Application of Differential Quadrature Method to the Analysis of Delamination Buckling of Laminated Composites

by

Shapour Moradi

A Thesis Submitted to the
Faculty of Engineering
in Partial Fulfillment of the Requirements
for the Degree of

DOCTOR OF PHILOSOPHY

Major Subject: *Mechanical Engineering*

DALHOUSIE UNIVERSITY – DALTECH

Halifax, Nova Scotia 1998

DEDICATION

To the Memories of My Mother and Father

TABLE OF CONTENTS

LIST OF TABLES

LIST OF FIGURES

NOMENCLATURE

A	Matrix (Extensional stiffness matrix)
a	delamination length, length
$A_{11}^{(k)}$	The first element of the extension stiffness matrix of the k^{th} region
B	Matrix (Bending-extensional stiffness matrix)
$B_{11}^{(k)}$	The first element of the bending-extension stiffness matrix of the k^{th} region
b	Length
$C_{ijk}^{(r)}$	Weighting coefficients for the r^{th} derivative
$c_{ij}^{(n)}$	Weighting coefficients for the n^{th} derivative
D_k	Flexural stiffness of the k^{th} derivative region
$\overline{D}$	Reduced bending stiffness
$D_{11}^{(k)}$	The first element of the bending stiffness matrix of the k^{th} region
$d_{11}^{(k)}$	The first element of the reduced bending stiffness matrix of the k^{th} region
E_i	Young's modulus along i^{th} direction (i can be x, y, z or 1, 2, 3)
F	Nonlinear function vector
G	Shear modulus
G_i	Fracture modes (i=I, II, III)
H	Thickness of the lower delaminated region
h	Thickness of the upper delaminated region
J	Jacobian matrix
J_d	Desired number of iterations for the convergence in the current load step
J_{m-1}	Actual number of iterations required for the convergence in the m-1^{th} load step
K	Matrix of the gradient of the force/displacement
k_s	Shear factor
L	Length
M	Moment
M	Moment matrix

M(x)=	$\prod_{j=1}^{N}(x-x_j)$
$M^{(1)}(x)$	First derivative of M(x)
N	Force vector
N	Load, Number
$N_i(\xi,\eta)$	Shape function
n_x, n_y	Directional cosines
P	Axial load, Compressive load
P_k	Axial load
$P_k(x)$	Polynomial of order k
P_N^*	Legendre Polynomial of order N
Q	Shear force
$r_k(x)$	Lagrange interpolation function of order k
s	Shear deformation factor, $s=\frac{4\pi^2 D}{k_s GTL^2}$
T	Beam's thickness
u	Inplane displacement
v	Inplane displacement
W_{ij}	Transverse deflection for the i^{th} point in the j^{th} region
W_b	Transverse deflection of the boundary points
W_i	Transverse deflection of the interior points
w	Transverse deflection
$\overline{w}$	Imperfection
w_o	Imperfection amplitude

α_1	Ration of the in-plane loads to the applied strain
β	Ratio of the two dimension
δ	Small distance
δ_{ij}	Kronecker delta
ε	Strain
ε_o	Strain of the reference surface
γ	Shear strain, Angle of fiber orientation
η	Natural axis
ξ	Natural axis
ϕ	Angle between normal to plate boundary and x-axis
φ	Transverse rotation
ψ	Nodal transverse rotation
κ	Curvature
λ	Loading factor
ν	Poisson's ratio

ACKNOWLEDGEMENTS

My thanks go first and foremost to God, who is the most merciful and compassionate, for giving me the power and energy to conduct this study.

I would like to convey my sincere appreciation and gratitude to my supervisor, Dr. Farid Taheri for his encouragement, support, guidance and most of all his friendship. I truly benefited from our discussions and his advises throughout the course of this study and thesis preparation. Thanks also go to the other members of my thesis committee, Dr. A. Kalamkarov, Dr. R. Bauer, Dr. G. Fenton and the external examiner Dr. Z. Fawaz.

My wife deserves special thanks for her love, support and understanding. Also thanks are due to my children to whom I apologize for being oftentimes a part-time father during my tenure as a Ph.D. candidate. Many appreciation toward my family, especially my brother Mr. Shahrokh Moradi, for their support and encouragement throughout my long academic career.

I also wish to thank the Iranian nation and the Ministry of Culture and Higher Education of I.R. of Iran for giving me the opportunity to complete my studies by awarding me a scholarship. Also the administrative efforts of the representative of the Iranian Ministry of Culture and Higher Education in Canada, Dr. R. Hosseini is acknowledged.

The financial support provided through a grant that was awarded to Dr. F. Taheri by the Natural Sciences and Engineering Research Council of Canada is gratefully acknowledged.

I also wish to acknowledge Advanced Mechanics Engineering Company for allowing me to use their facilities.

ABSTRACT

Buckling and postbuckling analysis of composite laminated structures having delaminations were studied numerically. The analyses were performed using the differential quadrature method of Bellman et al (1972). Several one- and two-dimensional models were developed and showed to be capable of predicting the buckling and postbuckling responses of composite beams and plates.

Prediction of the buckling strength of the delaminated composite beams and the examination of the influencing factors were carried out by employing several models. The effects of the shear deformation and the bending-stretching coupling were added by incorporating a shear deformation beam theory. Different models containing multiple through-the-width delaminations, as well as single delamination were studied parametrically. The accuracy and efficiency of the proposed method were evaluated through several case studies. In addition to the effect of shear deformation, bending-stretching coupling, the influence of material properties, lamination sequence and fiber-orientation, through-the-thickness and through-the-length locations of delaminations on buckling and postbuckling responses were investigated.

Using the differential quadrature method, the buckling response of composite laminated plates having a thin elliptical delamination was also studied by employing two-dimensional models. Employing the serendipity shape functions, the elliptical delaminated region was transformed into a rectangular computational domain with clamped boundaries. Subsequently, the differential equilibrium equations of the sublaminate were solved based on classical plate theory. In order to reduce the computational efforts, and at the same time, to include the effect of the bending stretching coupling, the reduced bending stiffness of the plates was employed. Through investigating several parameters, such as the shape and size of the delamination, fiber orientation, and the bending stretching effect, the integrity of the current methodology

was compared with other numerical methods, and found to be computationally less complex, and numerically more accurate.

For the postbuckling analysis, the differential quadrature method combined with an arc-length strategy was used to model the postbuckling analysis of composite beams having single or multiple delaminations. The nonlinear Von Karman strain-displacements and the exact curvatures were used to formulate the problem. Moreover, geometric imperfections in the form of initial deflections were included in the analysis. Several case studies were presented and the effects of parameters such as the number of delaminations, the imperfection amplitudes and the delamination length were investigated.

Throughout the course of the research, the differential quadrature results were compared with those of published analytical and numerical investigations or with those obtained by analyzing problems with the use of the commercial finite element packages. The results show that the differential quadrature technique can be used as a powerful, reliable, accurate and efficient numerical tool in assessing the buckling and postbuckling responses of delaminated composite structures. Throughout the thesis, we will demonstrate several advantages of the method in comparison to the other popular numerical methods such as the finite difference, finite element and boundary element methods. Beside the excellent quality of results that can be obtained through DQM, the method is relatively simple to formulate, and it requires less effort to implement. Furthermore, the method consumes relatively less effort, both in terms of computational time and also in the user effort in setting up a problem. The only disadvantage at this time is its lack of robustness in treating complicated geometries. This point is however treatable, as one could take advantage of several mesh generation schemes that are commonly used in alleviating similar anomaly encountered in the finite difference method.

CHAPTER 1

INTRODUCTION

1.1. Introductory remarks

Laminated composite materials, especially in the form of fiber reinforced plastics, are being utilized increasingly in the design of various structural applications. This is mostly due to the fact that these materials enjoy a strength-to-weight ratio advantage over the ordinary engineering materials. In spite of their definite advantages, they suffer from a major problem, namely their weak strength in the through-the-thickness direction of laminate because of low cohesive strength between the layers.

The defect could be even worse if the composite contains delamination. Delamination in composites may develop during manufacturing because of the imperfections and/or faulty procedures, or during service, by impact of an external object. This can significantly reduce the compressive strength and stiffness of the laminate and thereby, lowering the buckling load of the laminate when subjected to a compressive load, causing growth of such delamination regions.

Furthermore, the delamination buckling may occur in different types of modal shapes. As shown in Figure 1.1, at the critical load level, a compressed beam having a single delamination may respond in three possible modes of instability. Delamination length and its position through-the-thickness are the two important parameters controlling the shape of these modes. If the entire beam buckles before any other mode of deflection could take place, the response is referred to as the "global" buckling mode. This usually occurs in relatively short and thick delaminated beams. In a global buckling mode, if the buckling shape is symmetric with respect to the midspan of the beam, it is identified as the "global symmetric" mode (Figure 1.1a). On the other hand, if the global buckling

mode tends to deform into a kinked shape, the buckling shape is called the "global antisymmetric" mode (Figure 1.1b). When the delamination is thin, the first region that buckles is the delaminated region. Such a buckling is declared as the "local" buckling mode (Figure 1.1c). Finally, in an axially compressed delaminated beam, if both the global and local buckling take place at the same time, then the response is referred to as the "mixed" buckling mode (Figure 1.1d). The situations for multiply delaminated beams are quite similar to the ones discussed for single delamination.

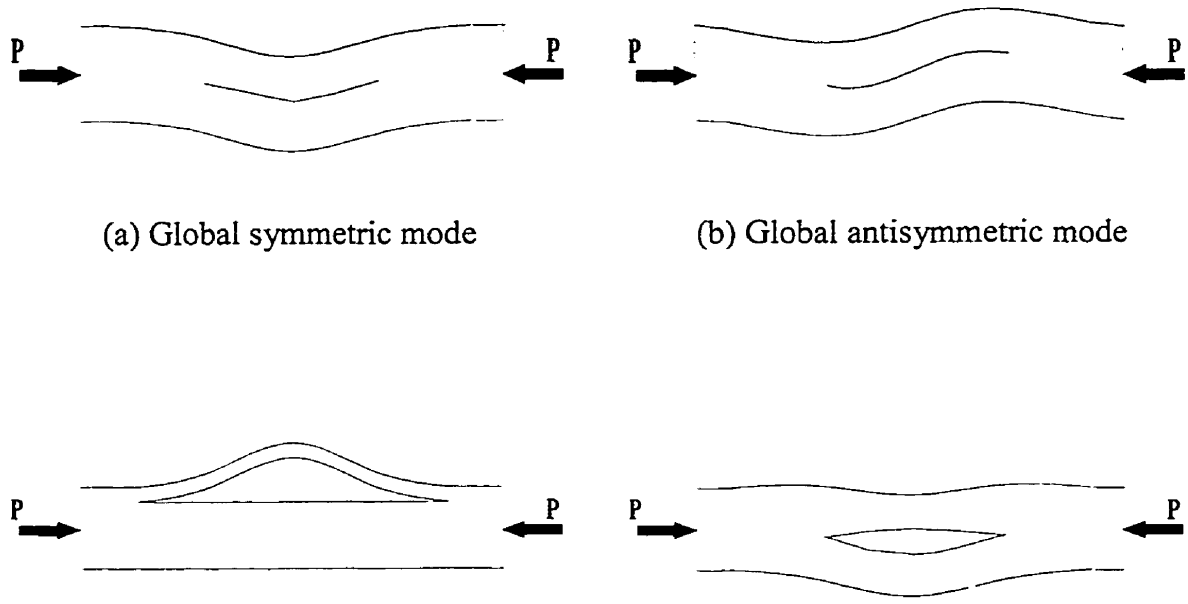

(a) Global symmetric mode (b) Global antisymmetric mode

(c) Local mode (d) Mixed mode

Figure 1.1. Buckling mode shapes for a delaminated composite.

1.2. Motivation

From the standpoint of analysis and design, it is of great importance to understand the behavior of the laminated composites containing one or several delaminations. The problem has been the focus of several research works and consequently, several methodologies and solutions have been developed. These methods can be classified under

three different categories: (i) experimental, (ii) analytical and (iii) numerical methods. The first method is usually costly and time consuming, often requiring special equipment and jigs, which makes it unsuitable for use in everyday applications. The second choice, in spite of being fast and efficient, is often limited to special cases. Because of the limitation of the analytical solutions, attention has been focused on the development of approximate and numerically oriented methods. The three most popular numerical techniques in use for solving partial differential equations are the Finite Difference Method (FDM), the Finite Element Method (FEM), and the Boundary Element Method (BEM). FDM is one of the simplest numerical methods (both in terms of its formulation and programming effort). To obtain an accurate result, however, considerable effort is required for representing (discretizing) the domain by a large number of grid points. FEM and BEM on the other hand require more skill and effort for algorithm development and implementation. Other numerical methods such as the Rayleigh-Ritz have also been used for solving such problems. Thus, the development of new methods from the standpoint of numerical accuracy, ease of formulation and computational efficiency is still of prime interest.

A relatively new numerical technique is the differential quadrature method (DQM). Bellman et al (1972) introduced the method in the early seventies for solving linear and nonlinear partial differential equations. Differential quadrature has been shown to perform extremely well in solving initial and boundary value problems (Bert and Malik (1996a)).

1.3. Objectives of the thesis

The main objective of this thesis is to develop a numerical approach, based on the differential quadrature method, to analyze the delamination buckling and postbuckling of composites. More specifically the objectives are:

1) To apply the differential quadrature analog to determine the buckling load of laminated composite beams having single or multiple delaminations. The effect of several parameters on the buckling response of a delaminated composite beam is considered, and the results obtained by DQM are compared with data available in the literature. The parameters considered are the number, through-the-thickness and along the span positions, and length of delaminations, material properties and stacking sequence of the laminates.

2) To identify and incorporate the necessary mapping functions, and to apply the differential quadrature technique to the buckling analysis of composite plates having a thin elliptical delamination.

3) To apply DQM to the postbuckling analysis, in conjunction with an arc length strategy to solve for the postbuckling response of a composite beam having single or multiple delaminations.

1.4. Layout of the thesis

The thesis is divided into seven chapters. In Chapter 2, a literature review of the past studies on delamination buckling and postbuckling is presented. In this state-of-the-art review, we categorize different aspects of the previous studies. This is followed by a literature survey on the differential quadrature method and its engineering applications. Details of the differential quadrature technique and its formulations are presented in Chapter 3. This includes the definition of the method and the derivation of the weighting coefficients for the first and higher order derivatives of single and multi variable functions. The chapter also discusses the concept of geometric mapping. Differential quadrature analogs of different types of delaminated beams and plates are presented in Chapter 4. Differential equilibrium equations of beams, having single or multiple delaminations and those of plates having elliptical delaminations, are presented. These

are followed by the presentation of the differential quadrature methodology used in transforming the differential equations into an equivalent eigenvalue system. Chapter 5 addresses the arc-length strategy used in the solution of nonlinear postbuckling problems. The same chapter also treats the nonlinear postbuckling analysis of composite beams having single or multiple delaminations. The details of several case studies used for assessing the validity, integrity, accuracy and efficiency of the method are given in Chapter 6, followed by the discussion of their results. Finally, Chapter 7 provides some conclusions and recommendations for future works.

CHAPTER 2

LITERATURE REVIEW

2.1. Introduction

In this chapter we will present a survey of the previous research on the delamination buckling and postbuckling behavior of laminated composite structures. Also, the chapter deals with a review of the research that has considered the differential quadrature method and its applications.

2.2. Delamination buckling and postbuckling

Previous studies on the delamination buckling and postbuckling of laminated composite structures can be classified within three general categories: experimental, analytical and numerical methods. The experimental methods are usually used to confirm the results produced by the other two methods; therefore, in here we will focus on the analytical and numerical works and will also mention their experimental validations. Later we will further subdivide the works based on different sub-categories, such as: one-, two- or three-dimension delamination modeling, single or multiple delaminations, etc.

2.2.1. Analytical studies

One of the earliest works in delamination buckling and growth analysis of beams was carried out by Chai et al (1981). They studied the behavior of an isotropic homogeneous beam-column under axial compression from a thin film model to the general case (when the supporting base laminate buckles globally, so that the zero-slope boundary condition for the thin sublaminate becomes invalid). In their model, the emphasis was on studying the delamination growth by employing the total energy release

rate of the system as a criterion. Perhaps the most important contribution of their work was to introduce the four-region model, obtained by dividing the delaminated beam into four different sections (Figure 2.1). Simitses et al (1985) also employed a similar model to study delamination buckling. They studied the effect of the location, length and thickness of delamination on the buckling load of a beam with clamped and simply supported ends, having a single across-the-width delamination. The perturbation method was used to solve the buckling equation.

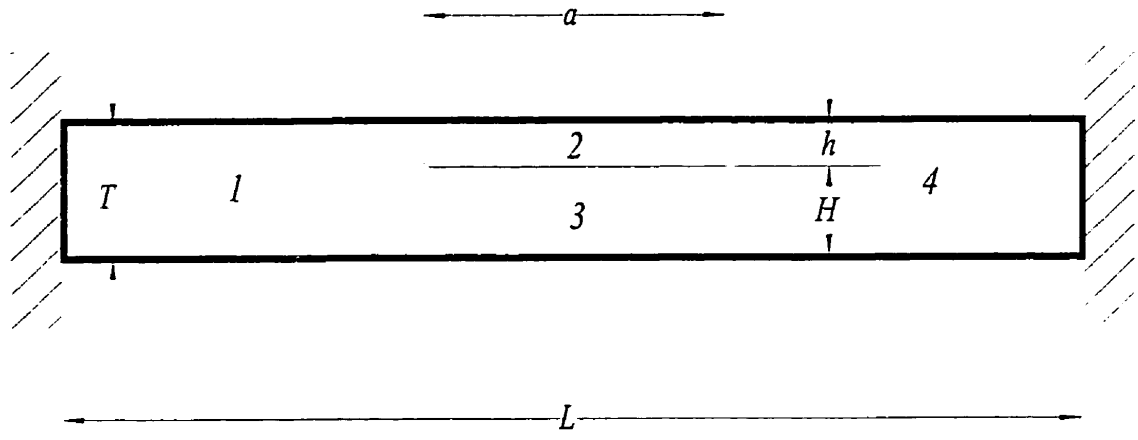

Figure 2.1. The four-region beam model.

Yin et al (1986) solved buckling and postbuckling problems of a one-dimensional beam-plate having an across-the-width delamination located symmetrically at an arbitrary depth. Their model was based on a special orthotropic plate with clamped edges and different delamination lengths. They obtained a general expression for the postbuckling behavior of the beam-plate. Kardomateas and Shmueser (1988) used perturbation technique to analyze the compressive stability of a one-dimensional across-the-width delaminated orthotropic homogeneous elastic beam. They also considered the transverse

shear effect on the buckling load and post-buckling behavior of the beam. Using the classical buckling equations, they accounted for the effects of the transverse shear by some correction terms. Using a variational energy approach and a shear-deformation theory, Chen (1991) formulated the same problem. According to his results, inclusion of the shear deformation causes reduction in the buckling and ultimate strength of delaminated composite plates. Kyoung and Kim (1995) used the variational principle to calculate the buckling load and delamination growth of an axially loaded beam-plate with a nonsymmetric (with respect to the center-span of the beam) delamination. They investigated the effects of shear deformation and various geometric parameters on the buckling strength and delamination growth of composite beams using their proposed solution and also an experimental investigation.

Chen and Chang (1994) used a first order shear-deformation theory to predict the delamination buckling loads for unsymmetric cross-ply delaminated plates with clamped edges. Their one-dimensional model was able to consider bending-extension coupling and transverse shear-deformation effects; the former parameter becomes significant in short and thick delaminations, while the latter has significant influence on delamination buckling loads.

Kardomateas (1993) and Kardomateas and Pelegri (1994) used perturbation techniques to study the initial post buckling and growth behavior of delaminations in plates. They also found closed form expressions for the energy release rate and the mixity ratio of mode I vs. mode II fracture at the delamination tips.

Wang et al (1997) used an analytical procedure to determine the buckling load of beams having multiple single-delaminations. Free and constrained models based on the beam-column theory were used to model the perfect and separated parts. Successive corrections made by removing the overlaps lead to physically permissible buckling mode.

Reference should be also made to the analysis of Bottega and Maewal (1983) who solved the problem of compression loaded homogeneous two layers plate with a centered circular delamination. Due to the circumferential symmetry, the problem could be reduced to one dimension. They considered nonlinear geometry by using the Von Karman nonlinear strain-displacement formulations. The load-deflection was calculated by an asymptotic expansion for the displacement fields.

Simitses and Chen (1988) investigated the buckling of a delaminated long cylindrical shell or panel under pressure. They divided the panel into four regions and assumed a separated solution for each part. It was found that the width and through-the-thickness position of delamination greatly affected the buckling load.

Sheinman and Adan (1993) used an analytical method to address the postbuckling analysis of a multiply delaminated beam. They used a function series composed of local and global eigenfunctions of a delaminated beam and applied them to nonlinear equilibrium equations. The resulting nonlinear system of algebraic equations was then solved numerically. Huang and Kardomateas (1997) applied a perturbation technique to transform the nonlinear equations of a beam having two central, through-the-thickness delaminations, under compressive load to a sequence of linear equations. Upon solving these equations they found an asymptotic solution of the postbuckling behavior of the beam. In both of the above works the contact between the delaminated layers and delamination growth was neglected.

Most of the investigations that have been done on compressive strength of composite laminates having single or multiple delaminations, employed the classical structural mechanics theory of beams and plates to estimate the buckling loads. Such approximate analyses greatly simplify the problem. Classical theory, due to its limitations, can not account for the effect of boundary conditions at the edges of delaminations; neither can it accurately represent the influence of different material

properties of the sublaminate and substrative. Hence, an exact analysis based on the mathematical theory of elasticity seems to be necessary. This approach, however, has its own difficulties due to complicated mathematical formulation and solution, specially in two or three dimensional problems. As a consequence, less attention has been given to such approaches.

Madenci and Westmann (1991) solved the local buckling problem of a layer containing a circular crack while Wang et al (1991) found the solution for local buckling of a half-space containing a through-the-width crack by using stability equations derived from the mathematical theory of elasticity. Wang and Takao (1995) solved the same problem, but with different material properties for the layer and the half-space. They solved the buckling differential equations by utilizing the Fourier integral transformation to establish a system of homogeneous singular integral equations and then solved this system numerically by employing the Gauss-Chebyshev integral formula.

2.2.2. Numerical studies

Because of the difficulties with the analytical methods used to solve the complicated delamination buckling and postbuckling problems, a great deal of attention has been given to the numerical solutions. Moreover, the availability of fast computers and various numerical algorithms have made this approach quite popular. In this section we will review the available numerical treatments of the delamination buckling and postbuckling of laminated composite structures.

Sheinman et al (1989) solved the differential equations of a delaminated composite beam under arbitrary loading and boundary conditions with a finite difference method. Bending-stretching coupling was taken into account which was shown to significantly influence the buckling loads.

Lee et al (1993) employed a one-dimensional finite element model (based on the layerwise plate theory) to solve the buckling of an axially loaded composite beam with multiple delaminations. The effects of several parameters, such as the number of delaminations, the lengths of delaminations, and their through-the-thickness and axial positions on the buckling strength of the beams, and their corresponding mode shapes, were investigated.

Lim and Parsons (1993) used an energy approach to predict the linearized buckling of a composite beam with single or multiple delaminations. Lagrange multipliers were used to enforce the kinematic constraints and boundary conditions. In their multiple delaminations model, all delaminations had the same lengths. They verified their results with those of finite element method and other published data.

Suemasu (1993) investigated the compressive buckling stability of composite panels with through-the-width, equally spaced multiple delaminations by performing numerical and experimental investigations. He used the Rayleigh-Ritz approximation technique and considered the Timoshenko type shear effects in his model. The results were compared with those of the finite element method and experimental investigations conducted on glass/epoxy composite panels.

Whitcomb (1981) performed a parametric study on the postbuckling response of laminated coupons having an across-the-width delamination. He conducted a geometrically nonlinear finite element analysis and calculated the stress distributions, strain energy release rates and lateral deflections for various delamination lengths, delamination depths and loading conditions. Kutlu and Chang (1992) developed a finite element code based on the updated Lagrangian formulation to compute the compression response of laminated composites containing multiple through-the-width delaminations. The model was one-dimensional, capable of accounting for multiple delaminations, including the interface contact phenomenon and delamination growth. Extensive

experiments on T300/976 graphite/epoxy composites were also performed which validated their analysis

Sheinman and Soffer (1991) used the finite difference method to solve the postbuckling problem of an imperfect composite laminate having a through-the-thickness delamination. They employed the commonly used one-dimensional beam model and formulated the response of the beam by dividing the delaminated beam into four regions. Using the Von Karman kinematic approach, the resulting non-linear differential equations were solved by the method of Newton-Raphson.

Lee et al (1995) used a one-dimensional finite element model (based on the layerwise plate theory), to solve the postbuckling problem of a beam having multiple delaminations. Their analysis included the effect of imperfections in the form of initial global deflection and initial delamination openings. They also adopted a contact analysis to prevent the overlapping of the delaminated segments of the beam. Lim (1994) applied a finite element analysis to study the postbuckling and delamination growth of a beam having a through-the-thickness delamination. His beam element was based on the Reissner's finite deformation beam theory. The nonlinear problem was solved by adopting an arc-length algorithm. To prevent the beam surfaces from overlapping, nonlinear springs were enforced and an initial imperfection in the form of a percentage of the first buckling mode was applied.

Chai and Babcock (1985) used the Rayleigh-Ritz method to solve the buckling and postbuckling problem of a laminated composite plate having elliptical delamination (Figure 2.2). The nonlinear Von Karman plate formulation was used to formulate the strain energy, while an energy balance criterion was used for the delamination growth. The delaminated region's thickness was assumed to be small compared to the base laminate thickness, so that the transverse displacement and slopes along the delamination boundary could be considered as null. Their solution was restricted to a special

orthotropic ellipse with the minor-axis parallel to the direction of loading. Their model, which used a simple energy balance criterion (G-criterion), exhibited interesting growth characteristics for different types of circular and elliptical delaminations in different materials.

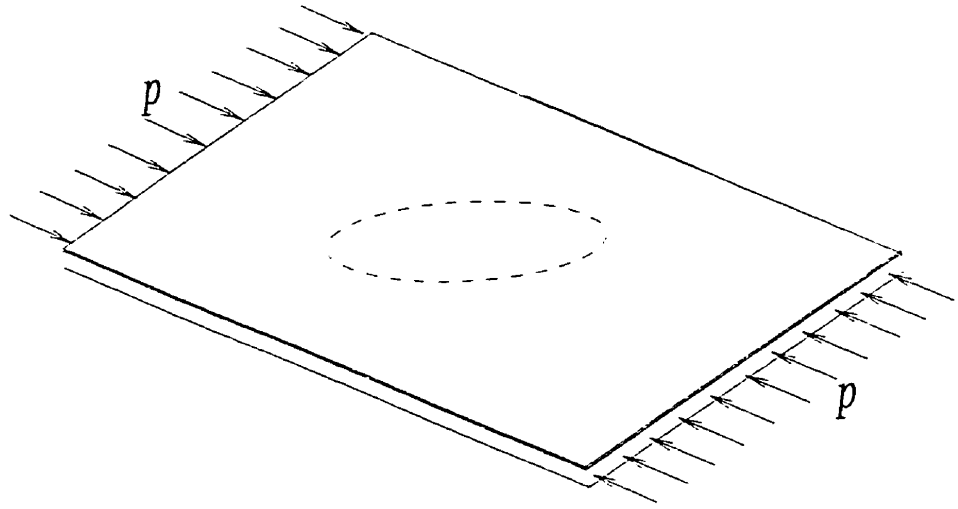

Figure 2.2. Plate with elliptical delamination under compressive load.

Shivakumar and Whitcomb (1985) presented an analysis for the same problem using Rayleigh-Ritz method and checked the results with finite element method. They found good agreement between the two methods. The Rayleigh-Ritz method was found to be simple and accurate, except for the highly anisotropic delaminated regions. The effects of the delamination shape and its orientation, material anisotropy and layup, on the buckling strains, were examined. It was shown that under certain conditions, the delaminated region would buckle when the laminate was loaded in tension. Heitzer and Feucht (1993) extended the Chai and Babcock (1985) work by taking into account all the couplings (which could result from an arbitrary nonsymmetric lay up) in the linear and nonlinear analyses. In their model, a thin laminate, which included an elliptical

delamination, was assumed to have been bonded to an infinitely thick homogeneous base laminate. The linear and nonlinear buckling problems were solved by Rayleigh-Ritz technique with up to 12 and 21 unknown terms, respectively, and the results were compared with those of the finite element method. In the nonlinear regime they used the Von Karman relations to account for large displacements in the thin film region. The energy release rates along the half axes were calculated for two unsymmetrical laminates and showed a monotonous rise with increasing load. The energies steeply decreased when the configuration switched to the second buckling mode. Heitzer and Feucht found that the Rayleigh-Ritz method, in addition to being too stiff at the higher modes of buckling, gives poor results for non-symmetric laminations.

Davidson (1991) used the Rayleigh-Ritz method to compute the buckling strains of a composite laminate containing an elliptical delamination. The influence of the bending-stretching coupling behavior of the delaminated region and the Poisson's ratio mismatch between the delaminated and base regions were also investigated. To reduce the computational efforts he used the reduced bending stiffness. The results correlated well with those obtained from experiments. In another work, the behavior of elliptical delamination in composite plates, under in-plane compressive, shear and thermal loads was investigated by Peck and Springer (1991), who also considered the contact effects. They extended the works of Chai and Babcock (1985) and Shivakumar and Whitcomb (1985) to include the transverse shear deformation, postbuckling deformation, contact effects, thermal loads and unsymmetric sublaminates. The Von Karman nonlinear strain-displacement formulations and a third order shear deformation theory, along with a through-the-thickness linearly varying contact force were used. The results were then compared with a series of experiments that were conducted on sandwich plates, made of graphite/epoxy laminates bonded to an aluminum honeycomb core, and reasonable agreement were obtained.

Yin and Jane (1992 part I ,II), have also used the Rayleigh-Ritz method with the Von Karman formulations to compute the buckling loads and postbuckling solutions of laminated anisotropic elliptical plates. By considering at least 33 undetermined coefficients in the Rayleigh-Ritz technique, they obtained reasonably accurate solutions for the membrane forces, bending and twisting moments and point wise energy release rates. Chai (1990 part I and II) extended the series expansion in the Rayleigh-Ritz method up to 77 terms for the analysis of a specially orthotropic plate with elliptical delamination. The plate's central deflections and bending moments converged quickly, even at higher buckling modes, whereas the membrane stresses showed a damped oscillatory type behavior as the number of displacement terms was increased. The solution was extended to take the point wise body contact into account. It turned out that the stresses changed significantly when the overlap was prevented.

Whitcomb and Shivakumar (1987) performed a finite element analysis of a post buckled rectangular delaminations using a crack closure technique. Using a geometrically nonlinear three dimensional finite element analysis, Whitcomb (1989) performed a fracture mode separation analysis, which could predict a pronounced mixed mode behavior along the crack front with large gradients in the modes I and II energy release rate components (G_I and G_{II}) and a negligible third mode energy component (G_{III}). The requirement of thin delamination was assured by choosing the base laminate to be ten times thicker than the sublaminate.

Chang and Kutlo (1989) developed a finite element code capable of computing the postbuckling behavior of composite plates and cylindrical shells containing multiple delaminations. In calculating the energy release rates they found that delamination growth was dominated by mode I fracture in flat plates and by mode II fracture in cylindrical panels.

Yeh and Tan (1994) studied the buckling behavior of composite laminated plates with elliptical delaminations, experimentally and analytically, using a nonlinear finite element method. To simulate delaminations, they used elliptical Teflon pieces and embedded them in the specimens at the ply interface. Based on the updated Lagrangian formulations, they developed a nonlinear finite element program (using degenerated shell elements) to analyze the buckling response of the laminated plates, which included large displacements and rotations. To evaluate the influence of the delamination size, fiber orientation, position of the delaminated region in the thickness direction, and the orientation of the major axis of the elliptical delamination with the loading axis, they varied these parameters and measured the plate responses both analytically and experimentally.

Kim et al (1996) used a nonlinear finite element formulation to study the buckling of a short orthotropic tube having a circumferential delamination under axial compression. The nonlinear finite element program was associated with a quadratic programming procedure to address the contact of delaminated faces. The load-carrying capacity of the delaminated tube and the stability of delamination growth were examined in terms of buckling load and energy release rate, respectively. Naganarayana and Atluri (1996) used nonlinear finite elements (2-noded curved beam and 3-noded shell) to model the delaminated stiffened laminated shells. To predict the postbuckling behavior, an arc length strategy was used. By computing the energy release rate at the delamination fronts, they studied the interaction of the postbuckling structural behavior and the delamination growth.

2.2.3. Classification of delamination buckling research

Although some of the important works in delamination buckling were reviewed in the previous sections, there are several other reported studies in this field. In this section we will classify them within different categories.

Table 2.1 presents a list of selected references in which the delamination buckling or postbuckling is evaluated based on experimental, analytical or numerical procedures. As seen through this table, most of the studies are based on numerical methods.

Table 2.1. Selected references classified based on the nature of the investigations used for the delamination buckling and postbuckling of structures.

Experimental	Analytical	Numerical
Suemasu (1993), Peck and Springer (1991), Ferrigno et al (1995),), Kōnig et al (1995), Yeh and Lee (1995), Wang et al (1985 b), Kutlu and Chang (1992), Kardomateas (1989), Cairns et al (1994),	Simitses et al (1985), Chen and Chang (1994), Huang and Kardomateas (1997), Moshaiov and Marshall (1991), Yin (1988), Wang and Cheng (1995), Chattopadhyay and Gu (1994), Wang et al (1997), Chai et al (1981), Kyoung and Kim (1995), Kardomateas and Schmueser (1988), Chen (1991, 1993), Yin et al (1986), Kardomateas (1989, 1993), Bottega and Maewal (1983), Simitses and Chen (1988), Yin and Fei (1988), Suemasu and Majima (1996), Wang and Takao (1995), Kardomateas and Pelegri (1994), Nilssin and Storåkers (1992), Madenci and Westmann (1991), Wang et al (1991), Cox (1994)	Sheinman et al (1989), Suemasu (1993), Lee et al (1993, 1995, 1996), Heitzer and Feucht (1993), Yin and Jane (1992 a,b), Davidson (1991), Chai (1990 a,b), Peck and Springer (1991), Chai and Babcock (1985), Shivakumar and Whitcomb (1985), Kyoung et al (1998), Sheinman and Soffer (1990, 1991), Sheinman and Adan (1993), Kim (1996, 1997), Davidson and Krafchak (1995), Moshaiov and Marshall (1991), Ferrigno et al (1995), Kōnig et al (1995), Yeh and Lee (1995), Mukherjee et al (1991), Barbero and Reddy (1991), Lim and Parsons (1993), Lim (1993), Srivatsa et al (1993), Naganarayana and Atluri (1996), Wang et al (1985 a, b), Kutlu and Chang (1992), Chang and Kutlu (1989), Kim et al (1996), Cairns et al (1994), Yeh an Tan (1994), Whitcomb (1981, 1989), Whitcomb and Shivakumar (1987), Gaudenzi (1997),

We further classified the works based on the number of geometric dimensionality used in the analysis, as presented in Table 2.2. In all one-dimensional analyses the delamination is across-the-width, while in the two or three dimensional analyses the crack is bounded by the intact laminate. This table signifies the appreciable attention that has been paid by researchers to the one-dimensional analysis.

Table 2.2. Selected references on the modeling of the delamination buckling and postbuckling based on the number of dimensions.

One-dimensional	Two-dimensional	Three-dimensional
Simitses et al (1985), Sheinman et al (1989), Suemasu (1993), Lee et al (1993, 1995, 1996), Chen and Chang (1994), Kyoung et al (1998), Sheinman and Soffer (1990, 1991), Huang and Kardomateas (1997), Sheinman and Adan (1993), Kim (1996,1997), Davidson and Krafchak (1995), Moshaiov and Marshall (1991), Yin (1988), Wang and Cheng (1995), Lim and Parsons (1993), Lim (1993), Wang et al (1997), Chai et al (1981), Wang et al (1985 a, b), Kyoung and Kim (1995), Kardomateas and Schmueser (1988), Chen (1991, 1993), Yin et al (1986), Kutlu and Chang (1992), Kardomateas (1989, 1993), Simitses and Chen (1988), Kim et al (1996), Whitcomb (1981), Kardomateas and Pelegri (1994),	Heitzer and Feucht (1993), Yin and Jane (1992 a,b), Davidson (1991), Chai (1990 a,b), Peck and Springer (1991), Babcock (1985), Shivakumar and Whitcomb (1985), Wang and Cheng (1995), Chattopadhyay and Gu (1994),), König et al (1995), Barbero and Reddy (1991), Naganarayana and Atluri (1996), Cairns et al (1994),	Kim (1996,1997), Ferrigno et al (1995),), König et al (1995), Yeh and Lee (1995), Mukherjee et al (1991), Srivatsa et al (1993), Yeh an Tan (1994), Whitcomb (1989),

Of those works dealing with one-dimensional problems, some have considered the problem of multiple delaminations. Table 2.3 categorizes the selected works based on single or multiple delaminations. To the author's best knowledge, none of the two- or three-dimensional investigations considered a laminate with multiple delaminations. In most of the two- or three-dimensional analyses the shape of delamination have been considered to be circular or elliptical. However, rectangular delamination was considered in some references such as Lee (1992) and Yeh and Tan (1995).

Table 2.3. Selected references classified based on single and multiple delaminations.

Single Delamination	Multiple Delaminations
Simitses et al (1985), Sheinman et al (1989), Lee et al (1993, 1996), Heitzer and Feucht (1993), Yin and Jane (1992 a,b), Davidson (1991), Chai (1990 a,b), Peck and Springer (1991), Babcock (1985), Shivakumar and Whitcomb (1985), Chen and Chang (1994), Sheinman and Soffer (1990, 1991), Huang and Kardomateas (1997), Sheinman and Adan (1993), Kim (1996, 1997), Davidson and Krafchak (1995), Moshaiov and Marshall (1991), Yin (1988), Wang and Cheng (1995), Ferrigno et al (1995), Chattopadhyay and Gu (1994),), Kõnig et al (1995), Yeh and Lee (1995), Mukherjee et al (1991), Lim and Parsons (1993), Lim (1993), Srivatsa et al (1993), Wang et al (1985 a, b), Naganarayana and Atluri (1996), Wang et al (1997), Chai et al (1981), Kyoung and Kim (1995), Kardomateas and Schmueser (1988), Chen (1991, 1993), Yin et al (1986), Kutlu and Chang (1992), Kardomateas (1989, 1993), Bottega and Maewal (1983), Simitses and Chen (1988), Kim et al (1996), Cairns et al (1994), Yeh an Tan (1994),	Suemasu (1993), Lee et al (1993, 1995, 1996), Kyoung et al (1998), Huang and Kardomateas (1997), Sheinman and Adan (1993), Davidson and Krafchak (1995), Wang and Cheng (1995), Lim and Parsons (1993), Larsson (1991), Wang et al (1997), Wang et al (1985 a, b), Kutlu and Chang (1992), Chang and Kutlu (1989), Suemasu and Majima (1996),

Classification of the selected numerical methods based on the nature of their formulations is presented in Table 2.4. As seen from this table, the Rayleigh-Ritz method has received a considerable attention.

Table 2.4. Selected references classified based on the modeling approaches used in the numerical studies.

Finite Difference	Finite Element	Rayleigh-Ritz
Sheinman et al (1989), Sheinman and Soffer (1990, 1991).	Lee et al (1993, 1995, 1996), Kyoung et al (1998), Kim (1996, 1997), Davidson and Krafchak (1995), Ferrigno et al (1995),), König et al (1995), Yeh and Lee (1995), Mukherjee et al (1991), Barbero and Reddy (1991), Lim (1993), Srivatsa et al (1993), Naganarayana and Atluri (1996), Wang et al (1985 a, b), Kutlu and Chang (1992), Chang and Kutlu (1989), Kim et al (1996), Yeh an Tan (1994), Whitcomb (1981, 1989), Whitcomb and Shivakumar (1987), Gaudenzi (1997),	Suemasu (1993), Heitzer and Feucht (1993), Yin and Jane (1992 a,b), Davidson (1991), Chai (1990 a,b), Peck and Springer (1991), Babcock (1985), Shivakumar and Whitcomb (1985), Moshaiov and Marshall (1991), Wang et al (1985 a, b), Cairns et al (1994),

Based on the nature of the formulation used to represent the problem and the incorporation of the bending-stretching coupling effect, Table 2.5 is constructed.

Table 2.5. Selected references classified based on the theoretical approaches used for the modeling of the delamination buckling and postbuckling.

Classical Lamination Theory	Higher order Theory	Bending-Stretching Effect
Simitses et al (1985), Sheinman et al (1989), Heitzer and Feucht (1993), Yin and Jane (1992 a,b), Davidson (1991), Chai (1990 a,b), Babcock (1985), Shivakumar and Whitcomb (1985), Sheinman and Soffer (1990, 1991), Huang and Kardomateas (1997), Sheinman and Adan (1993), Moshaiov and Marshall (1991), Yin (1988), Wang and Cheng (1995), Lim and Parsons (1993), Srivatsa et al (1993), Wang et al (1997), Chai et al (1981), Kardomateas and Schmueser (1988), Yin et al (1986), Simitses and Chen (1988),	Suemasu (1993), Lee et al (1993, 1995, 1996), Peck and Springer (1991), Chen and Chang (1994), Kyoung et al (1998), Kim (1996, 1997), Chattopadhyay and Gu (1994), Mukherjee et al (1991), Barbero and Reddy (1991), Lim (1993), Naganarayana and Atluri (1996), Wang et al (1985 a, b), Kyoung and Kim (1995), Chen (1991, 1993), Kutlu and Chang (1992), Cairns et al (1994),	Sheinman et al (1989), Heitzer and Feucht (1993), Davidson (1991), Peck and Springer (1991), Chen and Chang (1994), Kyoung et al (1998), Sheinman and Soffer (1990, 1991), Lee et al (1995), Sheinman and Adan (1993), Kim (1997), Yin (1988), Mukherjee et al (1991), Kim (1996), Chen (1993), Kutlu and Chang (1992), Chen (1993),

2.3. Differential Quadrature Method

Differential Quadrature Method (DQM), introduced by Bellman et al (1972), is based on the weighted sum of function values as an approximation to the derivatives of that function. Bellman et al (1972), (1986) stated that partial derivative of a function with respect to a space variable could be approximated by a weighted linear combination of function values evaluated at some intermediate points in the domain of that variable. Compared to FEM or FDM, DQM is relatively a new method used for solving a system of differential equations. In addition to the less complex algorithm, in comparison to

FEM, DQM also offers increased efficiency of the solution by demanding less number of grid points (hence, equations) to model the problem. Therefore, owing to the improved performances of DQM, this method has gained increasing popularity in solving a variety of engineering problems.

One of the areas in which the method has been applied frequently is in structural mechanics. Jang et al (1989) used DQM for the static analysis of structural components. They applied the method to find the deflection and buckling of beams and plates. Bert et al (1988) applied the method to the vibration analysis of beams and plates. Their results demonstrated that the method could be employed effectively in structural analysis.

Kukerti and Farsa (1992), Farsa et al (1993) and Farsa and Kukerti (1993) applied the method to the frequency analysis of isotropic, generally orthotropic and anisotropic plates. Bert et al (1993), (1994) used DQM for static and free vibration analysis of anisotropic plates, while Laura and Gutierrez (1994) used the method in vibration analysis of rectangular plates with non-uniform boundary conditions.

Sherbourne and Padney (1991) and Padney and Sherbourne (1991) used DQM to analyze the buckling of composite beams and plates. They used different number of grid spacing in their analysis. The same problem was addressed by Wang (1995), who also used different grid spacing. He found that employing uniform grid spacing could result in an inaccurate solution; therefore, caution should be exercised when using such spacing.

Liew et al (1996) used the method for the analysis of thick symmetric cross-ply laminates with first order shear deformation while Kang et al (1996) used it to address the vibration and buckling analysis of circular arches. Shu and Du (1997a) used DQM to address the analysis of free vibration of laminated composite cylindrical shells.

In most of the works done using DQM, the geometry of the problem has been considered to be simple. Straight lines and simple rectangles or in general, shapes with edges parallel to the curvilinear coordinate axes have been considered in the analysis. In actual situations, however, there may be irregular domains and thus, the solution strategy should be capable of covering these types of problems. In recent years more studies have been done to address this class of problems by mapping the physical domain into a computational domain. In this approach the physical domain, which contains the actual shape of the structure, can have curvilinear edges, while the computational domain would have straight edges, so that DQM can be applied to this domain. Lam (1993) used the mapping approach to solve some second order problems. Bert and Malik (1996b) used a mapping approach with cubic serendipity shape functions to analyze the vibration problem of some non-rectangular plates. They expressed the first derivative of a function in physical domain based on its differential quadrature in the computational domain, and Jacobian of the transformation. They then build the higher order derivatives of the function by inter-multiplying the lower order derivatives. Han and Liew (1997) used a mapping with quadratic shape functions to solve the bending of quadrilateral Reissner/Mindlin plates with curvilinear boundaries. The geometrical mapping was used to transform the physical domain (which its edges could have quadratic shapes) into the computational domain. The main advantage of the Han and Liew work over that of Bert and Malik is in the reduction of its numerical procedures. Bert and Malik analysis is, however, more efficient when applied to higher order problems.

Application of DQM in nonlinear analysis of structures has been also reported in several studies. Bert et al (1989) analyzed the large deflection problem of a thin orthotropic rectangular plate in bending. The three nonlinear differential equations of equilibrium of the plate were transformed into differential quadrature form and solved numerically using the method of Newton-Raphson. Lin et al (1994) used the same procedures to solve the problem of large deflection of isotropic plates under thermal

loading. In their analysis they used the generalized differential quadrature of Shu and Richards (1992).

As it can be seen from the definition of DQM, two important factors control the quality of the approximation resulting from the application of DQM. These are (i) the values of weighting coefficients and (ii) the positions of the discrete variables.

In order to determine the weighting coefficients for the first order derivatives, Bellman et al (1972) used two different approaches. The first approach, which was widely adopted in the earlier years, requires that the approximation to the function be exact for all power polynomials with degree less than or equal to one less than the number of the sampling points. This results in a set of linear algebraic equations, which is solved to obtain the weighting coefficients. The coefficients of the higher order derivatives can be obtained by multiplication of lower order matrix coefficients. This technique results in a Vandermonde matrix, which becomes ill-conditioned as the number of sampling points are increased. The second approach is to use the roots of the shifted Legendre polynomials as the coordinates of the grid points in a simple algebraic formulation. Most previous applications of differential quadrature use Bellman's first method to obtain the weighting coefficients because it lets the coordinate of the gird points to be chosen arbitrarily. Quan and Chang (1989) and Shu and Richards (1992) derived a recursive formula to obtain these coefficients directly and irrespective of the number and positions of the sampling points. In their approach they used the Lagrangian polynomials as the trial functions and found a simple recurrence formula for the weighting coefficients.

The location of the sampling points also plays a significant role in the accuracy of the solution of differential equations. Some of the researchers such as Sherbourne and Pandy (1991) and Farsa et al (1993) have used the equally distanced sampling points. This choice is considered to be a convenient and easy method. However, when using

equally spaced grids, the solutions become sensitive in several applications such as in anisotropic plates (Sherbourne and Pandy (1991)) or delaminated beams (Moradi and Taheri (1998)). In most cases, one can obtain a more accurate solution by choosing a set of unequally spaced sampling points. A common method is to select the zeros of orthogonal polynomials. Bert et al (1993) used the roots of Chebyshev polynomials as the coordinates of the grid points. Wang (1995) used several grid spacing such as the Gaussian integration points as the sampling points in the buckling analysis of laminated composites. Moradi and Taheri (1998) used equally and unequally spaced sampling points in the delamination buckling analysis of beams. Bert and Malik (1996a) also examined the equally spaced grids as well as unequally spaced in several structural mechanics applications.

Another important problem in dealing with DQM is the consideration of the boundary conditions in higher order differential equations such as for beams and plates. At each boundary point one boundary condition can be satisfied. In the case of fourth or higher order differential equations, however, more than one boundary condition should be satisfied at each boundary. To solve this problem several strategies have been adopted by the researchers. These strategies will be briefly discussed below.

Jang et al (1989) proposed the so-called δ-technique. In this method, points are chosen at a small distance δ, adjacent to the boundary points. Then, the differential quadrature analogue of the two conditions at a boundary is written for the boundary point and its adjacent δ-point. In another approach, Wang and Bert (1993) proposed a method in which the weighting coefficient matrices for each order of the derivatives can be derived by incorporating the boundary conditions in the differential quadrature discretization. Malik and Bert (1996c) also explored the benefits and the limitations of this approach for simulating various types of boundary conditions. Shu and Du (1997b, c), proposed an approach in which the derivative conditions for the two opposite edges are coupled to provide two solutions at two neighboring points to the edges. The

solutions are then substituted into the governing equations. Chen et al (1997) proposed a method in which the derivatives of the boundary points are approximated in the same way as that of the non-boundary points, by extending the size of the weighting matrices by two.

CHAPTER 3

DIFFERENTIAL QUADRATURE METHOD

3.1. Introduction

The concept of the differential quadrature method (DQM) is discussed in this chapter. The chapter starts with the definition of the technique and the methodologies available for the evaluation of weighting coefficients for various orders of derivatives. Then, the methodology will be extended for the multi-variable functions. Selection of the grid points and treatment of the boundary conditions will be discussed, subsequently. Finally, the concept of irregular domains will be explained, where the differential quadrature will be reformulated by using the mapping of a general curvilinear domain into a square domain.

3.2.1. Differential quadrature formulation for functions with single variable

As mentioned earlier, DQM was presented for the first time by Bellman et al (1972), for solving differential equations. The DQM uses the basis of the quadrature method in deriving the derivatives of a function. It follows that the partial derivative of a function with respect to a space variable can be approximated by a weighted linear combination of function values at some intermediate points in that variable. In order to show the mathematical representation of DQM, consider a function $f=f(x)$ on the domain $a \le x \le b$; then the n^{th} order differential of the function f at an intermediate point x_i can be written as:

$$\frac{d^n f(x_i)}{d\,x^n} = \sum_{k=1}^{N} c_{ik}^{(n)} f(x_k) \qquad \begin{matrix} i = 1,\ldots,N \\ n = 1,\ldots,N-1 \end{matrix} \tag{3.1}$$

where the domain is divided into N discrete points and $c_{ik}^{(n)}$ are the weighting coefficients of the n^{th} derivative. As it can be seen from equation (3.1), two important factors control the quality of the approximation, resulting from the application of DQM. These are (i) the values of weighting coefficients and (ii) the positions of the discrete variables.

In order to determine the weighting coefficients in equation (3.1), *f(x)* must be approximated by some test functions. To select a suitable test function, one needs to satisfy the following conditions:

a) Differentiability; the test function of the differential equation must be differentiable at least up to the n^{th} derivative (n referring to the highest order of the differential equation).

b) Smoothness; f must be sufficiently smooth to allow one to write (a) (Bert and Malik (1996a)).

One way of ensuring that the above conditions are satisfied is to use the attributes of the classical quadrature method. That is, choose a test function (in the form of polynomials of order *N-1*), such that the condition of equation (3.1) holds for all polynomials up to *N-1* order. In the original work of Bellman et al (1972), they suggested two approaches to fulfill the requirement. The first approach was to use a test function of the form:

$$P_k(x) = x^{k-1} \qquad k = 1,\ldots,N \tag{3.2}$$

Substituting (3.2) in (3.1) with n=1, leads to the following equation for all discrete points:

$$\sum_{j=1}^{N} c_{ij}^{(1)} x_j^{k-1} = \frac{d}{dx}\left(x_i^{k-1}\right) \qquad \begin{matrix} k = 1,\ldots,N \\ i = 1,\ldots,N \end{matrix} \tag{3.3}$$

which represents N sets of linear simultaneous equations, and has a unique solution (the coefficient matrix $c_{ij}^{(1)}$ is a Vandermonde matrix). From equation (3.3) it is clear that

$$\left[c^{(n)}\right]=\left[c^{(1)}\right]\cdot\left[c^{(n-1)}\right] \tag{3.4}$$

The above relation gives the higher order weighting coefficient matrix based on the first order derivative weighting coefficients.

The procedure outlined above bears a major problem: as the number of sampling points are increased the system of equation (3.3) tends to becomes ill-conditioned (because it includes a Vandermonde matrix), and consequently, the weighting coefficients obtained by this method become inaccurate.

The weighting coefficients may be determined explicitly for all discrete points, irrespective of the number of sampling points. Bellman et al (1972) in their second method used the roots of the shifted Legendre polynomials of degree N, as the sampling points, and derived the following relation for the first order derivative weighting coefficients:

$$\begin{aligned} c_{ij}^{(1)} &= \frac{P_N'^{*}(x_i)}{(x_i-x_j)\cdot P_N'^{*}(x_j)} \qquad i,j=1,\ldots,N \quad \text{and} \quad j\neq i \\ c_{ii}^{(1)} &= \frac{(1-2x_i)}{2x_i\cdot(x_i-1)} \end{aligned} \tag{3.5}$$

$P_N^{*}(x)$ is defined in terms of the Legendre polynomials by the relation:

$$P_N^{*}(x)=P_N(1-2x) \tag{3.6}$$

where $P_N(x)$ is the N^{th} order Legendre polynomial for $-1 \le x \le 1$. As seen from the equation (3.5) the second method uses a simple algebraic formula in calculating $c_{ij}^{(1)}$. The coefficients for the higher order terms can be obtained using relation (3.4).

The first method of Bellman et al in computing the weighting coefficients attracted more attention from researchers than their second one (Shu and Du (1997b)). This was mainly because in the first method the grid points can be selected arbitrarily while in the second method, one is restricted to choose only some specific points (the roots of the shifted Legendre polynomials). As mentioned above, however, using the first method may cause ill-conditioned coefficient matrix and therefore should not be used with high number of sampling points (say more than 13 points).

To overcome these drawbacks some researchers used other type of base polynomials. Quan and Chang (1989), Shu (1991) and Shu and Richards (1992) used the Lagrange interpolating functions and derived a recurrence formula which is independent of the number and position of sampling points. Using the Lagrange interpolation polynomial as the base polynomial

$$r_k(x) = \frac{M(x)}{(x - x_k) \cdot M^{(1)}(x_k)} \tag{3.7}$$

where

$$M(x) = \prod_{j=1}^{N} (x - x_j)$$

$$M^{(1)}(x) = \prod_{j=1, j \neq k}^{N} (x_k - x_j) \tag{3.8}$$

$M^{(1)}(x)$ is the first derivative of $M(x)$. Here x_i , $i=1,...,N$ are the coordinates of the sampling points which may be chosen arbitrarily. Then $f(x)$ can be expressed by

$$f(x)=\sum_{k=1}^{N} a_k \cdot r_k(x) \tag{3.9}$$

Substituting equation (3.9) into (3.1) and using (3.7) results in the following weighting coefficients (for more details see Shu (1991) and Shu and Du (1997b)):

$$\begin{aligned} c_{ij}^{(1)} &= \frac{\prod(x_i)}{(x_i-x_j)\cdot\prod(x_j)} && i,j=1,\ldots,N \quad \text{and} \quad j\neq i \\ c_{ij}^{(k)} &= k\left[c_{ii}^{(k-1)}\cdot c_{ij}^{(1)}-\frac{c_{ij}^{(k-1)}}{x_i-x_j}\right] && 2\le k\le N-1 \\ c_{ii}^{(m)} &= -\sum_{j=1,j\neq i}^{N} c_{ij}^{(m)} && m=1,\ldots,N-1 \end{aligned} \tag{3.10}$$

where

$$\prod(x_i)=\prod_{j=1,j\neq i}^{N}(x_i-x_j) \tag{3.11}$$

The above relations are not restricted to the number or position of the sampling points. Also there is substantial saving in computational time when the weighting coefficients are calculated by these formulae.

3.2.2. Weighting coefficients for functions with multi-variables

With the same approach, one can derive the quadrature analog of the multi-variables functions. To show it, consider a two-variables function $f=f(x,y)$; the n^{th} order derivative of function f with respect to x, the m^{th} order derivative of function f with respect to y and the $(n+m)^{\text{th}}$ order derivative of function f with respect to both x and y at

an intermediate discrete point x_i and y_j (where $i=1,\ldots,N_x$ and $j=1,\ldots,N_y$) can be approximated by the weighted linear sum of the function values as:

$$\frac{\partial^n}{\partial x^n} f(x_i, y_j) = \sum_{k=1}^{N_x} c_{ik}^{(n)} f(x_k, y_j) \qquad n = 1,\ldots,N_x - 1$$

$$\frac{\partial^m}{\partial y^m} f(x_i, y_j) = \sum_{k=1}^{N_y} c_{jk}^{(m)} f(x_i, y_k) \qquad m = 1,\ldots,N_y - 1 \tag{3.12}$$

$$\frac{\partial^{(n+m)}}{\partial x^n \partial y^m} f(x_i, y_j) = \sum_{k=1}^{N_x} c_{ik}^{(n)} \sum_{l=1}^{N_y} c_{jl}^{(m)} f(x_k, y_l) \qquad \begin{matrix} n = 1,\ldots,N_x - 1 \\ m = 1,\ldots,N_y - 1 \end{matrix}$$

where the domain is divided into N_x discrete points in the x-direction and N_y in the y-direction. $c_{ij}^{(n)}$ and $c_{ij}^{(m)}$ are the weighting coefficients of n^{th} and m^{th} order partial derivatives of $f(x,y)$ with respect to x and y, respectively.

3.3. Choice of the sampling points

The selection of locations of the sampling points plays a significant role in the accuracy of the solution of the differential equations. Using equally spaced points can be considered to be a convenient and an easy selection method. For a domain specified by $[a,b]$ and discretized by N points, then the coordinate of any point i can be evaluated by:

$$x_i = a + \frac{i-1}{N-1}(b-a) \tag{3.13}$$

But in most cases, one can obtain a more accurate solution by choosing a set of unequally spaced sampling points. A common method is to select the zeros of orthogonal polynomials. A simple and good choice can be the roots of shifted Chebyshev polynomials:

$$x_i = a + \frac{1}{2}\left(1 - \cos\frac{2i-1}{2N}\pi\right)(b-a) \tag{3.14}$$

Also use of zeros of the shifted Legendre polynomials have been known to give good results, while some authors have chosen the grid points based on trial (Sherbourne and Pandey (1991)). Wang (1995) suggested some useful schemes for selecting the sampling points for structural mechanics problems. In addition to the above grid schemes, later we will examine the effect of grid spacing through the use of the following sets of grid spacing in the normalized region $[0,1]$:

$$x_i = [0, (N-2) \text{ zeros of the shifted Legendre polynomial}, 1] \tag{3.15}$$

$$x_i = \left[\tfrac{1}{2}\left(1 - \cos[(i-1)\pi/(N-1)]\right)\right] \qquad i = 1,2,\ldots,N \tag{3.16}$$

$$x_i = \left[0, \tfrac{1}{2}\left(1 - \cos[(2i-3)\pi/(2N-4)]\right), 1\right] \qquad i = 2,3,\ldots,N-1 \tag{3.17}$$

A common property in these schemes is that the distribution of the sampling points is more concentrated at the ends of the region (i.e. around 0 and 1). This can lead to more accurate results as suggested by Shu (1991).

3.4. Treating Boundary Conditions

Essential and natural boundary conditions can be approximated by DQM; they are treated the same way as the differential equations are. In the resulting system of algebraic equations from DQM, each boundary condition replaces the corresponding field equation. Note that at each boundary point only one boundary condition can be satisfied. However, in the case of fourth order differential equations (such as those for beams and plates) or

the higher order, one must satisfy more than one boundary condition at each boundary. To overcome this problem several strategies have been adopted by the researchers.

Jang et al (1989) proposed the so-called "δ-technique". In this method points are selected at a small distance δ adjacent to the boundary points. Then, the differential quadrature analogue of the two conditions at a boundary is written for the actual boundary point and its adjacent δ-point. This technique offers an adequate means of applying the double boundary conditions for beams and plates, and has been successfully incorporated in the past (Farsa et al (1993), Sherbourne and Pandey (1991)). Nevertheless, there exist some drawbacks. First, since the second boundary is not applied at the actual boundary points, there is always some degree of error in the solution. Second, in order to reduce such an error, δ should be selected to be very small (say $\delta \cong 10^{-5}$). This may cause some convergence problems, such as the oscillation of the solution.

In another approach, Wang and Bert (1993) proposed a method in which the weighting coefficient matrices for each order derivative can be derived by incorporating the boundary conditions in the differential quadrature discretization. This method has significant limitations when dealing with the boundary conditions other than simply supported or clamped. Malik and Bert (1996c) also explored the benefits and the limitations of this method for various types of boundary conditions. Shu and Du (1997b, c) proposed another approach in which the derivative representing the two opposite edges are coupled to provide two solutions at two neighboring points to the edges. The solutions are then substituted into the governing equations. Shu and Du compared their results with those of Wang and Bert, and found that their results were inadequate in most cases. Chen et al (1997) proposed a method in which the derivatives representing the boundary points were approximated in the same way as those of the usual grid points by extending the size of the weighting matrices by two.

treatment of other type of the boundary conditions require no additional work. Moreover, our delamination buckling analysis indicated that the accuracy obtained by this technique in finding the buckling load was excellent.

3.5. Irregular domains

Based on its inherent nature, DQM can only consider domains with boundaries parallel to the coordinate axes. This means that the domain for a two dimensional problem should be rectangular. Thus, in order to solve an arbitrary shaped problem, one should map the physical domain into its equivalent rectangular. For this, there are currently two approaches. In one, which was suggested by Lam (1993) and Han and Liew (1997), the geometric coordinate transformation was employed to transform the governing differential equations and their corresponding boundary conditions from the physical to computational domain. Their approach however, is more efficient for problems that can be defined by differential equations up to second order. In the second approach as suggested by Bert and Malik (1996b) that is also utilized in this study, the quadrature rules were reformulated by using the mapping of a square domain into a general curvilinear region.

3.5.1. Geometric mapping

A general curvilinear quadrilateral domain with curve boundaries in the Cartesian x-y plane is shown in Figure 3.1. Each side of the plate can be described approximately by a cubic function. This domain can be mapped into a square domain, $-1 \leq \xi \leq 1$, $-1 \leq \eta \leq 1$ in the natural ξ-η plane by using the following cubic serendipity shape functions (Li et al (1986))

$$x = \sum_{i=1}^{12} N_i(\xi,\eta) \cdot x_i$$
$$y = \sum_{i=1}^{12} N_i(\xi,\eta) \cdot y_i \qquad (3.18)$$

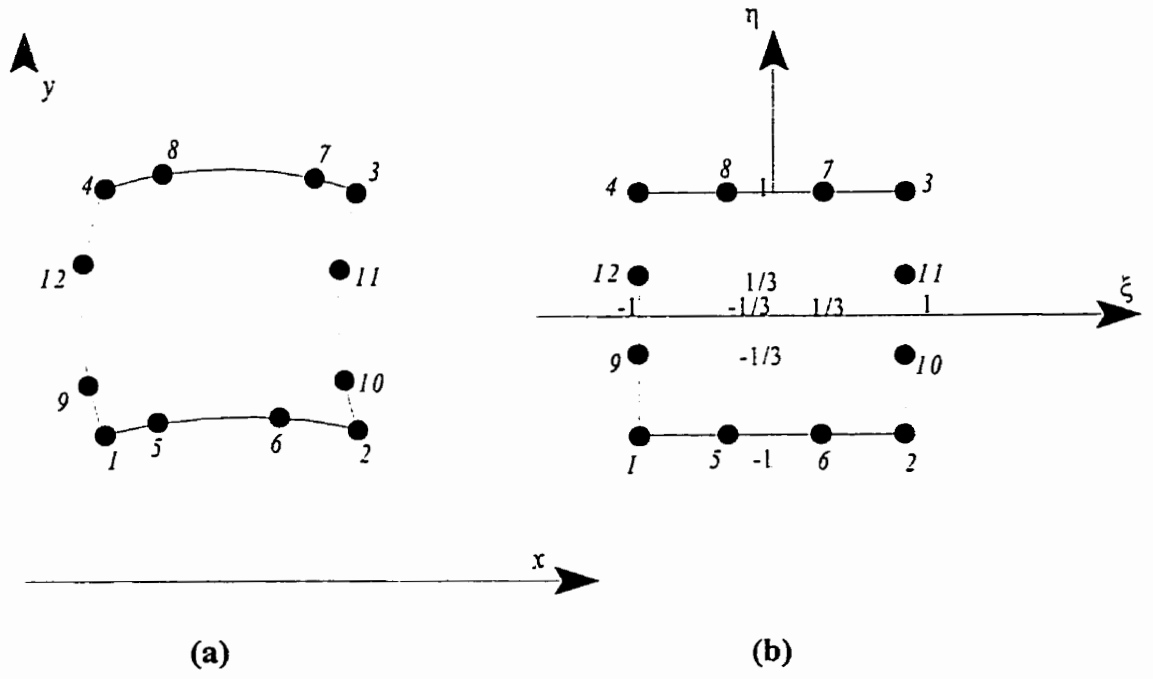

(a) **(b)**

Figure 3.1. Mapping from a) curvilinear quadrilateral physical domain to b) square parent computational domain.

where x_i and y_i are the coordinates of the i^{th} boundary node in the x-y plane, and $N_i(\xi,\eta)$ are the shape functions given by

$$N_i(\xi,\eta) = \tfrac{1}{32}(1+\xi_i\xi)\cdot(1+\eta_i\eta)\cdot\left[9(\xi^2+\eta^2)-10\right] \qquad i = 1,2,3,4$$

$$N_i(\xi,\eta) = \tfrac{9}{32}(1+\eta_i\eta)\cdot(1-\xi^2)\cdot(1+9\xi_i\xi) \qquad i = 5,6,7,8 \qquad (3.19)$$

$$N_i(\xi,\eta) = \tfrac{9}{32}(1+\xi_i\xi)\cdot(1-\eta^2)\cdot(1+9\eta_i\eta) \qquad i = 9,10,11,12$$

where ξ_i and η_i are the coordinates of the node i in the ξ-η plane. These shape functions have a value equal to unity at the i^{th} node and zero at all the remaining points. Next, by dividing the computational domain into N_ξ by N_η sampling points, we can derive the differential quadrature formulation of a function f in this domain. As a result, the first order derivatives $f_{,\xi}$ and $f_{,\eta}$ at a discrete point ξ_i, η_i can be defined as

$$f_{,\xi}(\xi_i,\eta_j) = \sum_{k=1}^{N_\xi} C_{ik}^{x(1)} f_{kj}$$
$$f_{,\eta}(\xi_i,\eta_j) = \sum_{l=1}^{N_\eta} C_{jl}^{\eta(1)} f_{il} \qquad (3.20)$$

where $C_{ik}^{x(1)}$ and $C_{jl}^{\eta(1)}$ are the weighting coefficients for the first order derivatives with respect to the ξ at ξ_i and η at η_j, respectively. The first order derivatives with respect to the physical coordinates x and y may be obtained from $f_{,\xi}$ and $f_{,\eta}$ by using the chain rule as

$$f_{,x} = \frac{1}{|J|}\left(y_{,\eta}\cdot f_{,\xi} - y_{,\xi}\cdot f_{,\eta}\right)$$
$$f_{,y} = \frac{1}{|J|}\left(-x_{,\eta}\cdot f_{,\xi} + x_{,\xi}\cdot f_{,\eta}\right) \qquad (3.21)$$

where $|J|$ is the determinant of the Jacobian matrix, which is

$$|J| = \left| x_{,\xi} \cdot y_{,\eta} - y_{,\xi} \cdot x_{,\eta} \right| \tag{3.22}$$

By substituting equation (3.20) in (3.21), the first order partial derivatives of f with respect to x and y at $\left(x(\xi,\eta), y(\xi,\eta)\right)_{ij}$ can be obtained by

$$\begin{aligned}
\left(f_{,x}\right)_{ij} &= \frac{1}{|J_{ij}|}\left[\left(y_{,\eta}\right)_{ij}\sum_{k=1}^{N_\xi} C_{ik}^{\prime(1)} f_{kj} - \left(y_{,\xi}\right)_{ij}\sum_{l=1}^{N\eta} C_{jl}^{\prime\prime(1)} f_{il}\right] \\
\left(f_{,y}\right)_{ij} &= \frac{1}{|J_{ij}|}\left[-\left(x_{,\eta}\right)_{ij}\sum_{k=1}^{N_\xi} C_{ik}^{\prime(1)} f_{kj} + \left(x_{,\xi}\right)_{ij}\sum_{l=1}^{N\eta} C_{jl}^{\prime\prime(1)} f_{il}\right]
\end{aligned} \tag{3.23}$$

Prescribing each sampling point with a unique index instead of two indices (i and j), one may rewrite equation (3.23) in a more compact form by:

$$\begin{aligned}
(f_{,x})_m &= \sum_{n=1}^{N_{\xi\eta}} C_{xmn}^{(1)} f_n \\
(f_{,y})_m &= \sum_{n=1}^{N_{\xi\eta}} C_{ymn}^{(1)} f_n
\end{aligned} \tag{3.24}$$

where $N_{\xi\eta} = N_\xi \times N_\eta$, $C_{xmn}^{(1)}$ and $C_{ymn}^{(1)}$ are the weighting coefficients for the first order derivatives with respect to the x and y and m and n are

$$\begin{aligned}
m &= (i-1)N_\xi + j \qquad i = 1,\ldots,N_\xi \\
n &= (i-1)N_\eta + j \qquad j = 1,\ldots,N_\eta
\end{aligned} \tag{3.25}$$

As seen from equation (3.24), the weighting coefficient matrices are of the order of $N_{\xi\eta}$. Having the weighting coefficients for the first order partial derivatives, one can easily obtain the weighting coefficients for the higher order derivatives. The general formula may be written as

$$(f_x^{(r)})_m = \sum_{n=1}^{N_{\xi\eta}} C_{xmn}^{(r)} f_n$$

$$(f_y^{(s)})_m = \sum_{n=1}^{N_{\xi\eta}} C_{ymn}^{(s)} f_n \qquad (3.26)$$

$$(f_{xy}^{(rs)})_m = \sum_{n=1}^{N_{\xi\eta}} C_{xymn}^{(rs)} f_n$$

where the first one represents the r^{th} order partial derivative of f with respect to x, the second one represents the s^{th} order partial derivative of f with respect to y and the third one is the $(r+s)^{\text{th}}$ order partial derivative of f with respect to both x and y. The weighting coefficient matrices of the higher order derivatives can be easily derived from the following formulae

$$\left[C_x^{(r)}\right] = \left[C_x^{(1)}\right] \cdot \left[C_x^{(r-1)}\right] \qquad r = 2,\ldots$$

$$\left[C_y^{(s)}\right] = \left[C_y^{(1)}\right] \cdot \left[C_y^{(s-1)}\right] \qquad s = 2,\ldots \qquad (3.27)$$

$$\left[C_{xy}^{(rs)}\right] = \left[C_x^{(r)}\right] \cdot \left[C_y^{(s)}\right] \qquad r,s = 1,\ldots$$

3.5.2. Domain Decomposition

For problems having complicated domains such as those in delaminated plates or beams or plates with cutouts, the concept of domain decomposition may be used for solving the problems. With this concept, first the domain is divided into several subdomains (Figure 3.2). A local mesh can be generated for each subdomain with more density near the boundaries. Then, the differential quadrature representation of the governing differential equations for each domain can be formulated. In this approach, each region may have different number of sampling points. Finally, the boundary conditions and the compatibility conditions at the subdomain interfaces should be taken into consideration and satisfied.

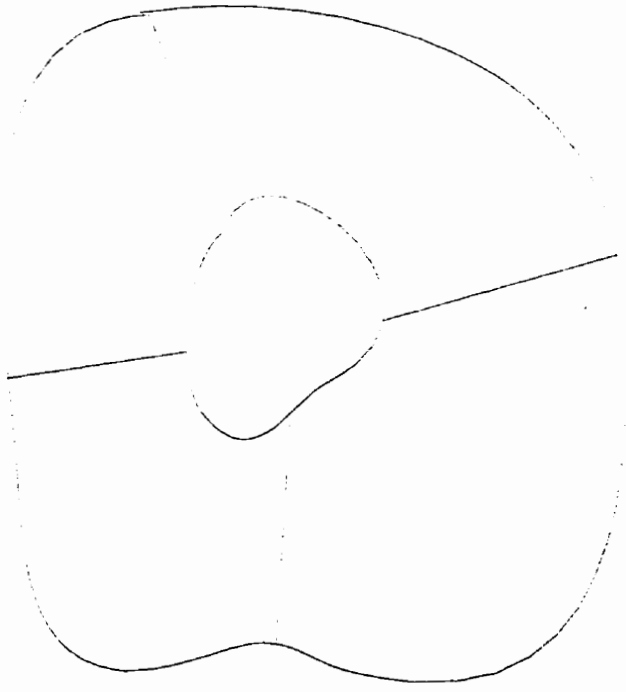

Figure 3.2. A complicated domain.

CHAPTER 4

DIFFERENTIAL QUADRATURE FORMULATION OF DELAMINATION BUCKLING

4.1. Introduction

In this chapter the differential quadrature analog of some delaminated beams and plates under compressive loads will be presented. The objective is to find the delamination buckling loads for the cases with single and multiple delaminations. For the delaminated beam problems with single delamination we have adopted the strategy in which the beam is divided into four regions. The extension of the similar approach is employed for modeling of laminated composite beams having multiple delaminations. The thin delamination model is used for the delaminated plate problems. The DQM will be applied to the differential equilibrium equations of each structure. Then appropriate boundary and interface compatibility conditions will be considered and treated. The results will be a linear system of eigenvalue equations. Solving this system results in delamination buckling loads and their corresponding mode shapes.

In the first part the formulation for the delaminated beams based on the classical lamination theory will be presented. This results in a forth order differential equation. Next a beam theory based on the first order shear deformation will be used to accommodate the effects of shear deformation, which results in a system of second order differential equations with two different type of variables. Then, the formulation for the general laminate will be presented which, in addition to the effects of shear deformation, includes bending-stretching coupling effects. Next, the quadrature analog of laminated composite beams with multiple delaminations will be derived. Finally the two-dimensional formulations for a plate having circular or elliptical delamination will be presented.

4.2. Delamination buckling formulation for beams

4.2.1. Delamination buckling for a specially orthotropic beam

The geometry of the one dimensional delaminated beam-plate is shown in Figure 4.1. This model contains an across-the-width delamination with the length a which is located in an arbitrary depth through the thickness of the plate. It is chosen to be symmetric with respect to the two restricted ends (The plate ends may have any form of constraints such as hinged or clamped). Note from Figure 4.1 that the delamination divides the beam into four regions. The region above the delamination plane with thickness h is referred to as the "upper" sublaminate, and the region below it with thickness H *is* referred to as the "lower" sublaminate. The sections before and after delamination where the beam is intact are referred to as the "base" laminate. Here we consider each of these regions as separate beams. The governing equations for these fields corresponding to the four parts are given by (Simitses et al (1985)):

$$D_k \frac{d^4 w_k}{dx^4} + P_k \frac{d^2 w_k}{dx^2} = 0 \qquad k = 1,2,3,4 \tag{4.1}$$

where D_k is the stiffness of the k^{th} region given by:

$$D_k = \frac{E_x t_k^3}{12(1 - \nu_{xz}\nu_{zx})} \tag{4.2}$$

P_k represents the axial force and t_k is the thickness of the k^{th} region. E_x is the Young's modulus along the x-direction and ν is the Poisson's ratio.

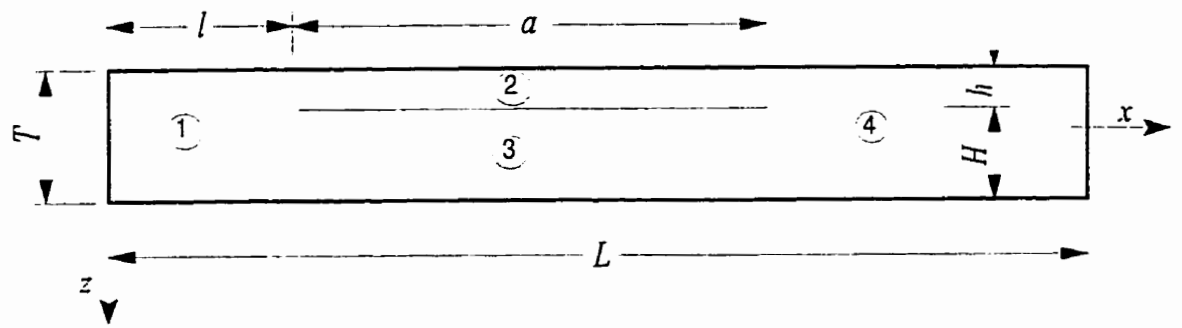

Figure 4.1. Geometry of a beam with single delamination.

The boundary conditions for different parts consist of in-plane and transverse boundary conditions, compatibility and continuity conditions. They are as follows:

The in-plane and transverse boundary conditions at both ends are:

at $x = 0$ $\qquad P_1 = -P$ (4.3a)

at $x = L$ $\qquad P_4 = -P$ (4.3b)

for clamped support ends:

at $x = 0$ $\qquad w_1 = \dfrac{dw_1}{dx} = 0$ (4.4a)

at $x = L$ $\qquad w_4 = \dfrac{dw_4}{dx} = 0$ (4.4b)

for simply supported ends:

at $x = 0$ $\qquad w_1 = \dfrac{d^2 w_1}{dx^2} = 0$ (4.4c)

at $x = L$ $\qquad w_4 = \dfrac{d^2 w_4}{dx^2} = 0$ (4.4d)

Continuity conditions at delaminated edges consist of transverse, moment, in-plane and shear force continuity:

at $x = l$

$$w_1 = w_2 = w_3 \tag{4.5a}$$

$$\frac{dw_1}{dx} = \frac{dw_2}{dx} = \frac{dw_3}{dx} \tag{4.5b}$$

$$M_1 - M_2 - M_3 + P_2(H/2) - P_3(h/2) = 0 \tag{4.5c}$$

$$P_1 - P_2 - P_3 = 0 \tag{4.5d}$$

$$-Q_1 + Q_2 + Q_3 = 0 \tag{4.5e}$$

at $x = l + a$

$$w_2 = w_3 = w_4 \tag{4.5f}$$

$$\frac{dw_2}{dx} = \frac{dw_3}{dx} = \frac{dw_4}{dx} \tag{4.5g}$$

$$M_2 + M_3 - M_4 - P_2(H/2) + P_3(h/2) = 0 \tag{4.5h}$$

$$P_2 + P_3 - P_4 = 0 \tag{4.5i}$$

$$-Q_2 - Q_3 + Q_4 = 0 \tag{4.5j}$$

Also applying the axial strain compatibility for the upper and lower sublaminates, it gives:

$$\frac{1}{2}\int_0^a \left(\frac{dw_2}{dx}\right)^2 dx + \frac{(1-\nu_{xz}\nu_{zx})P_2 a}{E_x h} = \frac{1}{2}\int_0^a \left(\frac{dw_3}{dx}\right)^2 dx + \frac{(1-\nu_{xz}\nu_{zx})P_3 a}{E_x H} + T\cdot\frac{dw(l)}{dx} \tag{4.6}$$

where $\frac{dw(l)}{dx}$ is the rotation angle at the delamination front. Note that for a non-symmetric delamination with respect to the longitudinal beam span, this angle should be replaced by $\frac{1}{2}\left(\frac{dw(l)}{dx} + \frac{dw(l+a)}{dx}\right)$. Equation (4.6) represents the postbuckling behavior of the delaminated beam. Before the onset of buckling, the values of $\left(\frac{dw}{dx}\right)^2$ are insignificant, so equation (4.6) reduces to:

$$P_2\frac{H}{2} - P_3\frac{h}{2} = \frac{T\cdot h\cdot H\cdot E_x}{2a\cdot(1-\nu_{xz}\nu_{zx})}\cdot\frac{dw(l)}{dx} \tag{4.7}$$

Also, from the primary state solution:

$$P_k = \frac{t_k}{T}P \tag{4.8}$$

Applying DQM approximation to Equation (4.1) for different regions and at each discrete point, one obtains:

$$\sum_{j=1}^{N_k} C_{ijk}^{(4)} W_{jk} = -\frac{P_k l_k^2}{D_k} \sum_{j=1}^{N_k} C_{ijk}^{(2)} W_{jk} \qquad \begin{matrix} i = 1,\ldots,N_k \\ k = 1,2,3,4 \end{matrix} \tag{4.9}$$

where $C_{ijk}^{(2)}$ and $C_{ijk}^{(4)}$ are the weighting coefficients for the second and forth derivatives along the non-dimensionalized X axis, respectively, W_{jk} is the deflection of the j^{th} point in the k^{th} region. N_k is the number of sampling points for the k^{th} region (Figure 4.2).

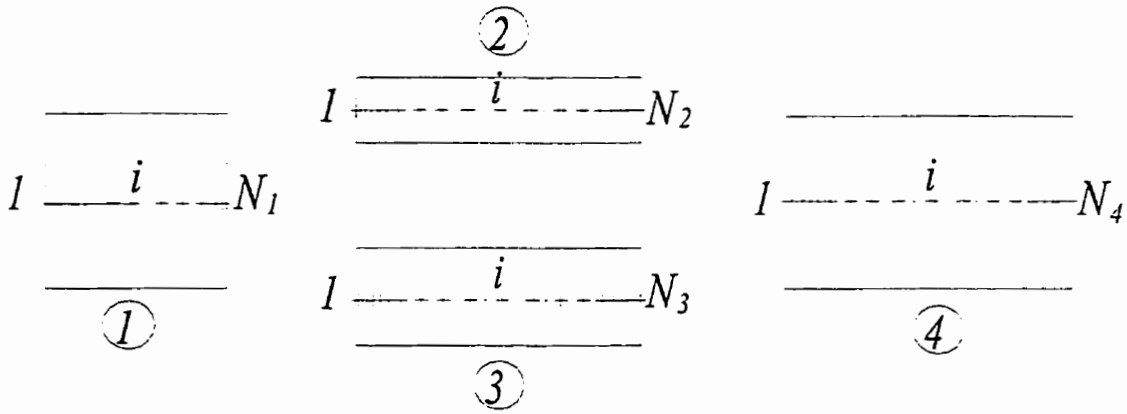

Figure 4.2. Sampling points for a beam with single delamination.

The kinematic boundary conditions in Equations (4.4a), (4.4b), (4.5a), (4.5b), (4.5f) and (4.5g) are transformed into the following differential quadrature format for a beam having clamped edges:

$$W_{11} = \sum_{j=1}^{N_1} C_{1j1}^{(1)} W_{j1} = 0 \tag{4.10a}$$

$$W_{N_4 4} = \sum_{j=1}^{N_4} C_{N_4 j4}^{(1)} W_{j4} = 0 \tag{4.10b}$$

$$W_{N_1 1} = W_{12} = W_{13} \tag{4.10c}$$

$$\frac{1}{l_1}\sum_{j=1}^{N_1} C_{N_1 j1}^{(1)} W_{j1} = \frac{1}{l_2}\sum_{j=1}^{N_2} C_{1j2}^{(1)} W_{j2} = \frac{1}{l_3}\sum_{j=1}^{N_3} C_{1j3}^{(1)} W_{j3} \tag{4.10d}$$

$$W_{N_2 2} = W_{N_3 3} = W_{14} \tag{4.10e}$$

$$\frac{1}{l_2}\sum_{j=1}^{N_2} C_{N_2 j2}^{(1)} W_{j2} = \frac{1}{l_3}\sum_{j=1}^{N_3} C_{N_3 j3}^{(1)} W_{j3} = \frac{1}{l_4}\sum_{j=1}^{N_4} C_{1j4}^{(1)} W_{j4} \tag{4.10f}$$

Using the following relations for M and Q:

$$\begin{aligned} M_k &= D_k \frac{d^2 w_k}{dx^2} \\ Q_k &= -D_k \frac{d^3 w_k}{dx^3} + P_k \frac{dw_k}{dx} \end{aligned} \tag{4.11}$$

and equations (4.5c-e), (4.5h-j) and (4.7), the moment and force boundary conditions at the delamination fronts become:

$$\frac{t_1^3}{l_1^2}\sum_{j=1}^{N_1} C_{N_1 j1}^{(2)} W_{j1} - \frac{t_2^3}{l_2^2}\sum_{j=1}^{N_2} C_{1j2}^{(2)} W_{j2} - \frac{t_3^3}{l_3^2}\sum_{j=1}^{N_3} C_{1j3}^{(2)} W_{j3} + \frac{6t_1 \cdot t_2 \cdot t_3}{l_1 \cdot l_2}\sum_{j=1}^{N_1} C_{N_1 j1}^{(1)} W_{j1} = 0 \tag{4.12a}$$

$$\frac{t_4^3}{l_4^2}\sum_{j=1}^{N_4} C_{1j4}^{(2)} W_{j4} - \frac{t_2^3}{l_2^2}\sum_{j=1}^{N_2} C_{N_2 j2}^{(2)} W_{j2} - \frac{t_3^3}{l_3^2}\sum_{j=1}^{N_3} C_{N_3 j3}^{(2)} W_{j3} - \frac{6t_1 \cdot t_2 \cdot t_3}{l_4 \cdot l_2}\sum_{j=1}^{N_4} C_{1j4}^{(1)} W_{j4} = 0 \qquad (4.12b)$$

$$\left(\frac{t_1}{l_1}\right)^3 \sum_{j=1}^{N_1} C_{N_1 j1}^{(3)} W_{j1} - \left(\frac{t_2}{l_2}\right)^3 \sum_{j=1}^{N_2} C_{1j2}^{(3)} W_{j2} - \left(\frac{t_3}{l_3}\right)^3 \sum_{j=1}^{N_3} C_{1j3}^{(3)} W_{j3} = 0 \qquad (4.12c)$$

$$\left(\frac{t_4}{l_4}\right)^3 \sum_{j=1}^{N_4} C_{1j4}^{(3)} W_{j4} - \left(\frac{t_2}{l_2}\right)^3 \sum_{j=1}^{N_2} C_{N_2 j2}^{(3)} W_{j2} - \left(\frac{t_3}{l_3}\right)^3 \sum_{j=1}^{N_3} C_{N_3 j3}^{(3)} W_{j3} = 0 \qquad (4.12d)$$

where t_k and l_k, (for $k = 1,2,3,4$) represent the thickness and length of each section, respectively. Imposing these boundary conditions make some of the equations in (4.9) redundant. In order to eliminate such a redundancy, the equations corresponding to $i = 1,2,(N_k - 1)$ and N_k in Equation (4.9) can be eliminated for all regions. Therefore, equation (4.9) becomes

$$\sum_{j=1}^{N_k} C_{ijk}^{(4)} W_{jk} = -\lambda \cdot \left(\frac{T}{t_k}\right)^2 \cdot \left(\frac{l_k}{L}\right)^2 \sum_{j=1}^{N_k} C_{ijk}^{(2)} W_{jk} \qquad \begin{matrix} i = 3,\ldots,(N_k - 2) \\ k = 1,2,3,4 \end{matrix} \qquad (4.13)$$

where

$$\lambda = \frac{12PL^2(1-\nu_{13}\nu_{31})}{4\pi^2 E_1 T^3} \qquad (4.14)$$

λ is the normalized buckling load which is the ratio of the compressive load to the Euler buckling load of a beam with clamped ends.

Combination of Equation (4.13) with the above sixteen boundary conditions gives the following system of linear equations

$$\begin{bmatrix} A_{bb} & A_{bi} \\ A_{ib} & A_{ii} \end{bmatrix} \begin{Bmatrix} \{W_b\} \\ \{W_i\} \end{Bmatrix} = \lambda \cdot \begin{bmatrix} 0 & 0 \\ B_{ib} & B_{ii} \end{bmatrix} \begin{Bmatrix} \{W_b\} \\ \{W_i\} \end{Bmatrix} \tag{4.15}$$

where the subscripts b and i refer to the locations of the boundary and the interior regions, respectively. The vectors $\{W_b\}$ and $\{W_i\}$ are the normal deflection vectors corresponding to the boundary and interior points. By transforming Equation (4.15) into a general eigenvalue form one obtains

$$[\mathrm{A}^*] \cdot \{W_i\} = \lambda [\mathrm{B}^*] \cdot \{W_i\} \tag{4.16}$$

where:

$$[\mathrm{A}^*] = [A_{ii} - A_{ib} \cdot A_{bb}^{-1} \cdot A_{bi}] \tag{4.17a}$$

$$[\mathrm{B}^*] = [B_{ii} - B_{ib} \cdot A_{bb}^{-1} \cdot A_{bi}] \tag{4.17b}$$

By solving the eigenvalue problem represented by Equation (4.16) with the help of a standard eigen solver, one will obtain the eigenvalues (i.e., the buckling loads), and the eigenvectors $\{W_i\}$ (i.e., the mode shapes).

4.2.2. Delamination buckling formulation for a specially orthotropic beam including shear deformation effects

Here, to include the effect of shear deformation, the same four-region model, which was considered in the last section is employed. The model contains an across-the-width

delamination with the length 'a' located arbitrarily through the thickness and along the span of the beam-plate. Using the shear deformation theory (Whitney (1989)), the equilibrium equations for each region can be written as:

$$P_{k,x} = 0 \tag{4.18a}$$

$$M_{k,x} - Q_i = 0 \qquad k = 1,2,3,4 \tag{4.18b}$$

$$Q_{k,x} - P_k w_{k,xx} = 0 \tag{4.18c}$$

where P_k, Q_k, M_k and w_k are the in-plane force, shear force, moment and the transverse deflection of each region k, respectively. By substituting

$$M_k = D_k \psi_{k,x} \tag{4.19a}$$

$$Q_k = k_s G t_k \left(\psi_k + w_{k,x}\right) \tag{4.19b}$$

into equations (4.18b) and (4.18c), the governing differential equations reduce to

$$D_k \psi_{k,xx} - k_s G t_k \left(\psi_k + w_{k,x}\right) = 0 \tag{4.20a}$$

$$k = 1,2,3,4$$

$$k_s G t_k \left(\psi_k + w_{k,x}\right)_{,x} - P_k w_{k,xx} = 0 \tag{4.20b}$$

where ψ_k and t_k are the transverse rotation angle and thickness of the k^{th} region, respectively; $G = G_{xz}$ is the shear modulus, k_s is the shear factor (i.e., $\frac{5}{6}$).

The boundary conditions for the different regions consist of the in-plane, transverse, continuity and compatibility conditions. The in-plane boundary conditions at both ends are the same as equations (4.3a,b). Also, for simply supported ends:

$$\text{at } x = 0 \qquad w_1 = \psi_{1,x} = 0 \tag{4.21a}$$

$$\text{at } x = L \qquad w_4 = \psi_{4,x} = 0 \tag{4.21b}$$

and if the ends are clamped, then:

$$\text{at } x = 0 \qquad w_1 = \psi_1 = 0 \tag{4.21c}$$

$$\text{at } x = L \qquad w_4 = \psi_4 = 0 \tag{4.21d}$$

Continuity conditions at the delaminated edges consist of the transverse, moment, in-plane and shear force continuity.

At at $x = l$

$$w_1 = w_2 = w_3 \tag{4.22a}$$

$$\psi_1 = \psi_2 = \psi_3 \tag{4.22b}$$

$$D_1\psi_{1,x} - D_2\psi_{2,x} - D_3\psi_{3,x} + (H/2)P_2 - (h/2)P_3 = 0 \tag{4.22c}$$

$$P_1 - P_2 - P_3 = 0 \tag{4.22d}$$

$$\left[k_s GT\left(\psi_1 + w_{1,x}\right) - k_s Gh\left(\psi_2 + w_{2,x}\right) - k_s GH\left(\psi_3 + w_{3,x}\right)\right] \tag{4.22e}$$

$$-\left(P_1 w_{1,x} - P_2 w_{2,x} - P_3 w_{3,x}\right) = 0$$

at $x = l + a$

$$w_2 = w_3 = w_4 \tag{4.22f}$$

$$\psi_2 = \psi_3 = \psi_4 \tag{4.22g}$$

$$D_2\psi_{2,x} + D_3\psi_{3,x} - D_4\psi_{4,x} - (H/2)P_2 + (h/2)P_3 = 0 \tag{4.22h}$$

$$P_2 + P_3 - P_4 = 0 \tag{4.22i}$$

$$\left[k_s Gh\left(\psi_2 + w_{2,x}\right) + k_s GH\left(\psi_3 + w_{3,x}\right) - k_s GT\left(\psi_4 + w_{4,x}\right)\right] \tag{4.22j}$$

$$-\left(P_2 w_{2,x} + P_3 w_{3,x} - P_4 w_{4,x}\right) = 0$$

It should be noted that the boundary conditions include terms containing the in-plane forces which makes the formation of the problem in a matrix form, and hence, the solution of the associated eigenvalues, impossible. Therefore, to convert the equilibrium and boundary condition equations into its equivalent matrix form, the terms associated with the in-plane forces in equation (4.22c), (4.22e), (4.22h) and (4.22j) must be eliminated. Substituting equations (4.22b), (4.22g) and (4.8) into equations (4.22c) and (4.22h) gives

$$Tw_{1,x} - hw_{2,x} - Hw_{3,x} = 0 \tag{4.23a}$$

and with the same way

$$Tw_{4,x} - hw_{2,x} - Hw_{3,x} = 0 \tag{4.23b}$$

which essentially indicates that the first derivatives of the transverse deformations at the delamination fronts are equal for the neighboring regions. Furthermore, applying the axial strain compatibility condition for the upper and lower sublaminates results in:

$$\frac{1}{2}\int_0^a (\frac{dw_2}{dx})^2 dx + \frac{(1-\nu_{xz}\nu_{zx})P_2 a}{E_x h} = \frac{1}{2}\int_0^a (\frac{dw_3}{dx})^2 dx + \frac{(1-\nu_{xz}\nu_{zx})P_3 a}{E_x H} + T\cdot\psi(l) \tag{4.24}$$

where $\psi(l)$ is the rotation angle at the delamination front. Equation (4.24) represents the postbuckling behavior of the delaminated beam. An important point to be noted is that by replacing the ψ term in equation (4.24) with $\frac{1}{2}\left(\psi(l)+\psi(l+a)\right)$, the above equation will become capable of treating a nonsymmetrical delamination. Before the onset of buckling, the magnitude of the $\left(\frac{dw}{dx}\right)^2$ term is insignificant, hence, equation (4.24) can be reduced into:

$$P_2\frac{H}{2} - P_3\frac{h}{2} = \frac{T\cdot h\cdot H\cdot E_x}{2a\cdot(1-\nu_{xz}\nu_{zx})}\cdot\psi(l) \tag{4.25}$$

Applying (4.25) to the moment continuity conditions (equation (4.22c) and (4.22h)) at the delamination fronts results in

$$D_1\psi_{1,x} - D_2\psi_{2,x} - D_3\psi_{3,x} + \frac{E_x ThH\psi(l)}{2a\cdot(1-\nu_{xz}\nu_{zx})} = 0 \tag{4.26a}$$

$$D_2\psi_{2,x} + D_3\psi_{3,x} - D_4\psi_{4,x} - \frac{E_x ThH\psi(l)}{2a\cdot(1-\nu_{xz}\nu_{zx})} = 0 \tag{4.26b}$$

At this stage DQM can be applied to the system of the differential equilibrium equations and their boundary conditions, forming:

$$\frac{s}{4\pi^2}\left(\frac{t_k}{T}\right)^2\left(\frac{L}{l_k}\right)^2\sum_{j=1}^{N_k} C_{ijk}^{(2)}\Psi_{jk} - \delta_{ij}\Psi_{jk} - \frac{1}{l_k}\sum_{j=1}^{N_k} C_{ijk}^{(1)}W_{jk} = 0 \qquad \begin{matrix} i = 1,\ldots,N \\ k = 1,2,3,4 \end{matrix} \tag{4.27a}$$

$$\sum_{j=1}^{N_k} C_{ijk}^{(1)}\Psi_{jk} + \frac{1}{l_k}\sum_{j=1}^{N_k} C_{ijk}^{(2)}W_{jk} = \lambda\cdot\left(\frac{s}{l_k}\right)\sum_{j=1}^{N_k} C_{ijk}^{(2)}W_{jk} \qquad \begin{matrix} i = 1,\ldots,N \\ k = 1,2,3,4 \end{matrix} \tag{4.27b}$$

where $C_{ijk}^{(1)}$ and $C_{ijk}^{(2)}$ are the weighting coefficients for the first and second derivatives along the non dimensional X-axis, respectively; W_{jk} and Ψ_{jk} are the deflection and rotation of the j^{th} point in the k^{th} section, respectively; δ_{ij} is the Kronecker delta, and s is the shear deformation parameter defined by:

$$s = \frac{4\pi^2 D_1}{k_s GTL^2} \tag{4.28}$$

which includes the effect of shear deformation. Defining λ as:

$$\lambda = \frac{P}{(4\pi^2 D_1/L^2)} \tag{4.29}$$

λ is called the normalized buckling load.

The boundary conditions of a beam-plate with its far edges clamped can be represented by:

$$W_{11} = \Psi_{11} = 0 \tag{4.30a}$$

$$W_{N_4 4} = \Psi_{N_4 4} = 0 \tag{4.30b}$$

$$W_{N_1 1} = W_{12} = W_{13} \tag{4.30c}$$

$$\Psi_{N_1 1} = \Psi_{12} = \Psi_{13} \tag{4.30d}$$

$$W_{N_2 2} = W_{N_3 3} = W_{14} \tag{4.30e}$$

$$\Psi_{N_2 2} = \Psi_{N_3 3} = \Psi_{14} \tag{4.30f}$$

$$\frac{t_1^3}{l_1}\sum_{j=1}^{N_1} C_{N_1 j1}^{(1)} \Psi_{j1} - \frac{t_2^3}{l_2}\sum_{j=1}^{N_2} C_{1j2}^{(1)} \Psi_{j2} - \frac{t_3^3}{l_3}\sum_{j=1}^{N_3} C_{1j3}^{(1)} \Psi_{j3} + \frac{6t_1 \cdot t_2 \cdot t_3}{l_2} \Psi_{N_1 1} = 0 \tag{4.30g}$$

$$\frac{t_4^3}{l_4}\sum_{j=1}^{N_4} C_{1j4}^{(1)} \Psi_{j4} - \frac{t_2^3}{l_2}\sum_{j=1}^{N_2} C_{N_2 j2}^{(1)} \Psi_{j2} - \frac{t_3^3}{l_3}\sum_{j=1}^{N_3} C_{N_3 j3}^{(1)} \Psi_{j3} - \frac{6t_1 \cdot t_2 \cdot t_3}{l_2} \Psi_{14} = 0 \tag{4.30h}$$

$$\frac{t_1}{l_1}\sum_{j=1}^{N_1} C_{N_1 j1}^{(1)} W_{j1} - \frac{t_2}{l_2}\sum_{j=1}^{N_2} C_{1j2}^{(1)} W_{j2} - \frac{t_3}{l_3}\sum_{j=1}^{N_3} C_{1j3}^{(1)} W_{j3} = 0 \tag{4.30i}$$

$$\frac{t_4}{l_4}\sum_{j=1}^{N_4} C_{1j4}^{(1)} W_{j4} - \frac{t_2}{l_2}\sum_{j=1}^{N_2} C_{N_2 j2}^{(1)} W_{j2} - \frac{t_3}{l_3}\sum_{j=1}^{N_3} C_{N_3 j3}^{(1)} W_{j3} = 0 \tag{4.30j}$$

where t_k and l_k, $(k = 1,2,3,4)$ represent the thickness and length of each section. The imposition of these boundary conditions makes some of the terms of equations (4.27a) and (4.27b) redundant. To eliminate this redundancy, the terms corresponding to $i = 1$ and N_k in equation (4.27a) and (4.27b), for all regions have to be omitted. The combination of equation (4.27a), (4.27b) and the above sixteen boundary conditions produce the following system of eigenvalue equations

$$\begin{bmatrix} A_{bb} & A_{bi} \\ A_{ib} & A_{ii} \end{bmatrix} \begin{Bmatrix} \begin{Bmatrix} \Psi_b \\ W_b \end{Bmatrix} \\ \begin{Bmatrix} \Psi_i \\ W_i \end{Bmatrix} \end{Bmatrix} = \lambda \cdot \begin{bmatrix} 0 & 0 \\ B_{ib} & B_{ii} \end{bmatrix} \begin{Bmatrix} \begin{Bmatrix} \Psi_b \\ W_b \end{Bmatrix} \\ \begin{Bmatrix} \Psi_i \\ W_i \end{Bmatrix} \end{Bmatrix} \tag{4.31}$$

where the subscripts b and i denotes for the boundary and interior points used for writing the differential quadrature, respectively. The vectors $\{\Psi\}$ and $\{W\}$ contain the rotations and normal deflections corresponding to the boundary and interior points. Transforming equation (4.31) into a general eigenvalue form in terms of $\{W_i\}$ results in

$$[\mathrm{A}^*] \cdot \{W_i\} = \lambda [\mathrm{B}^*] \cdot \{W_i\} \tag{4.32}$$

The solution of the above eigenvalue problem by a standard eigen solver, provides the eigenvalues, which are the buckling loads, and the eigenvectors $\{W_i\}$, which are the corresponding buckling mode shapes.

4.2.3. Delamination buckling formulation for a general laminated composite beam

The delaminated fiber reinforced composite beam-plate model under consideration is shown in Fig 4.1. Using the first order shear deformation lamination theory, the

equilibrium equations for the fields corresponding to these four parts are given by equations (4.18a-c). Let

$$Q_k = k_s A_{55}^{(k)} \left(\psi_k + w_{k,x} \right) \tag{4.33}$$

where again ψ_i is the rotation angle, k_s is the shear deformation factor and $A_{55}^{(k)}$ is the transverse shear stiffness defined as

$$A_{55}^{(k)} = \int_{-t_k/2}^{t_k/2} Q_{55}^{(k)} \cdot dz \tag{4.34}$$

and D_k in Equation (4.22) being the effective bending stiffness (otherwise known as the "apparent" or "reduced" flexural stiffness) of the k^{th} region defined by:

$$D_k = D_{11}^{(k)} - \frac{B_{11}^{(k)2}}{A_{11}^{(k)}} \tag{4.35}$$

where $A_{11}^{(k)}$, $B_{11}^{(k)}$ and $D_{11}^{(k)}$ are the extension, bending-extension and bending stiffness of the corresponding regions, respectively, and are defined as:

$$\left(A_{11}^{(k)}, B_{11}^{(k)}, D_{11}^{(k)} \right) = \int_{-t_k/2}^{t_k/2} Q_{11}^{(k)} \left(1, z, z^2 \right) \cdot dz \tag{4.36}$$

One can, therefore, rewrite the governing differential equations as:

$$D_k \psi_{k,xx} - k_s A_{55}^{(k)} \left(\psi_k + w_{k,x} \right) = 0 \tag{4.37a}$$

k=1,2,3,4

$$k_s A_{55}^{(k)} \left(\psi_k + w_{k,x} \right)_{,x} - P_k w_{k,xx} = 0 \tag{4.37b}$$

The boundary conditions for the different regions consist of the in-plane and transverse as well as the continuity and compatibility conditions. The in-plane and transverse boundary conditions at both ends are the same as equations (4.3a,b), (4.21a-d).

The continuity conditions at the delaminated edges must be satisfied for the transverse deflections, the moments, the in-plane and shear forces which can be represented at the first delamination front, that is at $x = l$ as equations (4.22a, b and d) plus

$$D_1\psi_{1,x} - D_2\psi_{2,x} - D_3\psi_{3,x} + \frac{A_{11}^{(2)}A_{11}^{(3)}}{A_{11}^{(1)}}\left(\frac{B_{11}^{(3)}}{A_{11}^{(3)}} - \frac{B_{11}^{(2)}}{A_{11}^{(2)}} + \frac{T}{2}\right)\left(\frac{P_2}{A_{11}^{(2)}} - \frac{P_3}{A_{11}^{(3)}}\right) = 0 \tag{4.38a}$$

$$\left[k_s A_{55}^{(1)}\left(\psi_1 + w_{1,x}\right) - k_s A_{55}^{(2)}\left(\psi_2 + w_{2,x}\right) - k_s A_{55}^{(3)}\left(\psi_3 + w_{3,x}\right)\right]$$

$$-\left(P_1 w_{1,x} - P_2 w_{2,x} - P_3 w_{3,x}\right) = 0 \tag{4.38b}$$

and at $x = l + a$, boundary conditions for the second delamination edge, taken the form of that of equations (4.22f, g and i), plus

$$D_2\psi_{2,x} + D_3\psi_{3,x} - D_4\psi_{4,x} - \frac{A_{11}^{(2)}A_{11}^{(3)}}{A_{11}^{(4)}}\left(\frac{B_{11}^{(3)}}{A_{11}^{(3)}} - \frac{B_{11}^{(2)}}{A_{11}^{(2)}} + \frac{T}{2}\right)\left(\frac{P_2}{A_{11}^{(2)}} - \frac{P_3}{A_{11}^{(3)}}\right) = 0 \tag{4.38c}$$

$$\left[k_s A_{55}^{(2)}\left(\psi_2 + w_{2,x}\right) + k_s A_{55}^{(3)}\left(\psi_3 + w_{3,x}\right) - k_s A_{55}^{(4)}\left(\psi_4 + w_{4,x}\right)\right]$$

$$-\left(P_2 w_{2,x} + P_3 w_{3,x} - P_4 w_{4,x}\right) = 0 \tag{4.38d}$$

In order to prepare the boundary equations for a matrix solution, the terms associated with the in-plane forces of these equations should be eliminated. Using the

method introduced in the last section and recognizing that the critical buckling load in each region can be expressed by:

$$P_k = \frac{A_{55}^{(k)}}{A_{55}^{(1)}} P \tag{4.39}$$

one can write

$$A_{55}^{(1)} w_{1,x} - A_{55}^{(2)} w_{2,x} - A_{55}^{(3)} w_{3,x} = 0 \tag{4.40a}$$

$$A_{55}^{(4)} w_{4,x} - A_{55}^{(2)} w_{2,x} - A_{55}^{(3)} w_{3,x} = 0 \tag{4.40b}$$

Furthermore, insuring the axial strain compatibility condition for the upper and lower sublaminates results in:

$$\frac{1}{2}\int_0^a \left(\frac{dw_2}{dx}\right)^2 dx + \frac{P_2 a}{A_{11}^{(2)}} = \frac{1}{2}\int_0^a \left(\frac{dw_3}{dx}\right)^2 dx + \frac{P_3 a}{A_{11}^{(3)}} + \left(\frac{B_{11}^{(3)}}{A_{11}^{(3)}} - \frac{B_{11}^{(2)}}{A_{11}^{(2)}} + T\right) \cdot \psi(l) \tag{4.41}$$

where $\psi(l)$ is the rotation angle at the delamination front. By replacing the ψ term in equation (4.41) with $\frac{1}{2}\left(\psi(l) + \psi(l+a)\right)$, the above equation will become capable of treating a nonsymmetrical delamination. Equation (4.41) represents the postbuckling behavior of the delaminated beam-plate. It should be noted that before the onset of buckling, the contribution of the $\left(\frac{dw}{dx}\right)^2$ terms is insignificant, therefore, they can be neglected. Equation (4.41) will then reduce to:

$$\frac{P_2}{A_{11}^{(2)}} - \frac{P_3}{A_{11}^{(3)}} = \left(\frac{B_{11}^{(3)}}{A_{11}^{(3)}} - \frac{B_{11}^{(2)}}{A_{11}^{(2)}} + T\right) \cdot \frac{\psi(l)}{a} \tag{4.42}$$

Applying (4.42) to the moment continuity conditions at the delamination fronts result in:

$$D_1\psi_{1,x} - D_2\psi_{2,x} - D_3\psi_{3,x} + \frac{A_{11}^{(2)}A_{11}^{(3)}}{A_{11}^{(1)}}\left(\frac{B_{11}^{(3)}}{A_{11}^{(3)}} - \frac{B_{11}^{(2)}}{A_{11}^{(2)}} + T\right)\cdot\left(\frac{B_{11}^{(3)}}{A_{11}^{(3)}} - \frac{B_{11}^{(2)}}{A_{11}^{(2)}} + \frac{T}{2}\right)\frac{\psi(l)}{a} = 0 \tag{4.43a}$$

$$D_2\psi_2 + D_3\psi_3 - D_4\psi_4 - \frac{A_{11}^{(2)}A_{11}^{(3)}}{A_{11}^{(1)}}\left(\frac{B_{11}^{(3)}}{A_{11}^{(3)}} - \frac{B_{11}^{(2)}}{A_{11}^{(2)}} + T\right)\cdot\left(\frac{B_{11}^{(3)}}{A_{11}^{(3)}} - \frac{B_{11}^{(2)}}{A_{11}^{(2)}} + \frac{T}{2}\right)\frac{\psi(l)}{a} = 0 \tag{4.43b}$$

Application of the DQM to the above systems of differential equilibrium equations and their boundary conditions results in a system of eigenvalue equations. First applying DQM to (4.37a,b) yields

$$\frac{D_k}{l_k^2}\sum_{j=1}^{N_k} C_{ijk}^{(2)}\Psi_{jk} - k_s A_{55}^{(k)}\left(\delta_{ij}\Psi_{jk} + \frac{1}{l_k}\sum_{j=1}^{N_k} C_{ijk}^{(1)}W_{jk}\right) = 0 \qquad \begin{matrix} i = 1,\ldots,N \\ k = 1,2,3,4 \end{matrix} \tag{4.44a}$$

$$\sum_{j=1}^{N_k} C_{ijk}^{(1)}\Psi_{jk} + \frac{1}{l_k}\sum_{j=1}^{N_k} C_{ijk}^{(2)}W_{jk} = \left(\frac{P}{k_s A_{55}^{(1)} l_k}\right)\sum_{j=1}^{N_k} C_{ijk}^{(2)}W_{jk} \qquad \begin{matrix} i = 1,\ldots,N \\ k = 1,2,3,4 \end{matrix} \tag{4.44b}$$

The kinematic boundary conditions for the beam with clamped edges can be presented by the same equations as in (4.30a-f), plus:

$$\frac{D_1}{l_1}\sum_{j=1}^{N_1} C^{(1)}_{N_1 j1}\Psi_{j1} - \frac{D_2}{l_2}\sum_{j=1}^{N_2} C^{(1)}_{1j2}\Psi_{j2} - \frac{D_3}{l_3}\sum_{j=1}^{N_3} C^{(1)}_{1j3}\Psi_{j3}$$

$$+\frac{A^{(2)}_{11}A^{(3)}_{11}}{A^{(1)}_{11}}\left(\frac{B^{(3)}_{11}}{A^{(3)}_{11}} - \frac{B^{(2)}_{11}}{A^{(2)}_{11}} + T\right)\left(\frac{B^{(3)}_{11}}{A^{(3)}_{11}} - \frac{B^{(2)}_{11}}{A^{(2)}_{11}} + \frac{T}{2}\right)\frac{1}{l_2}\Psi_{N_1 1} = 0 \tag{4.45a}$$

$$\frac{D_4}{l_4}\sum_{j=1}^{N_4} C^{(1)}_{1j4}\Psi_{j4} - \frac{D_2}{l_2}\sum_{j=1}^{N_2} C^{(1)}_{N_2 j2}\Psi_{j2} - \frac{D_3}{l_3}\sum_{j=1}^{N_3} C^{(1)}_{N_3 j3}\Psi_{j3}$$

$$-\frac{A^{(2)}_{11}A^{(3)}_{11}}{A^{(1)}_{11}}\left(\frac{B^{(3)}_{11}}{A^{(3)}_{11}} - \frac{B^{(2)}_{11}}{A^{(2)}_{11}} + T\right)\left(\frac{B^{(3)}_{11}}{A^{(3)}_{11}} - \frac{B^{(2)}_{11}}{A^{(2)}_{11}} + \frac{T}{2}\right)\frac{1}{l_2}\Psi_{14} = 0 \tag{4.45b}$$

$$\frac{A^{(1)}_{55}}{l_1}\sum_{j=1}^{N_1} C^{(1)}_{N_1 j1}W_{j1} - \frac{A^{(2)}_{55}}{l_2}\sum_{j=1}^{N_2} C^{(1)}_{1j2}W_{j2} - \frac{A^{(3)}_{55}}{l_3}\sum_{j=1}^{N_3} C^{(1)}_{1j3}W_{j3} = 0 \tag{4.45c}$$

$$\frac{A^{(4)}_{55}}{l_4}\sum_{j=1}^{N_4} C^{(1)}_{1j4}W_{j4} - \frac{A^{(2)}_{55}}{l_2}\sum_{j=1}^{N_2} C^{(1)}_{N_2 j2}W_{j2} - \frac{A^{(3)}_{55}}{l_3}\sum_{j=1}^{N_3} C^{(1)}_{N_3 j3}W_{j3} = 0 \tag{4.45d}$$

where t_k and l_k, $(k = 1,2,3,4)$ represent the thickness and length of each region. By using these boundary conditions some of the terms of equations (4.44a) and (4.44b) become redundant. To eliminate the redundancy, equations corresponding to $i = 1$ and N_k can be omitted for all regions; hence the combination of (4.44a), (4.44b) and the above sixteen boundary conditions can be represented by a system of eigenvalue equations similar to the one in (4.31), which can be simplified to the form of (4.32).

The solution of the eigenvalue problem of equation (4.32), by a standard eigen solver produces the buckling loads and the associated buckling mode shapes.

4.3. Buckling formulation for a laminated composite beam with multiple delamination

In the previous sections the formulations of a beam-plate having a single across-the-width delamination were presented. However in most situations, when a composite structure is impacted by an external object or due to other phenomena, a number of through-the-thickness delaminations may occur. In a multi-delaminated beam, number, size, position through-the-thickness and along the longitudinal span of the delaminations are some of the parameters that can influence the delamination response of the composite. In this section, we derive the differential quadrature formulation of a beam-plate having multiple delaminations.

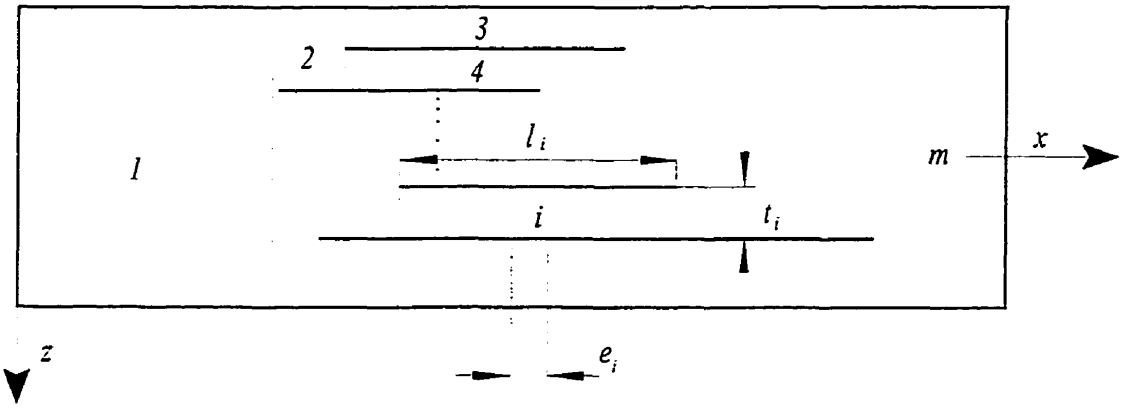

Figure 4.3. Geometry of a beam with multiple delaminations.

Figure (4.3) shows the side view of a laminated composite beam, which is assumed to have a number of delaminations prior to loading. The delaminations are in arbitrary location through-the-thickness, with arbitrary length and position along the beam span. As noted earlier, the sections before and after delamination regions, where the plate is intact are named "base" laminates, and the delaminated regions are referred to as the

"sublaminates". The delaminations divide the beam into m geometrically continuous regions (shown in the figure as doted lines). t_i and l_i are the thickness and length of each region, respectively. The position of each region along the beam span is defined by e_i. The beam is under an axial compressive load. Using the first order shear deformation theory to treat each region as a separate beam, the governing equilibrium equations corresponding to each region can be written as:

$$D_k \psi_{k,xx} - k_s A_{55}^{(k)} \left(\psi_k + w_{k,x}\right) = 0 \qquad (4.46a)$$

$$k=1,2,\ldots,m$$

$$k_s A_{55}^{(k)} \left(\psi_k + w_{k,x}\right)_{,x} - P_k w_{k,xx} = 0 \qquad (4.46b)$$

where w_k, ψ_k and P_k are transverse deflection, transverse rotation and the resulting compressive force of the k^{th} region, $A_{55}^{(k)}$ and D_k are the stiffness of each region as defined in (4.34) and (4.35). The boundary conditions for a multiply delaminated beam with clamped ends consist of the in-plane, transverse, continuity and compatibility conditions given by:

at x=0 $\qquad P_1 = -P \qquad w_1 = \psi_1 = 0 \qquad (4.47a)$

at x=L $\qquad P_m = -P \qquad w_m = \psi_m = 0 \qquad (4.47b)$

At the delaminated edges, the geometric boundary conditions consist of vertical deformation and rotation compatibility equations as:

$$w_i = w_j = \ldots = w_k \qquad (4.47c)$$

$$\psi_i = \psi_j = \ldots = \psi_k \qquad (4.47d)$$

where $i,j,...,k$ are the region numbers surrounding a crack tip.

The other boundary conditions at delamination fronts consist of the in-plane force, shear force and moment equations as follow:

$$P_i - P_j - \cdots - P_k = 0 \tag{4.47e}$$

$$Q_i - Q_j - \cdots - Q_k - \left(P_i w_{i,x} - P_j w_{j,x} - \cdots - P_k w_{k,x}\right) = 0 \tag{4.47f}$$

$$M_i - M_j - \cdots - M_k + P_i z_i + P_j z_j + \cdots + P_k z_k = 0 \tag{4.47g}$$

where z is the distance between the mid-plane of each region and the appropriate moment point. Shear force Q and moment M are defined by (4.33) and (4.19a) for each region, respectively.

In order to solve for the buckling load, the axial compressive load P in (4.47f, g) should be eliminated. To do this, one can combine the strain compatibility equation for the regions between delaminations, the relation between the loads at the critical buckling state given by (4.39) and kinematic relations of (4.47c-d). This results in a series of equations such as those given in (4.43a,b).

Applying the differential quadrature technique to the differential equilibrium equations of all the regions results in a system of discrete algebraic equations as:

$$\frac{D_k}{l_k^{\,2}} \sum_{j=1}^{N_k} C_{ijk}^{(2)} \Psi_{jk} - k_s A_{55}^{(k)} \left(\delta_{ij} \Psi_{jk} + \frac{1}{l_k} \sum_{j=1}^{N_k} C_{ijk}^{(1)} W_{jk} \right) = 0 \qquad \begin{matrix} i = 1,\ldots,N \\ k = 1,\ldots,m \end{matrix} \tag{4.48a}$$

$$\sum_{j=1}^{N_k} C_{ijk}^{(1)} \Psi_{jk} + \frac{1}{l_k} \sum_{j=1}^{N_k} C_{ijk}^{(2)} W_{jk} = \left(\frac{P}{k_s A_{55}^{(1)} l_k} \right) \sum_{j=1}^{N_k} C_{ijk}^{(2)} W_{jk} \qquad \begin{matrix} i = 1,\ldots,N \\ k = 1,\ldots,m \end{matrix} \qquad (4.48b)$$

Applying the differential quadrature to the boundary conditions, together with the above equations produce a system of eigenvalue equations. This system can be solved in the same way as presented in the previous sections to give the delamination buckling loads and corresponding modal shapes.

In our case studies we also consider a model where all the delaminations have equal lengths (Figure (4.4)). Some researchers like Suemasu (1993) and Lim and Parsons (1993) have used such models. For this case the number of regions, and therefore, the efforts required for formulation and solving the problem is reduced extensively. The number of regions is reduced to *k+3* where *k* is the number of delaminations.

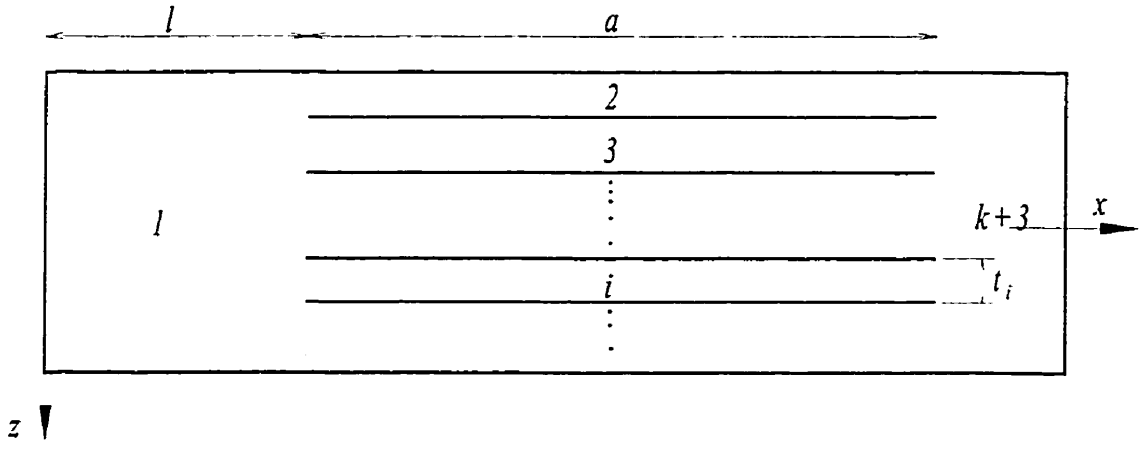

Figure 4.4. Geometry of a beam having multiple delaminations with equal length.

4.4. Delamination buckling formulation for a general laminated composite plate

In this part the differential quadrature formulation of a composite laminated plate containing a single elliptical delamination will be presented (Figure 4.5).

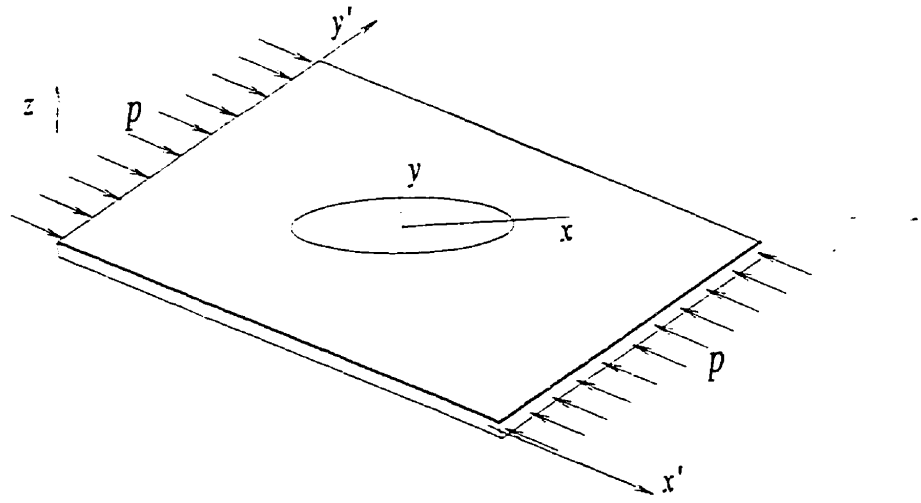

Figure 4.5. Delaminated plate under axial compression.

The geometry of the problem is shown in Figure 4.6. As shown, the global coordinate system $x'-y'-z'$ is oriented such that the x'-axis is along the loading direction. The laminate is under a compressive strain ε_x (a positive value indicates a tensile strain) in the x' direction. The delamination, which is located at the center of the plate, exists prior to the loading. The delamination, which is assumed to be thin, divides the laminate into two regions. The upper thin part, delaminated from the laminate is referred to as the "sublaminate" and the remaining part is known as the "base" laminate. From the top view the delaminated part is an ellipse with the principal axis of x and y and the major and minor semi-axes length of a and b. The local coordinate system x-y is rotated at an angle θ, which is called as sublaminate angle, with respect to the load

direction x'. γ is the angle of fiber orientation in each lamina with respect to x'. The thickness of the base laminate is considered to be much larger than the sublaminate, so the sublaminate boundaries can not be bent.

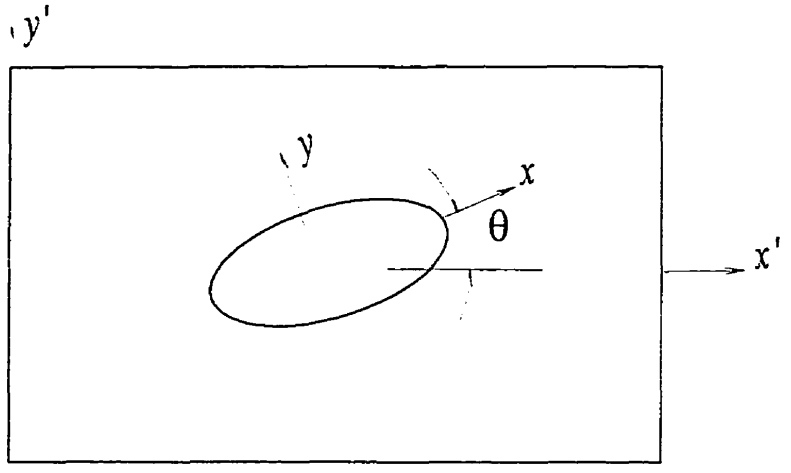

Figure 4.6. Geometry of a plate with elliptical delamination.

4.4.1. Equilibrium equations

In this study the classical laminated plate theory (CLPT) has been used to formulate the plate problem. This will result in differential equilibrium equations with derivatives up to forth order. Using CLPT, the differential equilibrium equations for a plate can be written as (Whitney (1987)):

$$N_{x,x} + N_{xy,y} = 0 \tag{4.49a}$$

$$N_{xy,x} + N_{y,y} = 0 \tag{4.49b}$$

$$M_{x,xx} + M_{xy,xy} + M_{y,yy} + N_x \cdot w_{,xx} + 2N_{xy} \cdot w_{,xy} + N_y \cdot w_{,yy} = 0 \tag{4.49c}$$

where w represents the out of plane deflection, N_x, N_y, N_{xy}, M_x, M_y, M_{xy} are the resultant forces and moments obtained by:

$$(N_x, N_y, N_{xy}) = \int (\sigma_x, \sigma_y, \sigma_{xy}) \cdot dz \tag{4.50a}$$

$$(M_x, M_y, M_{xy}) = \int (\sigma_x, \sigma_y, \sigma_{xy}) \cdot z \cdot dz \tag{4.50b}$$

Substituting stress-strain and strain-displacement relations in (4.49a) to (4.49c) yields the following equilibrium equations in terms of in-plane displacements u and v and out of plane deflection w

$$A_{11}u_{,xx} + 2A_{16}u_{,xy} + A_{66}u_{,yy} + A_{16}v_{,xx} + (A_{12} + A_{66})v_{,xy} + A_{26}v_{,yy}$$

$$- B_{11}w_{,xxx} - 3B_{16}w_{,xxy} - (B_{12} + 2B_{66})w_{,xyy} - B_{26}w_{,yyy} = 0 \tag{4.51a}$$

$$A_{16}u_{,xx} + (A_{12} + A_{66})u_{,xy} + A_{26}u_{,yy} + A_{66}v_{,xx} + 2A_{26}v_{,xy} + A_{22}v_{,yy}$$

$$- B_{16}w_{,xxx} - (B_{12} + 2B_{66})w_{,xxy} - 3B_{26}w_{,xyy} - B_{22}w_{,yyy} = 0 \tag{4.51b}$$

$$D_{11}w_{,xxxx} + 4D_{16}w_{,xxxy} + 2(D_{12} + 2D_{66})w_{,xxyy} + 4D_{26}w_{,xyyy} + D_{22}w_{,yyyy}$$

$$- B_{11}u_{,xxx} - 3B_{16}u_{,xxy} - (B_{12} + 2B_{66})u_{,xyy} - B_{26}u_{,yyy} \tag{4.51c}$$

$$- B_{16}v_{,xxx} - (B_{12} + 2B_{66})v_{,xxy} - 3B_{26}v_{,xyy} - B_{22}v_{,yyy} = N_x w_{,xx} + 2N_{xy}w_{,xy} + N_y w_{,yy}$$

where A, B and D are the stiffness terms. The first two equations are concerned with the in-plane equilibrium while the last one represents the buckling equation. A close look at equation (4.51c) indicates that the coefficients of in-plane displacements u and v are those which are only associated with the bending-stretching coupling terms. So, if one can eliminate these terms from (4.51c) then, one can determine the buckling strains by only one equation (i.e., 4.51c). This will dramatically reduce the computational efforts.

For symmetric delaminated plates, B_{ij}=0 and thus, the extension and bending are uncoupled. One therefore, only needs to solve equation (4.51c). But in general, the delaminated regions do not possess mid-plane symmetry (even if the laminate is symmetric), and therefore, bending-stretching coupling exists. In this case, some researchers have recommended the reduced bending stiffness approximation (Davidson 1991). In this approach, the effect of coupling terms B_{ij}, is implicitly accounted for by reducing the flexural stiffness matrix such as:

$$[\overline{D}]=[D]-[B][A]^{-1}[B] \tag{4.52}$$

The accuracy of the reduced bending stiffness approximation in analyzing the delamination buckling of composite laminates was examined by Dost et al (1988). They performed finite element analysis on delaminated composite plates and found that the results with reduced bending stiffness agree well with those with the usual bending and bending-stretching stiffness matrices. Therefore the delamination buckling equations of (4.51a-c) reduce to the following form:

$$\overline{D}_{11}w_{,xxxx}+4\overline{D}_{16}w_{,xxxy}+2(\overline{D}_{12}+2\overline{D}_{66})w_{,xxyy} \tag{4.53}$$

$$+4\overline{D}_{26}w_{,xyyy}+\overline{D}_{22}w_{,yyyy}=N_x w_{,xx}+2N_{xy}w_{,xy}+N_y w_{,yy}$$

4.4.2. Loading and Boundary Conditions

The laminate is loaded by a far field strain $\varepsilon_{x'}$ in the x' direction (where a positive sign refers to a tensile strain). Due to the Poisson effect, ν_{lam}, a strain with the magnitude of $-\nu_{lam}\varepsilon_{x'}$ acts in the y' direction. The in-plane stresses acting on the sublaminate region can be expressed based on the coordinates x-y. The problem can be reduced to an elliptical plate under axial loads as shown in Figure (4.7).

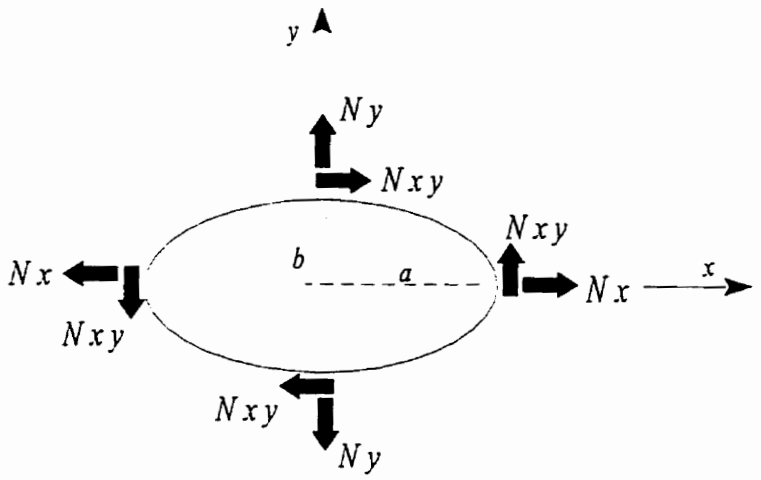

Figure 4.7. Acting forces on the sublaminate.

Therefore the in-plane stress resultant can be expressed as

$$N_x = A_{11}\varepsilon_x + A_{12}\varepsilon_y + A_{16}\varepsilon_{xy} \tag{4.54a}$$

$$N_y = A_{12}\varepsilon_x + A_{22}\varepsilon_y + A_{26}\varepsilon_{xy} \tag{4.54b}$$

$$N_{xy} = A_{16}\varepsilon_x + A_{26}\varepsilon_y + A_{66}\varepsilon_{xy} \tag{4.54c}$$

where the strains are expressed with respect to the sublaminate coordinates. These strains can be related to the laminate strain $\varepsilon_{x'}$, its Poisson's ratio ν_{lam} and the sublaminate angle θ (see Figure 4.6) by:

$$\varepsilon_x = (\cos^2\theta - \nu_{lam}\sin^2\theta)\cdot\varepsilon_{x'} \tag{4.55a}$$

$$\varepsilon_y = (\sin^2\theta - \nu_{lam}\cos^2\theta)\cdot\varepsilon_{x'} \tag{4.55b}$$

$$\varepsilon_{xy} = -\tfrac{1}{2}(1+\nu_{lam})\cdot\sin 2\theta\cdot\varepsilon_{x'} \tag{4.55c}$$

The boundary conditions are assumed to be clamped around its perimeter, which can be represented by:

$$w = 0 \tag{4.56a}$$

$$w_{,n} = 0 \tag{4.56b}$$

where n is the normal direction to the boundary edges. Using directional derivatives, equation (4.56b) can be written as

$$w_{,x}\cdot n_x + w_{,y}\cdot n_y = 0 \tag{4.57}$$

in which n_x and n_y are direction cosines of n.

Therefore, the buckling problem of a composite laminated plate under compressive axial load having a thin elliptical delamination can be represented by the buckling of a symmetric elliptical composite laminated plate, with clamped boundary under general in-plane load. In order to solve the problem by DQM, we recall that DQM inherently can only consider domains with boundaries parallel to the coordinate axes. This indicates that the domain for such two dimensional problems should be in the form of a rectangle. Thus, in order to solve the elliptical domain, one should map the actual domain into an equivalent computational domain in the form of a rectangle. For this, we use the method suggested by Bert and Malik (1996b) in which the quadrature rules are reformulated by mapping of a general curvilinear region into a square domain.

By using the mapping scheme introduced in Chapter 3, one can transfer the elliptical domain into the equivalent computational domain with the dimensions [-1,1]. Then applying the DQM to the equation (4.53) yields

$$\overline{D}_{11}\sum_{k=1}^{N_\xi} C_{ik}^{(4)} W_{kj} + 4\overline{D}_{16}\beta \sum_{k=1}^{N_\xi} C_{ik}^{(3)} \sum_{m=1}^{N_\eta} C_{jm}^{(1)} W_{km} + 2(\overline{D}_{12} + 2\overline{D}_{66})\beta^2 \sum_{k=1}^{N_\xi} C_{ik}^{(2)} \sum_{m=1}^{N_\eta} C_{jm}^{(2)} W_{km} +$$

$$4\overline{D}_{26}\beta^3 \sum_{k=1}^{N_\xi} C_{ik}^{(1)} \sum_{m=1}^{N_\eta} C_{jm}^{(3)} W_{km} + \overline{D}_{22}\beta^4 \sum_{k=1}^{N_\eta} C_{jk}^{(4)} W_{ik} = \qquad \begin{matrix} i = 1,\ldots,N_\xi \\ j = 1,\ldots,N_\eta \end{matrix} \qquad (4.58)$$

$$\lambda \cdot a^2 \left(\alpha_x \sum_{k=1}^{N_\xi} C_{ik}^{(2)} W_{kj} + 2\alpha_{xy}\beta \sum_{k=1}^{N_\xi} C_{ik}^{(1)} \sum_{m=1}^{N_\eta} C_{jm}^{(1)} W_{km} + \alpha_y \beta^2 \sum_{k=1}^{N_\eta} C_{jk}^{(2)} W_{ik} \right)$$

Note that N_ξ and N_η in the above are the number of grid points in the ξ and η directions of the computational rectangular domain, respectively (see Figure 4.8). W_{ij} is the deflection of the grid point laying on the intersection of the i^{th} point in the ξ-direction and j^{th} point in the η-direction. $\beta = a/b$, $\lambda = \varepsilon_x$, and

$$\alpha_l = \frac{N_l}{\varepsilon_{x'}} \qquad l = x, y, xy \tag{4.59}$$

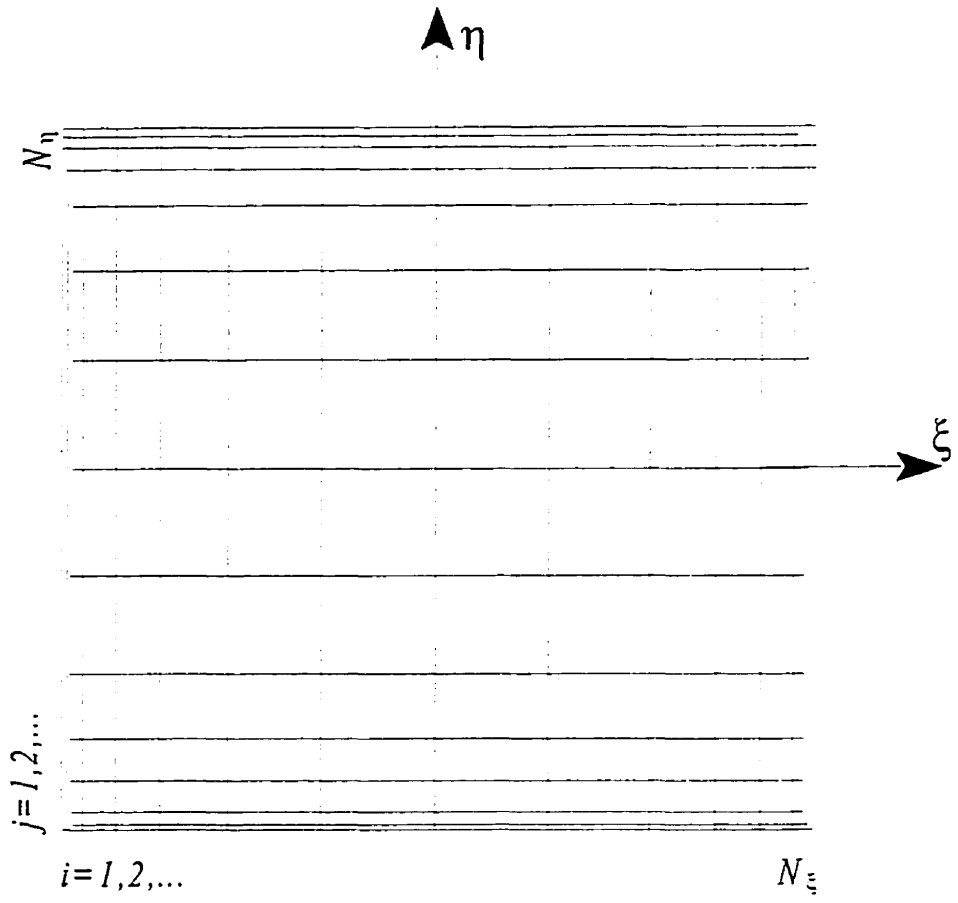

Figure 4.8. The sampling points in the transformed domain.

The differential quadrature representation of the boundary conditions of (4.56a) and (4.57) can be written as

$$W_{1j} = W_{N_\xi j} = W_{i1} = W_{iN_\eta} = 0 \qquad \begin{matrix} i = 1,\ldots,N_\xi \\ j = 2,\ldots,N_\eta - 1 \end{matrix} \tag{4.60a}$$

$$\cos\phi \cdot \sum_{k=1}^{N_\xi} C_{ik}^{(1)} W_{kl} + \sin\phi \cdot \beta \cdot \sum_{k=1}^{N_\eta} C_{lk}^{(1)} W_{ik} = 0 \qquad \begin{matrix} i = 2,\ldots,N_\xi - 1 \\ l = 2, N_\eta - 1 \end{matrix} \tag{4.60b}$$

$$\cos\phi \cdot \sum_{k=1}^{N_\xi} C_{lk}^{(1)} W_{kj} + \sin\phi \cdot \beta \sum_{k=1}^{N_\eta} C_{jk}^{(1)} W_{lk} = 0 \qquad \begin{matrix} j = 3,\ldots,N_\eta - 2 \\ l = 2, N_\xi - 1 \end{matrix} \tag{4.60c}$$

where ϕ is the angle between normal to the plate boundary and the x-axis.

By using these boundary conditions, some of the terms of equations (4.58) become redundant. To eliminate this redundancy, equations corresponding to the first and second points around the boundary (i.e. $i = 1,2,N_\xi - 1,N_\xi$ and $j = 1,2,N_\eta - 1,N_\eta$) can be omitted. Therefore, the combination of (4.58) and (4.60) can be represented by a system of eigenvalue equations such as the one represented by equation (4.15). Reducing this system of equations to the one with only $\{W_i\}$ as unknowns results in eigenvalue problem in the form of equation (4.16).

The solution of this eigenvalue problem by a standard eigen solver produces the buckling strains and the associated buckling mode shapes.

CHAPTER 5

POSTBUCKLING ANALYSIS

5.1. Introduction

As stated previously, delamination buckling has been a major concern in compressive applications of composite materials. Structures such as beams or plates, even in the delaminated form, have the capability to carry loads beyond their buckling limits. Such damaged structures may undergo a large amount of postbuckling deformation before their final failure. Also, it has been known that introducing a small imperfection may change the buckling load and postbuckling response dramatically. Consequently, the problem of postbuckling analysis of imperfect composite laminates having delaminations has been the focus of several investigations, and as a result several methodologies and solutions have been developed. This class of problems is often treated with numerical methods such as finite elements or finite differences combined with a nonlinear solution strategy.

In this chapter, the differential quadrature method combined with an arc-length strategy is used to model the postbuckling analysis of imperfect laminated composite beams having a single or multiple delaminations. Here the contact effect between the delaminated parts has been neglected. Also, the delamination growth due to the opening of the delaminated sections under the compressive load will not be considered in the analysis. First, the arc-length strategy employed in this study will be explained with the aid of an example to show the effectiveness of the method. In this example, DQM will be applied for the first time to analyze the postbuckling response of laminated plates. Then the differential quadrature formulation of imperfect laminated composite beam having a single or multiple delaminations will be presented.

5.2. Arc-length method

In the past few years a great deal of effort has been put toward improving the nonlinear solution schemes used in treating various nonlinear stability of structural responses. The conventional Newton-Raphson iterative algorithms, which have been used extensively to solve nonlinear problems, develop difficulties when tracing the points near buckling or limit points of the equilibrium path. In these algorithms load controls the path; that is, the load is incremented by constant values and the iteration is performed on the nodal displacements, only. In these algorithms, the solution often halts near the limit points. To resolve this problem, several strategies have been suggested by researchers (see for example Clarke and Hancock (1990)). In some of the suggested methods, the iterative procedure is controlled by displacement, where a constant displacement increment or a combination of, controls the equilibrium path (see Haisler and Stricklin (1977), Batoz (1979) and Powell and Simons (1981)).

In addition to the above methods, there is another strategy that uses a constraint to limit the load increment. The method, which was introduced by Wempner (1971) and by Riks (1979) independently, uses the arc length of the load-displacement path as the constraint equation, and therefore is referred to as the "arc-length" method. The method was modified by Crisfield (1981, 1983), thus being referred to as the "modified Riks" method.

There also exist other types of constraint equations such as the "constant external work". Clarke and Hancock (1990) performed a detailed study on the available incremental iterative strategies for the nonlinear analysis.

5.2.1. Arc-length formulation

An arc-length algorithm based on the Forde and Stiemer (1987) work is used to solve the nonlinear system of equations resulting from the application of DQM. The governing system of equilibrium equations is represented by:

$$\mathbf{F}(\mathbf{x}) = \lambda \mathbf{P} \tag{5.1}$$

where **F** is a nonlinear function of unknown displacements **x**, **P** is the fixed load vector and λ is the loading factor, which controls the applied load (Figure 5.1).

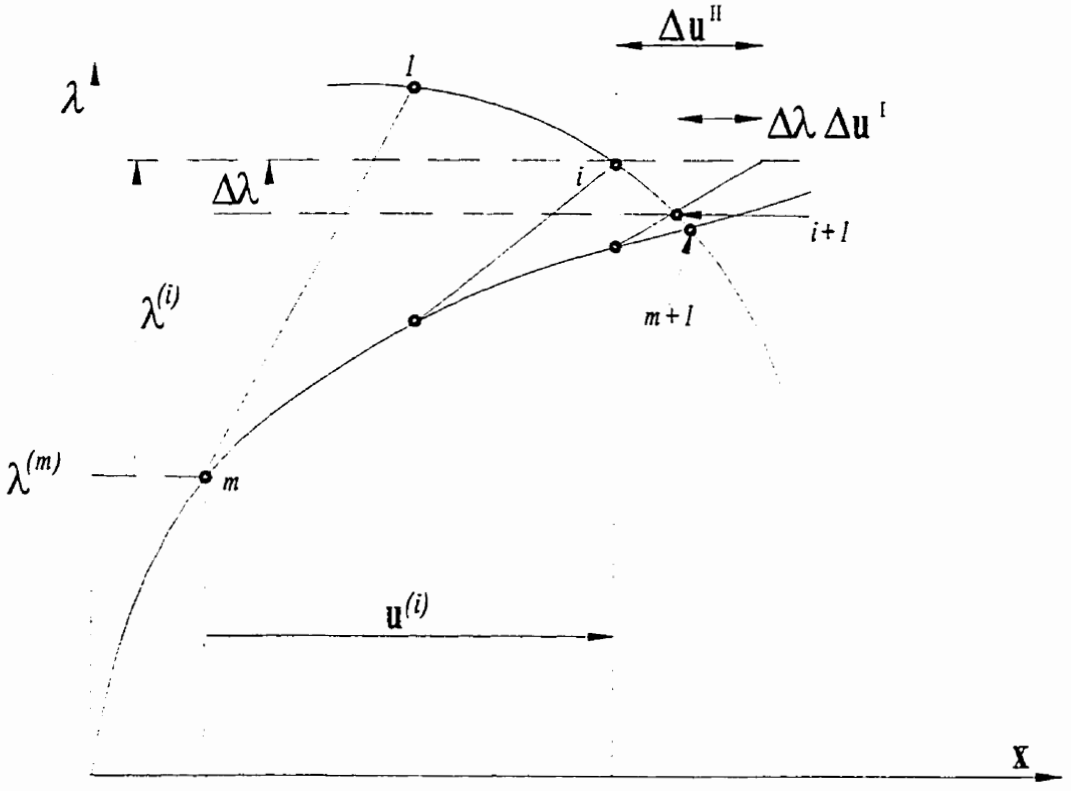

Figure 5.1. Arc-length incremental scheme.

Using a Newton incremental iterative solution, one can represent each iteration of the equilibrium relation by the following expression:

$$\mathbf{K}^{(i)}\Delta\mathbf{u} + \mathbf{F}(\mathbf{x}^{(i)}) = \lambda\mathbf{P} \tag{5.2}$$

where $\mathbf{K}$ is the first derivative of $\mathbf{F}$ with respect to $\mathbf{x}$ (or gradient of the force/displacement relationship), and

$$\Delta\mathbf{u} = \mathbf{x}^{(i+1)} - \mathbf{x}^{(i)} \tag{5.3}$$

The main difference between the arc-length method and the Newton technique is that in the Newton method the variables are unknown vector $\mathbf{x}$, while in the former procedure, the load factor λ is considered as a variable, too. Writing λ and $\mathbf{x}$ of equations (5.2), and (5.3) in incremental forms

$$\lambda^{(i+1)} = \lambda^{(m)} + \lambda^{(i)} + \Delta\lambda \tag{5.4a}$$

$$\mathbf{x}^{(i+1)} = \mathbf{x}^{(m)} + \mathbf{u}^{(i)} + \Delta\mathbf{u} \tag{5.4b}$$

where *m* represents a point on the load-displacement curve (see figure 5.1). Replacing λ and $\mathbf{x}$ in (5.2) by equations (5.4a,b) yields:

$$\mathbf{K}^{(i)}\Delta\mathbf{u} = (\lambda^{(m)} + \lambda^{(i)} + \Delta\lambda)\mathbf{P} - \mathbf{F}(\mathbf{x}^{(i)}) \tag{5.5}$$

The incremental displacement $\Delta\mathbf{u}$ can be written as:

$$\Delta\mathbf{u} = \Delta\lambda\Delta\mathbf{u}^{\mathrm{I}} + \Delta\mathbf{u}^{\mathrm{II}} \tag{5.6}$$

where

$$\mathbf{K}^{(i)}\Delta\mathbf{u}^{\mathrm{I}} = \mathbf{P} \tag{5.7a}$$

$$\mathbf{K}^{(i)}\Delta\mathbf{u}^{\mathrm{II}} = (\lambda^{(m)} + \lambda^{(i)})\mathbf{P} - \mathbf{F}(\mathbf{x}^{(i)}) \tag{5.7b}$$

The first term in equation (5.6) is due to a unit load vector multiplied by $\Delta\lambda$ (equation 5.7a) and the second term is due to the unbalanced load (equation 5.7b). In order to find the solution we need another equation to account for the unknown $\Delta\lambda$. For this, a general scalar equation is used to constrain the load and displacement increments. This equation, known as the arc-length equation can be written as:

$$\Delta l^2 = \lambda^{(i)^2} + \beta^2 \mathbf{u}^{(i)^T} \cdot \mathbf{u}^{(i)} \tag{5.8}$$

β is a scaling parameter (with units of displacement) to ensure the correct scale. Equation (5.8) holds for every substep in the iterations. When β =1 the method is known as "spherical arc-length", which was originally proposed by Crisfield (1981). However, using this equation results in a quadratic equation. The selection of one of the roots of this equation, which may also have one or two imaginary roots, needs additional computational efforts. In our investigation, we have used the method of the "explicit iteration on spheres" suggested by Forde and Stiemer (1987), which gives exactly the same results as those reported by Crisfield and yet, it does not use a quadratic equation. They used an iterative procedure to derive $\Delta\lambda$ as:

$$\Delta\lambda = \frac{R^{(i)} - \mathbf{u}^{(i)^T}\Delta\mathbf{u}^{\mathrm{II}}}{\lambda^{(i)} + \mathbf{u}^{(i)^T}\Delta\mathbf{u}^{\mathrm{I}}} \tag{5.9}$$

where, R is a scalar residual. Using equation (5.7) and (5.9) one can obtain $\Delta\mathbf{u}$. The solution is updated based on equations (5.4) and (5.5) until the specified convergence is reached. The procedure continues up to the desired load. At the beginning of each load step, an initial load increment $\lambda^{(1)}$ should be chosen to ensure the efficiency of the algorithm. Using a large load step may cause slow or no convergence, while a small load step may cost deficiency of the method. Moreover, using an automatic load increment strategy mostly depends on the nature of the problem, and therefore, makes it difficult to specify an exact formula for the load incrementation. In this study the following formula as suggested by Ramm (1981), is used for the automatic load incrementation:

$$\lambda^{(1)} = \bar{\lambda}^{(1)} \cdot \sqrt{\frac{J_d}{J_{m-1}}} \tag{5.10}$$

where J_d is the desired number of iterations for convergence, typically between 3 to 5, J_{m-1} is the actual number of iterations required for the m-1th load step and $\bar{\lambda}^{(1)}$ is the load increment for the m-1th load step.

5.2.2. Postbuckling analysis of a laminated composite plate

In this part the DQM and the arc-length method are combined to produce a numerical scheme for solving the nonlinear postbuckling equations of composite structures. To the author's best knowledge, there has been no attempt in the past to analyze the postbuckling response of composite plates by DQM. In order to examine the applicability of the DQM to the postbuckling analysis of delaminated structures we will first apply it to the postbuckling analysis of a laminated composite plate.

A thin composite laminated plate under compressive load is shown in Figure 5.2. Geometrical imperfections in the form of out of plane deflection are assumed to exist prior to the loading.

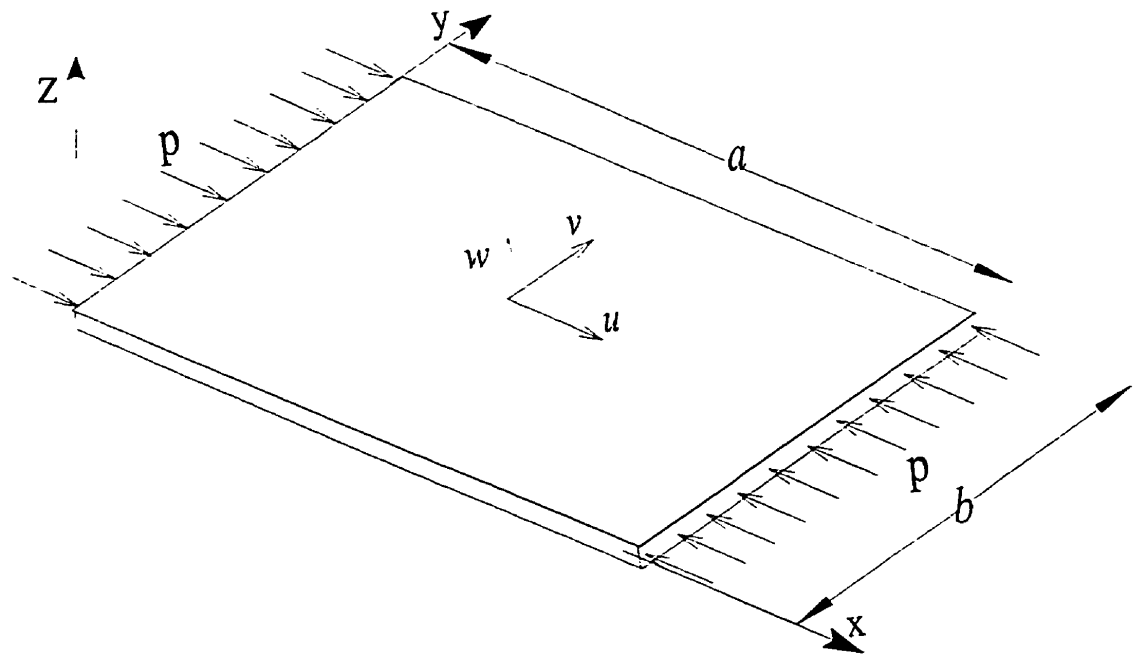

Figure 5.2. Geometry of the plate and the applied load.

In this study, the nonlinear von Karman strain-displacement relations are used to express the in-plane strains of the plate. Moreover, the distribution of the through-the-thickness strains is assumed to be based on the Kirchhoff-Love plate theory. These assumptions result in the following strain-displacement relations:

$$\varepsilon_x = u_{,x} + \tfrac{1}{2} w_{,x}^{\,2} + w_{,x}\overline{w}_{,x} + z\kappa_x \tag{5.11a}$$

$$\varepsilon_y = v_{,y} + \tfrac{1}{2} w_{,y}^{\,2} + w_{,y}\overline{w}_{,y} + z\kappa_y \tag{5.11b}$$

$$\gamma_{xy} = u_{,y} + v_{,x} + w_{,x}w_{,y} + w_{,x}\overline{w}_{,y} + w_{,y}\overline{w}_{,x} + z\kappa_{xy} \tag{5.11c}$$

where u, v and w represent the displacements of any point on the mid-plane along the x-, y- and z-directions, respectively; $\overline{w}$ is the imperfection function and κ are the curvatures, defined as:

$$\kappa_x = -w_{,xx}\,; \qquad \kappa_y = -w_{,yy}\,; \qquad \kappa_{xy} = -2w_{,xy} \tag{5.12}$$

The differential equilibrium equations of a thin laminated plate can be expressed in the following forms:

$$N_{x,x} + N_{xy,y} = 0 \tag{5.13a}$$

$$N_{xy,x} + N_{y,y} = 0 \tag{5.13b}$$

$$M_{x,xx} + 2M_{xy,xy} + M_{y,yy} + N_x(w+\overline{w})_{,xx} + 2N_{xy}(w+\overline{w})_{,xy} + N_y(w+\overline{w})_{,yy} = 0 \tag{5.13c}$$

where N and M represent the resulting forces and moments, respectively. The relation between the forces and strains in classical laminated theory can be expressed in vector and matrix forms by

$$\mathbf{N} = \mathbf{A}\varepsilon + \mathbf{B}\kappa \tag{5.14a}$$

$$\mathbf{M} = \mathbf{B}\varepsilon + \mathbf{D}\kappa \tag{5.14b}$$

where $\mathbf{N}$ and $\mathbf{M}$ are the force and moment vectors, respectively, and

$$(A_{ij}, B_{ij}, D_{ij}) = \int_{-h/2}^{h/2} Q_{ij}(1, z, z^2)\,dz \qquad i, j = 1,2,6 \tag{5.15}$$

Substituting (5.11) and (5.12) in (5.13) and using (5.14), the differential equations of equilibrium for a symmetric laminate can be expressed in terms of displacements as follows:

$$A_{11}\left(u_{,xx}+w_{,xx}\overline{w}_{,x}+w_{,x}(w_{,xx}+\overline{w}_{,xx})\right)+A_{12}\left(v_{,xy}+w_{,xy}\overline{w}_{,y}+w_{,y}(w_{,xy}+\overline{w}_{,xy})\right)+$$

$$A_{66}\left(u_{,yy}+v_{,xy}+w_{,x}(w_{,yy}+\overline{w}_{,yy})+w_{,yy}\overline{w}_{,x}+w_{,xy}(w_{,y}+\overline{w}_{,y})+w_{,y}\overline{w}_{,xy}\right)=0 \tag{5.16a}$$

$$A_{12}\left(u_{,xy}+w_{,xy}\overline{w}_{,x}+w_{,x}(w_{,xy}+\overline{w}_{,xy})\right)+A_{22}\left(v_{,yy}+w_{,yy}\overline{w}_{,y}+w_{,y}(w_{,yy}+\overline{w}_{,yy})\right)+$$

$$A_{66}\left(u_{,xy}+v_{,xx}+w_{,y}(w_{,xx}+\overline{w}_{,xx})+w_{,xx}\overline{w}_{,y}+w_{,xy}(w_{,x}+\overline{w}_{,x})+w_{,x}\overline{w}_{,xy}\right)=0 \tag{5.16b}$$

$$D_{11}w_{,xxxx}+2(D_{12}+2D_{66})w_{,xxyy}+D_{22}w_{,yyyy}+$$

$$\left[A_{11}\left(u_{,x}+\tfrac{1}{2}w_{,x}^{\,2}+w_{,x}\overline{w}_{,x}\right)+A_{12}\left(v_{,y}+\tfrac{1}{2}w_{,y}^{\,2}+w_{,y}\overline{w}_{,y}\right)\right]\cdot(w_{,xx}+\overline{w}_{,xx})+$$

$$2A_{66}\left(u_{,y}+v_{,x}+(w_{,x}+\overline{w}_{,x})\cdot(w_{,y}+\overline{w}_{,y})-\overline{w}_{,x}\overline{w}_{,y}\right)\cdot(w_{,xy}+\overline{w}_{,xy})+ \tag{5.16c}$$

$$\left[A_{12}\left(u_{,x}+\tfrac{1}{2}w_{,x}^{\,2}+w_{,x}\overline{w}_{,x}\right)+A_{22}\left(v_{,y}+\tfrac{1}{2}w_{,y}^{\,2}+w_{,y}\overline{w}_{,y}\right)\right]\cdot(w_{,yy}+\overline{w}_{,yy})=0$$

For a rectangular plate, simply supported along its edges, the boundary conditions are expressed by:

$$\text{at } x=0,a \qquad w=0, \quad M_x=0, \quad N_{xy}=0, \quad N_x=P \tag{5.17a}$$

$$\text{at } y=0,b \qquad w=0, \quad M_y=0, \quad N_{xy}=0, \quad N_y=0 \tag{5.17b}$$

Applying DQM to (5.16) result in:

$$A_{11}\left\{a\sum_{k=1}^{n_x}B_{ik}^{(2)}U_{kj}+\left(\sum_{k=1}^{n_x}B_{ik}^{(2)}W_{kj}\right)\left(\overline{W}_{.X}\right)_{ij}+\left(\sum_{k=1}^{n_x}B_{ik}^{(1)}W_{kj}\right)\left[\left(\sum_{k=1}^{n_x}B_{ik}^{(2)}W_{kj}\right)+\left(\overline{W}_{.XX}\right)_{ij}\right]\right\}+$$

$$A_{12}\beta^2\left\{b\sum_{k=1}^{n_x}B_{ik}^{(1)}\sum_{m=1}^{n_y}C_{jm}^{(1)}V_{km}+\left(\sum_{k=1}^{n_x}B_{ik}^{(1)}\sum_{m=1}^{n_y}C_{jm}^{(1)}W_{km}\right)\left(\overline{W}_{.Y}\right)_{ij}+\left(\sum_{k=1}^{n_y}C_{jk}^{(1)}W_{ik}\right)\cdot\right. \tag{5.18a}$$

$$\left.\left[\left(\sum_{k=1}^{n_x}B_{ik}^{(1)}\sum_{m=1}^{n_y}C_{jm}^{(1)}W_{km}\right)_{ij}+\left(\overline{W}_{.XY}\right)_{ij}\right]\right\}+A_{66}\beta^2\left\{a\sum_{k=1}^{n_y}C_{jk}^{(2)}U_{ik}+b\sum_{k=1}^{n_x}B_{ik}^{(1)}\sum_{m=1}^{n_y}C_{jm}^{(1)}V_{km}+\right.$$

$$\left(\sum_{k=1}^{n_x}B_{ik}^{(1)}W_{kj}\right)\left[\left(\sum_{k=1}^{n_y}C_{jk}^{(2)}W_{ik}\right)+\left(\overline{W}_{.YY}\right)_{ij}\right]+\left(\sum_{k=1}^{n_y}C_{jk}^{(2)}W_{ik}\right)\left(\overline{W}_{.X}\right)_{ij}+$$

$$\left.\left(\sum_{k=1}^{n_x}B_{ik}^{(1)}\sum_{m=1}^{n_y}C_{jm}^{(1)}W_{km}\right)\left[\left(\sum_{k=1}^{n_y}C_{jk}^{(1)}W_{ik}\right)+\left(\overline{W}_{.Y}\right)_{ij}\right]+\left(\sum_{k=1}^{n_y}C_{jk}^{(1)}W_{ik}\right)\left(\overline{W}_{.XY}\right)_{ij}\right\}=0$$

$$\frac{A_{12}}{\beta^2}\left\{a\sum_{k=1}^{n_x}B_{ik}^{(1)}\sum_{m=1}^{n_y}C_{jm}^{(1)}U_{km}+\left(\sum_{k=1}^{n_x}B_{ik}^{(1)}\sum_{m=1}^{n_y}C_{jm}^{(1)}W_{km}\right)\left(\overline{W}_{.X}\right)_{ij}+\right.$$

$$\left.\left(\sum_{k=1}^{n_x}B_{ik}^{(1)}W_{kj}\right)\left[\left(\sum_{k=1}^{n_x}B_{ik}^{(1)}\sum_{m=1}^{n_y}C_{jm}^{(1)}W_{km}\right)+\left(\overline{W}_{.XY}\right)_{ij}\right]\right\}+$$

$$A_{22}\left\{b\sum_{k=1}^{n_y}C_{jk}^{(2)}V_{ik}+\left(\sum_{k=1}^{n_y}C_{jk}^{(2)}W_{ik}\right)\left(\overline{W}_{.Y}\right)_{ij}+\left(\sum_{k=1}^{n_y}C_{jk}^{(1)}W_{ik}\right)\left[\left(\sum_{k=1}^{n_y}C_{jk}^{(2)}W_{ik}\right)+\left(\overline{W}_{.YY}\right)_{ij}\right]\right\}+ \tag{5.18b}$$

$$\frac{A_{66}}{\beta^2}\left\{a\sum_{k=1}^{n_x}B_{ik}^{(1)}\sum_{m=1}^{n_y}C_{jm}^{(1)}U_{km}+b\sum_{k=1}^{n_x}B_{ik}^{(2)}V_{kj}+\left(\sum_{k=1}^{n_y}C_{jk}^{(1)}W_{ik}\right)\left[\left(\sum_{k=1}^{n_x}B_{ik}^{(2)}W_{kj}\right)+\left(\overline{W}_{.XX}\right)_{ij}\right]+\right.$$

$$\left(\sum_{k=1}^{n_x}B_{ik}^{(2)}W_{kj}\right)\left(\overline{W}_{.Y}\right)_{ij}+\left(\sum_{k=1}^{n_x}B_{ik}^{(1)}\sum_{m=1}^{n_y}C_{jm}^{(1)}W_{km}\right)\left[\left(\sum_{k=1}^{n_x}B_{ik}^{(1)}W_{kj}\right)+\left(\overline{W}_{.X}\right)_{ij}\right]+$$

$$\left.\left(\sum_{k=1}^{n_x}B_{ik}^{(1)}W_{kj}\right)\left(\overline{W}_{.XY}\right)_{ij}\right\}=0$$

$$D_{11}\left(\sum_{k=1}^{n_x} B_{ik}^{(4)} W_{kj}\right) + 2(D_{12} + 2D_{66})\beta^2\left(\sum_{k=1}^{n_x} B_{ik}^{(2)} \sum_{m=1}^{n_y} C_{jm}^{(2)} W_{km}\right) + D_{22}\beta^4\left(\sum_{k=1}^{n_y} C_{jk}^{(4)} W_{ik}\right) +$$

$$\left\{A_{11}\left[a\sum_{k=1}^{n_x} B_{ik}^{(1)} U_{kj} + \frac{1}{2}\left(\sum_{k=1}^{n_x} B_{ik}^{(1)} W_{kj}\right)^2 + \left(\sum_{k=1}^{n_x} B_{ik}^{(1)} W_{kj}\right)\left(\overline{W}_{,X}\right)_{ij}\right] +\right.$$

$$\left. A_{12}\beta^2\left[b\sum_{k=1}^{n_y} C_{jk}^{(1)} V_{ik} + \frac{1}{2}\left(\sum_{k=1}^{n_y} C_{jk}^{(1)} W_{ik}\right)^2 + \left(\sum_{k=1}^{n_y} C_{jk}^{(1)} W_{ik}\right)\left(\overline{W}_{,Y}\right)_{ij}\right]\right\} \cdot$$

$$\left(\sum_{k=1}^{n_x} B_{ik}^{(2)} W_{kj} + \left(\overline{W}_{,XX}\right)_{ij}\right) + 2A_{66}\beta^2 \cdot \left\{a\sum_{k=1}^{n_y} C_{jk}^{(1)} U_{ik} + b\sum_{k=1}^{n_x} B_{ik}^{(1)} V_{kj} +\right.$$

$$\left.\left(\sum_{k=1}^{n_x} B_{ik}^{(1)} W_{kj} + \left(\overline{W}_{,X}\right)_{ij}\right) \cdot \left(\sum_{k=1}^{n_y} C_{jk}^{(1)} W_{ik} + \left(\overline{W}_{,Y}\right)_{ij}\right) - \left(\overline{W}_{,X}\right)_{ij} \cdot \left(\overline{W}_{,Y}\right)_{ij}\right\} \cdot \qquad (5.18c)$$

$$\left(\sum_{k=1}^{n_x} B_{ik}^{(1)} \sum_{m=1}^{n_y} C_{jm}^{(1)} W_{km} + \left(\overline{W}_{,XY}\right)_{ij}\right) +$$

$$\left\{A_{12}\beta^2\left[a\sum_{k=1}^{n_x} B_{ik}^{(1)} U_{kj} + \frac{1}{2}\left(\sum_{k=1}^{n_x} B_{ik}^{(1)} W_{kj}\right)^2 + \left(\sum_{k=1}^{n_x} B_{ik}^{(1)} W_{kj}\right)\left(\overline{W}_{,X}\right)_{ij}\right] +\right.$$

$$A_{22}\beta^2 \cdot \left[\sum_{k=1}^{n_y} C_{jk}^{(1)} V_{ik} + \frac{1}{2}\left(\sum_{k=1}^{n_y} C_{jk}^{(1)} W_{ik}\right)^2 +\right.$$

$$\left.\left.\left(\sum_{k=1}^{n_y} C_{jk}^{(1)} W_{ik}\right)\left(\overline{W}_{,Y}\right)_{ij}\right]\right\} \cdot \left(\sum_{k=1}^{n_y} C_{jk}^{(2)} W_{ik} + \left(\overline{W}_{,YY}\right)_{ij}\right) = 0$$

where $X = \frac{x}{a}$, $Y = \frac{y}{b}$, $\beta = \frac{a}{b}$, $i = 1,\ldots,n_x$, $j = 1,\ldots,n_y$ and $\left(\overline{W}_{.}\right)_{ij}$ represents the derivatives of the imperfection function evaluated at X_i and Y_j. $B_{ij}^{(k)}$ and $C_{ij}^{(k)}$ are the weighting coefficients for the k^{th} derivative along the non-dimensionalized X and Y axes, respectively. Similar expressions can also be found for the boundary conditions noted in (5.17).

Using the arc-length method, one can solve the nonlinear system of equations resulting from the application of DQM to the system of differential equations and their associated boundary conditions and to obtain the response of the plate under increasing compressive load.

5.2.3. Case Studies

To verify the analytical formulations presented, several case studies were used to evaluate the geometrically nonlinear response of various composite plates. In all cases the boundaries were assumed to be simply supported, while other boundary conditions can easily be implemented. The geometric imperfection functions are represented in terms of the buckling mode shape with different amplitudes by:

$$\overline{w} = w_0 \sin\left(\frac{n\pi x}{a}\right) \cdot \sin\left(\frac{m\pi y}{b}\right) \tag{5.19}$$

To illustrate the application of DQM, two case studies will be discussed here. The first case study examines the response of a square plate (unit length (a) × unit width (b) × 0.02 unit thick (h)), subjected to an axial compressive stress. The material forming the plate is orthotropic with the following properties:

$E_{11} = 104.6\times10^9$ Pa; $E_{22} = 8.66\times10^9$ Pa; $\nu_{12} = 0.276$; $G_{12} = 2.92\times10^9$ Pa

Three different imperfection amplitudes were applied to the plate and the resulting out of plane deformations are shown in Figure 5.3. The equilibrium path obtained from a commercial finite elements program (NISA) is also illustrated in the same figure. In the figure, the ordinate represents the applied load normalized with respect to the buckling load. For DQM, 13×13 grid points were used to discretized the plate. As shown by the figure, DQM was capable to predict the post critical response of the plate accurately, and efficiently compared to the finite element solution. Also, it can be seen that increasing the amplitude of imperfection dramatically influences the response of the plate.

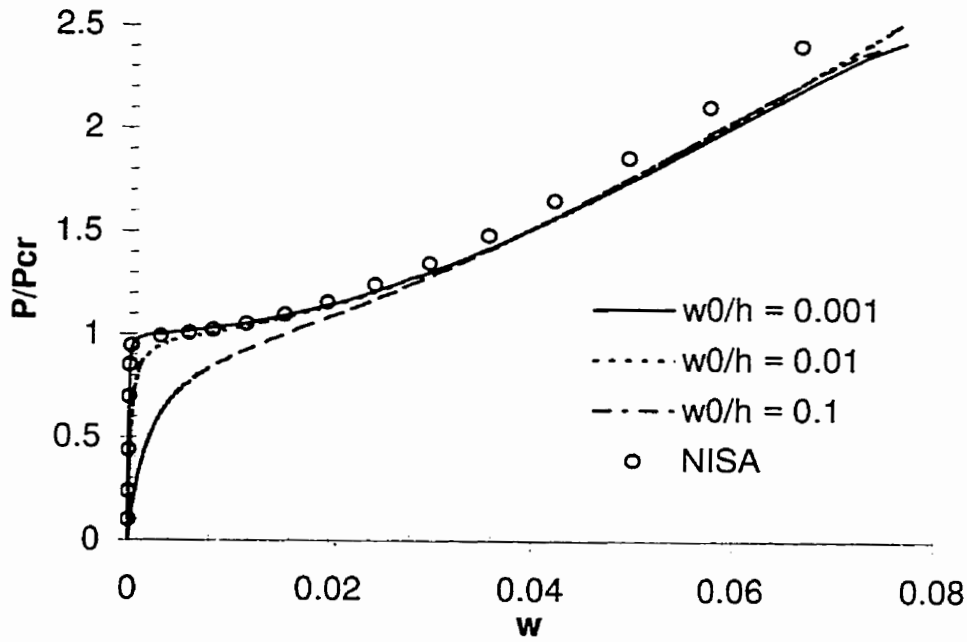

Figure 5.3. Load vs. max. deflection (at x=0.5a, y=0.5a) for the simply supported square plate.

In the second case study, the postbuckling response of the rectangular plate (a/b=3, h=0.1), of Lanzo et al (1995), was considered. They combined a High-Continuity finite elements plate model with the Koiter's asymptotic strategy to solve for the buckling and postbuckling response of the rectangular plates. The results are shown in Figure 5.4. Again the DQM shows excellent agreement with Lanzo et al.'s finite elements method.

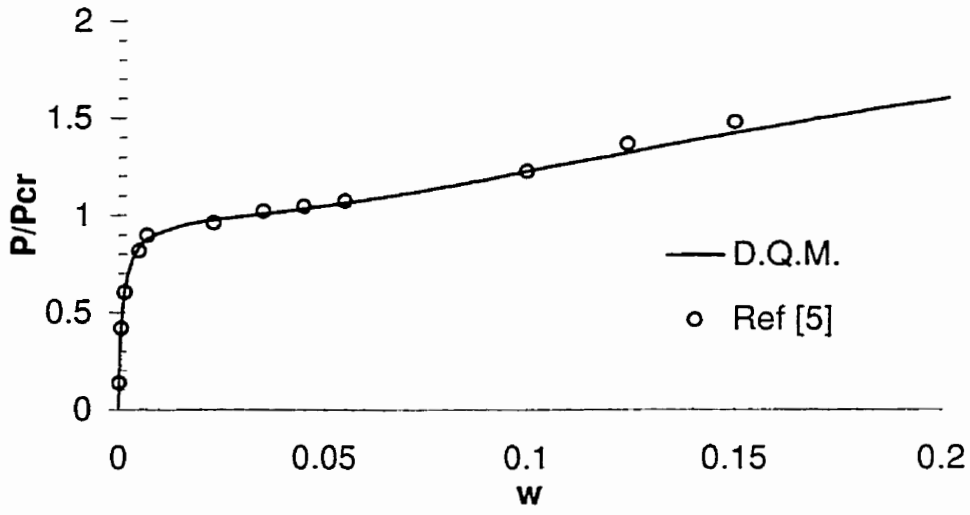

Figure 5.4. Load vs. max. deflection for the rectangular plate (a/b=3, $E=2.1\times10^6$, ν=0.25, h=0.1).

5.3. Postbuckling analysis of composite laminated beams having single delamination

In the following, DQM will be applied to the differential equations describing the postbuckling response of a delaminated composite beam under axial compression. The beam contains a single delamination prior to the loading. The case of multiple delaminations will be also considered later in this chapter. The geometry of a one-dimensional delaminated beam-plate used in this investigation is shown in Figure 4.2. This model contains an across-the-width delamination with the length 'a', located

arbitrarily through the thickness and along the span of the beam. As before, the delamination divides the beam into four regions.

To formulate the problem, we consider each of these regions as separate beams. Moreover, it is also assumed that prior to loading the beam has a natural imperfection, $\overline{w}$, in the form of the beam's preferred buckling mode shape, and the material is assumed to follow Hookian elasticity. Furthermore, delamination growth and the contact between the delaminated regions throughout the loading are neglected. Using the Kirchhoff-Love hypothesis, there are two independent variables: the axial displacement, u and the normal deflection, w. Writing the kinematical relationship for each region of the beam, one obtains:

$$\varepsilon^{(k)} = \varepsilon_0^{(k)} - z\kappa^{(k)}(x) \tag{5.20}$$

where $\varepsilon^{(k)}$ is the strain at any depth z in region k, κ is the flexural curvature of the reference (middle) surface and ε_0 is the axial strain of the same surface defined by

$$\varepsilon_0^{(k)} = u_{k,x} + \tfrac{1}{2} w_{k,x}^2 + w_{k,x}\overline{w}_{k,x} \tag{5.21}$$

Using the classical lamination theory the load/moment-strain/curvature relations can be represented as:

$$N_k = A_{11}^{(k)}\varepsilon_0^{(k)} - B_{11}^{(k)}\kappa^{(k)} \tag{5.22a}$$

$$M_k = B_{11}^{(k)}\varepsilon_0^{(k)} - D_{11}^{(k)}\kappa^{(k)} \tag{5.22b}$$

where N and M are the axial force and the bending moment, respectively, and A_{11}, B_{11} and D_{11} are the stiffness properties given by (4.36). The equilibrium equations for each region can be written as:

$$N_{k,x} = 0 \qquad (5.23a)$$

k=1,2,3,4

$$M_{k,x} - N_k(w_{k,xx} + \overline{w}_{k,xx}) = 0 \qquad (5.23b)$$

The curvature can be represented exactly by:

$$\kappa = \frac{w_{,xx}}{\left(1 + (w_{,x})^2\right)^{3/2}} \qquad (5.24)$$

As in the case of the elastic curve of a beam, the slope $w_{,x}$ is very small, and its square is negligible, therefore most beam formulations ignore the term $(w_{,x})^2$. But by neglecting this term when computing the postbuckling response of beams, one can introduce a substantial error, as the delaminated regions may undergo large deformations.

Using the kinematical expressions and the equilibrium equations developed above, we can write the non-linear differential equations describing each region in terms of the displacement components, as:

$$A_{11}^{(k)}\left(u_{k,xx} + w_{k,x}w_{k,xx} + w_{k,xx}\overline{w}_{k,x} + w_{k,x}\overline{w}_{k,xx}\right)$$

k=1,2,3,4 (5.25a)

$$- B_{11}^{(k)} \frac{w_{k,xxx}(1 + (w_{k,x})^2 - 3w_{k,x}(w_{k,xx})^2}{(1 + (w_{k,x})^2)^{\frac{5}{2}}} = 0$$

$$d_{11}^{(k)}\left(\frac{w_{k,xxxx}}{(1+(w_{k,x})^2)^{\frac{3}{2}}}-\frac{9w_{k,x}w_{k,xx}w_{k,xxx}}{(1+(w_{k,x})^2)^{\frac{5}{2}}}-\frac{3w_{k,xx}^3(1-4(w_{k,x})^2)}{(1+(w_{k,x})^2)^{\frac{7}{2}}}\right)-$$

k=1,2,3,4 (5.25b)

$$\left(A_{11}^{(k)}(u_{k,x}+\tfrac{1}{2}(w_{k,x})^2+w_{k,x}\overline{w}_{k,x})-B_{11}^{(k)}\frac{w_{k,xx}}{(1+(w_{k,x})^2)^{\frac{3}{2}}}\right)\cdot(w_{k,xx}+\overline{w}_{k,xx})=0$$

where $d_{11}^{(k)}=D_{11}^{(k)}-(B_{11}^{(k)})^2/A_{11}^{(k)}$. The boundary conditions are the given values of:

u or N
w or Q (5.26)
$w_{,x}$ or M

which are specified at the outside edges and along the interfaces of the regions. Q is the shear force and is defined by:

$$Q=M_{,x}+N(w_{,x}+\overline{w}_{,x}) \tag{5.27}$$

If the beam is simply supported, its boundary conditions can be written in the form:

At $x=0$ $\quad w_1=0 \;;\; M_1=0 \;;\; N_1=P_{appl}$ (5.28a)

At $x=L$ $\quad w_4=0 \;;\; M_4=0 \;;\; u_4=0$ (5.28b)

where P_{appl} is the applied load.

At the crack tip $x=l$

$$u_2 = u_1 - \frac{H}{2} w_{1,x} \quad ; \quad u_3 = u_1 + \frac{h}{2} w_{1,x} \tag{5.28c}$$

$$w_1 = w_2 = w_3 \quad ; \quad w_{1,x} = w_{2,x} = w_{3,x} \tag{5.28d}$$

$$M_1 - M_2 - M_3 + \frac{H}{2} N_2 - \frac{h}{2} N_3 = 0 \tag{5.28e}$$

$$Q_1 - Q_2 - Q_3 = 0 \tag{5.28f}$$

$$N_1 - N_2 - N_3 = 0 \tag{5.28g}$$

At $x = l+a$ the continuity conditions are the same as $x = l$, except the subscript '4' is replaced by '1'.

Using the non-dimensionalized variable $X = x/L$ and applying the DQM to the differential equations and their boundary conditions for all the regions results in:

$$A_{11}^{(k)} \left[l_k \sum_{j=1}^{n_k} C_{ijk}^{(2)} U_{jk} + \left(\sum_{j=1}^{n_k} C_{ijk}^{(1)} W_{jk} \right) \cdot \left(\sum_{j=1}^{n_k} C_{ijk}^{(2)} W_{jk} \right) + \right.$$

$$\left. \left(\sum_{j=1}^{n_k} C_{ijk}^{(1)} W_{jk} \right) \cdot \left(\overline{W}_{,XX} \right)_{ik} + \left(\sum_{j=1}^{n_k} C_{ijk}^{(2)} W_{jk} \right) \cdot \left(\overline{W}_{,X} \right)_{ik} \right] - \qquad \begin{matrix} i = 2,\ldots, n_k - 1 \\ k = 1,2,3,4 \end{matrix} \tag{5.29a}$$

$$B_{11}^{(k)} \frac{1}{V^{\frac{5}{2}}} \left[\left(\sum_{j=1}^{n_k} C_{ijk}^{(3)} W_{jk} \right) \cdot V^{-1} - \frac{3}{l_k^2} \left(\sum_{j=1}^{n_k} C_{ijk}^{(1)} W_{jk} \right) \cdot \left(\sum_{j=1}^{n_k} C_{ijk}^{(2)} W_{jk} \right)^2 \right] = 0$$

$$d_{11}^{(k)}\left[\left(\sum_{j=1}^{n_k} C_{ijk}^{(4)} W_{jk}\right) V^{\frac{3}{2}} - 9\frac{1}{l_k^2}\left(\sum_{j=1}^{n_k} C_{ijk}^{(1)} W_{jk}\right)\cdot\left(\sum_{j=1}^{n_k} C_{ijk}^{(2)} W_{jk}\right)\cdot\left(\sum_{j=1}^{n_k} C_{ijk}^{(3)} W_{jk}\right) V^{\frac{5}{2}} -\right.$$

$$\left. 3\frac{1}{l_k^2}\left(\sum_{j=1}^{n_k} C_{ijk}^{(2)} W_{jk}\right)^3\left(1-4\cdot\left(\frac{1}{l_k}\sum_{j=1}^{n_k} C_{ijk}^{(1)} W_{jk}\right)^2\right) V^{\frac{7}{2}}\right] - \tag{5.29b}$$

$$\left\{A_{11}^{(k)}\left[l_k\sum_{j=1}^{n_k} C_{ijk}^{(1)} U_{jk} + \frac{1}{2}\left(\sum_{j=1}^{n_k} C_{ijk}^{(1)} W_{jk}\right)^2 + \left(\sum_{j=1}^{n_k} C_{ijk}^{(1)} W_{jk}\right)\left(\overline{W}_{.X}\right)_{ik}\right] -\right.$$

$$\left. B_{11}^{(k)}\left(\sum_{j=1}^{n_k} C_{ijk}^{(2)} W_{jk}\right) V^{\frac{3}{2}}\right\}\cdot\left(\sum_{j=1}^{n_k} C_{ijk}^{(2)} W_{jk} + \left(\overline{W}_{.XX}\right)_{ik}\right) = 0 \qquad \begin{matrix} i = 3,\ldots,n_k - 2 \\ k = 1,2,3,4 \end{matrix}$$

where $C_{ijk}^{(r)}$ are the weighting coefficients for the r^{th} order derivative along the non-dimensionalized X axis, U_{jk} and W_{jk} are the in-plane and transverse displacements of the j^{th} point in the k^{th} section, respectively and V is:

$$V = \left(1 + \left(\frac{1}{l_k}\sum_{j=1}^{n_k} C_{ijk}^{(1)} W_{jk}\right)^2\right)^{-1} \tag{5.30}$$

The boundary conditions can be expressed in differential quadrature form as in the following:

At x=0

$$W_{11} = 0 \quad ; \quad \sum_{j=1}^{n_1} C_{1j1}^{(2)} W_{j1} = 0 \tag{5.31a}$$

$$A_{11}^{(1)} \left(\frac{1}{l_1} \sum_{j=1}^{n_1} C_{1j1}^{(1)} U_{j1} + \frac{1}{2} \left(\frac{1}{l_1} \sum_{j=1}^{n_1} C_{1j1}^{(1)} W_{j1} \right)^2 + \left(\frac{1}{l_1} \sum_{j=1}^{n_1} C_{1j1}^{(1)} W_{j1} \right) \left(\overline{W}_{.X} \right)_{11} \right) -$$

$$B_{11}^{(1)} \left(\frac{1}{l_1^2} \sum_{j=1}^{n_1} C_{1j1}^{(2)} W_{j1} \right) \cdot \left[1 + \left(\frac{1}{l_1} \sum_{j=1}^{n_1} C_{1j1}^{(1)} W_{j1} \right)^2 \right]^{-1} = P_{appl} \tag{5.31b}$$

At x = L

$$W_{n_4 4} = 0 \quad ; \quad \sum_{j=1}^{n_4} C_{n_4 j4}^{(2)} W_{j4} = 0 \quad ; \quad U_{n_4 4} = 0 \tag{5.31c}$$

At x = l

$$U_{12} = U_{n_1 1} - \frac{t_3}{2} \frac{1}{l_1} \sum_{j=1}^{n_1} C_{n_1 j1}^{(1)} W_{j1} \quad ; \quad U_{13} = U_{n_1 1} + \frac{t_2}{2} \frac{1}{l_1} \sum_{j=1}^{n_1} C_{n_1 j1}^{(1)} W_{j1} \tag{5.31d}$$

$$W_{n_1 1} = W_{12} = W_{13} \quad ; \quad \frac{1}{l_1} \sum_{j=1}^{n_1} C_{n_1 j1}^{(1)} W_{j1} = \frac{1}{l_2} \sum_{j=1}^{n_2} C_{1j2}^{(1)} W_{j2} = \frac{1}{l_3} \sum_{j=1}^{n_3} C_{1j3}^{(1)} W_{j3} \tag{5.31e}$$

$$\frac{D_{11}^{(1)}}{l_1^2}\left(\sum_{j=1}^{n_1} C_{n_1 j1}^{(2)} W_{j1}\right)\cdot V_{n_1 1}{}^{\frac{1}{2}} - \frac{B_{11}^{(1)}}{l_1}\left[\sum_{j=1}^{n_1} C_{n_1 j1}^{(2)} U_{j1} + \frac{1}{2l_1}\left(\sum_{j=1}^{n_1} C_{n_1 j1}^{(1)} W_{j1}\right)^2 + \right.$$

$$\left.\frac{1}{l_1}\left(\sum_{j=1}^{n_1} C_{n_1 j1}^{(1)} W_{j1}\right)\left(\overline{W}\right)_{n_1 1}\right] - \frac{D_{11}^{(2)}}{l_2^2}\left(\sum_{j=1}^{n_2} C_{1j2}^{(2)} W_{j2}\right)\cdot V_{12}{}^{\frac{1}{2}} +$$

$$\frac{B_{11}^{(2)}}{l_2}\left[\sum_{j=1}^{n_2} C_{1j2}^{(2)} U_{j2} + \frac{1}{2l_2}\left(\sum_{j=1}^{n_2} C_{1j2}^{(1)} W_{j2}\right)^2 + \frac{1}{l_2}\left(\sum_{j=1}^{n_2} C_{1j2}^{(1)} W_{j2}\right)\left(\overline{W}\right)_{12}\right] -$$

$$\frac{D_{11}^{(3)}}{l_3^2}\left(\sum_{j=1}^{n_3} C_{1j3}^{(2)} W_{j3}\right)\cdot V_{13}{}^{\frac{1}{2}} + \frac{B_{11}^{(3)}}{l_3}\left[\sum_{j=1}^{n_1} C_{1j3}^{(2)} U_{j3} + \frac{1}{2l_3}\left(\sum_{j=1}^{n_3} C_{1j3}^{(1)} W_{j3}\right)^2 + \right. \tag{5.31f}$$

$$\left.\frac{1}{l_3}\left(\sum_{j=1}^{n_3} C_{1j3}^{(1)} W_{j3}\right)\left(\overline{W}\right)_{13}\right] - \frac{1}{2}\left(t_3 P_2 - t_2 P_3\right) = 0$$

$$\frac{d_{11}^{(1)}}{l_1^3}\left[\left(\sum_{j=1}^{n_1} C_{n_1 j1}^{(3)} W_{j1}\right)\cdot V_{n_1 1}^{-1} - \frac{3}{l_1^2}\left(\sum_{j=1}^{n_1} C_{n_1 j1}^{(1)} W_{j1}\right)\left(\sum_{j=1}^{n_1} C_{n_1 j1}^{(2)} W_{j1}\right)^2\right]\cdot V_{n_1 1}{}^{\frac{5}{2}} -$$

$$\frac{d_{11}^{(2)}}{l_2^3}\left[\left(\sum_{j=1}^{n_2} C_{1j2}^{(3)} W_{j2}\right)\cdot V_{12}^{-1} - \frac{3}{l_2^2}\left(\sum_{j=1}^{n_2} C_{1j2}^{(1)} W_{j2}\right)\left(\sum_{j=1}^{n_2} C_{1j2}^{(2)} W_{j2}\right)^2\right]\cdot V_{12}{}^{\frac{5}{2}} - \tag{5.31g}$$

$$\frac{d_{11}^{(3)}}{l_3^3}\left[\left(\sum_{j=1}^{n_3} C_{1j3}^{(3)} W_{j3}\right)\cdot V_{13}^{-1} - \frac{3}{l_3^2}\left(\sum_{j=1}^{n_3} C_{1j3}^{(1)} W_{j3}\right)\left(\sum_{j=1}^{n_3} C_{1j3}^{(2)} W_{j3}\right)^2\right]\cdot V_{13}{}^{\frac{5}{2}} = 0$$

$$P_1 - P_2 - P_3 = 0 \tag{5.31h}$$

where P_1, P_2 and P_3 are

$$P_1 = \frac{A_{11}^{(1)}}{l_1^2}\left(l_1 \sum_{j=1}^{n_1} C_{n_1 j1}^{(1)} U_{j1} + \frac{1}{2}\left(\sum_{j=1}^{n_1} C_{n_1 j1}^{(1)} W_{j1} \right)^2 + \left(\sum_{j=1}^{n_1} C_{n_1 j1}^{(1)} W_{j1} \right)\left(\overline{W}_{,X}\right)_{n_1 1} \right) - \frac{B_{11}^{(1)}}{l_1^2}\left(\sum_{j=1}^{n_1} C_{n_1 j1}^{(2)} W_{j1} \right) V_{n_1 1}^{\frac{3}{2}} \tag{5.32a}$$

$$P_2 = \frac{A_{11}^{(2)}}{l_2^2}\left(l_2 \sum_{j=1}^{n_2} C_{1j2}^{(1)} U_{j2} + \frac{1}{2}\left(\sum_{j=1}^{n_2} C_{1j2}^{(1)} W_{j2} \right)^2 + \left(\sum_{j=1}^{n_2} C_{1j2}^{(1)} W_{j2} \right)\left(\overline{W}_{,X}\right)_{12} \right) - \frac{B_{11}^{(2)}}{l_2^2}\left(\sum_{j=1}^{n_2} C_{1j2}^{(2)} W_{j2} \right) V_{12}^{\frac{3}{2}} \tag{5.32b}$$

$$P_3 = \frac{A_{11}^{(3)}}{l_3^2}\left(l_3 \sum_{j=1}^{n_3} C_{1j3}^{(1)} U_{j3} + \frac{1}{2}\left(\sum_{j=1}^{n_3} C_{1j3}^{(1)} W_{j3} \right)^2 + \left(\sum_{j=1}^{n_3} C_{1j3}^{(1)} W_{j3} \right)\left(\overline{W}_{,X}\right)_{13} \right) - \frac{B_{11}^{(3)}}{l_3^2}\left(\sum_{j=1}^{n_3} C_{1j3}^{(2)} W_{j3} \right) V_{13}^{\frac{3}{2}} \tag{5.32c}$$

Similar continuity boundary conditions can be applied at $x = l+a$. Obviously, the resulting system of equations is nonlinear. Therefore, an arc-length strategy, as discussed in section 5.2, will be used to solve them.

5.4. Postbuckling analysis of composite laminated beams having multiple delaminations

Using the same procedure presented for postbuckling analysis of beams with single delamination, one can derive the quadrature analog formulation for the case of multiple delaminations. Consider a laminated composite beam having a number of through-the-width delaminations (Figure 4.3). The delaminations size, its across-the-thickness, and along the beam span locations are chosen arbitrarily. Therefore, the delaminations divide the beam into m different regions. As before, each region can be considered as a separate beam with its own stiffness properties. The assumptions used in section 5.2 leads to the same differential equilibrium equations as (5.25a,b), for all the regions k=1,...,m. The boundary conditions for the beam being simply supported, will be

$$\text{At } x = 0 \qquad w_1 = 0 \;\; ; \;\; M_1 = 0 \;\; ; \;\; N_1 = P_{appl} \tag{5.33a}$$

$$\text{At } x = L \qquad w_m = 0 \;\; ; \;\; M_m = 0 \;\; ; \;\; u_m = 0 \tag{5.33b}$$

At the crack tips the continuity boundary conditions require that

$$u_i + \frac{z_i}{2} w_{i,x} = u_j + \frac{z_j}{2} w_{j,x} = \ldots = u_k + \frac{z_k}{2} w_{k,x} \tag{5.33c}$$

$$w_i = w_j = \ldots = w_k \tag{5.33d}$$

$$w_{i,x} = w_{j,x} = \ldots = w_{k,x} \tag{5.33e}$$

$$M_i - M_j - \cdots - M_k + N_i z_i + N_j z_j + \cdots + N_k z_k = 0 \tag{5.33f}$$

$$Q_i - Q_j - \cdots - Q_k = 0 \tag{5.33f}$$

$$N_i - N_j - \cdots - N_k = 0 \tag{5.33g}$$

where $i,j,...,k$ are the region numbers surrounding a crack tip and z is the distance between the mid-plane of each beam and the appropriate moment point.

Applying DQM to the differential equilibrium equations and their boundary conditions result in a system of nonlinear algebraic equations in terms of the axial deformation u and transverse deflection w of sampling points as the variables. Employing the arc-length algorithm, this system of equations can be solved to give the response of the delaminated beam under progressive compressive axial load.

CHAPTER 6

VERIFICATION OF THE DQM

6.1. Introduction

In the following chapter, the capability of the DQM in solving the delamination buckling and postbuckling problems in laminated composite structures will be examined. The case studies include the buckling analysis of various beams containing single or multiple delaminations and laminated plates having single elliptical delamination. Moreover, postbuckling analysis of beams with single and multiple delaminations will be discussed. For all the one-dimensional models, it is assumed that the delaminations are across-the-width. The formulations presented in the chapters 4 and 5 were implemented into computer programs, some of which are presented in appendices. The DQM results will be compared with either those in the published literature or those of the finite element investigations conducted by the author.

6.2. Case studies for buckling of a specially orthotropic beam with a single delamination

The formulation presented in the section 4.2.1 was implemented as a computer code for evaluating the delamination buckling response of a panel containing a through-the-width delamination as shown in Figure 4.1. This investigation demonstrates the capability of the selected numerical method.

6.2.1. Delamination buckling load

The results for a clamped beam having a symmetric delamination are calculated. Table 6.1 tabulates the resulting buckling loads for various delamination lengths (a/L),

and thickness (h/T) ratios. In this table the buckling loads are normalized with respect to the Euler buckling load for a perfect column, that is:

$$\overline{P}_{cr} = \frac{P_{cr}}{4\pi^2 D_1 / L^2} \tag{6.1}$$

where D_1 is the flexural stiffness of the first region (base laminate).

Table 6.1: Normalized buckling load for the beam-plate with clamped ends.

a/L	h/T						
	0.02	0.05	0.10	0.20	0.30	0.40	0.5
0.025	0.64000	1.00000	1.00000	1.00000	1.00000	1.00000	1.00000
0.050	0.16000	0.99485	0.99976	1.00000	1.00000	1.00000	1.00000
0.100	0.04000	0.24994	0.97994	0.99966	0.99978	0.99987	0.99988
0.150	0.01778	0.11109	0.44347	0.99659	0.99852	0.99890	0.99898
0.200	0.01000	0.06249	0.24954	0.92647	0.99240	0.99505	0.99556
0.250	0.00640	0.03999	0.15974	0.62559	0.96621	0.98354	0.98593
0.300	0.00444	0.02777	0.11094	0.43712	0.85825	0.95434	0.96384
0.350	0.00327	0.02041	0.08152	0.32207	0.67802	0.89118	0.91479
0.400	0.00250	0.01562	0.06242	0.24705	0.53140	0.78832	0.84808
0.450	0.00198	0.01234	0.04933	0.19549	0.42492	0.67193	0.77446
0.500	0.00160	0.01000	0.03996	0.15855	0.34691	0.56755	0.68958
0.550	0.00132	0.00826	0.03303	0.13118	0.28842	0.48164	0.61060
0.600	0.00111	0.00694	0.02776	0.11034	0.24354	0.41240	0.54115
0.650	0.00095	0.00592	0.02365	0.09411	0.20839	0.35654	0.48159
0.700	0.00082	0.00510	0.02040	0.08122	0.18036	0.31111	0.43098
0.750	0.00071	0.00444	0.01777	0.07082	0.15766	0.27379	0.38800
0.800	0.00063	0.00391	0.01562	0.06230	0.13901	0.24282	0.35143
0.850	0.00055	0.00346	0.01384	0.05523	0.12352	0.21685	0.32016
0.900	0.00049	0.00309	0.01234	0.04930	0.11050	0.19488	0.29331

The integrity of the presented method and its capability in treating the delamination buckling problems is confirmed by the excellent agreement of the results presented in this study with those of Simitses et al (1985). In fact, the discrepancies between our results and those in Simitses et al are less than 0.01%, therefore, they were not rewritten on the table. The normalized buckling loads are also shown graphically in Figure 6.1. The results are derived using different rotations at the delamination fronts (equation (4.6)).

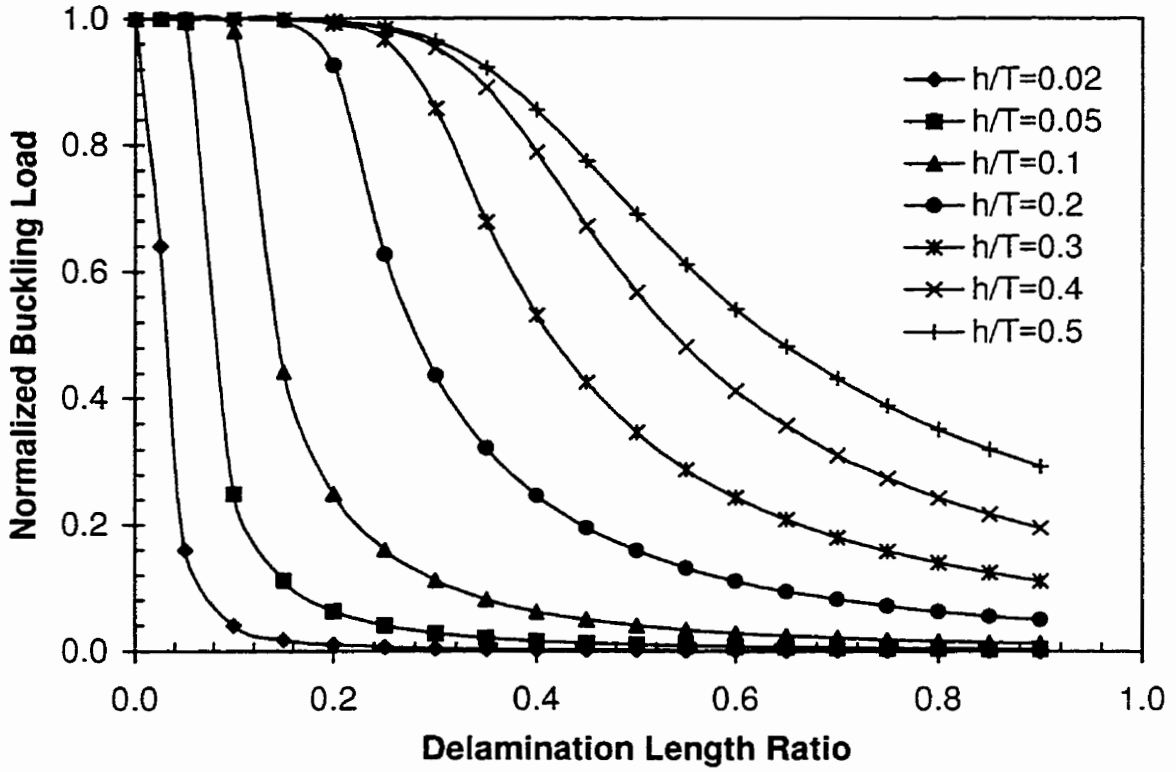

Figure 6.1. Influence of the delamination length on the buckling load of a beam with clamped ends.

Table 6.2 tabulates the buckling loads obtained by DQM for a specially-orthotropic composite laminate containing a delamination at its mid-plane (i.e., h/T=0.5). This

problem is analyzed for various delamination length ratios (a/L). The buckling loads are normalized with respect to the Euler buckling load of a perfect column. The "symmetric" and "anti-symmetric" notations in Table 6.2 conform to the terminology used in chapter 1.

Table 6.2. Comparison of normalized buckling loads for a beam with single delamination, h/T=0.5.

			Lee et al.(1993)		DQM (present study)	
	Simitses	Chen		Anti-		Non-
a/L	(1985)	(1991)	Symmetric	symmetric	Symmetric	symmetric
0.1	0.9999	0.9999	0.9999	1.9480	0.9999	0.9999
0.2	0.9956	0.9956	0.9956	1.4360	0.9956	0.9956
0.3	0.9638	0.9638	0.9639	1.0240	0.9638	0.9638
0.4	**0.8481**	**0.8561**	**0.8562**	**0.8482**	**0.8561**	**0.8481**
0.5	0.6896	0.6896	0.6898	0.7967	0.6896	0.6896
0.6	0.5411	0.5411	0.5413	0.7929	0.5411	0.5411
0.7	0.4310	0.4310	0.4311	0.7629	0.4310	0.4310
0.8	0.3514	0.3514	0.3515	0.6857	0.3514	0.3514
0.9	0.2923	0.2933	0.2934	0.5947	0.2933	0.2933

For comparison, the analytical results of Simitses et al (1985) and Chen (1991), followed by the results form the finite element layer wise approach of Lee et al (1993) are also tabulated. Note that the results reported by Chen were obtained by imposing the symmetry condition in the axial direction, while Simitses et al did not apply such an imposition. This is an important consideration as the anti-symmetric buckling mode can occur at specific a/L ratios (see Figure 15 and 16 of Lee (1992)); therefore, by imposing

the symmetry condition, accurate simulation of the buckling modes for all *a/L* ratios is not achievable. The result reported by Lee et al are provided for the two possible conditions. Also, note that the "nonsymmetric" terminology used to identify some of the DQM results conforms to the terminology used by Simitses et al. As it can be seen, there is an excellent agreement between the results obtained by DQM and those of Simitses et al, Chen, and Lee et al. Indeed, the DQM results are closer to the results obtained based on the analytical solutions (Simitses et al and Chen), than those calculated based on the finite element analysis of Lee et al. Also note that, while Lee et al used two different models to obtain the symmetric and antisymmetric buckling loads, the same results could be achieved by DQM by only using different rotations at crack tips. Table 6.3 shows the first three buckling loads derived from DQM for the same configuration (i.e. clamped ends and *h/T*=0.5) and different delamination ratios.

Table 6.3. Comparison of the first three normalized buckling loads for a beam with single delamination, h/T=0.5.

	Present study			Lee et al.(1993)		
	Buckling Load			Global	Local	Anti-
a/L	1st	2nd	3rd	Symmetric	Symmetric	symmetric
0.1	0.9999	1.9486	3.9900	0.9999	15.320	1.9480
0.2	0.9956	1.4358	3.6398	0.9956	6.0963	1.4360
0.3	0.9638	1.0243	2.5159	0.9639	2.7176	1.0240
0.4	0.8481	0.8561	1.5625	0.8562	1.5358	0.8482
0.5	0.6896	0.7966	1.0000	0.6898	0.9864	0.7967
0.6	0.5411	0.6945	0.7926	0.5413	0.6868	0.7929
0.7	0.4310	0.5102	0.7627	0.4311	0.5058	0.7629
0.8	0.3514	0.3903	0.6856	0.3515	0.3883	0.6857
0.9	0.2933	0.3086	0.5946	0.2934	.03077	0.5947

Comparison of these buckling loads with those of Lee et al shows that the first buckling loads in Table 6.3 is essentially the minimum value of the three possible mode shapes.

6.2.2 Number of sampling points

The influence of the number of sampling points on the predicted results obtained by the proposed method was also investigated. The resulting buckling loads as a function of the number of sampling points for isotropic beam-plates with clamped edges, having thin and thick delaminations are shown in Figure 6.2 and 6.3, respectively.

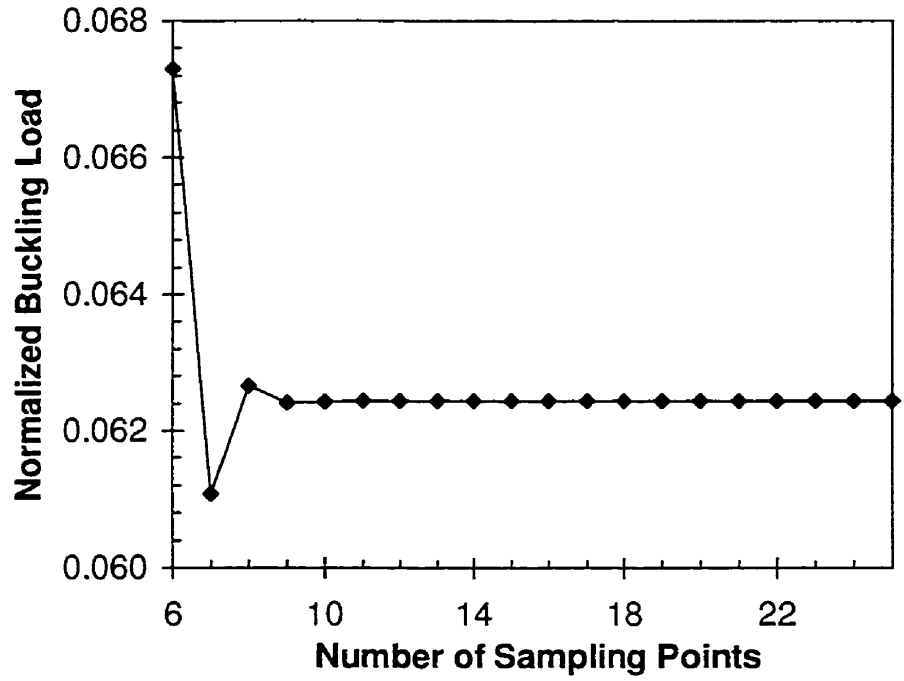

Figure 6.2. Effect of number of sampling points on the buckling load of a plate with a thin delamination (h/T=0.1, a/L=0.4).

For these case studies, all sub-regions had equal number of sampling points. As can be seen from these figures, the stability of the DQM is excellent and even with lower number of sampling points the convergence of the method is good. It can be concluded that for obtaining accurate results one needs to discretize each section by only 9 to 11 sampling points.

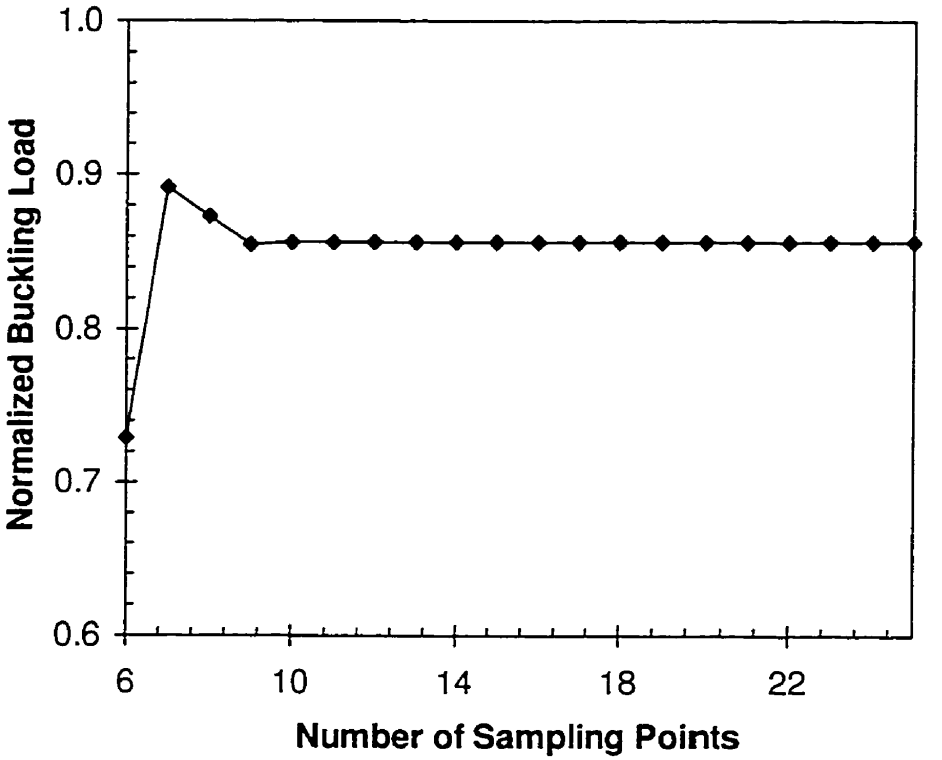

Figure 6.3. Effect of number of sampling points on the buckling load of a plate with a thick delamination (h/T=0.5, a/L=0.4).

6.2.3. Effect of grid spacing

As mentioned earlier, there are several possible grid spacing schemes when using DQM. In general, in applications that are sensitive to grid spacing, like buckling of composite structures, selection of the grid spacing is of critical importance (see Wang (1995) and Sherbourne and Pandey (1991)). One useful method is to use the δ-technique as used in conventional differential quadrature method (Bert and Malik (1996)). The other is to use unequally spaced sampling points. Here we examine the effect of grid spacing through the use of the equations (3.13-17) in the normalized region $[0,1]$.

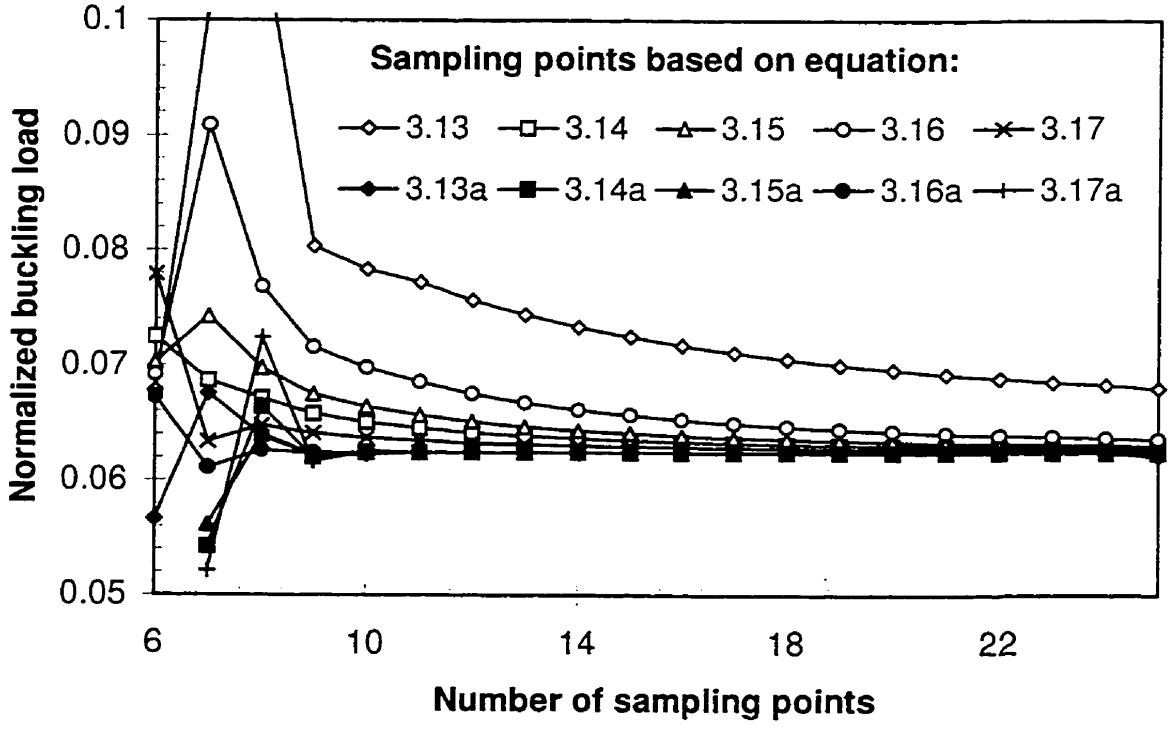

Figure 6.4. Convegence of DQM with different grid schemes for the case of a thin delamination ("a" indicate the δ-technique was used).

It must be noted that none of these schemes use the δ-technique, while the equation of the δ-technique bears little difference with the above relations. The results obtained for the various grid spacing schemes, for thin and thick delaminations of the last example are shown in Figures 6.4 and 6.5, respectively. The figures illustrate the performance of the above mentioned relations with and without the use of the δ-technique. In these figures, suffix "a" indicates that the relations incorporated the δ-technique.

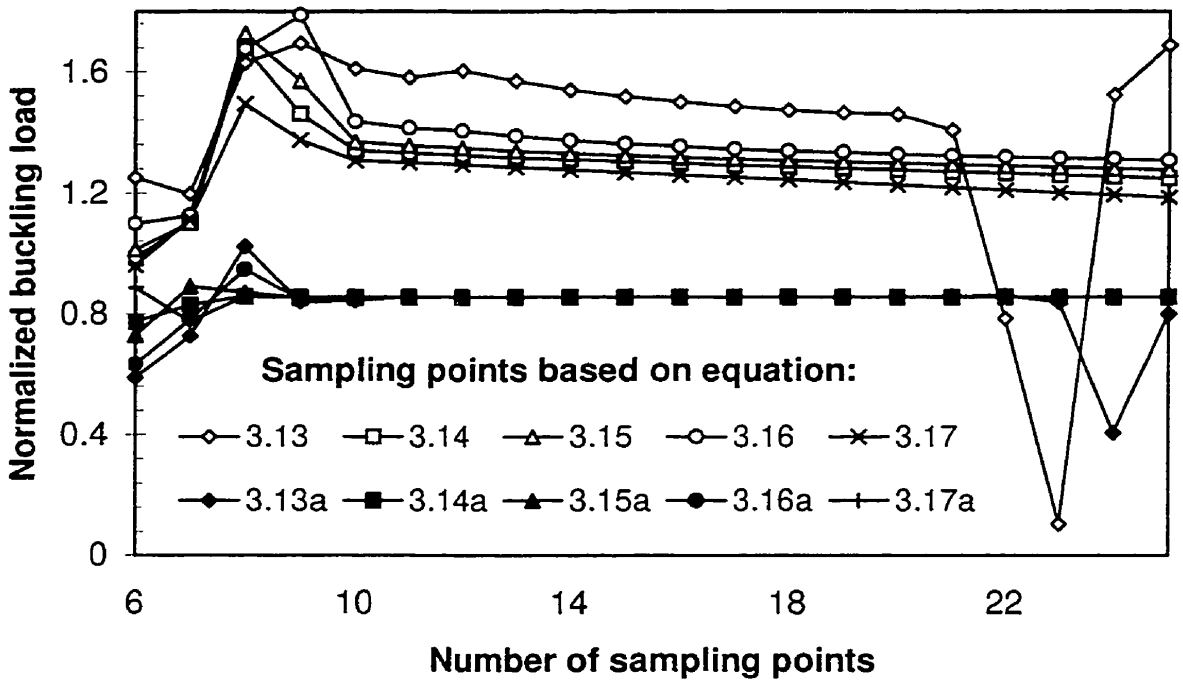

Figure 6.5. Convergence of DQM with different grid schemes for the case of thick delamination ("a" indicate the δ-technique was used).

Figure 6.4 (h/T=0.1 and a/L=0.4) indicates that inaccurate buckling loads can be expected when the δ-technique is not used in conjunction with the uniform grid spacing when treating thin delamination problems; while the other grid spacing schemes converge

to the analytical solution. It should be noted, however, that when the δ-technique was used, the solutions for all grid spacing schemes converged rapidly to the analytical solution (when each section was discretized by only 9 grid points). Moreover, the use of Chebyshev spacing produces the best convergence among all the schemes.

In the case of thick delamination problems (h/T=0.5 and a/L=0.4), Figure 6.5 indicates that all the grid spacing schemes can produce unacceptable results without the use of the δ-technique (especially, the case with the uniform spacing producing the worst results). However, incorporation of the δ-technique produces fast convergence (with the exception of the equal spacing), with eqation (3.14) producing the fastest convergence. When using the equal spacing scheme, the results produced by the larger even sampling points, (see results for the 24 sampling points in Figure 6.5, for example), bear considerable error; where the results for the odd sampling points show no discrepancy. Therefore, this may be considered as the reason to why most authors use odd number of grid points (Bert and Malik (1996a)).

6.3. Case studies for buckling of a specially orthotropic beam with shear deformation having single delamination

As shown in chapter 4, including the effect of shear deformation in the buckling analysis of delaminated beams affects the results considerably. This result in a system of second order differential equation with two different types of variables, namely the transverse deflection, w and rotation angle, φ. As a result the grid spacing can be chosen without employing the δ-technique. As in the last section the influence of several parameters on the buckling response of laminated beams was investigated. It was assumed that the beam-plates' outermost edges were clamped.

6.3.1. Effect of shear deformation on the buckling load

One of the parameters investigated in the study was the influence of the shear deformation. For this, the resulting buckling response of beams having a symmetric delamination with various configurations and a shear deformation factor, *s=0.2,* are shown in Figure 6.6.

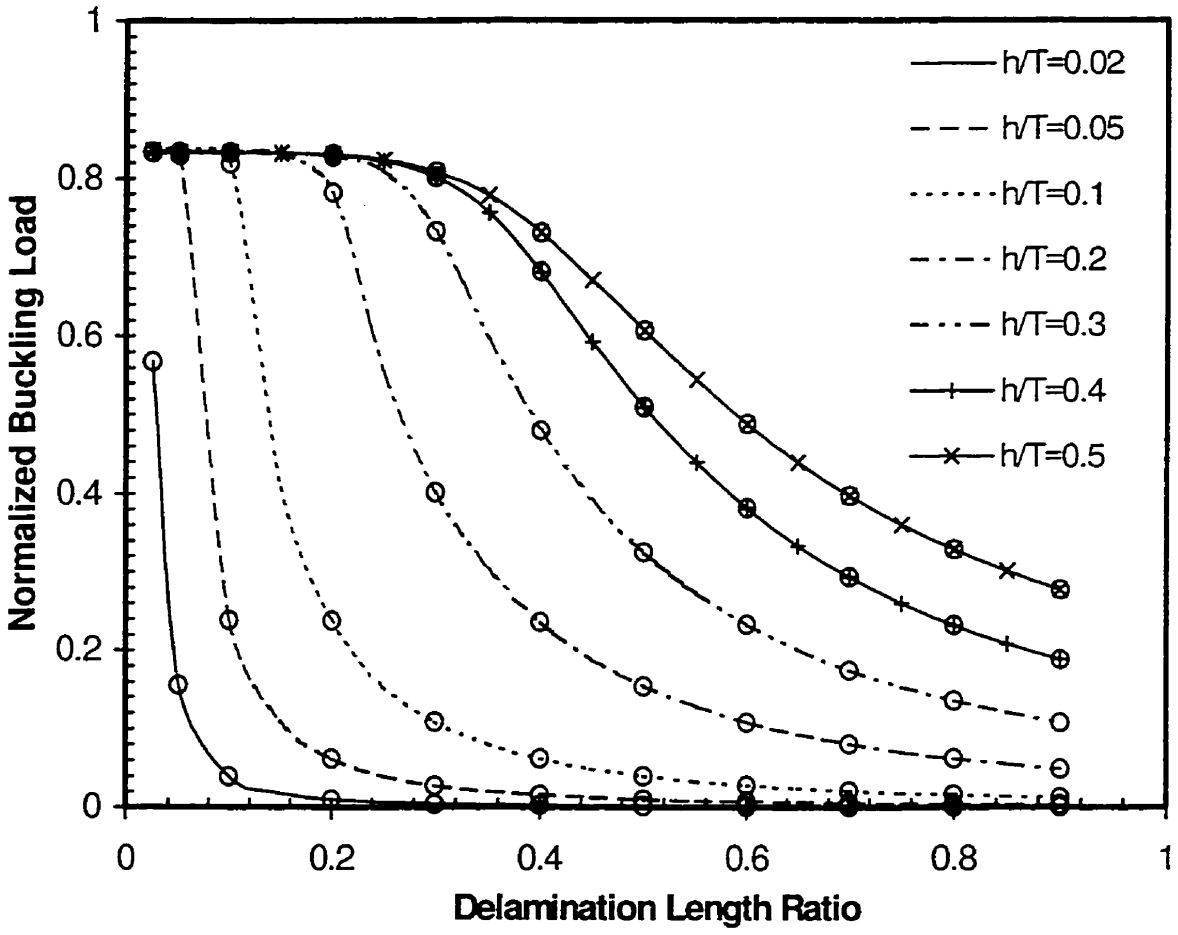

Figure 6.6. Buckling loads for different delamination configurations (s=0.2).

The variables considered were the length and the through-the-thickness location of the delamination. As shown in the figure, the DQM results are in excellent agreement with those obtained from the analytical solution of Chen (1991), to the extent that the differences are indistinguishable. Moreover, as shown, the classical laminate theory generally overestimates the buckling response of the composites, especially those with short delamination length. This phenomenon is more noticeable in Figures 6.7 and 6.8, where the buckling strength of beams having h/T = 0.05 and h/T = 0.5, and various delamination lengths are calculated for a practical range of shear deformation factors.

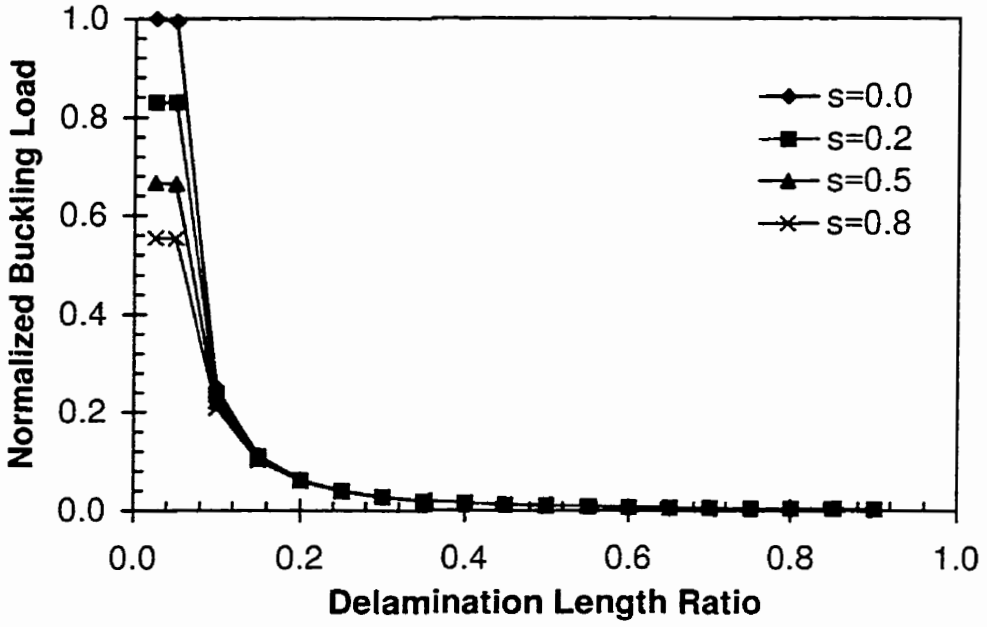

Figure 6.7. Effect of shear deformation on the buckling strength of beam-plates with h/T=0.05.

The figure illustrates that the buckling strength of composites having thicker sublaminates (h/T = 0.5), decreases as their shear deformation increases. This behavior is

quite consistent, regardless of the length of delamination, yet it is more significant for delaminations with $a/L < 0.6$. On the other hand, when the sublaminate is thin, the shear effect becomes noticeable only at very small delamination lengths (i.e.: $a/L < 0.1$).

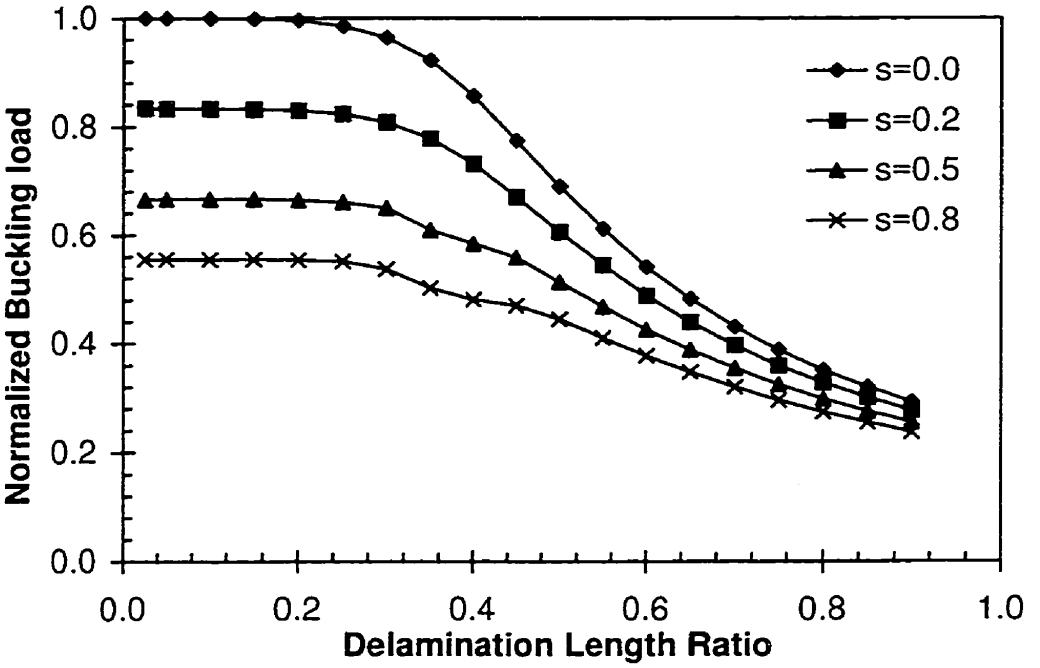

Figure 6.8. Effect of shear deformation on the buckling strength of beam-plates with h/T=0.5.

6.3.2. Effect of the longitudinal position of delamination

The influence of the longitudinal delamination position on the buckling response of the beams is shown in Figure 6.9 for beam with $h/T = 0.5$. For the delamination length ratios $0.2 < a/L < 0.6$, the buckling response varies depending on the location of the delamination along the span of the beams. As expected, the highest buckling strength is obtained when the delamination is at the center of the span of the beam. The behavior is

consistent throughout, including in beams with *h/T* ratios other than 0.5, as illustrated in Figure 6.9.

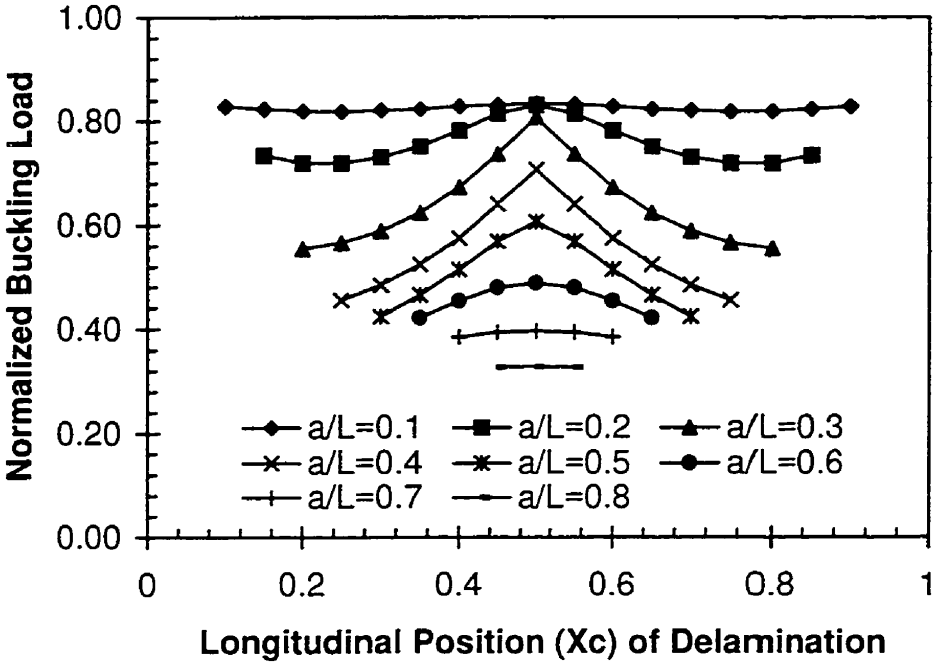

Figure 6.9. Effect of the delamination position on the buckling strength of beam-plates with h/T=0.5.

6.4. Case studies for buckling of a general laminated composite beam having single delamination

The formulations presented in chapter 4 for the buckling analysis of a general composite laminated beam with a single delamination were implemented in a computer program. Several case studies were investigated to insure the integrity and applicability of the proposed method. The effect of the material types, stacking sequence, delamination

position and delamination length, on the buckling response of a series of composite beam-plates were investigated.

To assess the overall convergence efficiency of the DQM, the response of two delaminated asymmetric cross-ply composite beam-plates (Chen and Chang (1994)), with ply sequence of $\left[(90_4/0_4)//(90_4/0_4)_3\right]$ and $\left[(90/0)_4//(90/0)_{12}\right]$, and several of symmetric laminates were investigated. The designation "//" is used to denote the position of delamination through the laminates. The material properties that are of a typical graphite/epoxy composite are tabulated in Table 6.4.

Table 6.4. Material properties of the laminates.

Material	Graphite/epoxy	Glass/epoxy	Kevlar/epoxy
E_1 (Gpa)	137.9	46	75.8
E_2 (Gpa)	9.65	13	5.5
G_{12} (GPa)	5.5	5	2.3
ν_{12}	0.3	0.3	0.34
G_{23} (GPa)	4.14	4.6	2.

It is assumed that each ply has a thickness of 0.127mm (0.005in) and the delamination thickness ratio is h/T=0.25. Both laminates have the same $A_{11}^{(i)}$, $A_{55}^{(i)}$ and $D_{11}^{(i)}$, but different bending-extension stiffnesses (denoted by $B_{11}^{(i)}$, where $B_{11}^{(i)}$ for the first laminate are about four times the values of those of the second laminate). The resulting buckling loads of the two laminates for different delamination ratios, a/L, are shown graphically in Figure 6.10. In this figure the buckling loads are normalized with respect to the Euler buckling load of an intact laminate, that is:

$$\overline{P}_{cr} = \frac{P_{cr}}{4\pi^2 D_{11}/L^2} \tag{6.2}$$

As seen in Figure 6.10, the bending-extension coupling reduces the delamination buckling load as the delamination length ratio increases. These results are in excellent agreement with the results of analytical and the finite element analysis of Chen and Chang (1994).

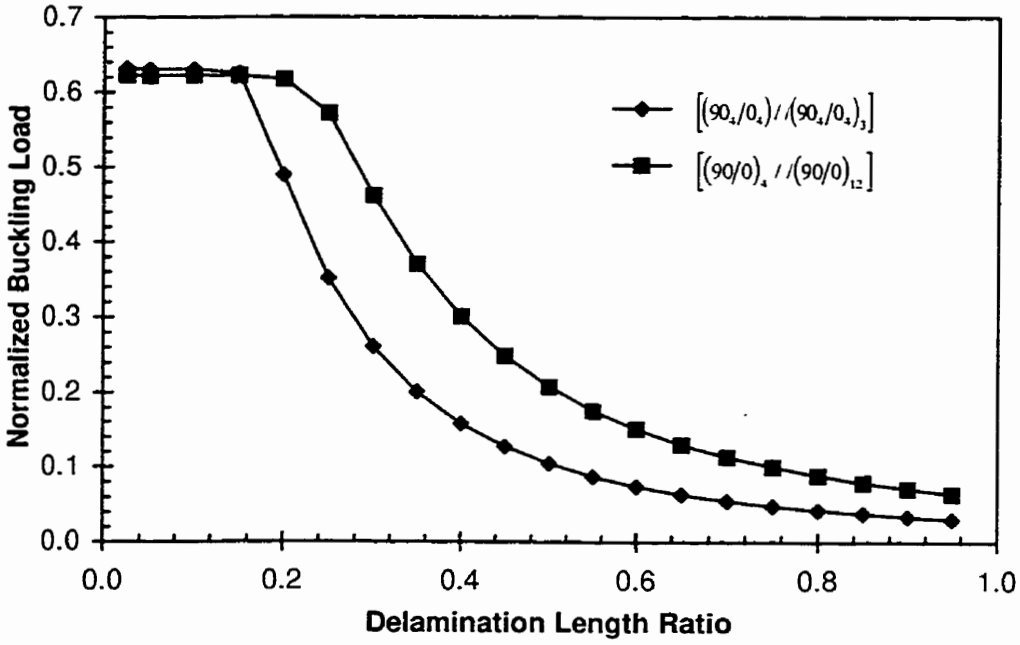

Figure 6.10. Delamination buckling load for different delamination lengths.

6.4.1. Effect of slenderness ratio (L/T)

The effect of the slenderness ratio, L/T, on the buckling load for $[(\pm 45)_4//(\pm 45)_{12}]$ laminates is shown in Figure 6.11. Note that the bending-extension

stiffness of all sublaminates of these laminates are effectively zero. Also shown in the figure is the effect of some thick laminates (i.e., $L/T<20$), for which the shear deformation effect becomes quite significant. Nevertheless, the laminates that have relatively large delamination length (i.e., delamination length ratios > 0.4), exhibit similar buckling response, regardless of their L/T ratios.

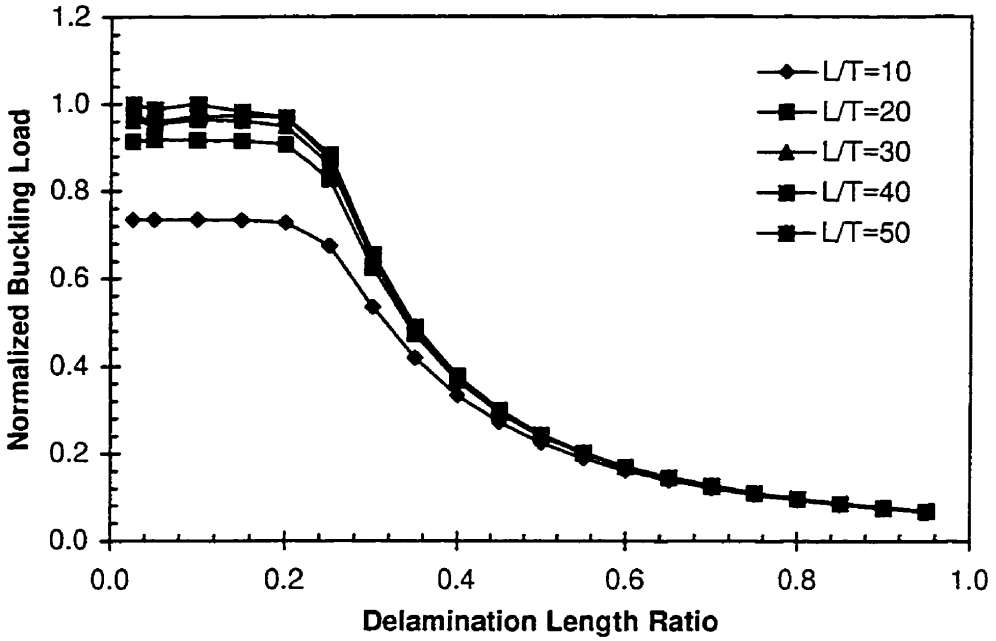

Figure 6.11. Effect of slenderness ratio on delamination buckling load.

6.4.2. Effect of fiber orientation

The influence of fiber orientation on the buckling strength of a thick delamination is shown in Figure 6.12. This investigation considers symmetric laminates of $[(\pm\theta)_{16}]$ with a delamination ratio of $a/L=0.2$, all having thick delamination ($h/T=\frac{1}{2}$). The

buckling loads are normalized with respect to that of an intact $[0_{32}]$ laminate. As the figure shows, the buckling strength decreases as the fiber orientation angle increases.

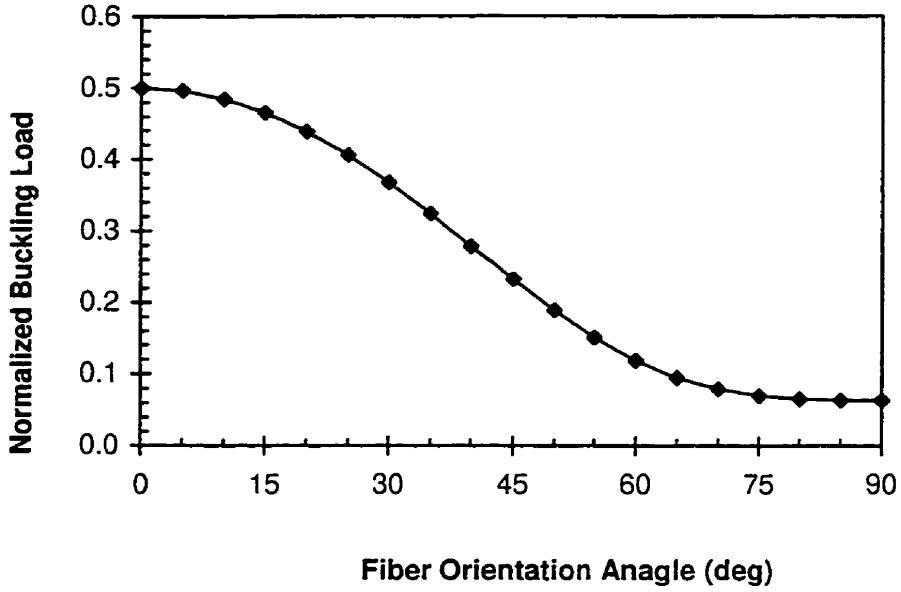

Figure 6.12. Effect of fiber orientation on buckling load for a thick delamination ($h/T = \frac{1}{2}$).

6.4.3. Effect of the through-the-thickness position of delamination

Figure 6.13 shows the influence of the through-the-thickness position of the delamination in $[(\pm 45)_{16}]$ laminates with a/L=0.2 and L/T=10. The figure illustrates that for relatively thick delaminations (i.e., h/T>0.2), the buckling strength is independent of the through-the-thickness position of the delamination. The same investigation was carried out for cross ply $[(90/0)_{16}]$ laminates and the resulting buckling loads are shown in Figure 6.14.

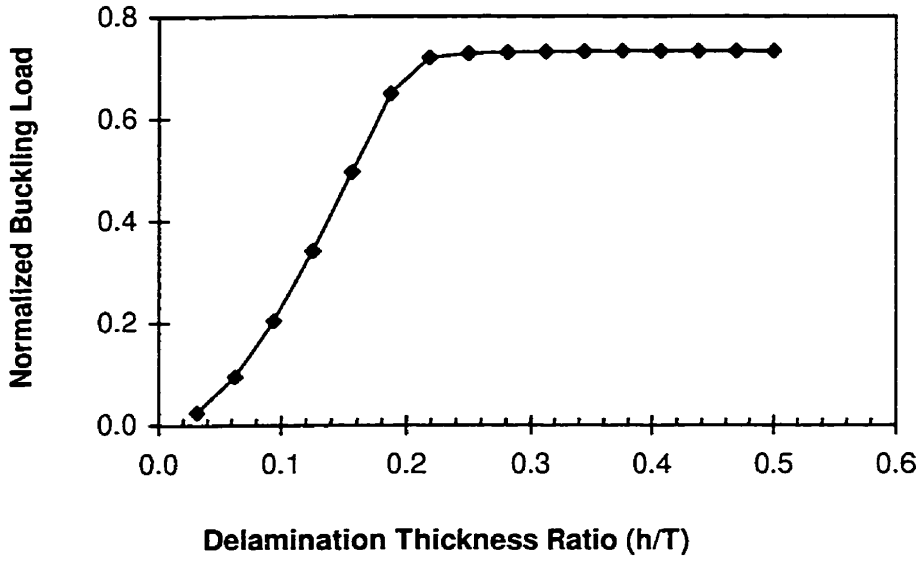

Figure 6.13. Effect of through-the-depth position of delamination on buckling load of $[(\pm 45)_{16}]$ laminates.

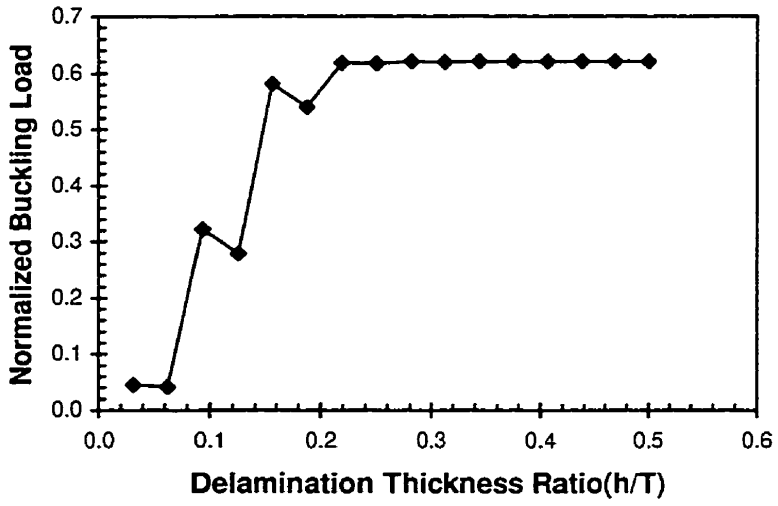

Figure 6.14. Effect of through-the-depth position of delamination on buckling load of $\left[(90/0)_{16}\right]$ laminates.

The buckling load oscillates in the beam-plates with thin delaminations; however, the response becomes quite consistent in the beams with thick delamination.

The effect of the same set of parameter for composites having a different ply sequence of $[(90_4/0_4)_4]$, is shown in Figure 6.15. The results indicate that when the delamination is located in between similarly oriented plies, the transition of the buckling load is smooth; on the other hand, when the delamination is located in between two dissimilarly oriented plies, the buckling response of the composite changes abruptly.

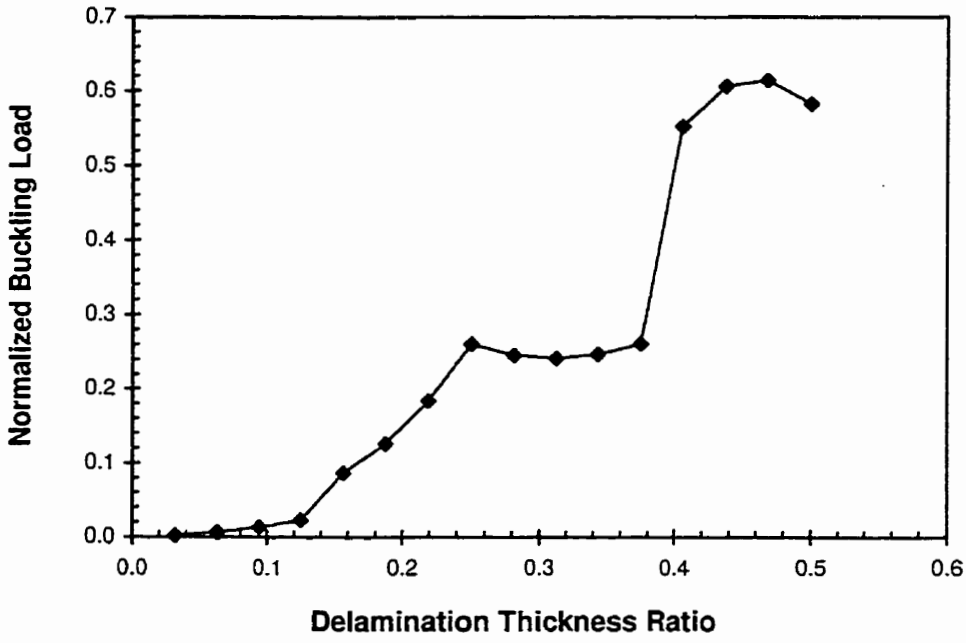

Figure 6.15. Effect of through-the-depth position of delamination on buckling load of $[(90_4/0_4)_4]$ laminates.

6.4.4. Effect of material properties

The type of materials used in formation of the composite was found to also have influence on the buckling response. Figure 6.16 illustrates the effects for three different types of composites, namely: graphite/epoxy, glass/epoxy and Kevlar/epoxy, having various delamination length ratios (a/L). Typical mechanical properties for these composites are tabulated in Table 6.4. All composites have ply sequence of $\left[(90/0)_4 / /(90/0)_{12}\right]$ with the delamination thickness ratio of h/T=0.25. Normalization of the buckling loads in Figure 6.16 was performed with respect to the modulus of glass/epoxy. The figure illustrates that the composite having the largest modulus (i.e., the graphite/epoxy) exhibits the highest buckling capacity regardless of delamination length, as it was expected.

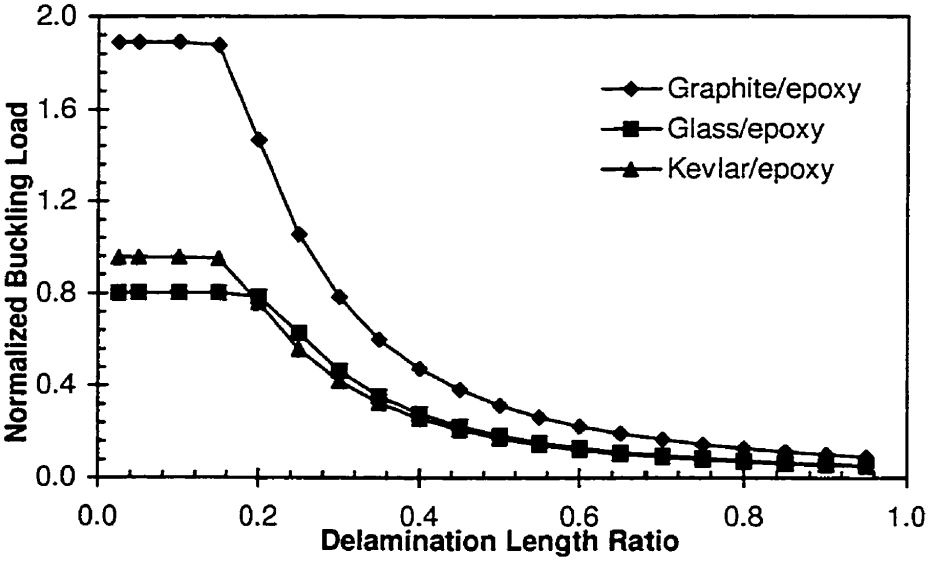

Figure 6.16. Effect of material properties on the buckling load.

6.4.5. Effect of the longitudinal position of delamination

The buckling response of $[(90_4/0_4)_4]$ graphite/epoxy beam-plates with a delamination positioned at various locations along their length is shown in Figure 6.17. The figure depicts the response of the laminate with thickness ratio of h/T=0.5, and $x_c = l + \frac{1}{2}a$. The results confirm that the buckling strength is significantly influenced by the location of the delamination. As it can be seen from Figure 6.17, the phenomenon is also a function of the delamination length. The decrease in the buckling strength is more significant in beam-plates with delamination length ratios between 0.2 to 0.6.

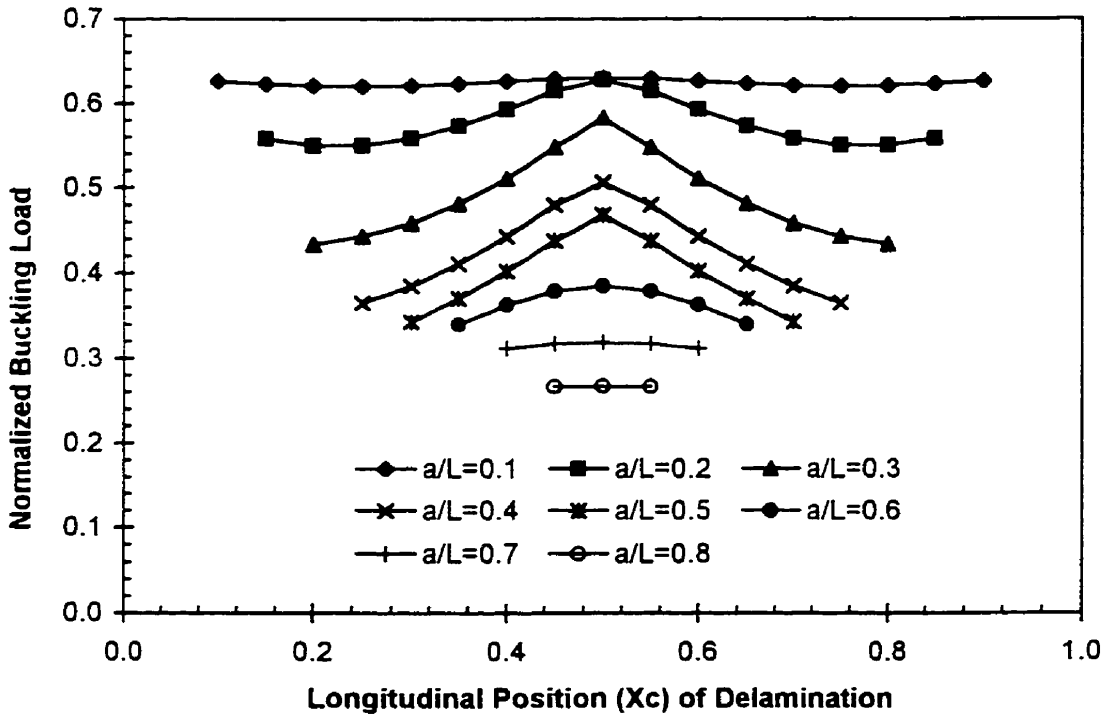

Figure 6.17. Effect of the longitudinal position of delamination on buckling load for a $[(90_4/0_4)_4]$ graphite/epoxy beam (h/T=0.5).

The influence of the longitudinal position of delamination on the buckling response of composite beam-plates, as the delamination position moves through the thickness of the beam-plates is shown in Figure 6.18. Here, the delamination has a length of a/L=0.3. It can be seen that the buckling load is affected only in those laminates with relatively thick delamination (when the delamination is on the interface of 12^{th} to 16^{th} plies).

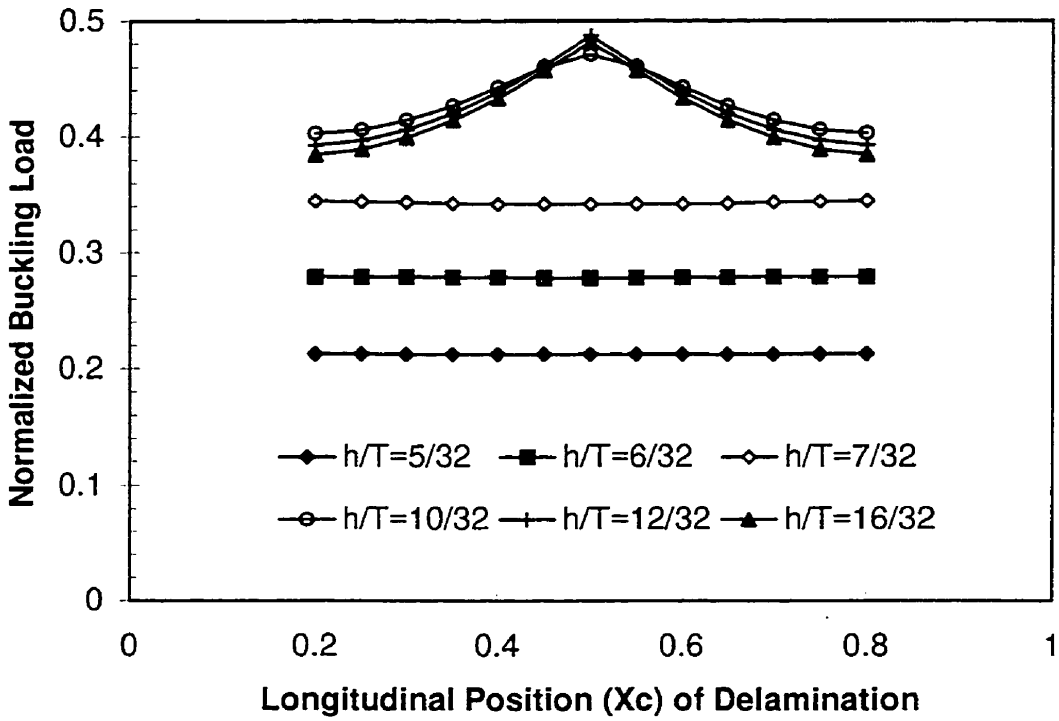

Figure 6.18. Effect of delamination location on buckling load for $[0]_{32}$ laminate.

6.4.6. Comparison between DQM and layer-wise model

Throughout this chapter the accuracy of the DQM, compare to finite element and analytical methods was shown for different delamination buckling models. Also its

efficiency was shown through the small number of sampling points needed to model the problem. A problem such as the delamination buckling analysis of a composite beam, with the inclusion of the shear deformation and bending-stretching coupling effects, could be modeled accurately by only 11 sampling points for each region of the model, or a total of 88 degrees of freedom (d.o.f), for the entire model.

The same problem was solved by Lee (1992) who employed a layer-wise finite element approach. Ten quadratic one-dimensional elements were used to model the full length of the beam. He used 252 d.o.f for the models without the coupling stiffness terms and 462 d.o.f for the cases including the coupling stiffness terms. Comparing the d.o.f used in the two methods clearly shows the efficiency of the DQM.

6.5. Case studies for buckling of a beam having multiple delaminations

In this part we will examine the case where beams having a number of delaminations, are subjected to compressive buckling load. As a first case, consider a specially orthotropic beam having equal length delaminations. The delaminations are through-the-width and could be anywhere through the beam longitudinal span.

6.5.1. Effect of the number of delaminations on the buckling load

Figure 6.19 shows the effect of number of delaminations on the buckling strength of the beam. This example is reconsidered from Suemasu (1993), where he used Rayleigh-Ritz approximation to solve for the buckling response of a multiply delaminated beam. The material properties are given in Table 6.5. The length and thickness of the beam are considered to be 160 mm and 3.8 mm, respectively. The effect of shear deformation is accounted by the shear deformation factor s. The number of delaminations is represented by N. They divide the clamped-clamped beam into $(N+1)$ regions with equal thickness.

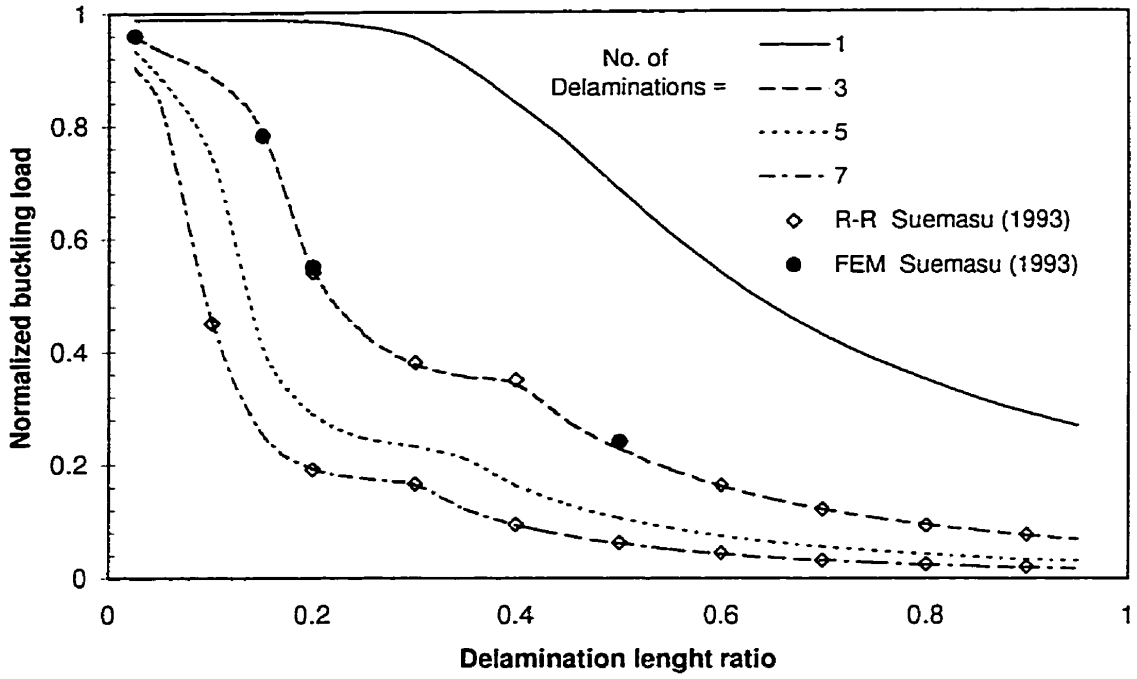

Figure 6.19. Normalized buckling load vs. delamination length ratio for multiple delaminations.

Here the buckling load is normalized with respect to the Euler buckling load of an intact beam. As shown in the figure, the results of the DQM are in very good agreement with those of the finite element and Rayleigh-Ritz calculations given by Suemasu (1993). Increasing the number of delaminations (and therefore reducing the thickness of delaminations) reduces the buckling load. Also the sharp changes in the curvature of all the curves are due to the changes in buckling modes. The first and the last regions of the curves are govern by symmetric modes while in the mid-region, the antisymmetric modes are the dominant modal shapes.

Table 6.5. Material properties used by Suemasu (1993).

E_1	20.2 Gpa
E_2	21.0 Gpa
E_3	10.0 Gpa
υ_{12}	0.16
υ_{13}	0.30
G_{12}	4.15 Gpa
G_{13}	4.0 Gpa

6.5.2. Effect of the longitudinal position of delaminations

The effects of the longitudinal position of delaminations on the buckling load are shown in figures 6.20 to 6.23 for different number of delaminations. As expected, the maximum buckling loads occur when the delaminations are in the center span of the beam. Changing the delamination position results in a decrease in the buckling load. This effect is more obvious in the case of small delaminations. Also, increasing the number of delaminations makes the beam less sensitive to the change in the longitudinal position of the delaminations. This is emphasized in Figure 6.24, where the normalized buckling loads are shown versus different delamination positions for different number of delaminations.

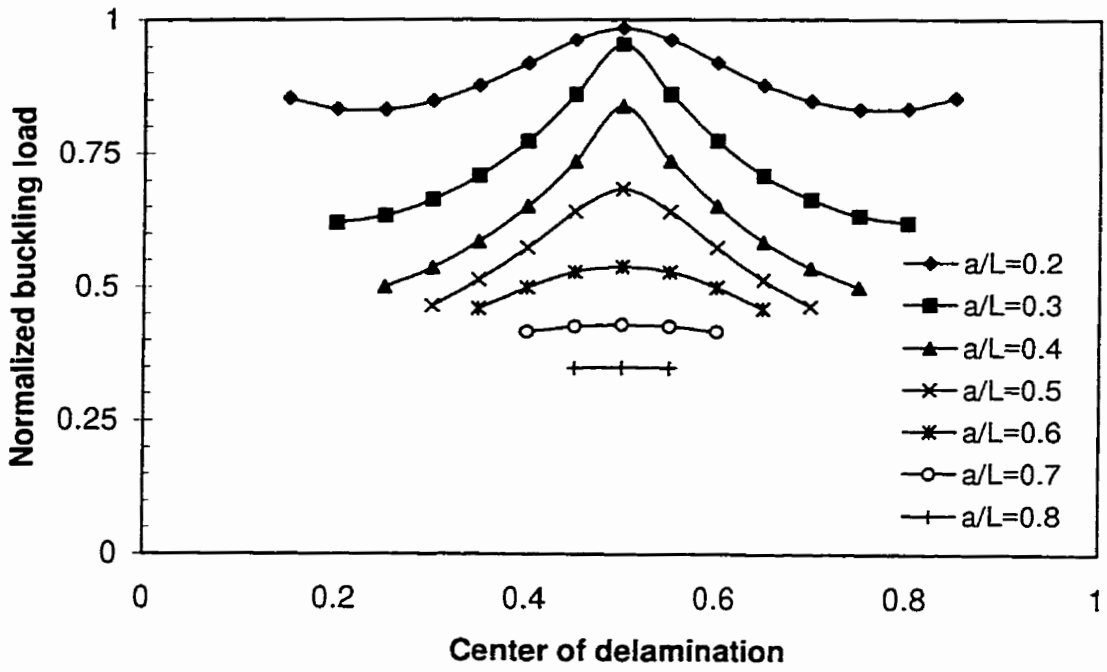

Figure 6.20. Effect of the longitudinal position of delamination on the buckling strength for a beam with single delamination.

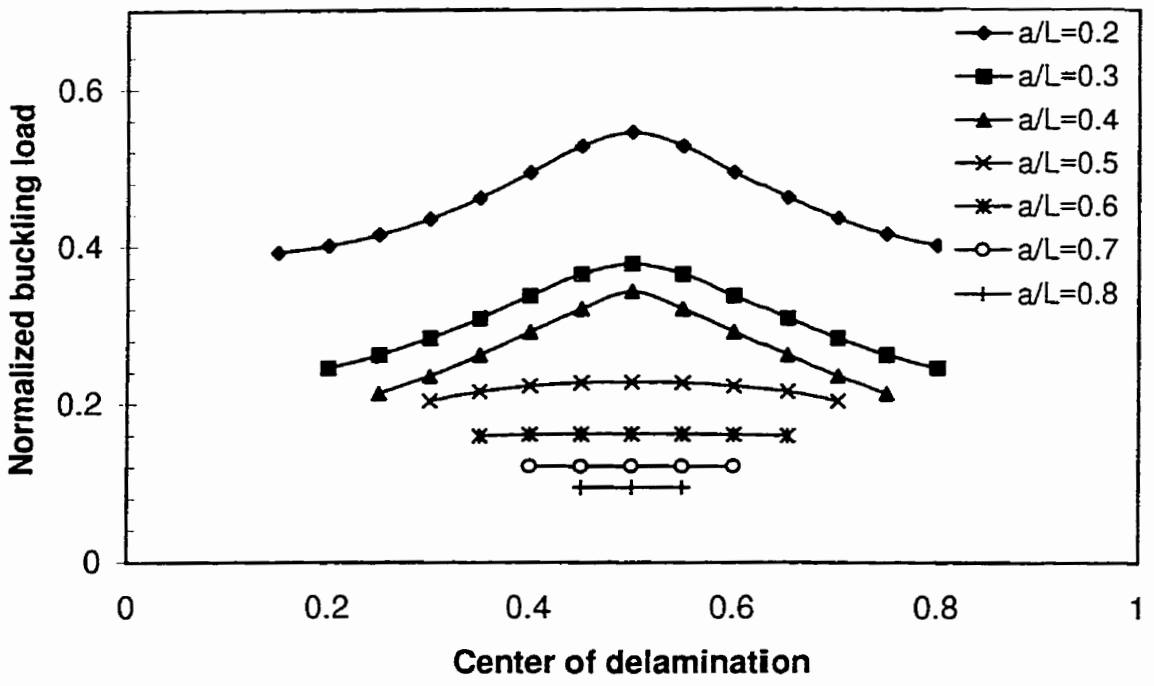

Figure 6.21. Effect of the longitudinal position of delamination on the buckling strength for a beam with three delaminations.

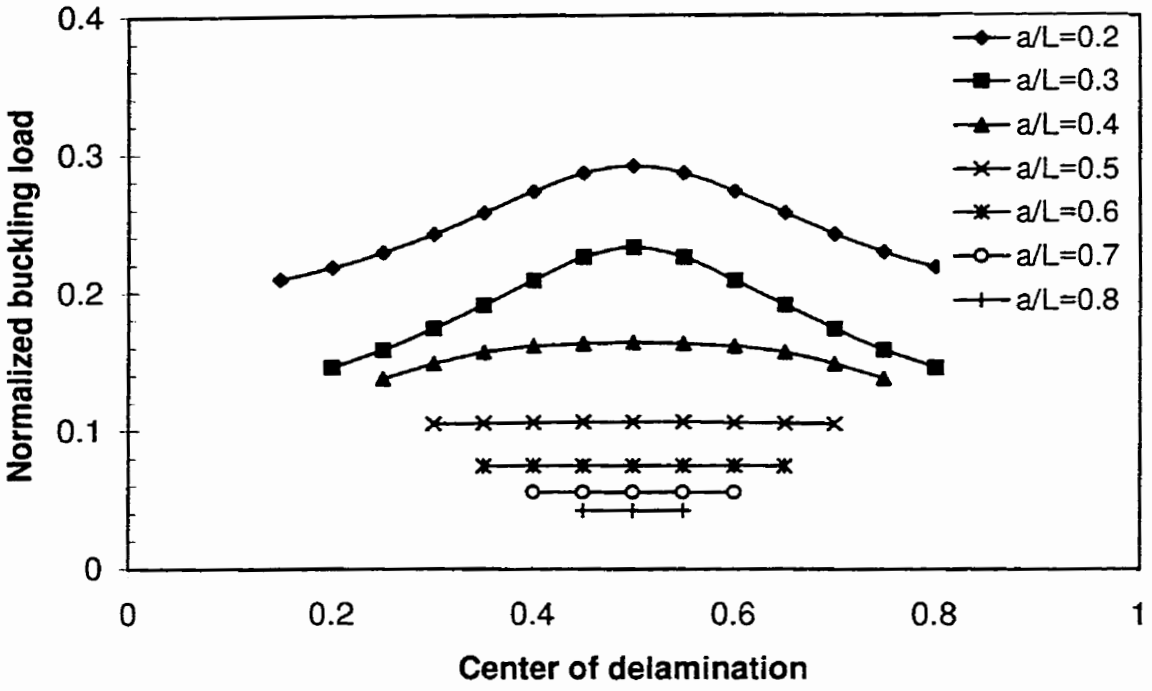

Figure 6.22. Effect of the longitudinal position of delamination on the buckling strength for a beam with five delaminations.

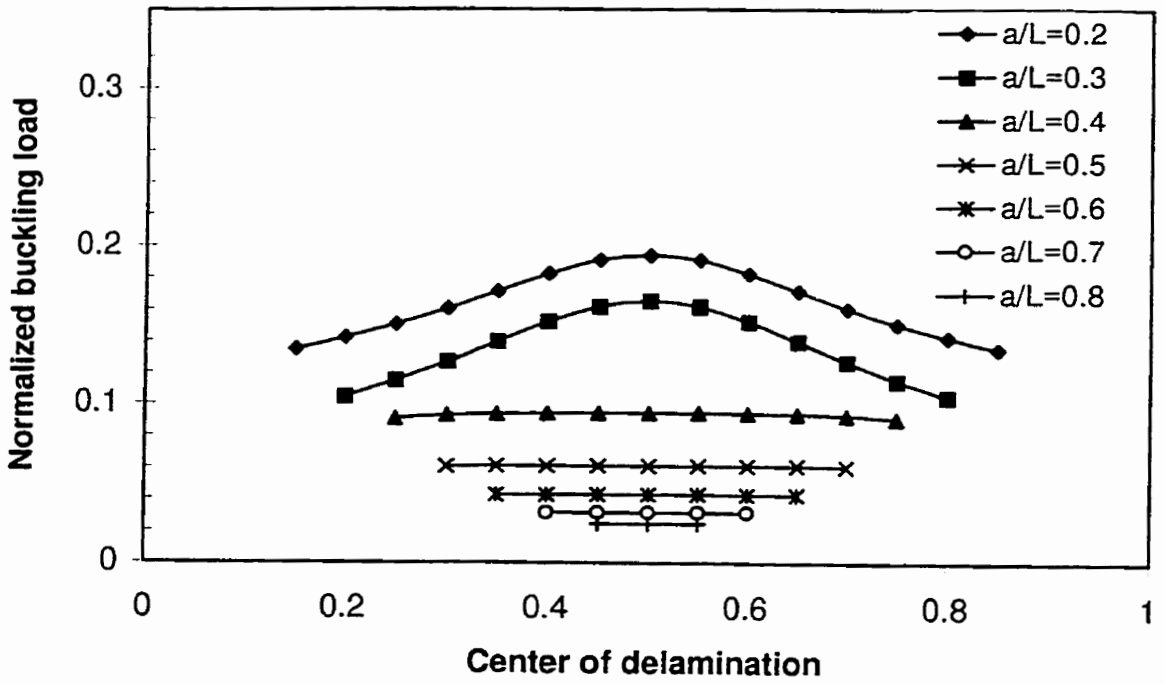

Figure 6.23. Effect of the longitudinal position of delamination on the buckling strength for a beam with seven delaminations.

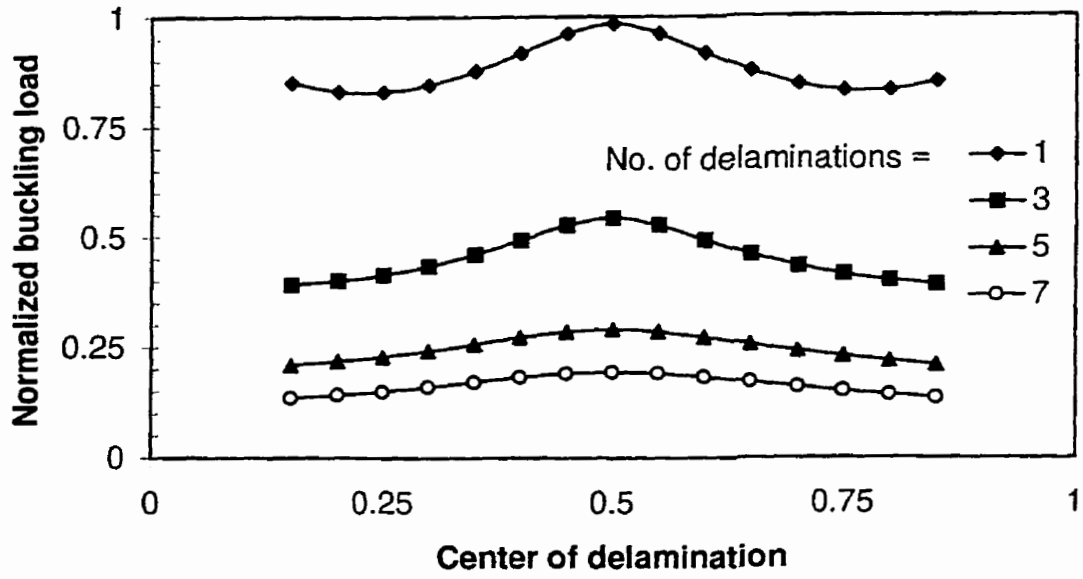

Figure 6.24. Comparison the effect of delamination longitudinal position on the buckling strength for a beam with different number of delaminations (a/L=0.2).

6.5.3. Effect of the length of delaminations

The effect of the different delamination lengths on the buckling load is shown in Figure 6.25. Here we consider clamped-clamped beams having two delaminations with different lengths, located symmetrically with respect to their mid-spans. Moreover, the delaminations are positioned symmetrically with respect to the mid-plane of the beams. While the length of the upper delamination in these beams varies, but the length of the lower one is fixed (a/L=0.3,0.4). The non-dimensional buckling load as a function of the non-dimensional delamination length of the upper delaminations for the case of thin (t/T=0.125) and thick (t/T=0.3) delaminations are presented in the figure. The results are

compared with those obtained from the finite element analysis conducted using the commercial package NISA (1996). Also, the results for the beams with a single delamination are shown in the figure. The figure indicates that as long as the length of the lower delamination is less than the length of the upper delamination (i.e. $a_2 > a_1$), the buckling strength of the beam is governed by the length of the upper delamination. This response is similar to the case where the beam hosts a single delamination.

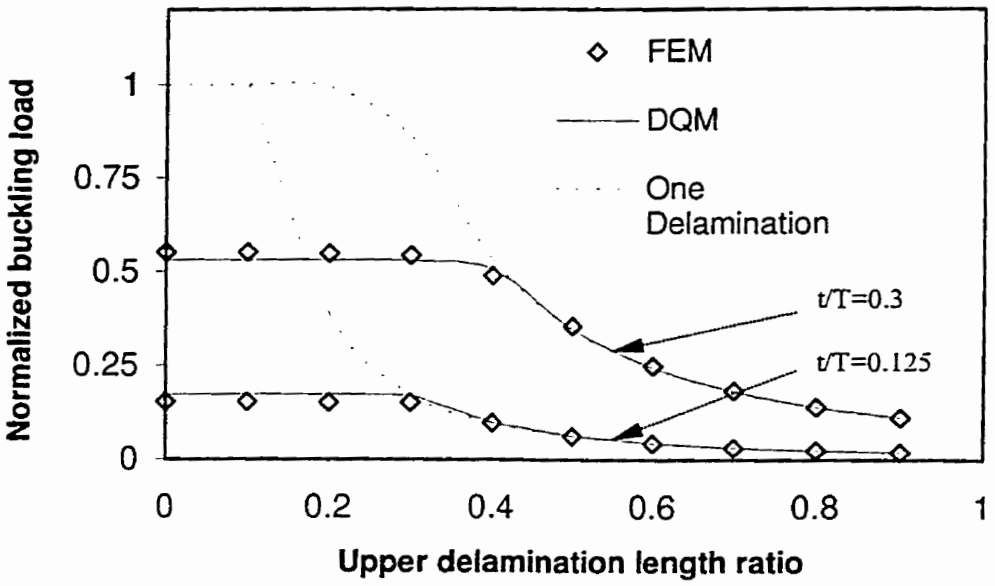

Figure 6.25. Response of beams hosting multiple delaminations with different lengths.

6.6. Case studies for buckling analysis of composite laminated plates with elliptical delamination

In this part the results of the application of DQM to the buckling analysis of laminated composite plates having elliptical delamination is discussed. These examples

are aimed at illustrating the numerical accuracy and efficiency of the proposed method. In particular, the differential quadrature results are compared with those of Shivakumar and Whitcomb (1985) and Heitzer and Feucht (1993). In both studies the authors used the Rayleigh-Ritz method and compared their solutions with the finite element results.

Using the mapping scheme introduced in chapter 3, the elliptical domain can be transferred into the equivalent computational domain. The calculations were carried out using cubic serendipity shape functions (even though the elliptical boundaries are quadratic, the mapping presented here can carry more complicated boundaries). The positions of the 12 points needed for this transformation are shown in Figure 6.26.

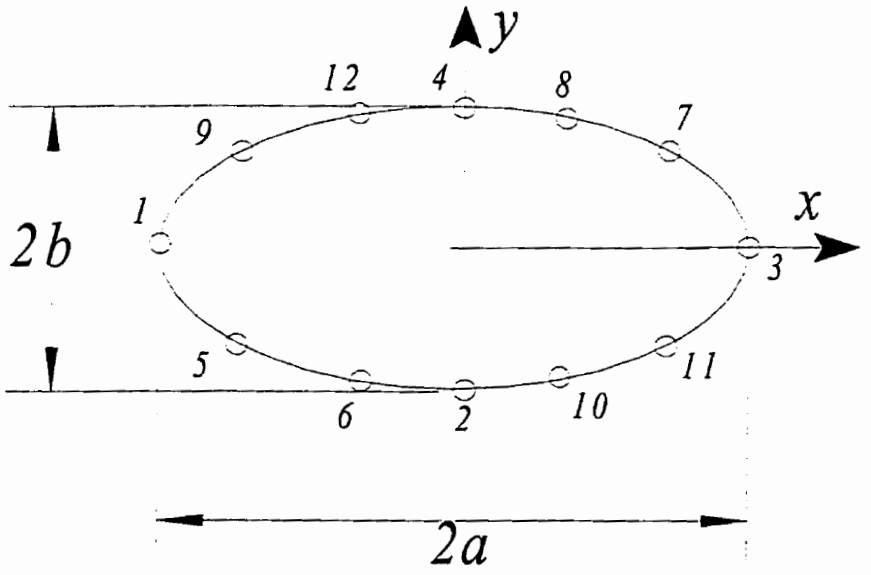

Figure 6.26. An elliptical domain.

The non-uniform sampling points along with δ-technique, as suggested by Bert and Malik (1996), are used by the following relations (see Figure 4.8):

$$\xi_1 = -1; \qquad \xi_2 = -1+\delta$$

$$\xi_i = -\cos\frac{(i-2)\pi}{N_\xi - 3} \qquad i = 3,4,\ldots,(N_\xi - 2) \tag{6.3}$$

$$\xi_{n_\xi - 1} = 1-\delta; \qquad \xi_{n_\xi} = 1$$

Similar sampling points were used for the η-direction. The material properties used here are those reported by Shivakumar and Whitcomb (1985) and Heitzer and Fuecht (1993), and are tabulated in Table 6.6.

Table 6.6. Material properties used by Shivakumar and Whitcomb (1985) and Heitzer and Feucht (1993).

	Shivakumar and Whitcomb (1985)		Heitzer and Feucht (1993)
	Aluminum	Graphite/epoxy	
E_1	68.95 GPa	131.0 GPa	230.0 GPa
E_2	68.95 GPa	13.0 GPa	7.0 GPa
υ_{12}	0.31	0.34	0.30
G_{12}	26.32 GPa	6.4 GPa	5.0 GPa

6.6.1. Effect of the sublaminate width on the buckling strain

Figure 6.27 shows the buckling strains versus different values of ellipse semi axis *b* for isotropic and specially orthotropic sublaminates ([0] laminate). The value of *a* is fixed at 25.4 mm, t=0.51mm and θ=0°. The finite element and Rayleigh-Ritz results by Shivakumar and Whitcomb are also shown in the figure. Their finite element model used triangular plate elements with eighteen degree-of-freedom to model a quarter of the

elliptical plate. A 8×12 mesh was used to model the isotropic and specially orthotropic sublaminates, while a 8×32 mesh was employed in modeling the anisotropic cases. As seen in the Figure 6.27, the DQM results agree well with those of the finite elements and the Rayleigh-Ritz methods.

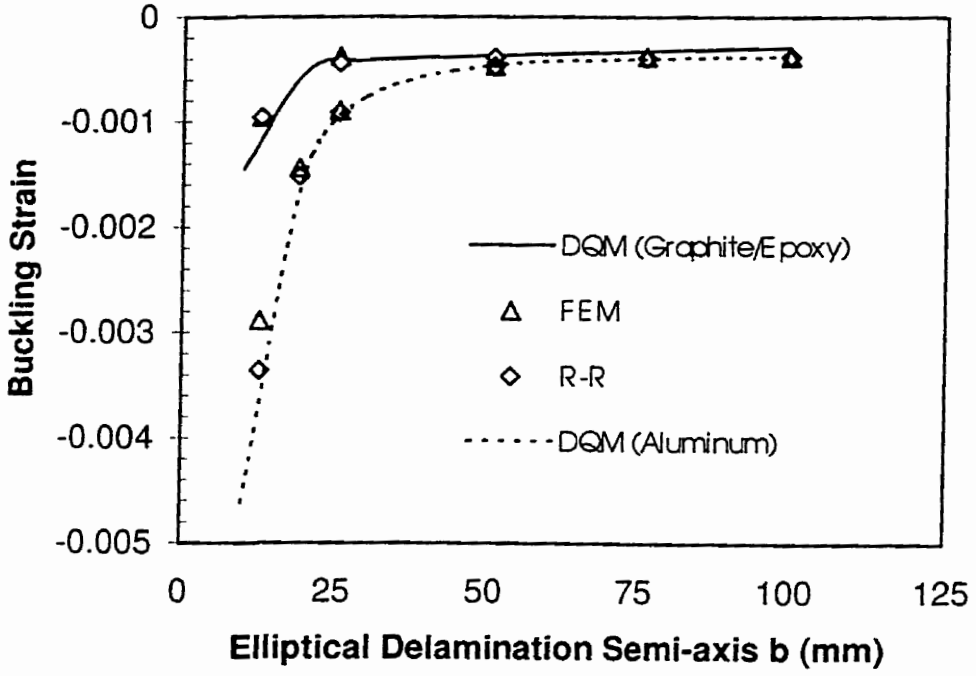

Figure 6.27. Effect of sublaminate width on buckling strain for different materials.

6.6.2. Effect of the fiber orientation on the buckling strain

The effect of the fiber orientation on the buckling strain for different delamination aspect ratios (a/b) is shown in Figure 6.28. The sublaminate fiber angle is successively rotated from 0° to 90° (with respect to the longitudinal, x-axis) for three different aspect ratios and the buckling strains are plotted. The finite element results are derived from Shivakumar and Whitcomb and plotted in the figure. The compression buckling strain

increases with the increasing fiber angle, but at a certain fiber angle the sublaminate can buckle under tensile strain (when the base laminate is loaded in tension). This is due to the mismatch between the Poisson ratios of the base laminate and the sublaminate (see Shivakumar and Whitcomb (1985)). As seen from the figure, increasing the aspect ratio results in an increase in the magnitude of the buckling strain.

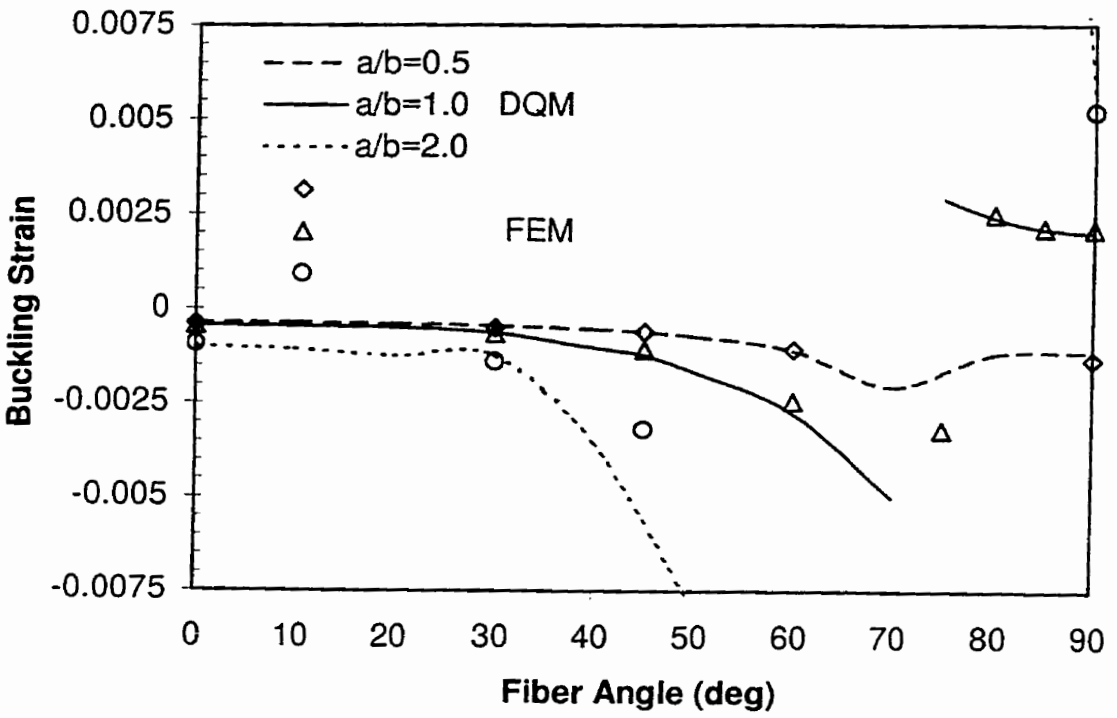

Figure 6.28. Effect of fiber angle on buckling strain for different aspect ratios (*a*=25.4 *mm*).

Figure 6.29 shows the effect of fiber angle on the buckling strain for an unsymmetric sublaminate. This example revisits the work of Heitzer and Feucht (1993), where their composite's sublaminate consisted of two plies, each of thickness 0.005 mm. One of the plies was successively rotated up to 90 degree. The delamination was

considered to have circular shape with a=1 mm. The results computed by DQM along with those of the finite elements and Rayleigh-Ritz of Heitzer and Feucht are plotted in this figure. They used two different meshes to model the circular and the elliptical delaminations. The circular mesh consisted of 784 four-noded plate elements and the elliptical mesh for the delamination with a=3mm and b=1mm, consisted of 652 three-noded plate elements. As for Rayleigh-Ritz method, they used a formulation with 12 and 21 constants. As seen, the DQM results are in better agreement with the FEM compared to the R-R. The inaccuracy in results of the R-R is contributed to the poor expansion of the in-plane displacements u and v used in their formulation. On the other hand, the in-plane displacements were not used in the DQM formulation (by using reduced stiffness concept).

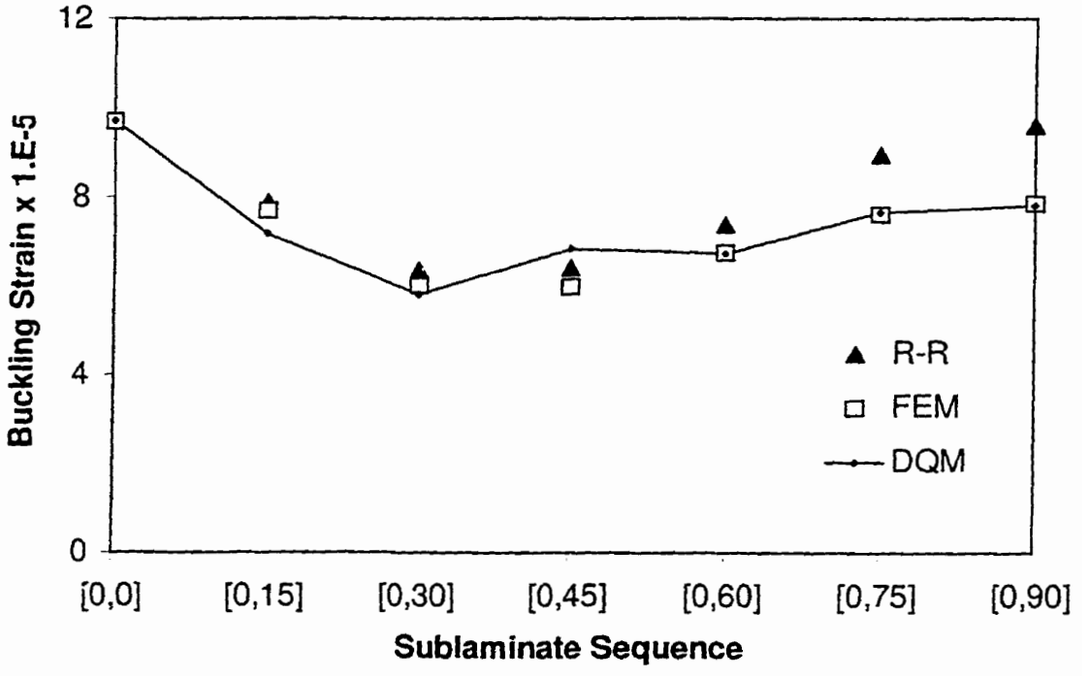

Figure 6.29. Effect of sublaminate sequence on buckling strain for circular delamination (a=1 mm).

6.6.3. Higher buckling modes

The comparisons between different numerical methods in computation of higher buckling modes are shown in Table 6.7. The first three buckling modes for an elliptical delamination (with a=3mm, b=1mm and t=0.01) composed of an unsymmetric [0/90] layup, oriented at θ=90° with respect to the loading direction is presented in this table. For the R-R method, only the first buckling mode is acceptable (compare to the finite element method) and the method exhibits fictitious higher stiffness for the higher modes. DQM, however, produces acceptable results for all the buckling modes.

Table 6.7. Buckling strains of higher modes for an elliptical delamination.

Mode	FEM	R-R	Error (%)	DQM	Error(%)
1	-3.41×10^{-5}	-3.51×10^{-5}	2.9	-3.24×10^{-5}	4.8
2	-4.76×10^{-5}	-1.31×10^{-4}	63	-4.55×10^{-5}	4.3
3	-6.77×10^{-5}	-1.84×10^{-4}	64	-6.19×10^{-5}	8.6

6.6.4. Effect of the number of sampling points on the buckling strain

Figure 6.30 shows the effect of the number of sampling points on the convergence of the buckling strain. The effect of grid spacing is shown for a circular delamination with a=1mm, b=1mm and an elliptical delamination with a=3mm, b=1mm. In both examples, the material is orthotropic, with thickness t=0.01mm and fiber angle θ=0°. Note that here, the numbers indicated on the horizontal axis represent the grid points in both horizontal and vertical directions, on the geometry. Therefore, the total numbers of grid points are the square of the number noted on the graph. Increasing the density of the

meshes, obviously improves the results, however, a 15×15 grid spacing is adequate for producing acceptable solutions.

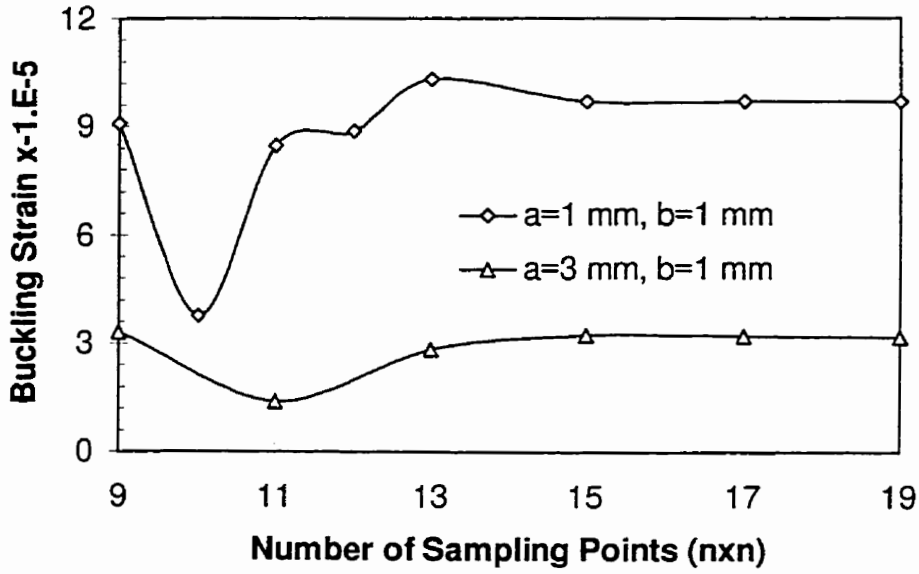

Figure 6.30. Effect of the no. of grid points on buckling strain for elliptical delamination.

6.7. Case studies for postbuckling analysis of laminated composite beams having single delamination

To show the validity of DQM in the postbuckling analysis of composite laminated beams with single delamination, some case studies were investigated. The first example is taken from Sheinman and Soffer (1991). A delaminated beam with the length L=4 m and thickness of T=0.08 m is shown in Figure 6.31.

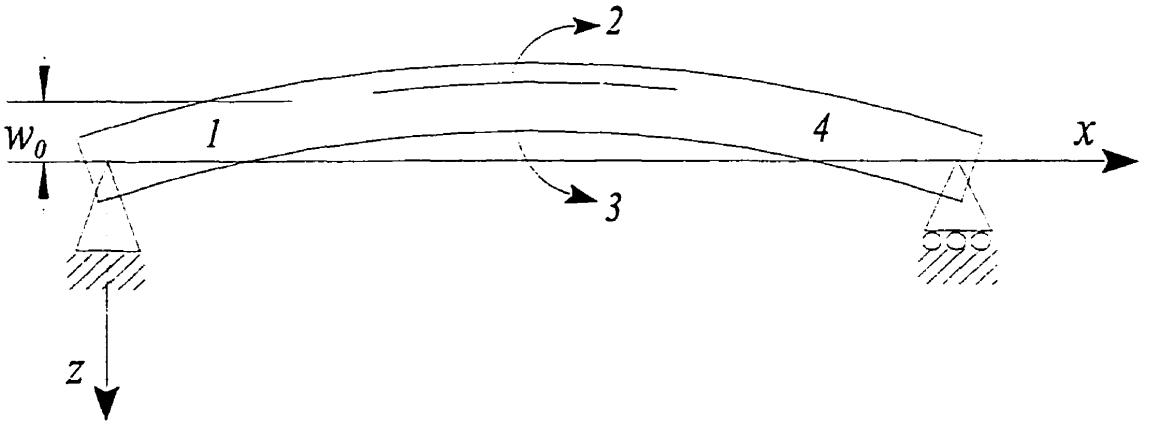

Figure 6.31. Geometry of an imperfect simply supported beam with a single delamination.

An across-the-width delamination with the length of a=1.5 m and thickness h=0.01 m is set at the mid-span of the beam (Figure 4.1). An initial imperfection exists in the form of $\overline{w}(x) = w_0 \sin(\pi x / L)$ (where w_0 is the imperfection amplitude). The material is isotropic. Figure 6.32 illustrates the resulting load-deflection curve evaluated at the midpoints of the sublaminates for positive imperfection amplitude. In this figure, the compressive load is normalized with respect to the Euler buckling load of the beam, as if it was intact. As seen in the figure, as the load reaches near the delamination buckling

load (P=0.442P_{cr}), the upper sublaminate starts to deflect in the positive direction and it buckles. By increasing the load the lower delamination starts to deflect and finally at a load near P=0.67P_{cr}, the system loses its load-carrying capacity.

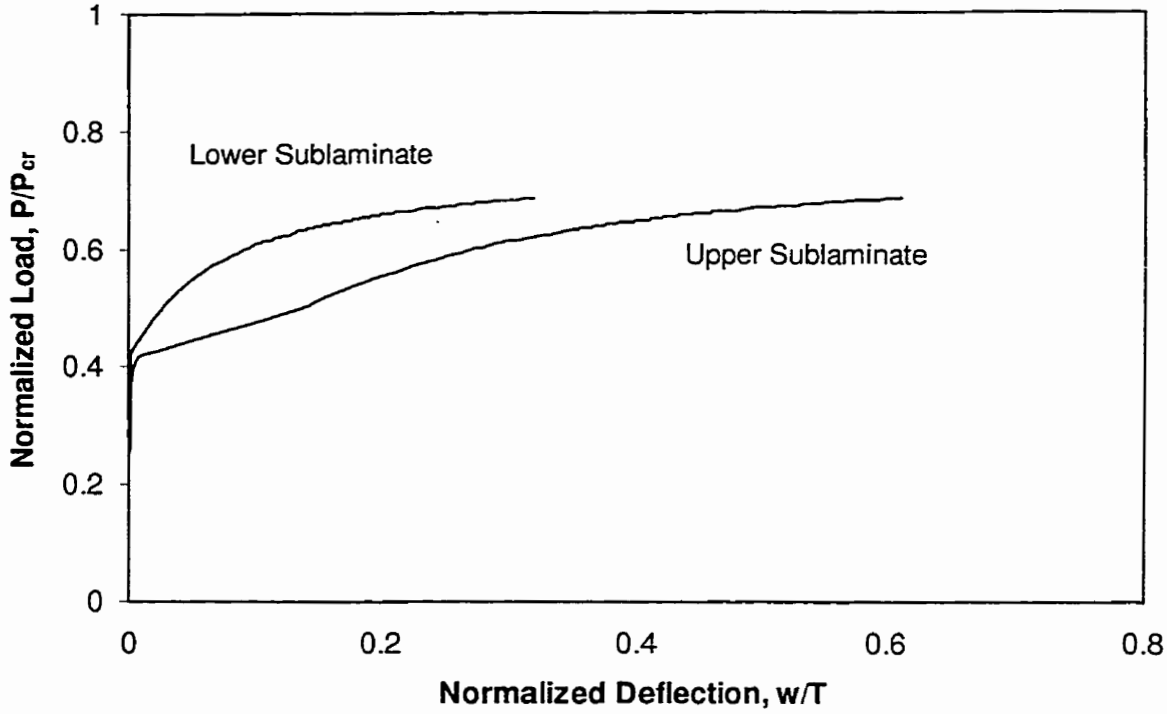

Figure 6.32. Load vs. mid-span deflection for w_0 =1×10^{-4}.

The same system produces a totally different response when the imperfection has a negative mode. As shown in Figure 6.33, as the load approaches the buckling load, the upper sublaminate start to deflect in the negative direction and the lower part gradually deflect in the positive direction. This causes the upper part to change its direction and

after a while it deflects in the positive direction. In the same graph the DQM results are compared with those of Sheinman et al (1993), and the results are in good agreement.

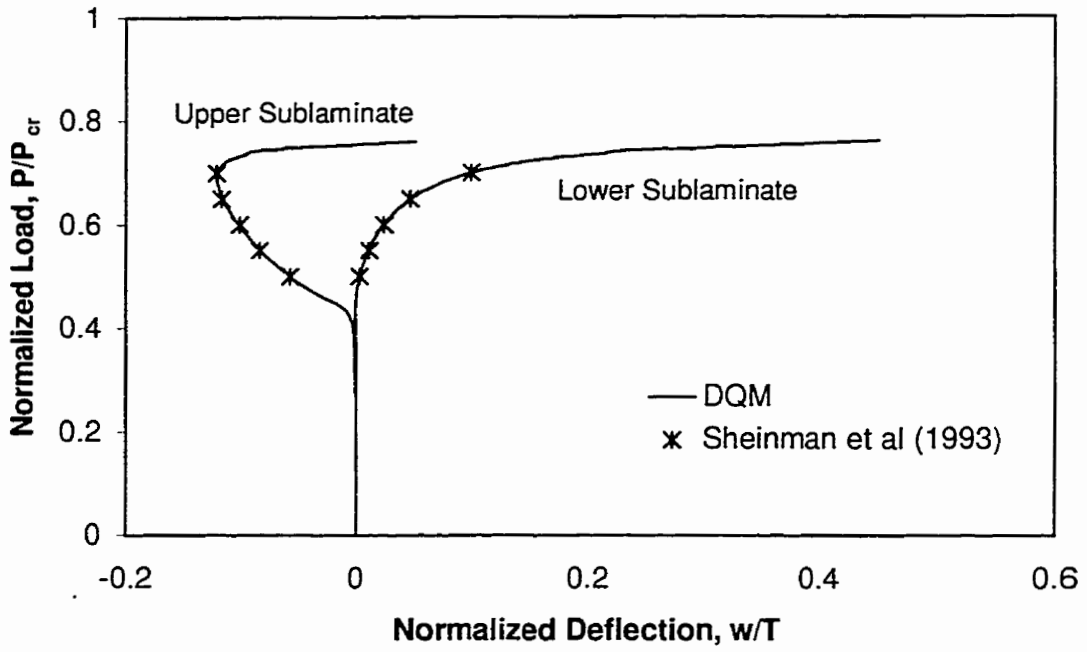

Figure 6.33. Load vs. mid-point deflection for $w_0 = -1\times10^{-4}$.

The response of a series of beams, each having a different delamination length, is shown in Figure 6.34. The results show that by increasing the delamination length, the buckling load decreases and the instability mode turns to a local buckling mode, and a decrease in the final load carrying capacity of the beam. This observation confirms that of Kim (1996). For a/L=0.2, the beam buckles globally, therefore, the upper and lower parts both buckle, almost simultaneously. On the other hand, for a relatively large delamination length ratio (i.e. a/L=0.6), the local buckling precedes the other buckling modes. In this case the upper part undergoes a large deformation before the buckling of the lower part.

For the intermediate delamination length ratios (i.e. a/L=0.4), both the upper and lower parts undergo considerable amount of deformation and the buckling mode is a combination of local and global modes which is usually referred to as mixed buckling mode.

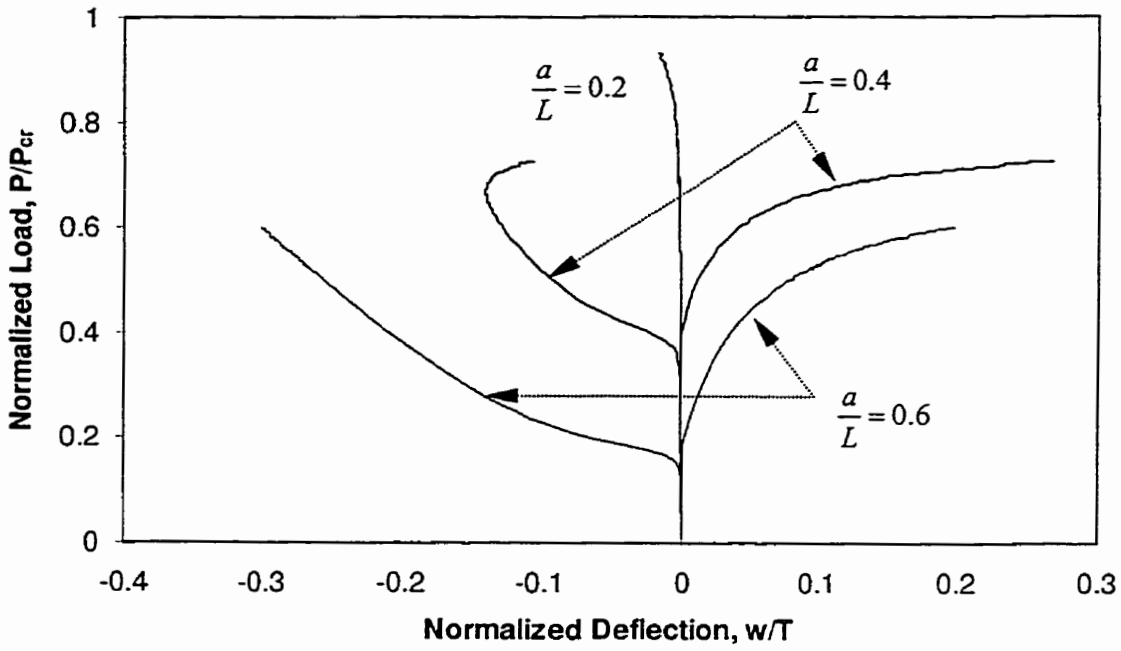

Figure 6.34. Load vs. mid-span deflection for various delamination lengths.

The effect of compressive load on the axial deformation of beams with different delamination length ratios is shown in Figure 6.35. Prior to buckling, the slopes of curves of the axial deformation vs. compressive applied load are the same for all delamination lengths. After the onset of buckling, beams start to lose their stiffness and the slope of the curves varies. The diverging in the stiffness accelerates near the final load capacity.

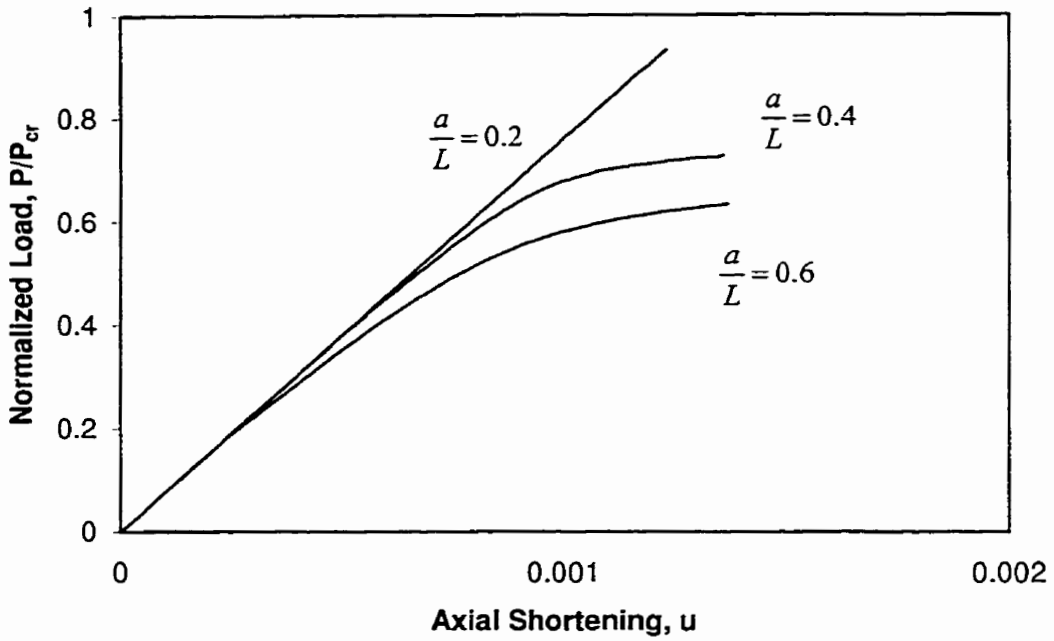

Figure 6.35. Load vs. axial shortening for various delamination lengths.

The effect of the imperfection amplitude on the load-carrying capacity of the beam is shown in Figure 6.36. Here, the same beam as discussed earlier is considered, but with different imperfection amplitudes. As seen in the figure, increasing the imperfection amplitude results in a significantly different response of the delaminated sublaminates; in the case of $w_o = -1\times10^{-2}$ the buckling behavior of the upper and lower sublaminates are almost indistinguishable.

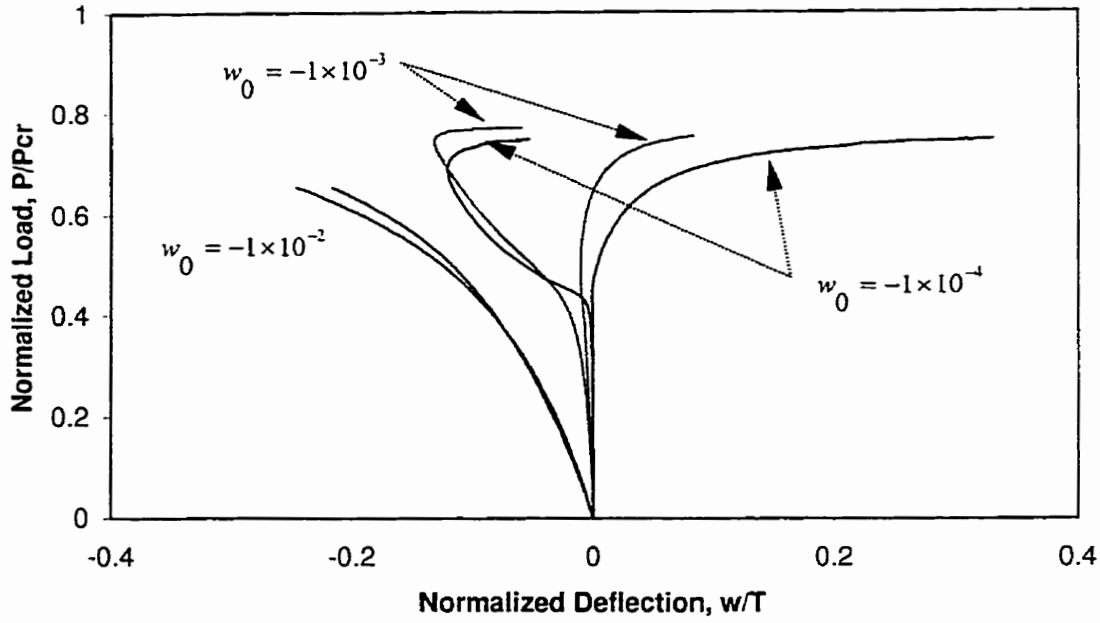

Figure 6.36. Load vs. mid-span deflection for various initial imperfections.

The next example considers a clamped-ended delaminated beam, derived from Lee (1992). A specially orthotropic composite laminated beam containing a single across-the-width delamination at its center with h/T=0.2 and a/L=0.3 is under axial compressive load. The material being used is T300/5208 graphite/epoxy, whose properties are given in Table 6.8. The thickness-to-span ratio is assumed to be T/L=1/400. The initial imperfection is in the form of

$$\overline{w} = \tfrac{1}{2} w_0 \left[1 - \cos\left(\frac{2\pi x}{L} \right) \right] \tag{6.4}$$

The response of the beam for an initial imperfection of w_o = -1×10^{-3} is shown in Figure 6.37 and 6.38. As the load approaches its buckling value, the upper sublaminate starts

deflecting in the negative direction (Figure 6.37), while the lower sublaminate gradually deflects in the positive direction. This will cause the upper sublaminate to reverse its displacement at a load about $P=0.7P_{cr}$, and then the layers lose their load-carrying capacity at around $P=0.8P_{cr}$. As shown in the figure, the DQM results are in good agreement with those extracted from Lee. The axial end shortening of the beam is shown in Figure 6.38. As the load nears the buckling load of the delaminated beam, the system starts losing its stiffness, and the phenomenon further accelerates as the load progresses toward the ultimate capacity of the beam.

Table 6.8. Material properties used by Lee (1992).

	T300/5208	(SMC-R50)
E_1	181.0 GPa	10.9 GPa
E_2	10.3 GPa	7.58 GPa
υ_{12}	0.28	0.31
υ_{13}	0.28	0.22
G_{12}	7.17 GPa	2.48 GPa
G_{13}	7.17 GPa	2.48 GPa

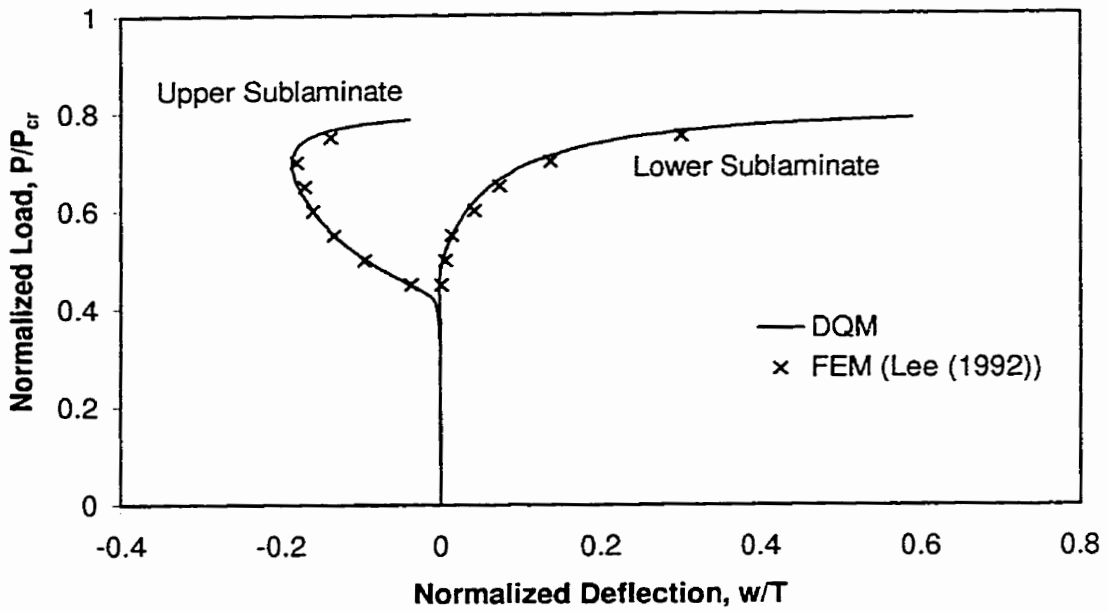

Figure 6.37. Load vs. mid-span deflection for a clamped beam.

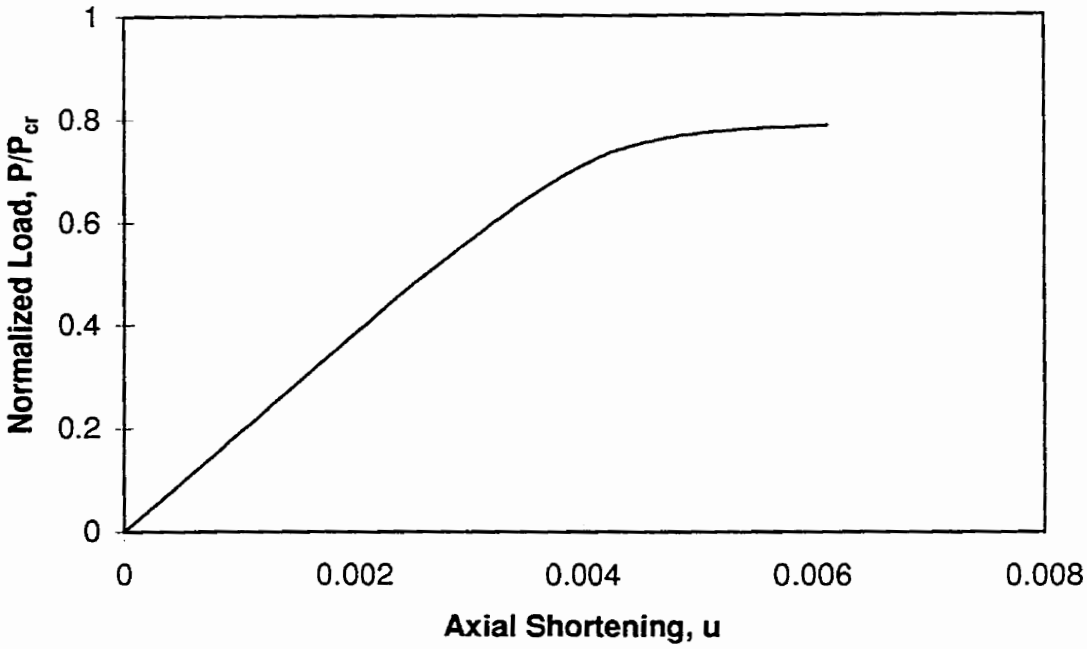

Figure 6.38. Load vs. axial shortening for a clamped beam.

6.8. Case studies for postbuckling analysis of composite laminated beams having multiple delaminations

To further verify the DQM, we also considered beams with multiple delaminations. For this, Lee et al's (1995) laminated composite clamped beam, having two equal length delaminations, symmetrically located with respect to the beam mid-plane was considered (Figure 6.39). The delaminations position, and length are h_1/T=0.125, h_2/T=0.125, a_1/L=0.3 and a_2/L=0.3, respectively. The material forming the beam was random short-fiber SMC-R50 composite with properties tabulated in Table 6.8. Dimensions of the beam were L=50 mm and T=1 mm as used by Kyoung et al (1998) (who considered the same problem).

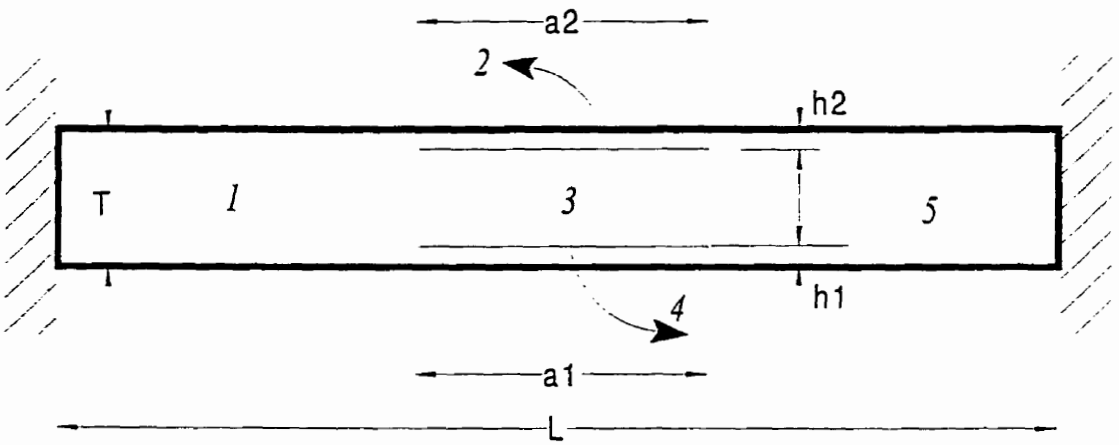

Figure 6.39. A clamped beam with two symmetric delaminations.

For this beam, the first two buckling modes were very close to each other. The initial imperfection shape, however, governed the buckling modes. The first buckling mode occurs when the initial imperfection of $w_o = 1\times10^{-3}$ is used for only the upper

sublaminate (in the shape of the first buckling mode). The load-deflection curve is shown in Figure 6.40. Here, the second delamination remains closed as if the beam contained only the upper delamination.

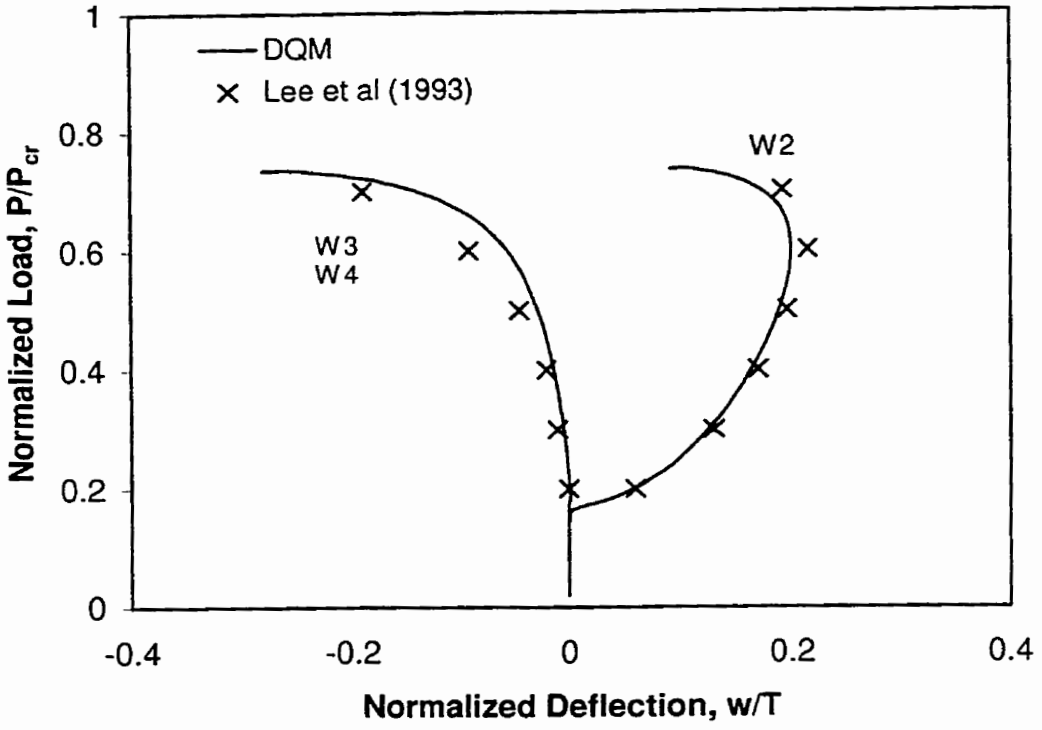

Figure 6.40. Load vs. mid-span deflection for clamped beam having two symmetric delaminations with imperfection of the first buckling mode (W2, W3 and W4 refer to the deflection of delaminated regions shown in Figure 6.39).

The progression of the compressive load through the delaminated region (region 2) is shown in Figure 6.41. Here P_{cr2} is the buckling load of the region 2. As seen from the figure, the increase of the load through the delaminated parts is proportional to the load increment up to the buckling point. After buckling, the stiffness in the upper delamination decreases, resulting in redistribution of the load among the sublaminates, and keeping the load in the upper sublaminate close to the buckling load.

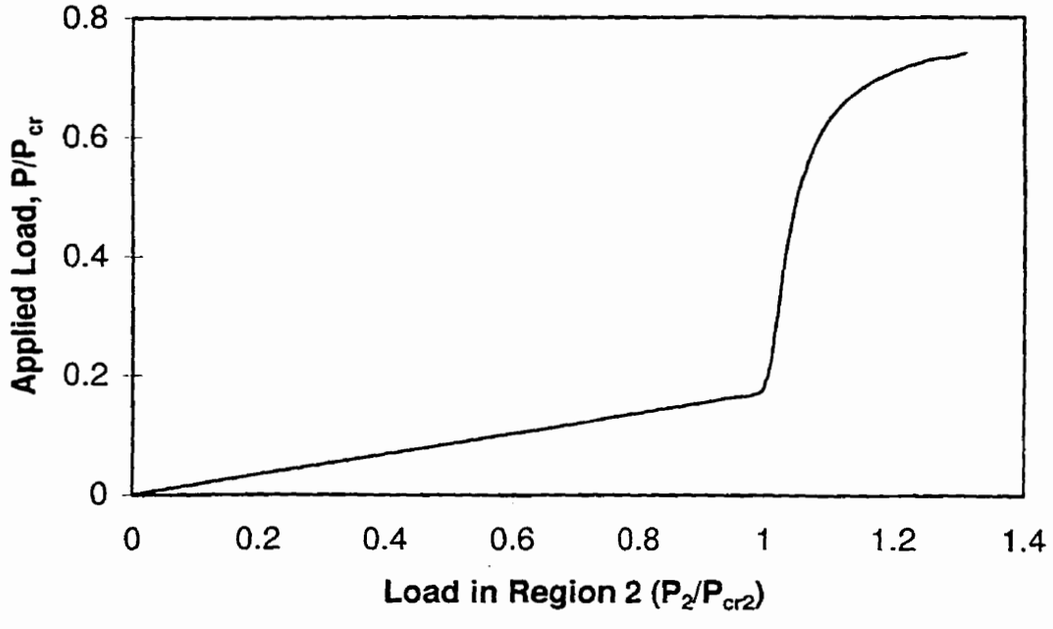

Figure 6.41. Variation of the load in region 2 (Figure 6.39) for a clamped beam having two symmetric delaminations with imperfection of the first buckling mode.

Applying an initial imperfection in the form of the second buckling mode (i.e., in the form that both upper and lower parts deform in opposite direction) results in opening of both upper and lower laminates, as shown in Figure 6.42.

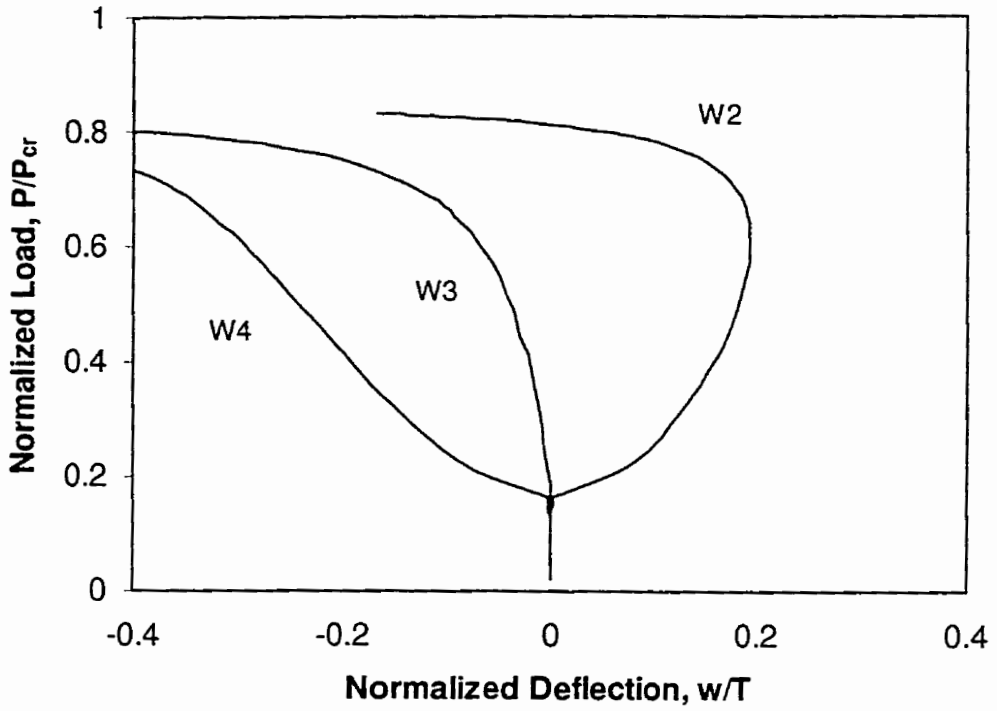

Figure 6.42. Load vs. mid-point deflection for clamped beam having two symmetric delaminations with imperfection of the second buckling mode (W2, W3 and W4 refer to the deflection of delaminated regions shown in Figure 6.39).

CHAPTER 7

CONCLUSIONS

7.1. Summary

Delamination buckling and postbuckling responses of composite laminated beams and plates were investigated. Using the differential quadrature method, one- and two-dimensional models were developed. The models were demonstrated to be capable of predicting the exact values of delamination buckling strengths and also accurately predicting the postbuckling response of the structures. For that, different configurations, such as beams with single and multiple through-the-width delaminations and plates with elliptical delaminations were studied. Several parameters, including the effect of shear deformation, the bending-stretching coupling, material properties, lamination sequence and fiber-orientation, were investigated. Also, the shape, size, number, initial geometrical imperfection, through-the-thickness and through-the-length location of the delaminations were studied parametrically.

Throughout the thesis, the DQM results were compared with those of the published analytical and numerical works or with those obtained by analyzing problem through the use of a commercial finite element package.

7.2. Conclusions

Based on the results of the author's investigations presented in the previous chapters, the following concluding remarks are made:

1) The thesis reports the first attempt in applying the differential quadrature analog to the delamination buckling of composite laminated structures.

2) DQM was shown to be capable of determining all possible buckling loads and their corresponding modes.

3) For a forth order differential equation (i.e., differential equilibrium equation of the Euler beam), the use of the δ-technique was found to enhance the accuracy of the solution. For such a problem, the use of the non-equally spaced grid schemes such as the Chebyshev or the Legendre, which allocate denser grid spacing near the boundaries, is recommended.

4) While using a grid spacing with an odd number of nodes is highly recommended, the author's experience indicates that a relatively low number of grid points can produce results with acceptable accuracy in the buckling analysis of delaminated composite structures. Mesh densities with 11 points per region for beams, and with 15 points per dimension for plates were shown to provide accurate results.

5) In delaminated beams, through-the-thickness and through-the-length position of the delamination can significantly influence their buckling behavior. An increase in the thickness of the delaminations with constant length can significantly boost their buckling strength. Also in beams with thick delaminations, and $0.2 < a/L < 0.6$, the eccentricity of the delaminations (with respect to the beam mid-span) can considerably alter their buckling strength. The buckling strength decreases as the delamination moves away from the mid-length of the beam.

6) The delamination buckling strength was found to be sensitive to the shear deformation. The buckling strengths are generally lower than those predicted by the classical laminate theory (CLT). Including the bending-stretching coupling effect, which is due to the non-symmetric laminations, significantly reduces the buckling load.

7) The buckling response of composite laminated plates having an elliptical thin delamination was also investigated by DQM. Using the serendipity shape functions, the physical domain was transferred into a quadrilateral computational domain. Then, the differential equilibrium equations of the sublaminate with clamped boundary conditions were formulated and solved. The DQM results were compared with those of the other numerical methods, and found to be numerically acceptable. The accuracy were achieved via less complex algorithms, compared to the other numerical approaches.

8) In order to solve for the buckling strains of an elliptical delamination, the author used the reduced bending stiffness approach. This resulted in a considerable reduction in the computational effort. In fact, instead of using the in-plane deformations (i.e. u and v) along with the out of plane deflection w as unknowns, it was shown that by using only one parameter, w, DQM could provide accurate results with minimal computational effort. The numerical results obtained as such were in good agreement with those obtained by the finite element method.

9) To the author's best knowledge, the present work is the first attempt in employing the DQM in the postbuckling analysis of composites. This was achieved by coupling the differential quadrature method with an arc-length strategy. The developed algorithm was applied to the postbuckling analysis of composite laminated plates, and single and multiply delaminated beams. The numerical results obtained through several case studies reconfirmed the excellent performance of the method.

The method was shown to have all the attributes and advantages that other popular numerical methods such as FDM, FEM and BEM have. In addition, it was shown that the method enjoys a mathematical foundation that is simpler to digest compared to those associated with the other numerical methods. Moreover, the implementation of the

method into a computer code is relatively easier. The efforts needed for setting up a problem, and for solving it with DQM is also relatively less in comparison to the other numerical methods. The only disadvantage of the proposed method at this stage of its evolution is that it is not as robust as FEM in accommodating problems with complicated geometries. This issue is however resolvable, as one can use the same type of remedy that is available for treating the same anomaly that exists with The FDM.

7.3. Recommendations for future works

The presented research was the basic step toward the implementation of differential quadrature technique for the buckling and postbuckling analysis of composite laminated structures having single or multiple delaminations. Therefore, in order to enhance the capability of the proposed approach, the following recommendations for future research are offered:

1) The presented approach may be employed in the buckling analysis of other laminated composite structures having delaminations, such as for composite shells with through-the-width or through-the-circumference delaminations.

2) The two-dimensional elliptical delamination model used in this study was based on the thin delamination approach. A more general approach for considering the position of a delamination (i.e., through-the-thickness and through-the-plane of the plate) should be explored. This requires a domain decomposition approach, and therefore, a significant increase in the size of the problem.

3) The presented postbuckling analysis of beams having single or multiple delaminations did not account for the growth of the delamination. Therefore, a crack growth analysis to account for the delamination propagation, and the implementation of appropriate failure criteria will be worth an initiative.

4) Moreover, the presented approaches did not account for contact between delaminated regions. Including this effect may change the response of the delaminated beams and plates significantly, therefore, research into inclusion of such a phenomenon is highly recommended.

5) Only the effect of compressive axial loads was considered in the current study. The buckling and postbuckling analyses of delaminated composite structures subjected to a combined state of loading, such as combinations of shear, bending, compressive and thermal loads are recommended.

6) The final matrices resulting from applying DQM to the different problems are non-symmetric, therefore require non-symmetric solvers. Incorporation of various methods for converting the matrices into symmetric matrices is also recommended. For this, one may use the idea of energy finite difference approach used in conjunction with the finite difference method.

REFERENCES

Barbero, E. J. and Reddy, J. N., (1991) Modeling of Delamination in Composite Laminates Using a Layer-Wise Plate Theory, International Journal of Solids and Structures, vol. 28, pp. 373-388.

Batoz, J. –L. and Dhatt, G., (1979) Incremental Displacement Algorithms for Nonlinear Problems, International Journal for Numerical Methods in Engineering, vol. 14, pp. 1262-1267.

Bellman, R. E., Kashef B. G. and Casti, J., (1972) Differential Quadrature: A Technique for Rapid Solution of Nonlinear Partial Differential Equations, J. Computer Physics, vol. 10, pp. 40-52.

Bellman, R. E. and Roth, R. S., (1986) in: Methods in Approximation, D Reidel Publishing, Dordrecht, Netherlands.

Bert, C. W., Jang, S. K. and Striz, A. G., (1988) Two New Approximate Methods For Analyzing Free Vibration of Structural Components, AIAA Journal, vol. 26, pp. 612-618.

Bert, C. W., Jang, S. K. and Striz, A. G., (1989) Nonlinear Bending Analysis of Orthotropic Rectangular Plates by the Method of Differential Quadrature, Computational Mechanics, vol. 5, pp. 217-226.

Bert, C. W., Wang, X. and Striz, A. G., (1993) Differential Quadrature for Static and Free Vibration Analysis of Anisotropic Plates, International Journal of Solids and Structures, vol. 30, pp. 1737-1744.

Bert, C. W., Wang, X. and Striz, A. G., (1994) Static and Free Vibration Analysis of Beams and Plates by Differential Quadrature Method, Acta Mechanica, vol. 102, pp. 11-24.

Bert, C. W. and Malik M., (1996a) Differential Quadrature Method in Computational Mechanics: A Review, Applied Mechanics Review, vol. 49, pp. 1-28.

Bert, C. W. and Malik M., (1996b) The differential Quadrature Method for Irregular Domains and Application to Plate Vibration, International Journal of Mechanical Science, vol. 38, pp. 589-606.

Bert, C. W. and Malik M., (1996c), Implementing Multiple Boundary Conditions in the DQ Solution of Higher-Order PDE's: Application to Free Vibration of Plates,

International Journal for Numerical Methods in Engineering, vol. 39, pp. 1237-1258.

Bhimaraddi, A., (1992) Buckling and Post-Buckling Behavior of Laminated Plates Using the Generalized Nonlinear Formulation, International Journal of Mechanical Science, vol. 34, pp. 703-715.

Bottega, W. J., and Maewal, A., (1983) Delamination Buckling and Growth in Laminates, Journal of Applied Mechanics, vol. 50, pp. 184-189.

Cairns, D. S., Minguet, P. J., and Abdallah, M. G., (1994) The Influence of Size and Location on the Response of Composite Structures with Delaminations Loaded in Compression, Proceedings of the 35th AIAA/ASME/ASCE/AHS/ASC Structures, Structural Dynamics, and Material Conference, v5, AIAA, New York, NY, USA, pp. 2815-2825.

Chai, H., Babcock, C. D., and Knauss, G., (1981) One Dimensional Modeling of Failure in Laminated Plates by Delamination Buckling, International Journal of Solids and Structures, vol. 17, pp. 1069-1083.

Chai, H., and Babcock, C. D., (1985) Two-Dimensional Modeling of Compressive Failure in Delaminated Laminates, J. of Composite Materials, vol. 19, pp. 67-98.

Chai, H., (1990a) Buckling and Post-Buckling Behavior of Elliptical Plates: Part I-Analysis, J. of Applied Mechanics, vol. 57, pp. 981-988.

Chai, H., (1990b) Buckling and Post-Buckling Behavior of Elliptical Plates: Part II-Results, Journal of Applied Mechanics, vol. 57, pp. 989-994.

Chang, F. K., and Kutlu, Z., (1989) Collapse Analysis of Composite Panels with Multiple Delaminations, Proceeding of AIAA/ASME/ASCE/AHS 30th Structures, Structural Dynamics, and Material Conference, Mobile, AL, USA, pp. 989-999.

Chattopadhyay, A. and Gu, H.,(1994) New Higher Order Plate Theory in Modeling Delamination Buckling of Composite Laminates, AIAA Journal, vol. 32, pp. 1709-1716.

Chen, H. P., (1991) Shear Deformation Theory for Compressive Delamination Buckling and Growth, AIAA Journal, vol. 29, pp. 813-819.

Chen, H. P., (1993) Transverse Shear Effects on Buckling and Postbuckling of Laminated and Delaminated Plates, AIAA Journal, vol. 31,pp. 163-169.

Chen, H. P. and Chang, W. C., (1994) Delamination Buckling Analysis for Unsymmetric Composite Laminates, 39th International SAMPE Symposium, pp. 2855-2867.

Chen, W., Striz, A. G., and Bert, C. W., (1997) A New Approach to the Differential Quadrature Method for Forth-Order Equations, International Journal for Numerical Methods in Engineering, vol. 40, pp. 1941-1956.

Clarke, M. J. and Hancock, G. J., (1990) A Study of Incremental-Iterative Strategies for Non-linear Analysis, International Journal for Numerical Methods in Engineering, vol. 29, pp. 1365-1391.

Cox, B. N., (1994) Delamination and Buckling in 3D Composites, Journal of Composite Materials, vol. 28, pp. 1114-1126.

Crisfield, M. A., (1981) A fast Incremental/Iterative Solution Procedure That Handles Snap Through, Computers & Structures, vol. 13, pp. 55-62.

Crisfield, M. A., (1983) An Arc-length Method Including Line Searches and Accelerations, International Journal for Numerical Methods in Engineering vol. 19, pp. 1269-1289.

Davidson, B. D., (1991) Delamination Buckling: Theory and Experiment, Journal of Composite Materials, vol. 25, pp. 1351-1378.

Davidson, B. D. and Krafchak, T. M., (1995) A Comparison of Energy Release Rates for Locally Buckled Laminates Containing Symmetrically and Asymmetrically Located Delaminations, Journal of Composite Materials, vol. 29, pp. 700-713.

Dost, E. F., Ilcewicz, L. B. and Gosse, J. H., (1988) Sublaminate Stability Based Modeling of Impact-Damaged Composite Laminates, Proceedings of the American Society for Composites, Third Technical Conference on Composite Materials, pp. 354-363.

El-Aini, Y. M., (1975) A Nonlinear Analysis for One-Way Buckling of a Laterally Loaded Column, Journal of Mechanical Engineering Science, vol. 17, pp. 150-154.

Farsa, J., Kukerti, A. R., and Bert, C. W., (1993) Fundamental Frequency Analysis of Single Specially Orthotropic, Generally Orthotropic and Anisotropic Rectangular Layered Plates by the Differential Quadrature Method, Computers & Structures, vol. 46, pp. 465-477.

Farsa, J. and Kukerti, (1993) Fundamental Frequency Analysis of Laminated Rectangular Plates by Differential Quadrature Method, International Journal for Numerical Methods in Engineering, vol. 36, pp. 2341-2356.

Ferrigno A., La Barbera A., and Perugini P., (1995) An engineering assessment of the static residual strength of composite laminates with impact induced damages: integrated procedure based on 3D FEM and 2D theoretical analysis and

experimental investigations, Proceedings of ICCM-10, Whistler, B. B., Canada, vol. 5, pp. 679-686.

Forde, B. W. R. and Stiemer, S. F., (1987) Improved Arc Length Orthogonality Methods for Nonlinear Finite Element Analysis, Computers & Structures, vol. 27, pp. 625-630

Gaudenzi, P., (1997) On Delamination Buckling of Composite Laminates Under Compressive Load, Composite Structures, vol. 39, pp. 21-30.

Haisler, W. E. and Stricklin, J. A., (1977) Displacement Incrementation in Nonlinear Structural Analysis by the Self-correcting Method, International Journal for Numerical Methods in Engineering, vol. 11, pp. 3-10.

Han, J. –B. and Liew, K. M., (1997) An Eight-node Curvilinear Differential Quadrature Formulation for Reissner/Mindlin Plates, Computer Methods in Applied Mechanics and Engineering, vol. 141, pp. 265-280.

Heitzer J., and Feucht M., (1993) Buckling and Postbuckling of Thin Elliptical Anisotropic Plates, Computers & Structures, vol. 48, pp. 983-992.

Huang, H. and Kardomateas, G. H., (1997) Post-Buckling Analysis of Multiply Delaminated Composite Plates, Journal of Applied Mechanics, vol. 64, pp. 842-846.

Jang, S. K., Bert, C. W., and Striz, A. G., (1989) Application of Differential Quadrature to Static Analysis of Structural Components, International Journal for Numerical Methods in Engineering, vol. 28, pp. 561-577.

Kang, K. J., Bert, C. W., and Striz, A. G., (1996) Vibration and Buckling Analysis of Circular Arches Using DQM, Computers & Structures, vol. 60, pp. 49-57.

Kardomateas, G. A. and Schmueser, D. W., (1988) Buckling and Postbuckling of Delaminated Composites Under Compressive Loads Including Transverse Shear Effects, AIAA Journal, vol. 26, pp. 337-343.

Kardomateas, G. A., (1989) Large Deformation Effects in the Postbuckling Behavior of Composites with Thin Delaminations, AIAA Journal, vol. 27, pp. 624-631.

Kardomateas, G. A., (1993) The Initial Post-Buckling and Growth Behavior of Internal Delaminations in Composite Plates, Journal of Applied Mechanics, vol. 60, pp. 903-910.

Kardomateas, G. A., and Pelegri, A. A., (1994) The Stability of Delamination Growth in Compressively Loaded Composite Plates, International Journal of Fracture, vol. 65, pp. 261-276.

Kim, Y., Na, M. S., and Im, S., (1996) Delamination Buckling of a Short Orthotropic Tube Under Axial Compression, Computers & Structures, vol. 58, pp. 173-182.

Kim, H. J., (1996) Effect of Delamination on Buckling Behavior of Quasi-Isotropic Laminates, Journal of Reinforced Plastics and Composites, vol. 15, pp. 1262-1277.

Kim, H. J., (1997) Postbuckling Analysis of Composite Laminates with a Delamination, Computers & Structures, vol. 62, pp. 975-983.

Kukerti, A. R., Farsa, J. , and Bert, C. W., (1992) Fundamental Frequency of Tapered Plates by Differential Quadrature, ASCE Journal of Engineering Mechanics, vol. 118, pp. 1221-1238.

Kutlu, Z., and Chang, F., (1992) Modeling Compression Failure of Laminated Composites Containing Multiple Through-the-Width Delaminations, Journal of Composite Materials, vol. 26, pp. 350-387.

Kyoung, W. M. and Kim, (1995) C. G., Delamination Buckling and Growth of Composite Laminated Plates with Transverse Shear Deformation, Journal of Composite Materials, vol. 29, pp. 2047-2068.

Kyoung, W. M., Kim, C. G., Hong, C. S., and Jun, S. M., (1998) Modeling of Composite Laminates with Multiple Delaminations Under Compressive Loading, Journal of Composite Materials, vol. 32, pp. 951-968.

König, M., Krüger, R., and Rinderknecht, S., (1995) Numerical Simulation of Delamination Buckling and Growth, Proceeding of ICCM-10, Whistler, B.C., Canada, vol. 1, pp. 269-276.

Lam, S. S. E., (1993) Application of the Differential Quadrature Method to Two-Dimensional Problems with Arbitrary Geometry, Computers & Structures, vol. 47, pp. 459-464.

Lanzo, A. D., Garcea, G. and Casiaro, R., (1995) Asymptotic Post-Buckling Analysis of Rectangular Plates by HC Finite Elements, International Journal for Numerical Methods in Engineering, vol. 38, pp. 2325-2345.

Larsson, P., (1991) On Multiple Delamination Buckling and Growth in Composite Plates, International Journal of Solids and Structures, vol. 27, pp. 1623-1637.

Laura, P. A. A. and Gutierrez, R. H., (1994) Analysis of Vibrating Rectangular Plates with Non-Uniform Boundary Conditions by Using the Differential Quadrature Method, Journal of Sound and Vibration, vol. 173, pp. 702-706.

Lee, J., (1992) Vibration, Buckling and Postbuckling of Laminated Composites with Delaminations, Ph.D. Thesis, Virginia Polytechnic Institute and State University, Blacksburg, VA, USA.

Lee, J., Gürdal, Z., and Griffin Jr., O. H., (1993) Layer-Wise Approach for the Bifurcation Problem in Laminated Composites with Delaminations, AIAA Journal, vol. 31, pp. 331-338.

Lee, J., Gürdal, Z., and Griffin Jr., O. H., (1995) Postbuckling of Laminated Composites with Delaminations, AIAA Journal, vol. 33, pp. 1963-1970.

Lee, J., Gürdal, Z., and Griffin Jr., O. H., (1996) Buckling and Postbuckling of Circular Plates Containing Concentric Penny-Shaped Delaminations, Computers & Structures, vol. 58, pp. 1045-1054.

Li, W. Y., Cheung, Y. K., and Tham, L. G., (1986) Spline Finite Strip Analysis of General Plates, ASCE Journal of Engineering Mechanics, vol. 112, pp. 43-54.

Liew, K. M., Han, J. –B., and Xiao, Z. M., (1996) Differential Quadrature Method for Thick Symmetric Cross-Ply Laminates with First-Order Shear Flexibility, International Journal of Solids and Structures, vol. 33, pp. 2647-2658.

Lim, Y. B. and Parsons, I. D., (1993) The Linearized Buckling Analysis of a Composite Beam with Multiple Delaminations, International Journal of Solids and Structures, vol. 30, pp. 3085-3099.

Lim, Y. B., (1994) Buckling and Postbuckling Analysis of Delaminated Beams Under Compressive Loads, Unpublished Ph.D. Thesis, University of Illinois at Urbana-Champaign, Illinois, USA.

Lin, R. M., Lim, M. K., and Du, H., (1994) Large Deflection Analysis of Plates Under Thermal Loading, Computer Methods in Applied Mechanics and Engineering, vol. 117, pp. 381-390.

Madenci, E., and Westmann, R. A., (1991) Local Delamination Buckling in Layered Systems, Journal of Applied Mechanics, vol. 58, pp. 157-166.

Moradi, S. and Taheri, F., (1998) Application of the Differential Quadrature Method to the Analysis of Delamination Buckling of Composite Beam-Plates, in: Advances in Computational Engineering Science, Edited by S. N. Atluri and G. Yagawa, Tech Science Press, Georgia, USA., pp. 1238-1243.

Moshaiov, A. and Marshall, J., (1991) Analytical Determination of the Critical Load of Delaminated Plates, Journal of Ship Research, vol. 35, pp. 87-90.

Mukherjee, Y. X., Xie, Z., and Ingraffea, A. R., (1991) Delamination Buckling of Laminated Plates, International Journal for Numerical Methods in Engineering, vol. 32, pp. 1321-1337.

Naganarayana, B. P. and Atluri, S. N., (1996) A Computational Model for Analysing Interactive Buckling and Delamination Growth in Composite Structures, vol. 21, Part 5, pp. 547-575.

Nilsson, K. –F. and Storåkers, B., (1992) On Interface Crack Growth in Composite Plates, Journal of Applied Mechanics, vol. 59, pp. 530-538.

NISA II user's manual, (1996), Engineering Mechanics Research Corporation, Troy, MI, U.S.A.

Pandey, M. D. and Sherbourne, A. N., (1991) Buckling of Anisotropic Composite Plates Under Stress Gradient, ASCE Journal of Engineering Mechanics, vol. 117, pp. 260-275.

Peck, S. C., and Springer, G. S., (1991) The Behavior of Delamination in Composite Plates- Analysis and Experimental Results, J. of Composite Materials, vol. 25, pp. 907-929.

Powell, G. and Simons, J., (1981) Improved Iteration Strategy for Nonlinear Structures, International Journal for Numerical Methods in Engineering, vol. 17, pp. 1455-1467.

Press, W. H., Flannery, B. P., Teukolsky, S. A., and Vetterling, W. T., (1986), Numerical Recipes: The Art of Scientific Computing, Cambridge University Press, NY, USA.

Quan, J. R. and Chang, C. T., (1989) New Insights in Solving Distributed System Equations by The Quadrature Method-I Analysis, Computers and Chemical Engineering, vol. 13, pp. 779-788.

Ramm, E., (1981) Strategies for Tracing the Nonlinear Response Near Limit Points, in nonlinear Finite Element Analysis in Structural Mechanics, Springer-Verlag, Berlin, Germany, pp. 63-89.

Riks, E., (1979) An Incremental Approach to the Solution of Snapping and Buckling Problems, International Journal of Solids and Structures, vol. 15, pp. 529-551.

Sheinman, I., Bass, U., and Ishai, O., (1989) Effect of Delamination on Stability of Laminated Composite Strip, Composite Structures, vol. 11, pp. 227-242.

Sheinman, I. and Soffer, M., (1990) Effect of Delamination on the Nonlinear Behavior of Composite Laminated Beams, Journal of Engineering Materials and Technology, vol. 112, pp. 393-397.

Sheinman, I. and Soffer, M., (1991) Post-buckling Analysis of Composite Delaminated Beams, International Journal of Solids and Structures, vol. 27, pp. 639-646.

Sheinman, I. and Adan, M., (1993) Post-buckling Analysis of Multiply Delaminated Beams, International Journal of Solids and Structures, vol. 30, pp. 1289-1300.

Sherbourne, A. N. and Pandey, M. D., (1991) Differential Quadrature Method in The Buckling Analysis of Beams and Composite Plates, Computers & Structures, vol. 40, pp. 903-913.

Shivakumar K. N. and Whitcomb J. D., (1985) Buckling of a Sublaminate in a Quasi-Isotropic Composite Laminate, Journal of Composite Materials, vol. 19, pp. 2-18.

Shu, C., (1991) Generalized Differential-Integral Quadrature and Application to the Simulation of Incompressible Viscous Flows Including Parallel Computation, Ph.D. Thesis, University of Glasgow.

Shu, C. and Richards, B. E., (1992) Application of Generalized Differential Quadrature to Solve Two-dimensional Incompressible Navier-Stokes Equations, International Journal for Numerical Methods in Fluids, vol. 15, pp. 791-798.

Shu, C. and Du, H., (1997a) Free Vibration Analysis of Laminated Composite Cylindrical Shells by DQM, , vol. , pp. 267-274.

Shu, C. and Du, H., (1997b) Implementation of Clamped and Simply Supported Boundary Conditions in the GDQ Free Vibration Analysis of Beams and Plates, International Journal of Solids and Structures, vol. 34, pp. 819-835.

Shu, C. and Du, H., (1997c) A General Approach for Implementing General Boundary Conditions in the GDQ Free Vibration Analysis of Plates, International Journal of Solids and Structures, vol. 34, pp. 837-846.

Simitses, G. J. Sallam, S. N., and Yin, W. L., (1985) Effect of Delamination of Axially Loaded Homogeneous Laminated Plates, AIAA Journal, vol. 23, pp. 1437-1444.

Simitses, G. J. and Chen, Z., (1988) Buckling of Delaminated, Long, Cylinderical Panels Under Pressure, Computers & Structures, vol. 28, pp. 173-184.

Srivatsa, K. S., Vidyashankar, B. R., Krishna Murty, A. V., and Vijaykumar, K., (1993) Buckling of Laminated Plates Containing Delaminations, Computers & Structures, vol. 48, pp. 907-912.

Suemasu, H., (1993) Effects of Multiple Delaminations on Compressive Buckling Behaviors of Composite Panels, J. of Composite Materials, vol. 27, pp. 1172-1192.

Suemasu, H. and Majima, O., (1996) Multiple Delaminations and Their Severity in Circular Axisymmetric Plates Subjected to Transverse Loading, Journal of Composite Materials, vol. 30, pp. 441-453.

Wang, S. S., Zahlan, N. M., and Suemasu, H., (1985) Compressive Stability of Delaminated Random Short-Fiber Composites, Part I- Modeling and Methods of Analysis, Journal of Composite Materials, vol. 19, pp. 296-316.

Wang, S. S., Zahlan, N. M., and Suemasu, H., (1985) Compressive Stability of Delaminated Random Short-Fiber Composites, Part II- Experimental and Analytical Results, Journal of Composite Materials, vol. 19, pp. 317-333.

Wang, X. and Bert, C. W., (1993) A New Approach in Applying Differential Quadrature to Static and Free Vibrational Analysis of Beams and Plates, Journal of Sound and Vibration, vol. 162, pp. 566-572.

Wang, X., (1995) Differential Quadrature for Buckling Analysis of Laminated Plates, Computers & Structures, vol. 57, pp. 715-719.

Wang, J. T., Cheng, S. H., and Lin, C. C., (1995) Local Buckling of Delaminated Beams and Plates Using Continuous Analysis, Journal of Composite Materials, vol. 29, pp. 1374-1402.

Wang, J. T., Pu, H., and Lin, C., (1997) Buckling of Beam-Plates Having Multiple Delaminations, Journal of Composite Materials, vol. 31, pp. 1002-1025.

Wang, W. X., Shen, W., Takao, Y., Shen, Z., and Chen, P., (1991) An Analysis of Compressive Stability of Elastic Solids Containing a Crack Parallel to the Surface, Engineering Fracture Mechanics, vol. 40, pp. 1023-1033.

Wang, W. X., and Takao, Y., (1995) Load Buckling of a Layer Bonded to a Half-Space with an Interface Crack, Journal of Applied Mechanics, vol. 62, pp. 64-70.

Wempner, G. A., (1971), Discrete Approximations Related to Nonlinear Theories of Solids, International Journal of Solids and Structures, vol. 7, pp. 1581-1599.

Whitcomb J. D., (1981) Finite Element Analysis of Stability Related Delamination Growth", Journal of Composite Materials, vol. 15, pp. 403-426.

Whitcomb, J. D., and Shivakumar, K. N., (1987) Strain-Energy Release Rate Analysis of a Laminate with a Post-Buckled Delamination, In Numerical Methods in Fracture Mechanics, Pineridge Press, Swansea, pp. 581-605.

Whitcomb, J. D., (1989) Three Dimensional Analysis of a Post-Buckled Embedded Delamination, Journal Composite Materials, vol. 23, pp. 862-889.

Whitney, J. M., (1987) Structural Analysis of Laminated Anisotropic Plates, Technomic, USA.

Yeh, M. K. and Lee, H. C., (1995) Buckling of Composite Plates with Rectangular Delamination, Proceeding of ICCM-10, Whistler, B.C., Canada, vol. 5, pp. 69-76.

Yeh, M. K., and Tan C. M., (1994) Buckling of Elliptically Delaminated Composite Plates, Journal of Composite Materials, vol. 28, pp. 36-52.

Yin, W. L., Sallam, S. N., and Simitses, G. J., (1986) Ultimate Axial Load Capacity of a Delaminated Beam-Plate, AIAA Journal, vol. 24, pp. 123-128.

Yin, W. L. and Fei, Z., (1988) Delamination Buckling and Growth in a Clamped Circular Plate, AIAA Journal, vol. 26, pp. 438-445.

Yin, W. -L., (1988) The Effects of Laminated Structures on Delamination Buckling and Growth , Journal of Composite Materials, vol. 22, pp. 502-517.

Yin, W. -L., and Jane, K. C., (1992) Refined Buckling and Postbuckling Analysis of Two-Dimensional Delaminations- I. Analysis and Validation, International Journal of Solids and Structures, vol. 29, pp. 591-610.

Yin, W. -L., and Jane, K. C., (1992) Refined Buckling and Postbuckling Analysis of Two-Dimensional Delaminations- II. Results for Anisotropic Laminates and Conclusion, International Journal of Solids and Structures, vol. 29, pp. 611-639.

APPENDICES

APPENDIX A1

Sample program ONEDSD for the buckling analysis of composite laminated beams having a single delamination. The routines balanc, elmhes, hqr and piksrt are taken from Press et al (1986).

```
c     Program ONEDSD for the buckling analysis of a general laminated
c     composite beam having single delamination.
c
c     Last update: October 18,1996
c
      CHARACTER*40  file1
-
      CHARACTER*40 file2,file3,file4
-
      DIMENSION a(200,200),b(100,100),c(100,100)
-
      DIMENSION x1(50),x2(50),x3(50),x4(50),s1(2,50,50)
-
     &          ,s2(2,50,50),s3(2,50,50),s4(2,50,50)
      DIMENSION wr(100),wi(100)
      DIMENSION pmx(50),ainv(100,100)
      DIMENSION ip(50,8)
      REAL*4 l(4),t(4),ltot,d11(4),a11(4),a55(4),b11(4)
      OPEN (5, FILE="onedsd.inp", STATUS="UNKNOWN")
      READ(5,*)file1,file2,file3,file4
      OPEN (1, FILE=file1, STATUS="UNKNOWN")
      OPEN (2, FILE=file2, STATUS="UNKNOWN")
      OPEN (3, FILE=file3, STATUS="UNKNOWN")
c
c   need also "mat.inp" which contains laminate layup.
c
      READ(1,*)n1,n2,n3,n4           !number of sampling points.
      READ(1,*)(t(i), i = 1 , 4)     !t(i)=thickness of each section.
      READ(1,*)(l(i), i = 1 , 4)     !l(i)=length of each section.
      CALL matprp(file4)
      OPEN (4, FILE="mat.dat", STATUS="UNKNOWN")
      DO i = 1 , 3
         READ(4,*)a11(i),a55(i),b11(i),d11(i)
      END DO
      a11(4) = a11(1)
      a55(4) = a55(1)
      b11(4) = b11(1)
      d11(4) = d11(1)
      ntot = n1+n2+n3+n4-4           !total number of nodes
      ltot = l(1) + l(2) + l(4)      !overall length
      nbc = 4
      sdf = 5./6.                    !shear factor
```

```
      d110 = d11(1)
      DO i = 1 , 4
         d11(i) = d11(i) - b11(i)**2/a11(i)
      END DO
      WRITE(*,*)'D11 = ',d11(1)
c
c   determining the global position of each local node.
c
      CALL global(n1,n2,n3,n4,ip)
c
c   computing sampling points in each section.
c

      CALL position(n1,x1)
      CALL position(n2,x2)
      CALL position(n3,x3)
      CALL position(n4,x4)
c
c   computing coefficients of DQM.
c
      CALL coef1d(x1,s1,2,n1,pmx)
      CALL coef1d(x2,s2,2,n2,pmx)
      CALL coef1d(x3,s3,2,n3,pmx)
      CALL coef1d(x4,s4,2,n4,pmx)
c
c   Applying boundary conditions for all the regions.
c
c
c   Clamped condition of both ends.
c
c
      a(nbc+1,ntot+1) = 1.                ! Zero deflection x=0
      a(2*nbc,2*ntot) = 1.                ! Zero deflection   x=L
      a(1,1) = 1.                         ! Zero slope
      a(nbc,ntot) = 1.                    ! Zero slope
c
c   moment continuity at the intersection of regions 1,2 and 3.
c
      DO i = 1 , n1
         a(2,ip(i,1)) = a(2,ip(i,1)) + s1(1,n1,i)*d11(1)/l(1)
      END DO
      DO i = 1 , n2
         a(2,ip(i,2)) = a(2,ip(i,2)) - s2(1,1,i)*d11(2)/l(2)
      END DO
      DO i = 1 , n3
         a(2,ip(i,3)) = a(2,ip(i,3)) - s3(1,1,i)*d11(3)/l(3)
      END DO
      fac = 0.5*a11(2)*a11(3)*(-b11(2)/a11(2)+b11(3)/a11(3)+t(1))
     &                *(-b11(2)/a11(2)+b11(3)/a11(3)+t(1)/2.)/a11(1)
      a(2,ip(n1,1)) = a(2,ip(n1,1))+fac/l(2)
      a(2,ip(n2,2)) = a(2,ip(n2,2))-fac/l(2)
c
c   shear force continuity at the intersection of regions 1,2 and 3.
c
```

```
      DO i = 1 , n1
         a(nbc+2,ip(i,5)) = a(nbc+2,ip(i,5)) + s1(1,n1,i)*(a55(1)/l(1))
      END DO
      DO i = 1 , n2
         a(nbc+2,ip(i,6)) = a(nbc+2,ip(i,6)) - s2(1,1,i)*(a55(2)/l(2))
      END DO
      DO i = 1 , n3
         a(nbc+2,ip(i,7)) = a(nbc+2,ip(i,7)) - s3(1,1,i)*(a55(3)/l(3))
      END DO
c
c   moment continuity at the intersection of regions 2,3 and 4.
c
      DO i = 1 , n4
         a(3,ip(i,4)) = a(3,ip(i,4)) + s4(1,1,i)*d11(4)/l(4)
      END DO
      DO i = 1 , n2
         a(3,ip(i,2)) = a(3,ip(i,2)) - s2(1,n2,i)*d11(2)/l(2)
      END DO
      DO i = 1 , n3
         a(3,ip(i,3)) = a(3,ip(i,3)) - s3(1,n3,i)*d11(3)/l(3)
      END DO
      a(3,ip(1,4)) = a(3,ip(1,4))-fac/l(2)
      a(3,ip(1,2)) = a(3,ip(1,2))+fac/l(2)
c
c   shear force continuity at the intersection of regions 2,3 and 4.
c
      DO i = 1 , n4
         a(nbc+3,ip(i,8)) = a(nbc+3,ip(i,8)) + s4(1,1,i)*(a55(4)/l(4))
      END DO
      DO i = 1 , n2
         a(nbc+3,ip(i,6)) = a(nbc+3,ip(i,6)) - s2(1,n2,i)*(a55(2)/l(2))
      END DO
      DO i = 1 , n3
         a(nbc+3,ip(i,7)) = a(nbc+3,ip(i,7)) - s3(1,n3,i)*(a55(3)/l(3))
      END DO
c
c   applying the buckling eqations for the rest of the nodes.
c
      DO i = 2 , n1-1                    !first section.
         DO j = 1 , n1
            a(7+i,ip(j,1)) = a(7+i,ip(j,1))+s1(2,i,j)
     &                              *d11(1)/(sdf*a55(1)*l(1)**2)
            a(7+i,ip(j,5)) = -s1(1,i,j)/l(1)
            IF(j .EQ. i)THEN
               a(7+i,ip(j,1)) = a(7+i,ip(j,1))- 1.
            END IF
            a(ntot+3+i,ip(j,1)) = s1(1,i,j)
            a(ntot+3+i,ip(j,5)) = s1(2,i,j)/l(1)
            b(i-1,ip(j,1)) = s1(2,i,j)*(t(1)/t(1))/(sdf*a55(1)*l(1))
         END DO
      END DO
      DO i = 2 , n2-1                    !second section.
         DO j = 1 , n2
            a(n1+5+i,ip(j,2)) = a(n1+5+i,ip(j,2))+s2(2,i,j)
```

```
     &                              *d11(2)/(sdf*a55(2)*l(2)**2)
            a(n1+5+i,ip(j,6)) = -s2(1,i,j)/l(2)
            IF(j .EQ. i)THEN
               a(n1+5+i,ip(j,2)) = a(n1+5+i,ip(j,2)) - 1.
            END IF
            a(ntot+n1+1+i,ip(j,2)) = s2(1,i,j)
            a(ntot+n1+1+i,ip(j,6)) = s2(2,i,j)/l(2)
            b(i+n1-3,ip(j,2)) = s2(2,i,j)*(t(2)/t(1))/(sdf*a55(2)*l(2))
         END DO
       END DO
       DO i = 2 , n3-1                        !third section.
         DO j = 1 , n3
            a(n1+n2+3+i,ip(j,3)) = a(n1+n2+3+i,ip(j,3))+s3(2,i,j)
     &                             *d11(3)/(sdf*a55(3)*l(3)**2)
            a(n1+n2+3+i,ip(j,7)) = -s3(1,i,j)/l(3)
            IF(j .EQ. i)THEN
               a(n1+n2+3+i,ip(j,3)) = a(n1+n2+3+i,ip(j,3)) - 1.
            END IF
            a(ntot+n1+n2-1+i,ip(j,3)) = s3(1,i,j)
            a(ntot+n1+n2-1+i,ip(j,7)) = s3(2,i,j)/l(3)
            b(i+n1+n2-5,ip(j,3)) = s3(2,i,j)*(t(3)/t(1))
     &                               /(sdf*a55(3)*l(3))
         END DO
       END DO
       DO i = 2 , n4-1                        !forth section.
         DO j = 1 , n4
            a(n1+n2+n3+1+i,ip(j,4)) = a(n1+n2+n3+1+i,ip(j,4))+s4(2,i,j)
     &                              *d11(4)/(sdf*a55(4)*l(4)**2)
            a(n1+n2+n3+1+i,ip(j,8)) = -s4(1,i,j)/l(4)
            IF(j .EQ. i)THEN
               a(n1+n2+n3+1+i,ip(j,4)) = a(n1+n2+n3+1+i,ip(j,4)) - 1.
            END IF
            a(ntot+n1+n2+n3-3+i,ip(j,4)) = s4(1,i,j)
            a(ntot+n1+n2+n3-3+i,ip(j,8)) = s4(2,i,j)/l(4)
            b(i+n1+n2+n3-7,ip(j,4)) = s4(2,i,j)*(t(4)/t(1))
     &                             /(sdf*a55(4)*l(4))
         END DO
       END DO
c
c  column pivoting.
c
       k1 = ip(n1,1)
       k2 = ip(1,4)
       k3 = ip(n4,4)
       k4 = ip(n1,5)
       k5 = ip(1,8)
       k6 = ip(n4,8)
       DO i = 1 , 2*ntot
          dummy = a(i,2)
          a(i,2) = a(i,k1)
          a(i,k1) = dummy
          dummy = a(i,3)
          a(i,3) = a(i,k2)
          a(i,k2) = dummy
```

```
            dummy = a(i,4)
            a(i,4) = a(i,k3)
            a(i,k3) = dummy
            dummy = a(i,ntot+2)
            a(i,ntot+2) = a(i,k4)
            a(i,k4) = dummy
            dummy = a(i,ntot+3)
            a(i,ntot+3) = a(i,k5)
            a(i,k5) = dummy
            dummy = a(i,ntot+4)
            a(i,ntot+4) = a(i,k6)
            a(i,k6) = dummy
            dummy = a(i,5)
            a(i,5) = a(i,ntot+1)
            a(i,ntot+1) = dummy
            dummy = a(i,6)
            a(i,6) = a(i,ntot+2)
            a(i,ntot+2) = dummy
            dummy = a(i,7)
            a(i,7) = a(i,ntot+3)
            a(i,ntot+3) = dummy
            dummy = a(i,8)
            a(i,8) = a(i,ntot+4)
            a(i,ntot+4) = dummy
         END DO
         DO i = 1 , ntot-nbc
            dummy = b(i,2)
            b(i,2) = b(i,k1)
            b(i,k1) = dummy
            dummy = b(i,3)
            b(i,3) = b(i,k2)
            b(i,k2) = dummy
            dummy = b(i,4)
            b(i,4) = b(i,k3)
            b(i,k3) = dummy
         END DO
c
c  preparing the matrices for the standard eigen solver.
c
         DO i = 1 , 2*nbc
            DO j = 1 , 2*nbc
               ainv(i,j) = a(i,j)
            END DO
         END DO
c
         CALL gaussj(ainv,2*nbc,2*nbc)
         DO i = 1 , 2*nbc
            DO j = 1 , 2*nbc
               a(i,j) = ainv(i,j)
            END DO
         END DO
c
         DO i = 1 , 2*nbc
            DO j = 1 , 2*(ntot-nbc)
```

```
            DO k = 1 , 2*nbc
               c(i,j) = c(i,j) + ainv(i,k)*a(k,j+2*nbc)
            END DO
         END DO
      END DO
c
      DO i = 1 , 2*(ntot-nbc)
         DO j = 1 , 2*(ntot-nbc)
            DO k = 1 , 2*nbc
               a(i+2*nbc,j+2*nbc) = a(i+2*nbc,j+2*nbc) -
     &                              a(i+2*nbc,k)*c(k,j)
            END DO
         END DO
      END DO
c
      DO i = 1 , (ntot-nbc)
         DO j = 1 , (ntot-nbc)
            DO k = 1 , nbc
               b(i,j+nbc) = b(i,j+nbc) - b(i,k)*c(k+nbc,j+ntot-nbc)
            END DO
         END DO
      END DO
c
      END DO
      DO i = 1 , ntot-nbc
         DO j = 1 , ntot-nbc
            ainv(i,j) = a(i+2*nbc,j+2*nbc)
         END DO
      END DO
c
      CALL gaussj(ainv,ntot-nbc,ntot-nbc)
c
      DO i = 1 , ntot-nbc
         DO j = 1 , ntot-nbc
            c(i,j) = 0.
            DO k = 1 , ntot-nbc
               c(i,j) = c(i,j) + ainv(i,k)*a(k+2*nbc,j+ntot+nbc)
            END DO
         END DO
      END DO
c
      DO i = 1 , ntot-nbc
         DO j = 1 , ntot-nbc
            DO k = 1 , ntot-nbc
               a(i+ntot+nbc,j+ntot+nbc) = a(i+ntot+nbc,j+ntot+nbc)
     &                          - a(i+ntot+nbc,k+2*nbc)*c(k,j)
            END DO
         END DO
      END DO
      DO i = 1 , ntot-nbc
         DO j = 1 , ntot-nbc
            ainv(i,j) = b(i,j+nbc)
         END DO
      END DO
```

```
c
      CALL gaussj(ainv,ntot-nbc,ntot-nbc)
      DO i = 1 , ntot-nbc
         DO j = 1 , ntot-nbc
            c(i,j) = 0.
            DO k = 1 , ntot-nbc
               c(i,j) = c(i,j) + ainv(i,k)*a(k+ntot+nbc,j+ntot+nbc)
            END DO
         END DO
      END DO
c
c   calling eigen solver
c
      CALL balanc(c,ntot-nbc,ntot-nbc)
      CALL elmhes(c,ntot-nbc,ntot-nbc)
      CALL hqr(c,ntot-nbc,ntot-nbc,wr,wi)
c
c   sorting the eigenvalues
c
      CALL piksrt(ntot-nbc,wr)
      DO i = 1 , ntot-nbc
         wr(i) = wr(i)/(4.*3.1415926**2*d110/ltot**2)
      END DO
      WRITE(*,*)'Real eigenvalues'
      WRITE(*,*)(wr(i),i=1,ntot-nbc)
      STOP
      END
c
c    Subroutine global for determining the global position of
c    each local node.
c
c    Last update: July 8,1996
c
c    PARAMETERS :
c     ip(i,j) = global node number of i-th local node belong to
c                  j-th section.
c     n = number of nodes in each section.
c
      SUBROUTINE global(n1,n2,n3,n4,ip)
      DIMENSION ip(50,8)
c
c  rotations
c
      DO i = 1 , n1
         ip(i,1) = i
      END DO
      ip(1,2) = n1
      DO i = 2 , n2
         ip(i,2) = n1+i-1
      END DO
      ip(1,3) = n1
      DO i = 2, n3-1
         ip(i, 3) = n1+n2+i-2
      END DO
```

```
      ip(n3,3) = n1+n2-1
      ip(1,4) = n1+n2-1
      DO i = 2 , n4
         ip(i,4) = n1+n2+n3+i-4
      END DO
c
c  deflections
c
      ntot=n1+n2+n3+n4-4
      DO i = 1 , n1
         ip(i,5) = i+ntot
      END DO
      ip(1,6) = n1+ntot
      DO i = 2 , n2
         ip(i,6) = n1+i-1+ntot
      END DO
      ip(1,7) = n1+ntot
      DO i = 2, n3-1
         ip(i, 7) = n1+n2+i-2+ntot
      END DO
      ip(n3,7) = n1+n2-1+ntot
      ip(1,8) = n1+n2-1+ntot
      DO i = 2 , n4
         ip(i,8) = n1+n2+n3+i-4+ntot
      END DO
      RETURN
      END
c
c    Subroutine position for computiong the sampling points in each
c    section.
c
c
c    Last update: July 8,1996
c
c
      SUBROUTINE position(n,x)
c
      DIMENSION  x(*)
c
      pi = 3.1415926
      DO i = 2 , n - 1
         x(i) = 0.5*(1. - COS((2*i-1)*pi/(2*n)))
      END DO
      x(1) = 0.
      x(n) = 1.
      RETURN
      END
c
c  Subroutine coef1d to compute the weighting coefficients.
c
c    Last update: July 8,1996
c
```

```
      SUBROUTINE coef1d(x,s,norder,n,pmx)
      DIMENSION x(*),s(2,50,50),pmx(*)
c
c  Computing the first derivatives of Lagrange polynomials
c  in x direction .
c
      DO i = 1 , n                !n=number of grid points in x dir.
         pmx(i) = 1.
         DO j = 1 , n
            IF (i .EQ. j) CYCLE
            pmx(i) = pmx(i)*(x(i)-x(j))
         END DO
      END DO
c
c  Determination the weighting coefficients for the first derivative.
c
      DO i = 1 , n
         DO j = 1 , n
            IF (i .EQ. j) CYCLE
            s(1,i,j) = pmx(i)/((x(i)-x(j))*pmx(j))
            s(1,i,i) = s(1,i,i)-s(1,i,j)
         END DO
      END DO
c
c  Computing the weight coefficients of successive derivatives.
c
      DO k = 2 , norder        ! norder= highest dervat. ord. in x dir.
         DO i = 1 , n
            DO j = 1 , n
               IF (i .EQ. j) CYCLE
               s(k,i,j)=k*(s(k-1,i,i)*s(1,i,j)-s(k-1,i,j)/(x(i)-x(j)))
               s(k,i,i) = s(k,i,i)-s(k,i,j)
            END DO
         END DO
      END DO
      RETURN
      END
```

APPENDIX A2

Sample program ONEDMD for the buckling analysis of composite laminated beams having multiple delaminations. The routines: balanc, elmhes, hqr and piksrt are taken from Press et al (1986).

```
c     Program ONEDMD for the buckling analysis of a general laminated
c     composite beam having multiple delaminations.
c
c     Last update: Jan. 10,1997
c
       IMPLICIT DOUBLE PRECISION(a-h,o-z)
       DIMENSION a(400,400),b(400,400),c(300,300)
       DIMENSION x1(20),x2(20),x3(20),s1(2,20,20)
      &          ,s2(2,20,20),s3(2,20,20)
       DIMENSION wr(300),wi(300)
       DIMENSION pmx(20),ainv(300,300)
       DIMENSION ip(20,20)
       REAL*8 l(10),t(10),dl(10),dt(10),ltot
       OPEN (1, FILE="onedm10.inp", STATUS="OLD")
c
c    l(2) length of delaminations
c
       READ(1,*)nod                    !no. of delamination.
       READ(1,*)n1,n2,n3               !no. of grid spacing in each region.
       READ(1,*)(t(i), i = 1 , nod+3)  !t(i)=thickness of each section.
       READ(1,*)(l(i), i = 1 , 3)      !l(i)=length of each section.
       READ(1,*)s
c
       ntot = n1+(nod+1)*n2+n3-2*(nod+1)    ! total number of nodes
       ltot = l(1)+l(2)+l(3)                ! overall length
       nbc = 4
       l(nod+3)=l(3)
       DO i = 2 , nod+2
          l(i)=l(2)
       END DO
       DO i = 1 , nod+3
          dt(i) = t(i)/t(1)
          dl(i) = ltot/l(i)
       END DO
       sbar = s/(4.*(3.1415926)**2)
c
c    determining the global position of each local node.
c
       CALL global(n1,n2,n3,nod,ip)
c
c    computiong sampling points in each section.
c
```

```
      CALL position(n1,x1)
      CALL position(n2,x2)
      CALL position(n3,x3)
c
c   computing coefficients of DQM.
c
      CALL coef1d(x1,s1,2,n1,pmx)
      CALL coef1d(x2,s2,2,n2,pmx)
      CALL coef1d(x3,s3,2,n3,pmx)
c
c   applying boundary conditions for all sections.
c   clamped condition of both ends.
c
      a(nbc+1,ntot+1) = 1.                !Zero deflection
      a(2*nbc,2*ntot) = 1.                !Zero deflection
      a(1,1) = 1.                         !Zero slope
      a(nbc,ntot) = 1.                    !Zero slope
c
c   moment continuity at the intersection of 1,2,3,.. and nod+2.
c
      DO i = 1 , n1
         a(2,ip(i,1)) = a(2,ip(i,1)) + s1(1,n1,i)*t(1)**3/l(1)
      END DO
      DO j = 2 , nod+2
         DO i = 1 , n2
            a(2,ip(i,j)) = a(2,ip(i,j)) - s2(1,1,i)*t(j)**3/l(j)
         END DO
      END DO
      sig = 0.
      DO i = 2 , nod+1
         DO j = i+1, nod+2
            sig = sig+t(i)*t(j)*(t(i)+t(j))
         END DO
      END DO
      a(2,ip(n1,1)) = a(2,ip(n1,1))+3.*sig/l(2)
      a(2,ip(n2,2)) = a(2,ip(n2,2))-3.*sig/l(2)
c
c   shear force continuity at the intersection of 1,2,3,.. and nod+2.
c
      DO i = 1 , n1
         a(nbc+2,ip(i,nod+4)) = a(nbc+2,ip(i,nod+4))+
     &                        s1(1,n1,i)*(t(1)/l(1))
      END DO
      DO j = 2 , nod+2
         DO i = 1 , n2
            a(nbc+2,ip(i,j+nod+3)) = a(nbc+2,ip(i,j+nod+3))
     &                             -s2(1,1,i)*(t(j)/l(j))
         END DO
      END DO
c
c   moment continuity at the intersection of 2,3,4,.. and nod+3.
c
      DO i = 1 , n3
         a(3,ip(i,nod+3)) = a(3,ip(i,nod+3))
```

```
     &                          +s3(1,1,i)*t(nod+3)**3/l(nod+3)
      END DO
      DO j = 2 , nod+2
         DO i = 1 , n2
            a(3,ip(i,j)) = a(3,ip(i,j)) - s2(1,n2,i)*t(j)**3/l(j)
         END DO
      END DO
      a(3,ip(1,nod+3)) = a(3,ip(1,nod+3))-3.*sig/l(2)
      a(3,ip(1,2)) = a(3,ip(1,2))+3.*sig/l(2)
c
c   shear force continuity at the intersection of 2,3,4,.. and nod+3.
c
      DO i = 1 , n3
         a(nbc+3,ip(i,2*(nod+3))) = a(nbc+3,ip(i,2*(nod+3)))
     &                           +s3(1,1,i)*(t(nod+3)/l(nod+3))
      END DO
      DO j = 2 , nod+2
         DO i = 1 , n2
            a(nbc+3,ip(i,j+nod+3)) = a(nbc+3,ip(i,j+nod+3))
     &                              -s2(1,n2,i)*(t(j)/l(j))
         END DO
      END DO
c
c   applying the buckling eqations for the rest of the nodes.
c
      no = 2*nbc
      DO i = 2 , n1-1                      !first section.
         DO j = 1 , n1
            a(no-1+i,ip(j,1)) = a(no-1+i,ip(j,1))+s1(2,i,j)
     &                                  *sbar*dl(1)**2*dt(1)**2
            a(no-1+i,ip(j,nod+4)) = -s1(1,i,j)/l(1)
            IF(j .EQ. i)THEN
               a(no-1+i,ip(j,1)) = a(no-1+i,ip(j,1))- 1.
            END IF
            a(ntot+nbc-1+i,ip(j,1)) = s1(1,i,j)
            a(ntot+nbc-1+i,ip(j,nod+4)) = s1(2,i,j)/l(1)
            b(i-1,ip(j,1)) = s1(2,i,j)*s/l(1)
         END DO
      END DO
      DO k = 2 , nod +2
         k1 = (k-2)*(n2-2)
      DO i = 2 , n2-1                      !delaminated sections.
         DO j = 1 , n2
            a(n1+no-3+i+k1,ip(j,k)) = a(n1+no-3+i+k1,ip(j,k))+s2(2,i,j)
     &                               *sbar*dl(k)**2*dt(k)**2
            a(n1+no-3+i+k1,ip(j,k+nod+3)) = -s2(1,i,j)/l(k)
            IF(j .EQ. i)THEN
               a(n1+no-3+i+k1,ip(j,k)) = a(n1+no-3+i+k1,ip(j,k)) - 1.
            END IF
            a(ntot+n1+nbc-3+i+k1,ip(j,k)) = s2(1,i,j)
            a(ntot+n1+nbc-3+i+k1,ip(j,k+nod+3)) = s2(2,i,j)/l(k)
            b(i+n1-3+k1,ip(j,k)) = s2(2,i,j)*s/l(k)
         END DO
      END DO
```

```
      END DO
      k1 = (nod+1)*(n2-2)
      DO i = 2 , n3-1                          !last section.
         DO j = 1 , n3
            a(n1+no-3+i+k1,ip(j,nod+3)) = a(n1+no-3+i+k1,ip(j,nod+3))
     &                          +s3(2,i,j)*sbar*dl(nod+3)**2*dt(nod+3)**2
            a(n1+no-3+i+k1,ip(j,2*(nod+3))) = -s3(1,i,j)/l(nod+3)
            IF(j .EQ. i)THEN
               a(n1+no-3+i+k1,ip(j,nod+3))=a(n1+no-3+i+k1,
     &                                       ip(j,nod+3))-1.
            END IF
            a(ntot+n1+nbc-3+i+k1,ip(j,nod+3)) = s3(1,i,j)
            a(ntot+n1+nbc-3+i+k1,ip(j,2*(nod+3))) = s3(2,i,j)/l(nod+3)
            b(i+n1-3+k1,ip(j,nod+3)) = s3(2,i,j)*s/l(nod+3)
         END DO
      END DO
c
c  column pivoting.
c
      k1 = ip(n1,1)
      k2 = ip(1,nod+3)
      k3 = ip(n3,nod+3)
      k4 = ip(n1,nod+4)
      k5 = ip(1,2*(nod+3))
      k6 = ip(n3,2*(nod+3))
      DO i = 1 , 2*ntot
         dummy = a(i,2)
         a(i,2) = a(i,k1)
         a(i,k1) = dummy
         dummy = a(i,3)
         a(i,3) = a(i,k2)
         a(i,k2) = dummy
         dummy = a(i,4)
         a(i,4) = a(i,k3)
         a(i,k3) = dummy
         dummy = a(i,ntot+2)
         a(i,ntot+2) = a(i,k4)
         a(i,k4) = dummy
         dummy = a(i,ntot+3)
         a(i,ntot+3) = a(i,k5)
         a(i,k5) = dummy
         dummy = a(i,ntot+4)
         a(i,ntot+4) = a(i,k6)
         a(i,k6) = dummy
         dummy = a(i,5)
         a(i,5) = a(i,ntot+1)
         a(i,ntot+1) = dummy
         dummy = a(i,6)
         a(i,6) = a(i,ntot+2)
         a(i,ntot+2) = dummy
         dummy = a(i,7)
         a(i,7) = a(i,ntot+3)
         a(i,ntot+3) = dummy
         dummy = a(i,8)
```

```
            a(i,8) = a(i,ntot+4)
            a(i,ntot+4) = dummy
         END DO
         DO i = 1 , ntot-nbc
            dummy = b(i,2)
            b(i,2) = b(i,k1)
            b(i,k1) = dummy
            dummy = b(i,3)
            b(i,3) = b(i,k2)
            b(i,k2) = dummy
            dummy = b(i,4)
            b(i,4) = b(i,k3)
            b(i,k3) = dummy
         END DO
c
c  preparing the matrices for the standard eigen solver.
c
         DO i = 1 , 2*nbc
            DO j = 1 , 2*nbc
               ainv(i,j) = a(i,j)
            END DO
         END DO
c
         CALL gaussj(ainv,2*nbc,2*nbc)
         DO i = 1 , 2*nbc
            DO j = 1 , 2*nbc
               a(i,j) = ainv(i,j)
            END DO
         END DO
c
         DO i = 1 , 2*nbc
            DO j = 1 , 2*(ntot-nbc)
               DO k = 1 , 2*nbc
                  c(i,j) = c(i,j) + ainv(i,k)*a(k,j+2*nbc)
               END DO
            END DO
         END DO
c
         DO i = 1 , 2*(ntot-nbc)
            DO j = 1 , 2*(ntot-nbc)
               DO k = 1 , 2*nbc
                  a(i+2*nbc,j+2*nbc) = a(i+2*nbc,j+2*nbc) -
     &                                 a(i+2*nbc,k)*c(k,j)
               END DO
            END DO
         END DO
c
         DO i = 1 , (ntot-nbc)
            DO j = 1 , (ntot-nbc)
               DO k = 1 , nbc
                  b(i,j+nbc) = b(i,j+nbc) - b(i,k)*c(k+nbc,j+ntot-nbc)
               END DO
            END DO
         END DO
```

```
c
      END DO
      DO i = 1 , ntot-nbc
         DO j = 1 , ntot-nbc
            ainv(i,j) = a(i+2*nbc,j+2*nbc)
         END DO
      END DO
      CALL gaussj(ainv,ntot-nbc,ntot-nbc)
c
      DO i = 1 , ntot-nbc
         DO j = 1 , ntot-nbc
            c(i,j) = 0.
            DO k = 1 , ntot-nbc
               c(i,j) = c(i,j) + ainv(i,k)*a(k+2*nbc,j+ntot+nbc)
            END DO
         END DO
      END DO
c
      DO i = 1 , ntot-nbc
         DO j = 1 , ntot-nbc
            DO k = 1 , ntot-nbc
               a(i+ntot+nbc,j+ntot+nbc) = a(i+ntot+nbc,j+ntot+nbc)
     &                           - a(i+ntot+nbc,k+2*nbc)*c(k,j)
            END DO
         END DO
      END DO
      DO i = 1 , ntot-nbc
         DO j = 1 , ntot-nbc
            ainv(i,j) = b(i,j+nbc)
         END DO
      END DO
      CALL gaussj(ainv,ntot-nbc,ntot-nbc)
      DO i = 1 , ntot-nbc
         DO j = 1 , ntot-nbc
            c(i,j) = 0.
            DO k = 1 , ntot-nbc
               c(i,j) = c(i,j) + ainv(i,k)*a(k+ntot+nbc,j+ntot+nbc)
            END DO
         END DO
      END DO
c
c   calling eigen solver
c
      CALL balanc(c,ntot-nbc,ntot-nbc)
      CALL elmhes(c,ntot-nbc,ntot-nbc)
      CALL hqr(c,ntot-nbc,ntot-nbc,wr,wi)
c
c   sorting the eigenvalues
c
      CALL piksrt(ntot-nbc,wr)
      WRITE(*,*)'Real eigenvalues'
      WRITE(*,*)(wr(i),i=1,ntot-nbc)
      STOP
      END
```

```
c
c     Subroutine global for determining the global position of
c     each local node.
c
c     PARAMETERS :
c
c     ip(i,j)=global node number of i^th local node belong to j^th section.
c     n=number of nodes in each section.
c
      SUBROUTINE global(n1,n2,n3,nod,ip)
      DIMENSION ip(20,*)
c
c  rotation
c
      DO i = 1 , n1
         ip(i,1) = i
      END DO
      ip(1,2) = n1
      DO i = 2 , n2
         ip(i,2) = i+n1-1
      END DO
      DO j = 3 , nod+2
         ip(1,j) = n1
         ip(n2,j) = n1+n2-1
         DO i = 2 , n2-1
           IF(j .EQ. 3) THEN
             ip(i,j) = ip(n2,j-1)+i-1
           ELSE
             ip(i,j) = ip(n2-1,j-1)+i-1
           END IF
         END DO
      END DO
      ip(1,nod+3) = ip(n2,2)
      DO i = 2 , n3
         ip(i,nod+3) = ip(n2-1,nod+2)+i-1
      END DO
c
c  deflection
c
      ntot = n1+(nod+1)*n2+n3-2*(nod+1)    !total number of nodes
      DO i = 1 , n1
         ip(i,nod+4) = ip(i,1) + ntot
      END DO
      DO j = 2 , nod+2
         DO i = 1 , n2
            ip(i,nod+3+j) = ip(i,j) + ntot
         END DO
      END DO
      DO i = 1 , n3
         ip(i,2*(nod+3)) = ip(i,nod+3) + ntot
      END DO
      RETURN
      END
```

APPENDIX A3

Sample program PLATBUC for the buckling analysis of composite laminated plates having an elliptical delamination. The routines balanc, elmhes, hqr and piksrt are taken from Press et al (1986).

```
c     Program PLATBUC for the buckling analysis of a general laminated
c     composite rectangular plate having an elliptical delamination.
c
c     Last update: Jan. 30, 1998
c
      IMPLICIT DOUBLE PRECISION(a-h,o-z)
      DIMENSION a(400,400),b(400,400),c(400,400)
      DIMENSION sx(400,400),sy(400,400),sxx(400,400),syy(400,400)
      DIMENSION sxxx(400,400),syyy(400,400),s1(50,50),s2(50,50)
      DIMENSION sxxxx(400,400),sxyyy(400,400),syyyy(400,400)
      DIMENSION sxxyy(400,400),sxxxy(400,400),sxy(400,400)
      DIMENSION wr(400),wi(400),x(12),y(12),rx(50),ry(50)
      DIMENSION ap(3,3),bp(3,3),dp(3,3)
      DIMENSION pmx(50),ainv(400,400)
      DIMENSION ip(50,50)
      EQUIVALENCE (sx,ainv),(sy,c)
      COMMON/set1/x,y
      CHARACTER*20 matfile
      OPEN (1, FILE="plate.inp", STATUS="UNKNOWN")
      OPEN (2, FILE="plate.out", STATUS="UNKNOWN")
      OPEN (3, FILE="plate.txt", STATUS="UNKNOWN")
      READ(1,*)nx,ny    !no. of sampling points in x and y directions.
      READ(1,*)ax,ay    !half axes of the ellipse.
      READ(1,*)teta     !angle between ellipse and laminate (x') axis.
      READ(1,*)matfile         !material properties file.
      CLOSE(1)
      pi = 2.*DASIN(1.d0)
      teta  = teta*pi/180.d0
      nbc = 4*(nx + ny - 4)      !number of boundary conditions.
      ntot = nx*ny               !total number of nodes
      beta = ax/ay
c
c   call matprp to compute the material properties.
c
      CALL matprp(matfile,ap,bp,dp,umu)
c
c   reduced stiffness D= D-B*inv(A)*B
c
      DO i = 1 , 3
         DO j = 1 , 3
            ainv(i,j) = ap(i,j)
         END DO
```

```
      END DO
      CALL gaussj(ainv,3,3)
      DO i = 1 , 3
         DO j = 1 , 3
            DO k = 1 , 3
               c(i,j) = c(i,j)+ ainv(i,k) *bp(k,j)
            END DO
         END DO
      END DO
      DO i = 1 , 3
         DO j = 1 , 3
            DO k = 1 , 3
               dp(i,j) = dp(i,j)- bp(i,k) *c(k,j)
            END DO
         END DO
      END DO
      IF(dp(1,1) .NE. 0.d0)THEN
         d11 = dp(1,1)
         DO i = 1 , 3
            DO j = 1 , 3
               ap(i,j) = ap(i,j)/d11
               bp(i,j) = bp(i,j)/d11
               dp(i,j) = dp(i,j)/d11
            END DO
         END DO
      END IF
      ex = DCOS(teta)**2 - umu*DSIN(teta)**2
      ey = DSIN(teta)**2 - umu*DCOS(teta)**2
      exy = -.5d0*(1.d0+umu)*DSIN(2.d0*teta)
      px = -(ap(1,1)*ex +     ap(1,2)*ey + ap(1,3)*exy)    !Nx
      py = -(ap(1,2)*ex + ap(2,2)*ey + ap(2,3)*exy)    !Ny
      pxy = -(ap(1,3)*ex + ap(2,3)*ey + ap(3,3)*exy)   !Nxy
      IF(DABS(px) .LT. 1.d-10) px = 0.d0
      IF(DABS(py) .LT. 1.d-10) py = 0.d0
      IF(DABS(pxy) .LT. 1.d-10) pxy = 0.d0
c
c  x,y of ellipse
c
      x(1) = -1.d0
      x(2) = 0.d0
      x(3) = 1.d0
      x(4) = 0.d0
      x(5) = -1.d0*DCOS(pi/6.)
      x(6) = -1.d0*DCOS(pi/3.)
      x(7) = -x(5)
      x(8) = -x(6)
      x(9) = x(5)
      x(10) = x(8)
      x(11) = x(7)
      x(12) = x(6)
      y(1) = 0.d0
      y(2) = -1.d0
      y(3) = 0.d0
      y(4) = 1.d0
```

```
      y(5) = -1.d0*DSIN(pi/6.)
      y(6) = -1.d0*DSIN(pi/3.)
      y(7) = -y(5)
      y(8) = -y(6)
      y(9) = -y(5)
      y(10) = y(6)
      y(11) = y(5)
      y(12) = -y(6)
      CALL global(nx,ny,ip)       !global position of each local node.
      CALL position(nx,rx,1)      !sampling points in each dir.
      CALL position(ny,ry,1)
      CALL coef1d(rx,s1,nx,pmx)   !coefficients of DQM.
      CALL coef1d(ry,s2,ny,pmx)
c
c   compute the coefficients of first order D.Q.
c
      DO i = 1 , nx
         DO j = 1 , ny
            m = ip(i,j)
            CALL mapping(rx(i),ry(j),djac,dxdr,dxds,dydr,dyds)
            DO k = 1 , nx
               n = ip(k,j)
               sx(m,n) = sx(m,n) + s1(i,k)*dyds/djac
               sy(m,n) = sy(m,n) - s1(i,k)*dxds/djac
            END DO
            DO l = 1 , ny
               n = ip(i,l)
               sx(m,n) = sx(m,n) - s2(j,l)*dydr/djac
               sy(m,n) = sy(m,n) + s2(j,l)*dxdr/djac
            END DO
         END DO
      END DO
c
c   computing the coefficients of higher order derivatives.
c
      DO i = 1 , ntot
         DO j = 1 , ntot
            DO k = 1 , ntot
               sxx(i,j) = sxx(i,j) + sx(i,k)*sx(k,j)
               syy(i,j) = syy(i,j) + sy(i,k)*sy(k,j)
               sxxx(i,j) = sxxx(i,j) + sx(i,k)*sxx(k,j)
               syyy(i,j) = syyy(i,j) + sy(i,k)*syy(k,j)
            END DO
         END DO
      END DO
      DO i = 1 , ntot
         DO j = 1 , ntot
            DO k = 1 , ntot
               sxxxx(i,j) = sxxxx(i,j) + sxx(i,k)*sxx(k,j)
               syyyy(i,j) = syyyy(i,j) + syy(i,k)*syy(k,j)
               sxxxy(i,j) = sxxxy(i,j) + sxxx(i,k)*sy(k,j)
               sxyyy(i,j) = sxyyy(i,j) + sx(i,k)*syyy(k,j)
               sxxyy(i,j) = sxxyy(i,j) + sxx(i,k)*syy(k,j)
               sxy(i,j) = sxy(i,j) + sy(i,k)*sx(k,j)
```

```
            END DO
         END DO
      END DO
c
c   applying boundary conditions for clamped plate.
c
      DO i = 1 , ntot
         DO j = 1 , ntot
            a(i,j) = 0.d0
         END DO
      END DO
      DO j = 1 , ny
         a(ip(1,j),ip(1,j)) = 1.d0            !Zero deflection x=0
         a(ip(nx,j),ip(nx,j)) = 1.d0          !Zero deflection x=a
      END DO
      DO i = 2 , nx-1
         a(ip(i,1),ip(i,1)) = 1.d0            !Zero deflection y=0
         a(ip(i,ny),ip(i,ny)) = 1.d0          !Zero deflection y=b
      END DO
      DO j = 2 , ny-1
         CALL cmap(rx(2),ry(j),xx,yy)
         dnom = DSQRT(ay**4*xx**2   + ax**4*yy**2)
         cost1 = DCOS(ay**2*xx/dnom)
         sint1 = DSIN(ax**2*yy/dnom)
         CALL cmap(rx(nx-1),ry(j),xx,yy)
         dnom = DSQRT(ay**4*xx**2   + ax**4*yy**2)
         cost2 = DCOS(ay**2*xx/dnom)
         sint2 = DSIN(ax**2*yy/dnom)
         DO k = 1 , nx
            DO m = 1 , ny
            a(ip(2,j),ip(k,m)) = cost1*sx(ip(2,j),ip(k,m))/ax +
     &           sint1*sy(ip(2,j),ip(k,m))/ay    !Zero rotation x=0
            a(ip(nx-1,j),ip(k,m))= cost2*sx(ip(nx-1,j),ip(k,m))/ax +
     &           sint2*sy(ip(nx-1,j),ip(k,m))/ay !Zero rotation x=a
            END DO
         END DO
      END DO
      DO i = 3 , nx-2
         CALL cmap(rx(i),ry(2),xx,yy)
         dnom = DSQRT(ay**4*xx**2   + ax**4*yy**2)
         cost1 = DCOS(ay**2*xx/dnom)
         sint1 = DSIN(ax**2*yy/dnom)
         CALL cmap(rx(i),ry(ny-1),xx,yy)
         dnom = DSQRT(ay**4*xx**2   + ax**4*yy**2)
         cost2 = DCOS(ay**2*xx/dnom)
         sint2 = DSIN(ax**2*yy/dnom)
         DO k = 1 , nx
            DO m = 1 , ny
            a(ip(i,2),ip(k,m)) = cost1*sx(ip(i,2),ip(k,m))/ax +
     &           sint1*sy(ip(i,2),ip(k,m))/ay   !Zero rotation y=0
            a(ip(i,ny-1),ip(k,m)) = cost2*sx(ip(i,ny-1),ip(k,m))/ax +
     &           sint2*sy(ip(i,ny-1),ip(k,m))/ay !Zero rotation y=b
            END DO
         END DO
```

```
      END DO
c
c   applying the buckling eqation for internal nodes.
c
      DO k = nbc+1 , ntot
         DO i = 1 , nx
            DO j = 1 , ny
               a(k,ip(i,j)) = a(k,ip(i,j)) + dp(1,1)*sxxxx(k,ip(i,j))+
     &                        4.d0*dp(1,3)*beta*sxxxy(k,ip(i,j)) +
     &          2.d0*beta**2*(dp(1,2)+2.d0*dp(3,3))*sxxyy(k,ip(i,j))+
     &                    4.d0*beta**3*dp(2,3)*sxyyy(k,ip(i,j)) +
     &                        beta**4*dp(2,2)*syyyy(k,ip(i,j))
               b(k-nbc,ip(i,j)) = b(k-nbc,ip(i,j))+px*sxx(k,ip(i,j))+
     &         2.d0*beta*pxy*sxy(k,ip(i,j)) + beta**2*py*syy(k,ip(i,j))
            END DO
         END DO
      END DO
c
c  computing eigenvalues of A.W = B.W
c
      DO i = 1 , nbc                          !inv(a11)
         DO j = 1 , nbc
            ainv(i,j) = a(i,j)
         END DO
      END DO
      CALL gaussj(ainv,nbc,nbc)
      DO i = 1 , nbc                          !inv(a11)*a12
         DO j = 1 , ntot-nbc
            c(i,j) = 0.d0
            DO k = 1 , nbc
               c(i,j) = c(i,j) + ainv(i,k)*a(k,j+nbc)
            END DO
         END DO
      END DO
      DO i = 1 , ntot-nbc                     !A
         DO j = 1 , ntot-nbc
            DO k = 1 , nbc
               a(i+nbc,j+nbc) = a(i+nbc,j+nbc) - a(i+nbc,k)*c(k,j)
            END DO
         END DO
      END DO
      DO i = 1 , ntot-nbc                     !B
         DO j = 1 , ntot-nbc
            DO k = 1 , nbc
               b(i,j+nbc) = b(i,j+nbc) - b(i,k)*c(k,j)
            END DO
         END DO
      END DO
      DO i = 1 , ntot-nbc
         DO j = 1 , ntot-nbc
            c(i,j) = a(i+nbc,j+nbc)
            ainv(i,j) = b(i,j+nbc)
         END DO
      END DO
```

```
      CALL gaussj(ainv,ntot-nbc,ntot-nbc)
      DO i = 1 , ntot-nbc                              !inv(B)*A
         DO j = 1 , ntot-nbc
            a(i,j) = 0.d0
            DO k = 1 , ntot-nbc
               a(i,j) = a(i,j) + ainv(i,k)*c(k,j)
            END DO
         END DO
      END DO
c
c   Solve inv(B)*A for it's eigenvalues
c
      CALL balanc(a,ntot-nbc,ntot-nbc)
      CALL elmhes(a,ntot-nbc,ntot-nbc)
      CALL hqr(a,ntot-nbc,ntot-nbc,wr,wi)
      CALL piksrt(ntot-nbc,wr)                !sorting eigenvalues
      DO i = 1 , ntot-nbc
         wr(i) = wr(i)/ax**2
      END DO
      WRITE(*,*)'Real eigenvalues'
      WRITE(*,*)(wr(i),i=1,ntot-nbc)
      WRITE(*,*)'Imaginary eigenvalues'
      WRITE(*,*)(wi(i),i=1,ntot-nbc)
      STOP
      END
c
c    Subroutine global for determining the global position of
c    each local node.
c
      SUBROUTINE global(nx,ny,ip)
      DIMENSION ip(50,50)
c
c   First put the boundry points
c
      DO i = 1 , 2                 !The first and the last two columns
         DO j = 1 , ny
            ip(i,j) = (i-1)*ny+j
            ip(nx-2+i,j) = (i+1)*ny+j
         END DO
      END DO
      DO j = 1 , 2                 !The first and the last two rows
         DO i = 3 , nx-2
            ip(i,j) = 4*ny + (j-1)*(nx-4)+(i-2)
            ip(i,ny-2+j) = 4*ny + (j+1)*(nx-4)+(i-2)
         END DO
      END DO
c
c   Then the internal nodes
c
      DO i = 3 , nx-2
         DO j = 3 , ny-2
            ip(i,j) = 4*(nx+ny-4)+(i-3)*(ny-4)+(j-2)
         END DO
      END DO
```

```
      RETURN
      END
c
c     Subroutine position for computiong sampling points in each
c     direction. It is based on unequally spaced sampling points
c     with adjacent delta-points.
c
      SUBROUTINE position(n,x,k)
      IMPLICIT DOUBLE PRECISION(a-h,o-z)
      DIMENSION  x(*)
      pi = 2.d0*DASIN(1.d0)
      delta = 1.d-5
      IF(k .EQ. 1)THEN
         DO i = 3 , n - 2
            x(i) =  - DCOS((i-2)*pi/(n-3))
         END DO
         x(1) = -1.d0
         x(2) = -1.d0 + delta
         x(n-1) = 1.d0 - delta
         x(n) = 1.d0
      ELSE IF (k .EQ. 2)THEN
         DO i = 2 , n-1
            x(i) = ((i-1)/DFLOAT(n-1))
         END DO
      END IF
      RETURN
      END
c
c
c   SUBROTINE mapping to map the physical domain into computational
c   domain by using cubic serendipity shape functions.
c
      SUBROUTINE mapping(rc,sc,djac,dxdr,dxds,dydr,dyds)
      IMPLICIT DOUBLE PRECISION(a-h,o-z)
      DIMENSION sfd(12,2),x(12),y(12),r(12),s(12)
      COMMON/set1/x,y
      DATA r/-1.d0,1.d0,1.d0,-1.d0,-.3333333333333,.3333333333333,
     &      .33333333333333,-.33333333333333,-1.d0,1.d0,1.d0,-1.d0/
      DATA s/-1.d0,-1.d0,1.d0,1.d0,-1.d0,-1.d0,1.d0,1.d0,
     &      -.33333333333333,-.33333333333333,
     &       .33333333333333,.33333333333333/
c
c   Compute the derivatives of shape functions at rc and sc.
c
      DO i = 1 , 12
         SELECT CASE (i)
         CASE(1,2,3,4)
            sfd(i,1) = (1.d0/32.d0)*(1.d0+sc*s(i))*(r(i)*
     &       (9.d0*(rc**2+sc**2)-10.d0) +18.d0*rc*(1.d0+rc*r(i)))
            sfd(i,2) = (1.d0/32.d0)*(1.d0+rc*r(i))*(s(i)*
     &       (9.d0*(rc**2+sc**2)-10.d0) +18.d0*sc*(1.d0+sc*s(i)))
         CASE(5,6,7,8)
            sfd(i,1) = (9.d0/32.d0)*(1.d0+sc*s(i))*(9.d0*r(i)*
     &       (1.d0-rc**2) -2.d0*rc*(1.d0+9.d0*rc*r(i)))
```

```
            sfd(i,2)=(9.d0/32.d0)*s(i)*(1.d0+9.d0*rc*r(i))*(1.d0-rc**2)
         CASE(9,10,11,12)
            sfd(i,1)=(9.d0/32.d0)*r(i)*(1.d0+9.d0*sc*s(i))*(1.d0-sc**2)
            sfd(i,2)=(9.d0/32.d0)*(1.d0+rc*r(i))*(9.d0*s(i)*
     &       (1.d0-sc**2) -2.d0*sc*(1.d0+9.d0*sc*s(i)))
         END SELECT
       END DO
c
c   Jacobian evaluation at rc and sc.
c
       dxdr = 0.d0
       dxds = 0.d0
       dydr = 0.d0
       dyds = 0.d0
       DO i = 1 , 12
          dxdr = dxdr + sfd(i,1)*x(i)
          dxds = dxds + sfd(i,2)*x(i)
          dydr = dydr + sfd(i,1)*y(i)
          dyds = dyds + sfd(i,2)*y(i)
       END DO
       djac = DABS(dxdr*dyds - dxds*dydr)              !Jacobian
       IF(djac .EQ. 0.)THEN
       WRITE(*,100)rc,sc
       STOP
       END IF
100    FORMAT('**** SINGULARITY ****',/,'At point r =',e11.4,
     &      ' ,s =',e11.4,'  Jacobian is zero')
       RETURN
       END
c
c   SUBROUTINE cmap to give the physical coordinate from computational
c   domain by using cubic Serendipity shape functions.
c
       SUBROUTINE cmap(rc,sc,xx,yy)
       IMPLICIT DOUBLE PRECISION(a-h,o-z)
       DIMENSION sf(12),x(12),y(12),r(12),s(12)
       COMMON/set1/x,y
       DATA r/-1.d0,1.d0,1.d0,-1.d0,-.3333333333333,.3333333333333,
       &      .33333333333333,-.33333333333333,-1.d0,1.d0,1.d0,-1.d0/
       DATA s/-1.d0,-1.d0,1.d0,1.d0,-1.d0,-1.d0,1.d0,1.d0,
       &      -.33333333333333,-.33333333333333,
       &      .33333333333333,.33333333333333/
c
c   Compute shape functions at rc and sc.
c
       DO i = 1 , 12
          SELECT CASE (i)
          CASE(1,2,3,4)
             sf(i) = (1.d0/32.d0)*(1.d0+rc*r(i))*(1.d0+sc*s(i))*
     &         (9.d0*(rc**2+sc**2)-10.d0)
          CASE(5,6,7,8)
             sf(i) = (9.d0/32.d0)*(1.d0+sc*s(i))*(1.d0-rc**2)*
     &                        (1.d0+9.d0*rc*r(i))
          CASE(9,10,11,12)
```

```
            sf(i) = (9.d0/32.d0)*(1.d0+rc*r(i))*(1.d0-sc**2)*
     &              (1.d0+9.d0*sc*s(i))
          END SELECT
        END DO
        xx = 0.d0                          !x coordinate
        yy = 0.d0                          !y coordinate
        DO i = 1 , 12
           xx = xx + sf(i)*x(i)
           yy = yy + sf(i)*y(i)
        END DO
        RETURN
        END
c
c   subroutine matprp to compute the material properties.
c
c   ap(3,3) = extensional stiffness
c   bp(3,3) = bending-extensional stiffness
c   dp(3,3) = flexural stiffness
c   umu = base lamin. Poisson's ratio for time being =.3
c
        SUBROUTINE matprp(matfile,ap,bp,dp,umu)
        IMPLICIT DOUBLE PRECISION(a-h,o-z)
        CHARACTER*20 matfile
        DIMENSION deg(50),n1(50),z(0:50),t(50),ap(3,3),dp(3,3),
     &          qbar(3,3),bp(3,3)
        OPEN (1, FILE=matfile, STATUS="UNKNOWN")
        READ(1,*)e1,e2,g13,v12
        READ(1,*)n
        pi = 2.d0*DASIN(1.d0)
        DO i = 1 , n
           READ(1,*)n1(i),deg(i),t(i)
           deg(i) = deg(i)*pi/180.d0
        END DO
        CLOSE(1)
        umu = 0.3d0
        v21 = v12*e2/e1
        fac1 = 1. - v12*v21
        q11 = e1/fac1
        q12 = v12*e2/fac1
        q21 = v12*e2/fac1
        q22 = e2/fac1
        q33 = g13
        DO i = 1 , n+1
           IF(i .EQ. n+1) t(i) = t(n)
           z(i-1) = -((n/2.)-(i-1))*t(i)
        END DO
        DO i = 1 , 3
           DO j = 1 , 3
              ap(i,j) = 0.d0
              bp(i,j) = 0.d0
              dp(i,j) = 0.d0
           END DO
        END DO
        DO i = 1 , n
```

```
      qbar(1,1) =q11*(DCOS(deg(i)))**4 + q22*(DSIN(deg(i)))**4 +
     &      2.d0*(q12+2.d0*q33)*(DCOS(deg(i))*DSIN(deg(i)))**2
      qbar(1,2) =(q11+q22-4.d0*q33)*(DCOS(deg(i))*DSIN(deg(i)))**2 +
     &      q12*(DSIN(deg(i))*DCOS(deg(i)))**4
      qbar(2,2) =q11*(DSIN(deg(i)))**4 + q22*(DCOS(deg(i)))**4 +
     &      2.d0*(q12+2.d0*q33)*(DCOS(deg(i))*DSIN(deg(i)))**2
      qbar(1,3) =(q11-q12-2.d0*q33)*DCOS(deg(i))**3*DSIN(deg(i)) +
     &      (q22-q12-2.d0*q33)*DSIN(deg(i))**3*DCOS(deg(i))
      qbar(2,3) =(q11-q12-2.d0*q33)*DCOS(deg(i))*DSIN(deg(i))**3 +
     &       (q22-q12-2.d0*q33)*DSIN(deg(i))*DCOS(deg(i))**3
      qbar(3,3) =(q11+q22-2.d0*q12-2.d0*q33)*(DCOS(deg(i))*
     &       DSIN(deg(i)))**2 + q33*(DSIN(deg(i))**4+DCOS(deg(i))**4)
      DO j = 1 , 3
         DO k = 1 , 3
            ap(j,k) =ap(j,k) + qbar(j,k)*(z(i)-z(i-1))
            bp(j,k) =bp(j,k) + 0.5d0*qbar(j,k)*(z(i)**2-z(i-1)**2)
            dp(j,k) =dp(j,k)+(1.d0/3.)*qbar(j,k)*(z(i)**3-z(i-1)**3)
         END DO
      END DO
   END DO
   ap(2,1) = ap(1,2)
   ap(3,1) = ap(1,3)
   ap(3,2) = ap(2,3)
   bp(2,1) = bp(1,2)
   bp(3,1) = bp(1,3)
   bp(3,2) = bp(2,3)
   dp(2,1) = dp(1,2)
   dp(3,1) = dp(1,3)
   dp(3,2) = dp(2,3)
   RETURN
   END
```

APPENDIX A4

Sample program ONEDSDP for the postbuckling analysis of composite laminated beams having a single delamination. The routines mnewt, lubksb and ludcmp are taken from Press et al (1986).

```
c    Program ONEDSDP for postbuckling analysis of a composite laminated
c    clamped beam having a single delamination.
c
c    Last update: Aug. 29, 98
c
c    Routines :
c
c        mnewt, lubksb, ludcmp (all from numerical recipes book)
c
       IMPLICIT DOUBLE PRECISION (A-H,O-Z)
       DIMENSION x(250),x0(250),xx1(250),xx2(250),fvec(250),a(250,250)
       DIMENSION x1(200),s1(4,50,50),x2(100),u1(250),u2(250),xx3(250)
       DIMENSION pmx(100),ip(50,8),g(250,250),xx(250),xx4(250)
      &    ,indx(250),ev(250),x00(250)
       REAL*8 ltot,lan0,load,landa,landa1,delan
       REAL*8 l(4),t(4)
       DIMENSION a11(4),a55(4),b11(4),d11(4)
       COMMON/set1/l,t,ltot,s1,n1,n2,n3,n4,aa,ip,xx
       COMMON/set2/ nload
       COMMON/set3/ a11,a55,b11,d11
       CHARACTER*20 matfile
       OPEN (1, FILE="arc.inp", STATUS="UNKNOWN")
       OPEN (2, FILE="arc.out", STATUS="UNKNOWN")
       OPEN (5, FILE="wdef.xls", STATUS="UNKNOWN")
       OPEN (6, FILE="udef.xls", STATUS="UNKNOWN")
       READ(1,*)n1,n2,n3,n4
       READ(1,*)(t(i), i = 1 , 4)     !thickness of each section.
       READ(1,*)(l(i), i = 1 , 4)     !length of each section.
       READ(1,*)aa                    !imperfection amplitude
       READ(1,*)delta                 !load increament
       READ(1,*)matfile               !material properties file.
       READ(1,*)itnum                 !no. of iterations.
       CLOSE(1)
c
       pi = 2.d0*DASIN(1.d0)
       ltot = l(1) + l(2) + l(4)      !overall length
       ntot = n1+n2+n3+n4-4           !total number of nodes
       n = 2*ntot+4                   !number of variables.
       nload = 19                     !position of load n-nload
       radmax = 1.d-1                 !Max radious of arc-length
       radmin = 2.d-2                 !Min radious of arc-length
       prdit = 5.                     !Desired number of iteration
```

```
      icon2 = 10           !Max no. of iter. in each arc length search
      icon4 = 5            !Max no. of bisection in each iter.
      kk = n1/2 +1
c
c  iprint=0 print for one run
c  iprint=1 print at the end of last run (for multiple runs)
c
      iprint = 0
c
c   call matprp to compute the material properties.
c
      CALL matprp(matfile)
      pcr = 4.*pi**2*d11(1)/ltot**2   !Critical load of intact beam
c
c   global position of each local node.
c
      CALL global(n1,n2,n3,n4,ip)
c
c   computiong sampling points in each section.
c
      CALL position(n1,x1)
c
c   computing coefficients of DQM.
c
      CALL coef1d(x1,s1,4,n1,pmx)
c
c   position of sampling points along the beam length.
c
      DO i = 1 , n1
         xx(i) = x1(i)*l(1)
      END DO
      DO i = 1 , n2
         xx(n1+i) = l(1) + x1(i)*l(2)
      END DO
      DO i = 1, n3
         xx(n1+n2+i) = l(1) + x1(i)*l(3)
      END DO
      DO i = 1, n4
         xx(n1+n2+n3+i) = l(1) + l(2) + x1(i)*l(4)
      END DO
c
c     Initial starting point.
c
      aa1 = 1.d-2*aa
      DO i = 1 , ntot
         x(i) = aa1*(ltot - xx(i))
      END DO
      DO i = 1 , n1
         x(ip(i,5)) = 1.d-1*aa*(1. - DCOS(2.*pi*xx(ip(i,1))/ltot))
         x(ip(i,6)) = 1.d-1*aa*(1. - DCOS(2.*pi*xx(ip(i,2))/ltot))
         x(ip(i,7)) = 1.d-1*aa*(1. - DCOS(2.*pi*xx(ip(i,3))/ltot))
         x(ip(i,8)) = 1.d-1*aa*(1. - DCOS(2.*pi*xx(ip(i,4))/ltot))
      END DO
      x(ip(n4,4)) = 0.
```

```
      x(ip(1,5)) = 0.
      x(ip(n4,8)) = 0.
      load = 0.
c
c  Find a point on the load-disp. curve.
c
      delta0 = delta
102   load = load + delta
      tolx = 1.d-6
      tolf = 1.d-6
      iter = 30
      CALL mnewt(iter,x,n,tolx,tolf,load)
      ux0 = 0.
      wx0 = 0.
      DO j = 1 , n1
         ux0 = ux0 + s1(1,1,j)*x(ip(j,1))/l(1)
         wx0 = wx0 + s1(1,1,j)*x(ip(j,5))/l(1)
      END DO
      v = (1.d0+wx0**2)
      wbar1 = 0.
      p1 = (a11(1)/pcr)*(sig1 + .5d0*sig2**2 +sig2*wbar1)-
     &     (b11(1)/pcr)*wxx0/(1+sig1**2)**1.5
      WRITE(*,*)'--------------------'
      WRITE(*,*)'p at x=0    = ',p1
      WRITE(*,*)'--------------------'
      IF(iprint .EQ. 0)THEN
         WRITE(5,*)ABS(p1),(x(ip(kk,6))/t(1)),(x(ip(kk,7))/t(1))
         WRITE(6,*)DABS(p1),x(ip(1,1))
      ELSE
         DO WHILE (.NOT. EOF(5))
            READ(5,*,ERR=112,END=112)aaa1
         END DO
112      WRITE(5,*)ABS(p1),(x(ip(kk,6))/t(1)),(x(ip(kk,7))/t(1))
         DO WHILE (.NOT. EOF(6))
            READ(6,*,ERR=113,END=113)aaa1
         END DO
113      WRITE(6,*)DABS(p1),x(ip(1,1))
      END IF
      IF(kkk .NE. 1)THEN
         kkk = kkk+1
         GO TO 102
      END IF
c
c   Start arc length method.
c
      WRITE(*,*)'                Start arc length method'
      DO ite = 1 , itnum
         WRITE(*,2000)ite
         WRITE(*,*)'  At load ',load
         WRITE(*,1500)delta
         DO i = 1 , n
             x00(i) = x(i)
         END DO
         icon1 = 1
```

```
          icon3 = 0
          tolx = 5.d-4
          tolf = 5.d-4
          DO i = 1 , n
              x0(i) = x(i)
          END DO
          CALL usrfun(x0,n,a,fvec,1)     !stiffness mat. at x0
c
c    Solving K.X = delta to find the first u-i and landa1.
c
          DO i = 1 , n
             xx4(i) = 0.d0
          END DO
          xx4(n-nload) = -1.d0
          CALL ludcmp(a,n,np,indx,d)
          CALL lubksb(a,n,np,indx,xx4)
          uimax = 0.d0
          DO i = 1 , n
             uimax = DMAX1(uimax,DABS(xx4(i)))
          END DO
          beta1 = 1.d0
          dummy = 0.d0
          DO i = 1 , n
             x0(i) = x0(i)/uimax                !normalizing
             xx4(i) = xx4(i)/uimax
             dummy = dummy +xx4(i)**2
          END DO
104       landa1 = delta/DSQRT(beta1**2+dummy)       !landa1
          DO i = 1 , n
             xx1(i) = xx4(i)*landa1                  !U-1
          END DO
          dummy4 = 0.
          DO i = 1 , n
             dummy4 = dummy4 + xx1(i)**2
          END DO
          t1 = DSQRT(dummy4 + (beta1*landa1)**2)
          WRITE(*,*)' landa-i = ',landa1
          WRITE(2,*)' landa-i = ',landa1
103       DO i = 1 , n
             x(i) = (x0(i)+xx1(i))*uimax
          END DO
          WRITE(*,1530)ite,icon1
          CALL usrfun(x,n,a,fvec,1)
          DO i = 1 , n
             u1(i) = 0.d0
          END DO
          u1(n-nload) = -1.d0
          CALL ludcmp(a,n,np,indx,d)
          CALL lubksb(a,n,np,indx,u1)
          DO i = 1 , n
             u1(i) = u1(i)/uimax                     !UI
          END DO
          WRITE(*,*)' u-I ',u1(kk+n1)
c
```

```
c      compute UII
c
          DO i = 1 , n
             u2(i) = -fvec(i)
          END DO
          u2(n-nload) = u2(n-nload)-(load+landa1)
          CALL LUBKSB(a,n,np,indx,u2)
          DO i = 1 , n
             u2(i) = u2(i)/uimax                          !UII
          END DO
          WRITE(*,*)' u-II ',u2(kk+n1)
c
c  Compute delan
c
          dummy1 = 0.d0
          dummy2 = 0.d0
          DO i = 1 , n
             dummy1 = dummy1 - xx1(i)*u2(i)
             dummy2 = dummy2 + xx1(i)*u1(i)
          END DO
          delan = dummy1/(beta1**2*landa1 + dummy2)
          WRITE(*,*)' first estimate of delan = ',delan
          dummy3 = 0.d0
          DO i = 1 , n
             xx2(i) = u1(i)*delan + u2(i)
             dummy3 = dummy3 + xx2(i)**2
          END DO
          t2 = DSQRT(delta**2 + dummy3 + (beta1*delan)**2)
          WRITE(*,*)' t-i    ',t1
          WRITE(*,*)' t-i+1 ',t2
          r = -(delta**2/t2)*(t2 - delta)              !r = residual
          WRITE(*,*)' Residual =  ',r
          WRITE(2,*)' Residual =  ',r
c
c  New delan
c
          delan = (r + dummy1)/(beta1**2*landa1 + dummy2)
          WRITE(*,*)' final estimate of delan = ',delan
105       DO i = 1 , n
             xx2(i) = u1(i)*delan + u2(i)
          END DO
c
c  Control for the convergence.
c
          DO i = 1 , n
             x(i) = (x0(i)+xx1(i) + xx2(i))*uimax
          END DO
          landa = landa1 + delan
          WRITE(*,*)'Comp. Load = ', (load+landa)
          CALL converge(x,n,(load+landa),tolx,tolf,indicat)
          IF(indicat .EQ. 0)THEN              !indicat=0 converged
             WRITE(*,1000)icon1,tolx
c
c   check the distance of the new point to the last one.
```

```
c
            IF(landa .GT. delta) THEN      !violation
               DO i = 1 , n2
                  WRITE(*,1110)ip(i,1),(x(ip(i,6))/t(1)),ip(i,1)
     &                 ,(x(ip(i,7))/t(1))
               END DO
               WRITE(*,*)'landa = ', landa
               WRITE(*,*)'delta = ', delta
               WRITE(*,*)'p=', (load+landa)
               icon1 = 1
               delta = delta/2.d0        !reduction of arc length
               GO TO 104
            END IF
            IF((load+landa) .LT. load) THEN       !violate
               WRITE(*,*)'p=', (load+landa)
               icon1 = 1
               delta = delta/2.d0        !reduction of arc length
               GO TO 104
            END IF
            load = load + landa
            delta = delta*DSQRT(prdit/icon1)
            IF (delta .GT. radmax) delta = radmax
            IF (delta .LT. radmin) delta = radmin
         ELSE IF(indicat .EQ. 1)THEN     !indicat=1 not converged
            DO i = 1 , n
               xx1(i) = xx1(i) + xx2(i)
            END DO
            landa1 = landa1 + delan
            t1 = t2
            WRITE(*,*)'   Compressive load = ',(load+landa1)
            ux0 = 0.
            wx0 = 0.
            DO j = 1 , n1
               ux0 = ux0 + s1(1,1,j)*x(ip(j,1))/l(1)
               wx0 = wx0 + s1(1,1,j)*x(ip(j,5))/l(1)
            END DO
            v = (1.d0+wx0**2)
            wbar1 = 0.
            p1 = (a11(1)/pcr)*(sig1 + .5d0*sig2**2 +sig2*wbar1)-
     &           (b11(1)/pcr)*wxx0/(1+sig1**2)**1.5
            WRITE(*,*)'--------------------'
            WRITE(*,*)'p at x=0     = ',p1
            WRITE(*,*)'--------------------'
c
c   Check
c
            IF(icon1 .GT. icon2)THEN
               IF(DABS(p1-p2) .LT. 1.d-5)THEN
                  WRITE(*,*)'Convergence based on the value of P'
                  load = load + landa
                  delta = delta*(prdit/icon1)
                  IF (delta .GT. radmax) delta = radmax
                  IF (delta .LT. radmin) delta = radmin
                  GO TO 107
```

```
                END IF
                IF(icon3 .GT. icon4)THEN
                   WRITE(*,1520)ite
                   STOP
                END IF
                icon3 = icon3 + 1           !number of step reduction
                WRITE(*,1510)delta, (delta/2.)
                icon1 = 1
                delta = delta/2.d0          !reduction of arc length
                GO TO 104
             END IF
             icon1 = icon1 + 1
             GO TO 103
          END IF
107       ux0 = 0.
          wx0 = 0.
          DO j = 1 , n1
             ux0 = ux0 + s1(1,1,j)*x(ip(j,1))/l(1)
             wx0 = wx0 + s1(1,1,j)*x(ip(j,5))/l(1)
          END DO
          v = (1.d0+wx0**2)
          wbar1 = 0.
          p1 = (a11(1)/pcr)*(sig1 + .5d0*sig2**2 +sig2*wbar1)-
     &         (b11(1)/pcr)*wxx0/(1+sig1**2)**1.5
          WRITE(*,*)'--------------------'
          WRITE(*,*)'p at x=0    = ',p1
          WRITE(*,*)'--------------------'
          DO i = 1 , n2
             WRITE(*,1110)ip(i,1),(x(ip(i,6))/t(1)),ip(i,1)
     &                   ,(x(ip(i,7))/t(1))
          END DO
c
c writing the results on exell file.
c
          kk = n1/2 +1
          IF(iprint .EQ. 0)THEN
             WRITE(5,*)ABS(p1),(x(ip(kk,6))/t(1)),(x(ip(kk,7))/t(1))
             WRITE(6,*)DABS(p1),x(ip(1,1)),DABS(p2)
          ELSE
             DO WHILE (.NOT. EOF(5))
                READ(5,*,ERR=114,END=114)aaa1
             END DO
114          WRITE(5,*)ABS(p1),(x(ip(kk,6))/t(1)),(x(ip(kk,7))/t(1))
             DO WHILE (.NOT. EOF(6))
                READ(6,*,ERR=115,END=115)aaa1
             END DO
115          WRITE(6,*)DABS(p1),x(ip(1,1))
          END IF
          WRITE(*,2100)ite
       END DO
c
c  Formats
c
1000   FORMAT(' Convergence achieved after ',i3,'  iterations',/,
```

```
     &       ' Norm of error in f = ',d15.8,//)
1050  FORMAT(10x,'Solution :',/)
1100  FORMAT(5x,'u(',i3,')= ',e13.6,10x,'w(',i3,')= ',e13.6)
1150  FORMAT(/,10x,'Deflections of delaminated regions',/,
     &    10x,'Upper sublaminate',10x,'Lower sublaminate',/)
1200  FORMAT(5x,'x(',i2,')= ',d15.8)
1300  FORMAT(/,' Did not converge within the tolerances',/
     &  ,' The best solution with error in functions norm of '
     &  ,d15.8,' is: ',/)
1400  FORMAT(5x,'p = ',d15.8)
1450  FORMAT('----------------------',/,5x,'P at x=0 =   ',d15.8
     &     ,/,5x,'P at x=L/2 = ',d15.8,/,'----------------------',/)
1500  FORMAT(' Arc Length = ',e12.6)
1510  FORMAT(/,' Did not converge with arc length ',f8.5,/
     &  ,'Reducing the arc length to ',f8.5,/)
1520  FORMAT(/,' Did not converge at the iteration ',i3,/)
1530  FORMAT(//,' At load step ',i3,5x,'iteration no. ',i3,/70('-'))
2000  FORMAT(20x,'----------------------',/,20x,'Start of Ite. no. : '
     &        ,i3,/)
2100  FORMAT(20x,'End of Ite. no.   : ',i3,//)
      STOP
      END
c
c  Subroutine usrfun to calculate value of function and its gradient.
c
c  n       number of variables
c  g(n,n)  matrix containing derivatives of each function
c  f(n)    vector of functions
c
c
c
      SUBROUTINE usrfun(x,n,g,f,indi)
      IMPLICIT DOUBLE PRECISION (A-H,O-Z)
      DIMENSION x(*),g(n,n),f(*),f1(*)
      CALL fnc(x,n,f)
      IF(indi .EQ. 0)RETURN
      DO i = 1 , n
         h = 1.d-6*x(i)
         IF(h .EQ. 0.d0)h = 1.d-12
         x(i) = x(i) + h
         CALL fnc(x,n,f1)
         x(i) = x(i) - h
         DO j = 1 , n
            g(j,i) = (f1(j) - f(j))/h
         END DO
      END DO
      RETURN
      END
c
c
c   Subroutine fnc for computing the values of nonlinear equations
c   and boundary equations.
c
      SUBROUTINE fnc(x,n,fvec)
```

```
      IMPLICIT DOUBLE PRECISION(a-h,o-z)
      INTEGER n,ip(50,8),nk(4),iiu,iiw
      DIMENSION x(n),fvec(n)
      DIMENSION x1(*),xx(*)
      DIMENSION s1(4,50,50)
      REAL*8 l(4),t(4),ltot,d11c(4)
      DIMENSION a11(4),a55(4),b11(4),d11(4)
      COMMON/set1/l,t,ltot,s1,n1,n2,n3,n4,aa,ip,xx
      COMMON/set3/ a11,a55,b11,d11
      pi = 2.d0*DASIN(1.d0)
      nk(1) = n1
      nk(2) = n2
      nk(3) = n3
      nk(4) = n4
      ntot = n1+n2+n3+n4-4
      pcr = 4.*pi**2*d11(1)/ltot**2
c
c                        FUNCTION EVALUATION
c
      DO k = 1 , 4
         d11c(k) = d11(k)-b11(k)**2/a11(k)
         DO i = 2 , nk(k)-1
            SELECT CASE (k)
            CASE (1)
               iiu = ip(i,k)-1
               iiw = ip(i,4+k)-10
            CASE (2)
               iiu = ip(i,k)-3
               iiw = ip(i,4+k)-13
            CASE (3)
               iiu = ip(i,k)-5
               iiw = ip(i,4+k)-16
            CASE (4)
               iiu = ip(i,k)-7
               iiw = ip(i,4+k)-18
            END SELECT
            ux = 0.d0
            uxx = 0.d0
            wx = 0.d0
            wxx = 0.d0
            wxxx = 0.d0
            wxxxx = 0.d0
            DO j = 1 , nk(k)
               ux = ux + s1(1,i,j)*x(ip(j,k))
               uxx = uxx + s1(2,i,j)*x(ip(j,k))
               wx = wx + s1(1,i,j)*x(ip(j,4+k))
               wxx = wxx + s1(2,i,j)*x(ip(j,4+k))
               wxxx = wxxx + s1(3,i,j)*x(ip(j,4+k))
               wxxxx = wxxxx + s1(4,i,j)*x(ip(j,4+k))
            END DO
            ux = ux/l(k)
            uxx = uxx/l(k)**2
            wx = wx/l(k)
            wxx = wxx/l(k)**2
```

```
            wxxx = wxxx/l(k)**3
            wxxxx = wxxxx/l(k)**4
c
c    IMPERFECTION TERMS
c
            wbar1=(pi/ltot)*aa*DSIN(2*pi*xx(ip(i,k))/ltot) !1st derv.
            wbar2=2*(pi/ltot)**2*aa*DCOS(2*pi*xx(ip(i,k))
     &           /ltot)              !2nd derv.
            v = (1.d0+wx**2)
            c = (wxxx*(1.+wx**2)-3.d0*wx*wxx**2)/v**2.5
            fvec(iiu) =uxx + (wx+wbar1)*(wxx+wbar2) - wbar1*wbar2
     &                          -(b11(k)/a11(k))*c
            IF(i .EQ. 2 )CYCLE
            IF(i.EQ.n1-1 .OR.i.EQ.n2-1 .OR. i.EQ.n3-1.OR.
     &         i.EQ.n4-1)CYCLE
            pa = wxxxx/v**1.5d0 - 9.d0*wxxx*wxx*wx/v**2.5d0 -
     &                 3.d0*wxx**3*(1.d0-4.d0*wx**2)/v**3.5d0
            fvec(iiw)=pa-((a11(k)/d11c(k))*(ux+0.5d0*wx**2+wx*wbar1)
     &         -(b11(k)/d11c(k))*wxx/v**1.5)*(wxx+wbar2)  !second eq.
          END DO
        END DO
c
c    Boundary conditions at beam edges.
c
        ii = 2*(n1+n2+n3+n4-12)
        ux = 0.d0
        wx = 0.d0
        wxx = 0.d0
        DO j = 1 , n1
           ux = ux + s1(1,1,j)*x(ip(j,1))
           wx = wx + s1(1,1,j)*x(ip(j,5))
           wxx = wxx + s1(2,1,j)*x(ip(j,5))
        END DO
        ux = ux/l(1)
        wx = wx/l(1)
        wxx = wxx/l(1)**2
        wbar1 = 0.
        fvec(ii+1)=(a11(1)/pcr)*(ux+.5d0*wx**2+wx*wbar1)-  !Applied Load
       &          (b11(1)/pcr)*wxx/(1.+wx**2)**1.5
        wx = 0.d0
        DO j = 1 , n1
           wx = wx + s1(1,2,j)*x(ip(j,5))
        END DO
        fvec(ii+2) = wx
!rotation(x=0)=0
        wx = 0.d0
        DO j = 1 , n4
           wx = wx + s1(1,n4-1,j)*x(ip(j,8))
        END DO
        fvec(ii+3) = wx
!rotation(x=L)=0
        fvec(ii+4) = x(ip(n4,4))                          !u(x=L)=0
        fvec(ii+5) = x(ip(1,5))                           !w(x=0)=0
        fvec(ii+6) = x(ip(n4,8))                          !w(x=L)=0
```

```
wxa = 0.d0
DO j = 1 , n1
   wxa = wxa + s1(1,n1,j)*x(ip(j,5))/l(1)
END DO
fvec(ii+7) = x(ip(1,2))-x(ip(n1,1))-.5d0*t(3)*wxa        !u2(x=l)
fvec(ii+8) = x(ip(1,3))-x(ip(n1,1))+.5d0*t(2)*wxa        !u3(x=l)
wxb = 0.d0
DO j = 1 , n4
   wxb = wxb + s1(1,1,j)*x(ip(j,8))/l(4)
END DO
fvec(ii+9) = x(ip(n2,2))-x(ip(1,4))-.5d0*t(3)*wxb        !u(x=l+a)
fvec(ii+10) = x(ip(n3,3))-x(ip(1,4))+.5d0*t(2)*wxb       !u(x=l+a)
ux1 = 0.
ux2 = 0.
ux3 = 0.
wx1 = 0.
wxx1 = 0.
wxxx1 = 0.
wx2 = 0.
wxx2 = 0.
wxxx2 = 0.
wx3 = 0.
wxx3 = 0.
wxxx3 = 0.
DO j = 1 , n1
   ux1 = ux1 + s1(1,n1,j)*x(ip(j,1))
   wx1 = wx1 + s1(1,n1,j)*x(ip(j,5))
   wxx1 = wxx1 + s1(2,n1,j)*x(ip(j,5))
   wxxx1 = wxxx1 + s1(3,n1,j)*x(ip(j,5))
END DO
   ux1 = ux1/l(1)
   wx1 = wx1/l(1)
   wxx1 = wxx1/l(1)**2
   wxxx1 = wxxx1/l(1)**3
DO j = 1 , n2
   ux2 = ux2 + s1(1,1,j)*x(ip(j,2))
   wx2 = wx2 + s1(1,1,j)*x(ip(j,6))
   wxx2 = wxx2 + s1(2,1,j)*x(ip(j,6))
   wxxx2 = wxxx2 + s1(3,1,j)*x(ip(j,6))
END DO
ux2 = ux2/l(2)
wx2 = wx2/l(2)
wxx2 = wxx2/l(2)**2
wxxx2 = wxxx2/l(2)**3
DO j = 1 , n3
   ux3 = ux3 + s1(1,1,j)*x(ip(j,3))
   wx3 = wx3 + s1(1,1,j)*x(ip(j,7))
   wxx3 = wxx3 + s1(2,1,j)*x(ip(j,7))
   wxxx3 = wxxx3 + s1(3,1,j)*x(ip(j,7))
END DO
ux3 = ux3/l(3)
wx3 = wx3/l(3)
wxx3 = wxx3/l(3)**2
wxxx3 = wxxx3/l(3)**3
```

```
      v1 = (1.d0+wx1**2)
      v2 = (1.d0+wx2**2)
      v3 = (1.d0+wx3**2)
      c1 = (wxxx1*(1.+wx1**2)-3.d0*wx1*wxx1**2)/v1**2.5
      c2 = (wxxx2*(1.+wx2**2)-3.d0*wx2*wxx2**2)/v2**2.5
      c3 = (wxxx3*(1.+wx3**2)-3.d0*wx3*wxx3**2)/v3**2.5
      wbar1 =  (pi/ltot)*aa*DSIN(2.*pi*xx(ip(n1,1))/ltot)
      p1 = (ux1 +.5d0*wx1**2 + wx1*wbar1)
      p2 = (ux2 +.5d0*wx2**2 + wx2*wbar1)
      p3 = (ux3 +.5d0*wx3**2 + wx3*wbar1)
c
      fvec(ii+11)=p1-(a11(2)/a11(1))*p2-(a11(3)/a11(1))*p3
     &    -(b11(1)/a11(1))*wxx1/v1+(b11(2)/a11(1))*wxx2/v2
     &    +(b11(3)/a11(1))*wxx3/v3
      fvec(ii+12)= c1-(d11c(2)/d11c(1))*c2-(d11c(3)/d11c(1))*c3
      fvec(ii+13) = wxx1/v1**1.5-(d11(2)/d11(1))*wxx2/v2**1.5-
     &  (d11(3)/d11(1))*wxx3/v3**1.5-
     &   0.5d0*((t(3)*a11(2)/d11(1))*p2 -(t(2)*a11(3)/d11(1))*p3)-
     &  (b11(1)/d11(1))*p1+(b11(2)/d11(1))*p2 + (b11(3)/d11(1))*p3
      fvec(ii+14) = wx2 - wx1
      fvec(ii+15) = wx3 - wx1
      ux4 = 0.
      ux2 = 0.
      ux3 = 0.
      wx4 = 0.
      wxx4 = 0.
      wxxx4 = 0.
      wx2 = 0.
      wxx2 = 0.
      wxxx2 = 0.
      wx3 = 0.
      wxx3 = 0.
      wxxx3 = 0.
      DO j = 1 , n4
         ux4 = ux4 + s1(1,1,j)*x(ip(j,4))
         wx4 = wx4 + s1(1,1,j)*x(ip(j,8))
         wxx4 = wxx4 + s1(2,1,j)*x(ip(j,8))
         wxxx4 = wxxx4 + s1(3,1,j)*x(ip(j,8))
      END DO
      ux4 = ux4/l(4)
      wx4 = wx4/l(4)
      wxx4 = wxx4/l(4)**2
      wxxx4 = wxxx4/l(4)**3
      DO j = 1 , n2
         ux2 = ux2 + s1(1,n2,j)*x(ip(j,2))
         wx2 = wx2 + s1(1,n2,j)*x(ip(j,6))
         wxx2 = wxx2 + s1(2,n2,j)*x(ip(j,6))
         wxxx2 = wxxx2 + s1(3,n2,j)*x(ip(j,6))
      END DO
      ux2 = ux2/l(2)
      wx2 = wx2/l(2)
      wxx2 = wxx2/l(2)**2
      wxxx2 = wxxx2/l(2)**3
      DO j = 1 , n3
```

```
          ux3 = ux3 + s1(1,n3,j)*x(ip(j,3))
          wx3 = wx3 + s1(1,n3,j)*x(ip(j,7))
          wxx3 = wxx3 + s1(2,n3,j)*x(ip(j,7))
          wxxx3 = wxxx3 + s1(3,n3,j)*x(ip(j,7))
        END DO
        ux3 = ux3/l(3)
        wx3 = wx3/l(3)
        wxx3 = wxx3/l(3)**2
        wxxx3 = wxxx3/l(3)**3
        v4 = (1.d0+wx4**2)
        v2 = (1.d0+wx2**2)
        v3 = (1.d0+wx3**2)
        c4 = (wxxx4*(1.+wx4**2)-3.d0*wx4*wxx4**2)/v4**2.5
        c2 = (wxxx2*(1.+wx2**2)-3.d0*wx2*wxx2**2)/v2**2.5
        c3 = (wxxx3*(1.+wx3**2)-3.d0*wx3*wxx3**2)/v3**2.5
        wbar1 = (pi/ltot)*aa*DSIN(2.*pi*xx(ip(n1,2))/ltot)
        p4 = (ux4 +.5d0*wx4**2 + wx4*wbar1)
        p2 = (ux2 +.5d0*wx2**2 + wx2*wbar1)
        p3 = (ux3 +.5d0*wx3**2 + wx3*wbar1)
c
        fvec(ii+16) = p4 - (a11(2)/a11(4))*p2 - (a11(3)/a11(4))*p3
     &    -(b11(4)/a11(4))*wxx4/v4+(b11(2)/a11(4))*wxx2/v2
     &    +(b11(3)/a11(4))*wxx3/v3
        fvec(ii+17) =c4-(d11c(2)/d11c(4))*c2-(d11c(3)/d11c(4))*c3
        fvec(ii+18) = wxx4/v4**1.5-(d11(2)/d11(4))*wxx2/v2**1.5-
     &  (d11(3)/d11(4))*wxx3/v3**1.5-
     &  .5d0*((t(3)*a11(2)/d11(4))*p2 - (t(2)*a11(3)/d11(4))*p3) -
     &  (b11(4)/d11(4))*p4 +(b11(2)/d11(4))*p2 + (b11(3)/d11(4))*p3
        fvec(ii+19) = wx2 - wx4
        fvec(ii+20) = wx3 - wx4
        RETURN
        END

c
        SUBROUTINE MNEWT(NTRIAL,X,N,TOLX,TOLF,dlinc)
        IMPLICIT DOUBLE PRECISION (A-H,O-Z)
        PARAMETER (NP=250)
        DIMENSION X(n),g(n,n),BETA(np),INDX(np)
        COMMON/set2/ nload
        DO k = 1 ,ntrial
           CALL USRFUN(X,n,g,beta,2)
           DO i = 1 , n
              beta(i) = -beta(i)
           END DO
           beta(n-nload) = beta(n-nload) - dlinc
           ERRF=0.
           DO i = 1 , n
              ERRF=ERRF+DABS(BETA(I))
           END DO
           write(*,*)k,errf
           IF(ERRF.LE.TOLF)THEN
              RETURN
           END IF
           CALL LUDCMP(g,N,NP,INDX,D)
```

```
            CALL LUBKSB(g,N,NP,INDX,BETA)
            ERRX=0.
            DO i = 1 , n
               ERRX=ERRX+DABS(BETA(I))
               X(I)=X(I)+BETA(I)
            END DO
            write(*,*)k,errx
            write(*,*)'____'
            IF(ERRX.LE.TOLX)THEN
               RETURN
            END IF
         END DO
         RETURN
         END
c
c  Checking the convergence:
c
c        indicat = 0  Converged in fvec
c        indicat = 1  Didn't converge in fvec
c
         SUBROUTINE converge(x,nn,dload,tolx,tolf,indicat)
         IMPLICIT DOUBLE PRECISION (A-H,O-Z)
         DIMENSION x(*),fvec(250)
         COMMON/set2/ nload
         CALL fnc(x,nn,fvec)
         fvec(nn-nload) = fvec(nn-nload)+dload
         errf=0.
         DO i = 1 , nn
            errf = errf + DABS(fvec(i))
         END DO
         IF(errf .LE. tolf)THEN
            indicat = 0              !Converged
            tolx = errf
         ELSE
            indicat = 1              !Not Converged
         END IF
         WRITE(*,*)'     Tolerance in f = ',errf,indicat
         RETURN
         END
c
c    Subroutine global for determining the global position of
c    each local node.
c
         SUBROUTINE global(n1,n2,n3,n4,ip)
         DIMENSION ip(50,8)
c
c  u
c
         DO i = 1 , n1
            ip(i,1) = i
         END DO
         DO i = 1 , n2
            ip(i,2) = n1+i
         END DO
```

```
      DO i = 1, n3
         ip(i, 3) = n1+n2+i
      END DO
      DO i = 1 , n4
         ip(i,4) = n1+n2+n3+i
      END DO
      ntot1 = n1 + n2 + n3 + n4
c
c   w
c
      DO i = 1 , n1
         ip(i,5) = ip(i,1)+ntot1
      END DO
      ip(1,6) = ip(n1,5)
      DO i = 2 , n2
         ip(i,6) = ip(i,2)+ntot1 - 1
      END DO
      ip(1,7) = ip(1,6)
      DO i = 2 , n3-1
         ip(i,7) = ip(i,3)+ntot1 -2
      END DO
      ip(n3,7) = ip(n2,6)
      ip(1,8) = ip(n2,6)
      DO i = 2 , n4
         ip(i,8) = ip(i,4)+ntot1 -4
      END DO
      RETURN
      END
c
c     Subroutine position for computiong sampling points in each
c     section. It is based on unequally spaced sampling points
c     with adjacent ë-points. Points are normalized w.r.t. each
c     section length.
c
c
c     Reference : Bert, C. W., and Malik, M.,"Differential quadrature
c     method in computational mechanics: A review", Appl Mech Rev,
c     vol 49, no 1, Jan 1996, pp 1-28.
c
      SUBROUTINE position(n,x)
      IMPLICIT DOUBLE PRECISION(a-h,o-z)
      DIMENSION  x(*)
      pi = 2.d0*DASIN(1.d0)
      DO i = 3 , n - 2
         x(i) = 0.5*(1. - COS((2*i-3)*pi/(2*n-4)))
      END DO
      delta = 1.d-3
      x(1) = 0.d0
      x(2) = delta
      x(n-1) = 1. - delta
      x(n) = 1.d0
      RETURN
      END
c
```

```
c  Subroutine coef1d to compute the weighting coefficients.
c
      SUBROUTINE coef1d(x,s,norder,n,pmx)
      IMPLICIT DOUBLE PRECISION(a-h,o-z)
      DIMENSION x(*),s(4,50,50),pmx(*)
      DO i = 1 , n                ! n= number of grid points in x dir.
         pmx(i) = 1.
         DO j = 1 , n
            IF (i .EQ. j) CYCLE
            pmx(i) = pmx(i)*(x(i)-x(j))
         END DO
      END DO
c
c  weighting coefficients for the first order derivative.
c
      DO i = 1 , n
         DO j = 1 , n
            IF (i .EQ. j) CYCLE
            s(1,i,j) = pmx(i)/((x(i)-x(j))*pmx(j))
            s(1,i,i) = s(1,i,i)-s(1,i,j)
         END DO
      END DO
c
c  Computing the weighting coefficients of successive derivatives.
c
      DO k = 2 , norder        !norder= highest dervat. ord. in x dir.
         DO i = 1 , n
            DO j = 1 , n
               IF (i .EQ. j) CYCLE
               s(k,i,j)=k*(s(k-1,i,i)*s(1,i,j)-s(k-1,i,j)/(x(i)-x(j)))
               s(k,i,i) = s(k,i,i)-s(k,i,j)
            END DO
         END DO
      END DO
      RETURN
      END
```